Impact of material attributes & process parameters on critical quality attributes of the amorphous solid dispersion products obtained using hot melt extrusion

Aniket Deepak Sabnis

Submitted for the degree of Doctor of Philosophy

Faculty of Life Sciences

University of Bradford

2019

Impact of material attributes & process parameters on critical quality attributes of the amorphous solid dispersion products obtained using hot melt extrusion

Aniket Deepak Sabnis

Submitted for the degree of Doctor of Philosophy

Faculty of Life Sciences

University of Bradford

2019

Abstract

Keywords: Hot melt extrusion, solid dispersion, crystallisation, Ibuprofen, Polyox, Soluplus®, Affinisol™HPMC, controlled release.

The feasibility of hot melt extrusion (HME) was explored for development of amorphous solid dispersion systems. Controlled release formulations were developed using a cellulose based derivative, Affinisol™HPMC 100cP and 4M grades. BCS class II drugs ibuprofen and posaconazole were selected due to their difference in glass transition temperature and lipophilicity.

This study focused on investigation of the impact the material attributes and process parameters on the critical quality attributes in preparation of amorphous solid dispersions using hot melt extrusion. The critical quality attributes were sub divided into three main attributes of material, process and product.

Rheology of ibuprofen-Affinisol 100cP from melt phase to extrudate phase was tracked. A partial factorial design was carried out to investigate the critical parameters affecting HME. For optimisation of 40%IBU-Affinisol 100cP blends, a feed rate of 0.6kg/hr, screw speed of 500rpm and screw configuration with two mixing elements were found to be optimum for single phase extrudates. ATR-FTIR spectroscopy was found to be an indirect technique of choice in predicting the maximum ibuprofen drug load within extrudates. Prediction was based on the prepared extrudates without charging them to stability conditions.

An alternative strategy of incorporation of di-carboxylic acids to increase the dissolution of posaconazole-Affinisol 4M blends was investigated. Succinic acid and L- malic acid incorporation was found to increase the dissolution of posaconazole. Although, the extrudates crystallised out quicker than the naïve posaconazole-Affinisol 4M, but free posaconazole formed eutectic and co-crystal with succinic and L-malic acid within extrudates. This lead to an increase in dissolution of the extrudates compared to day 0.

Declaration

No portion of the work referred to in the thesis has been submitted in support of an application for another degree or qualification of this or any other university or other institute of learning

i. The author of this thesis (including any appendices and/or schedules to this thesis) owns certain copyright or related rights in it (the “Copyright”) and s/he has given The University of Bradford certain rights to use such Copyright, including for administrative purposes.

ii. Copies of this thesis, either in full or in extracts and whether in hard or electronic copy, may be made only in accordance with the Copyright, Designs and Patents Act 1988 (as amended) and regulations issued under it or, where appropriate, in accordance with licensing agreements which the University has from time to time. This page must form part of any such copies made.

iii. The ownership of certain Copyright, patents, designs, trade marks and other intellectual property (the “Intellectual Property”) and any reproductions of copyright works in the thesis, for example graphs and tables (“Reproductions”), which may be described in this thesis, may not be owned by the author and may be owned by third parties. Such Intellectual Property and Reproductions cannot and must not be made available for use without the prior written permission of the owner(s) of the relevant Intellectual Property and/or Reproductions.

iv. Further information on the conditions under which disclosure, publication and commercialisation of this thesis, the Copyright and an Intellectual Property University IP Policy see https://www.bradford.ac.uk/governance/ordinancesregulations/regulations/university-regulations/regulation-14/), in any relevant Thesis restriction declarations deposited in the University Library, The University Library's regulations (see https://www.bradford.ac.uk/library/about-us/regulations-and-policies/) and in the University's policy on Presentation of Theses.

Table of Contents

Abbreviations and symbols

Abbreviations

AA : Ascorbic acid

API : Active Pharmaceutical Ingredient

ASD : Amorphous solid dispersion

ATR : Attenuated total reflectance

BCS : Biopharmaceutical classification system

CM : Compression Moulding

CPP : Critical process parameters

CQA : Critical quality attributes

CR : Controlled release

DMA : Dynamic Mechanical Analysis

Do : Dose number

DSC : Differential Scanning Calorimetry

DVS : Dynamic Vapour Sorption

FDA : Food Drug Administration

FTIR : Fourier transformed infra-red

GIT : Gastro-intestinal tract

HME : Hot Melt Extrusion

HPMC: Hydroxy Propyl Methyl Cellulose

IBU : Ibuprofen

ICH	:	International Conference on Harmonization
IR	:	Immediate release
ITZ	:	Itraconazole
MA	:	L-malic acid
MeA	:	Maleic acid
MRT	:	Mean residence time
NCE	:	New chemical entity
NIR	:	Near infra-red
OA	:	Oxalic acid
PAT	:	Process Analytical Tools
Posa	:	Posaconazole
QbD	:	Quality by Design
RAF	:	Rigid amorphous fraction
rpm	:	Revolutions Per Minute
RTD	:	Residence time distribution
SA	:	Succinic acid
SEM	:	Scanning Electron Microscopy
SGF	:	Simulated gastric fluid
SIF	:	Simulated intestinal fluid
T_g	:	Glass transition temperature
TGA	:	Thermogravimetric Analysis

T_m	:	melting point temperature
TPS	:	Terahertz pulsed spectroscopy
USP	:	United States Pharmacopeia
UV	:	Ultraviolet
UV	:	Ultra-Violet Spectroscopy
WHO	:	World Health Organization
XRD	:	X -Ray Diffraction

List of Figures

List of Tables

Chapter 1: Introduction

Hot melt extrusion (HME) has been applied in the pharmaceutical industry mainly to prepare solid dispersions for improving solubility of poorly water soluble drugs delivered using instantaneous release (IR) formulations. This is now becoming an established technology for compounds with low solubility in the pharmaceutical industry. HME offers advantages over traditional pharmaceutical operations such as solvent free and continuous processing, thus eliminating the drawbacks of batch processing (Shah et al. 2013). It is easily scalable and has the capability of producing sustained, targeted and modified release, providing better content uniformity over a wide range of dosages, applicability to a wide range of dosage forms, ability to maintain good product stability and formulating clinically advantageous dosage forms such as drug abuse and dose dumping deterrent products. The use of HME technology to achieve controlled release is starting to gain popularity. Its application should translate into a more robust controlled release formulation (e.g. reduced food effect liability) compared to conventional controlled release (CR) matrices. Another key component in preparation of amorphous solid dispersion using HME is the availability of approved suitable polymers. Lack of polymers has led to slow emergence of HME in pharmaceutical industry. The choice of polymer governs the drug release mechanism of solid dispersion, solid state miscibility and solubility with the active pharmaceutical ingredient and processing conditions. A detailed history of success stories of HME products marketed will be provided in chapter 2.

Despite the potential for HME technology there are some important aspects which will affect critical quality attributes of any final drug product. Melt

attributes such as thermal properties and history of the polymer, melt rheology, drug miscibility and process parameters such as temperature, shear, feed rate, residence time, post extrusion processing conditions etc. are important variables (Crowley et al. 2007). These variables will affect critical quality attributes (CQA) such as level of dispersion, stability, mechanical properties, post extrusion processability, drug and polymer degradation and in vitro and in vivo performance. The large number of interdependent variables creates complexity in undertaking any study and its interpretation.

1.1 Research objectives

In order to study the interdependent variables of the application of HME, the focus of this work was on active pharmaceutical ingredients (APIs) known to be amorphous and were selected for formulation development using HME.

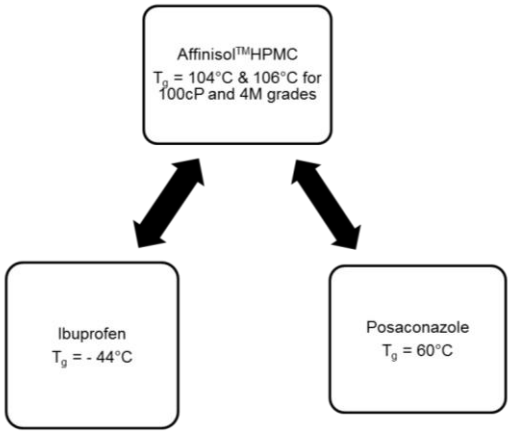

Figure 1.1 Drug-Polymer combinations used for processing using HME

Both APIs used during the study are categorised as poorly water-soluble drug according to BCS (Figure 1.1). Glass transition temperature and partition coefficient are one of the critical factors during formulation development of ASD. Taking them as reference factors, Ibuprofen and Posaconazole were selected. Ibuprofen has a low glass transition temperature and low partition

coefficient while Posaconazole has a high glass transition temperature and high partition coefficient. Additionally, Ibuprofen has a lower molecular weight compared to Posaconazole.

One of the key drawbacks for suitability of HME in the Pharma industry has been the lack of FDA approved polymers. Conventionally used polymers in Pharma had major drawbacks of high T_g, high melt viscosity, and thermal degradation (Serajuddin 1999). To overcome this, various new polymers were introduced either by co-polymerisation or substitution/replacement within the monomers of the polymers (Gupta et al. 2016). This has led to the introduction of new polymers like Soluplus® (copolymer of PVC-PVA-PEG), HPMCAS, HPMCP, and AffinisolTMHPMC. Affinisol^{TM}HPMC was recently launched as an improved HPMC especially for HME (Huang et al. 2016). Limited research data was available for the said polymer and hence was selected as a polymer of choice for the trials. Since the focus was on the sustained released formulation, higher molecular weight grades of 100cP and 4M were evaluated in the current studies.

Ibuprofen

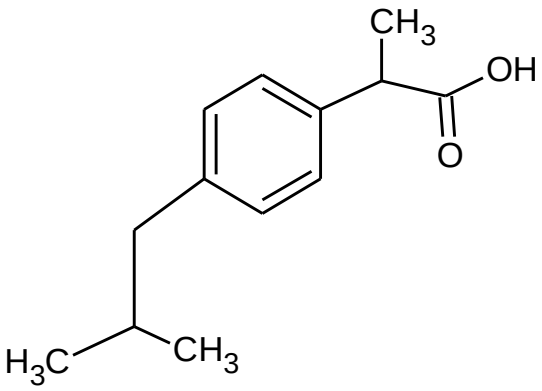

Molecular Formula:	$C_{13}H_{18}O_2$
Formula Weight:	206.28082
Composition:	C(75.69%) H(8.80%) O(15.51%)
Molar Refractivity:	60.77 ± 0.3 cm^3
Molar Volume:	200.3 ± 3.0 cm^3
Parachor:	497.6 ± 4.0 cm^3
Index of Refraction:	1.518 ± 0.02
Surface Tension:	38.0 ± 3.0 dyne/cm
Density:	1.029 ± 0.06 g/cm^3
Dielectric Constant:	Not available
Polarizability:	24.09 ± 0.5 $10^{-24} cm^3$
RDBE:	5
Monoisotopic Mass:	206.13068 Da
Nominal Mass:	206 Da
Average Mass:	206.2808 Da
M+:	206.130131 Da
M-:	206.131228 Da
[M+H]+:	207.137956 Da
[M+H]-:	207.139053 Da
[M-H]+:	205.122306 Da
[M-H]-:	205.123403 Da

Figure 1.2 Chemical Structure of Ibuprofen

Ibuprofen (IBU) or 2-(4-isobutylphenyl)propionic acid is a nonsteroidal anti-inflammatory drug (NSAID) (Figure 1.2). It is used for reducing inflammation and pain in the body (Lerdkanchanaporn and Dollimore 1997). The intended use of Ibuprofen is to reduce fever and treat pain or inflammation caused by many conditions such as a headache, toothache, back pain, arthritis, menstrual cramps, or minor injury.

Physical properties of Ibuprofen are summarised in table 1.1.

Chemical Formula	$C_{13}H_{18}O_2$
Appearance	White solid powder
Odour	Characteristic odour
Mol. Wt g/mol	206.29
Solid State	Crystalline
Melting Point °C	75
Vapour Density	7.1
Solubility	Soluble in most of the organic solvents and water. Insoluble in cold water.
Partition coefficient (Log P)	3.97
pKa	4.91
Glass transition temperature of the amorphous form (°C)	-44.25

Table 1.1 Typical properties of Ibuprofen

Posaconazole

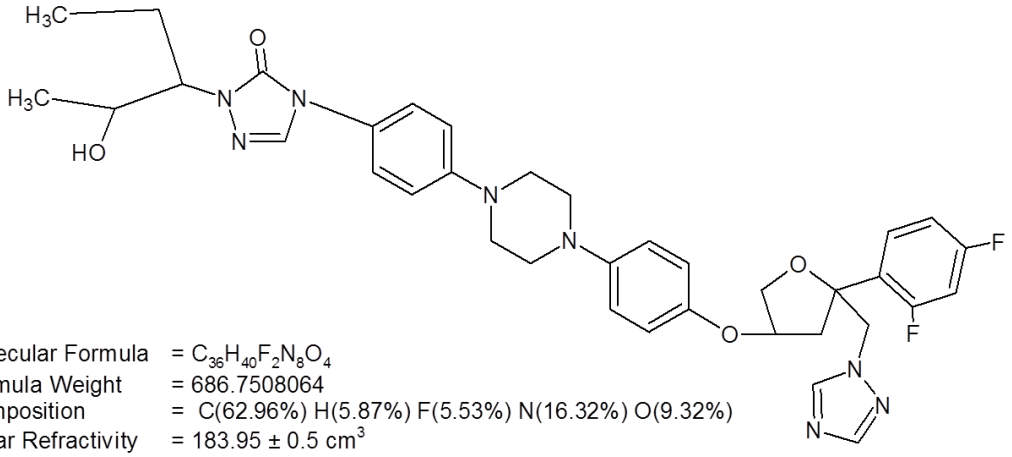

Molecular Formula	= $C_{36}H_{40}F_2N_8O_4$
Formula Weight	= 686.7508064
Composition	= C(62.96%) H(5.87%) F(5.53%) N(16.32%) O(9.32%)
Molar Refractivity	= 183.95 ± 0.5 cm^3
Molar Volume	= 496.0 ± 7.0 cm^3
Parachor	= 1340.5 ± 8.0 cm^3
Index of Refraction	= 1.663 ± 0.05
Surface Tension	= 53.3 ± 7.0 dyne/cm
Density	= 1.38 ± 0.1 g/cm^3
Dielectric Constant	= Not available
Polarizability	= 72.92 ± 0.5 $10^{-24}cm^3$
Monoisotopic Mass	= 686.314058 Da
Nominal Mass	= 686 Da
Average Mass	= 686.7508 Da

Figure 1.3 Chemical Structure of Posaconazole

Posaconazole (POSA) or 4-[4-[4-[4-[[(3R,5R)-5-(2,4-difluorophenyl)-5-(1,2,4-triazol-1-ylmethyl)oxolan-3-yl]methoxy]phenyl]piperazin-1-yl]phenyl]-2-[(2S,3S)-2-hydroxypentan-3-yl]-1,2,4-triazol-3-one is a broad spectrum, second generation, triazole compound with antifungal activity (Torres et al. 2005) (Figure 1.3). It is an antifungal agent structurally related to itraconazole. It is a drug derived from itraconazole through the replacement of the chlorine substituents with fluorine in the phenyl ring, as well as hydroxylation of the triazolone side chain. These modifications enhance the potency and spectrum of activity of the drug. Posaconazole can be either fungicidal or fungistatic in action.

It is a potent triazole antifungal agent used in the prevention of invasive fungal infections due to aspergillosis and candida in high-risk patients. Posaconazole

therapy is associated with transient, asymptomatic serum aminotransferase elevations and is a suspected but rare cause of clinically apparent acute drug-induced liver injury (Dekkers et al. 2016).

Physical properties of POSA are summarised in table 1.2.

Chemical Formula	$C_{36}H_{40}F_2N_8O_4$
Appearance	White solid powder
Odour	Characteristic odour
Mol. Wt g/mol	686.75
Solid State	Crystalline
Melting Point °C	170-172°C
Density	1.38g/cm^3
Solubility	Insoluble in water (0.027mg/L). Soluble in DMSO, DMF, Acetonitrile and Methanol.
Partition coefficient (Log P)	5.5
pKa	14.83
Glass transition temperature of the amorphous form (°C)	60.85°C

Table 1.2 Physical properties of Posa

Affinisol^{TM}HPMC

Hypromellose (HPMC) is one of the polymers of choice when it comes to preparation of solid dispersions of pharmaceutical drugs (Figure 1.4). The key advantage it holds over the other polymers is it is a water-soluble polymer and helps to maintain stable solid dispersion and inhibit API crystallisation in the solution. It is widely reported for its use in immediate as well as modified release formulations.

Although being amorphous in nature and water soluble, HPMC lacked certain aspects for being an ideal polymer of choice for HME. This was largely due to its high glass transition temperature (160-210°C), low decomposition temperatures (200-250°C) and high melt viscosity (Huang et al. 2016).

To overcome the disadvantages of traditional HPMC grades available in the market, a new substituted version named Affinisol^{TM}HPMC was marketed by DOW specifically for HME use. It is amorphous in nature and has a wide temperature window for melt processing. Three grades Affinisol^{TM}HPMC 15cP, 100cP and Affinisol 4M are commercially available grades of which only 100cP and 4M grades were evaluated simultaneously for feasibility as the target release of the formulation in this study was controlled release. Physical properties of the Affinisol can be found in Table 1.3.

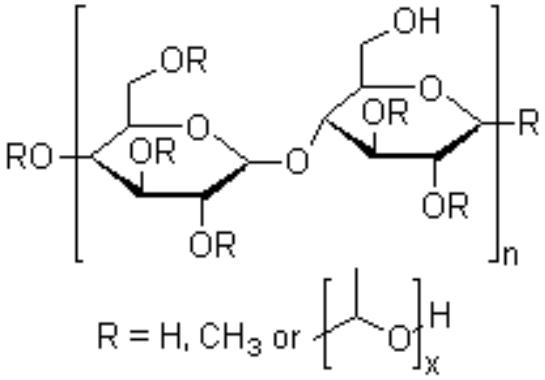

Figure 1.4 Chemical Structure of HPMC

Appearance	White free-flowing powder
Bulk Density (g/cc)	0.42
Tapped Density (g/cc)	0.55
True Density (g/cc)	1.2
Cloud Point (°C)	46
Loss on Drying (%)	1-3
The angle of Repose (°)	32
CARR Index	16.2

Table 1.3 Physical Properties of Affinisol^{TM}HPMC

Table 1.4 provides the difference between three grades of Affinisol^{TM}HPMC.

Properties	Affinisol^{TM}HPMC 15cP	Affinisol^{TM}HPMC 100cP	Affinisol^{TM}HPMC 4M
Mol wt (kDa)	83	179.3	552.8
Particle Size (D_{90}) (µm)	207.068	208.87	237.12
Hansen Solubility Parameter (Δδ) $(J/cc)^{1/2}$	18.0	17.9	17.8
Glass transition temperature (reported) (°C)	110-120°C	110-120°C	110-120°C

HME processing range	135-190°C	145-195°C	155-200°C
Decomposition temperature (°C)	Above 250°C	Above 250°C	Above 250°C

Table 1.4 Properties of different grades of Affinisol^{TM}HPMC

Affinisol^{TM}HPMC is shown to be soluble in a variety of organic solvents extending its versatility in the aqueous free formulations. It is pure HPMC without any addition of plasticiser or additives. Thus, the toxicity data is similar to the HPMC and is considered to be low on toxicity with daily food intake level to be around 20g/person/day.

Dicarboxylic acids as co-formers

To overcome effect of food on the oral bioavailability of Posa, dicarboxylic acids were used as additives. Dicarboxylic acids were used as co-formers for the screening of Eutectics and co-crystals with Posaconazole (Table 1.5).

Co-former name	**Source / Lot no**	**Chemical structure**
Succinic Acid (SA)	Sigma Aldrich, UK	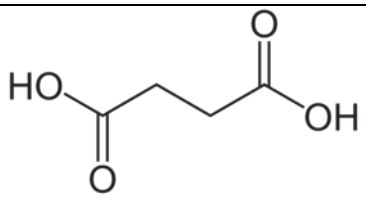 Chemical formula: $C_4H_6O_4$ Molecular weight: 118.09 g/mol Melting point: 185-190°C
L-Malic Acid (MA)	Sigma Aldrich, UK	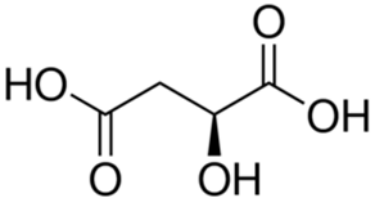 Chemical formula: $C_4H_6O_5$

		Molecular weight:134.087 g/mol Melting point: 104-107°C
Oxalic Acid (OA)	Sigma Aldrich, UK	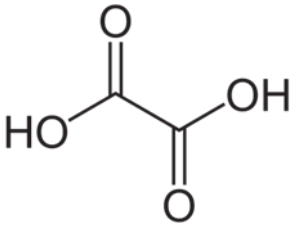 Chemical formula: $C_2H_2O_4$ Molecular weight: 90.1034g/mol Melting point: 188-189°C
Maleic Acid (MeA)	Sigma Aldrich, UK	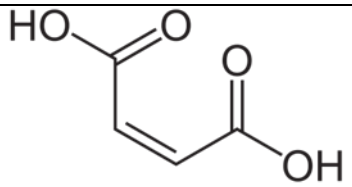 Chemical formula: $C_4H_4O_4$ Molecular weight:116.072 g/mol Melting point: 130-131°C
Ascorbic Acid (AA)	Sigma Aldrich, UK	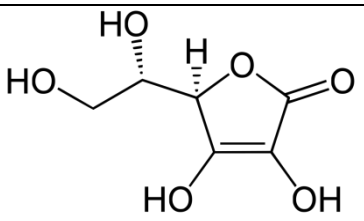 Chemical formula: $C_6H_8O_6$ Molecular weight:176.124 g/mol Melting point: 190-192°C

Table 1.5 Dicarboxylic acids used as co-formers

The research will be divided in to three attributes which are material, process and product respectively (Figure 1.5). It is mainly focussed on indentifying, characterising and proposing solutions to overcome the challenges that arise in the material, process and product attributes during preparation of amorphous solid dispersion products using HME.

Specific objectives of the study involve:

1. To develop robust HME process for amorphous solid dispersion products using amorphous polymer and poorly soluble APIs.
2. To identify and develop preformulatory methods to characterise the polymer and APIs.
3. To investigate the effect of API concentration on the processing history and mechanical properties of extrudates.
4. To study the effect of processing parameters on the performance of amorphous solid dispersion prepared using HME.
5. To identify, confirm and present an indirect analytical method to predict the solid state stability of the extrudates prepared using HME.
6. To understand effect of additives on the performance of amorphous solid dispersion products and suggest an alternative strategy to overcome the bioavailability issue due to effect of food.

To achieve the objectives, the research revolved around three main aspects:

1. Efficient experimental design of HME processing
2. Characterisation using appropriate off-line and in-line tools for improved understanding during processing
3. Product performance and characterisation.

Expected outcomes from the research:

1. Knowledge about use of study designs (in-line tools) and data analysis for HME process for manufacturing of controlled release formulations
2. In-dept understanding around characterisation (e.g. thermal, rheological, spectroscopic and chromatograpic analysis) of HME products.
3. Understanding effect of process vairables on final product critical quality attributes.
4. Use of additives as a strategy to tackle product perfomance affected due to presence of food for solid dispersion using HME.

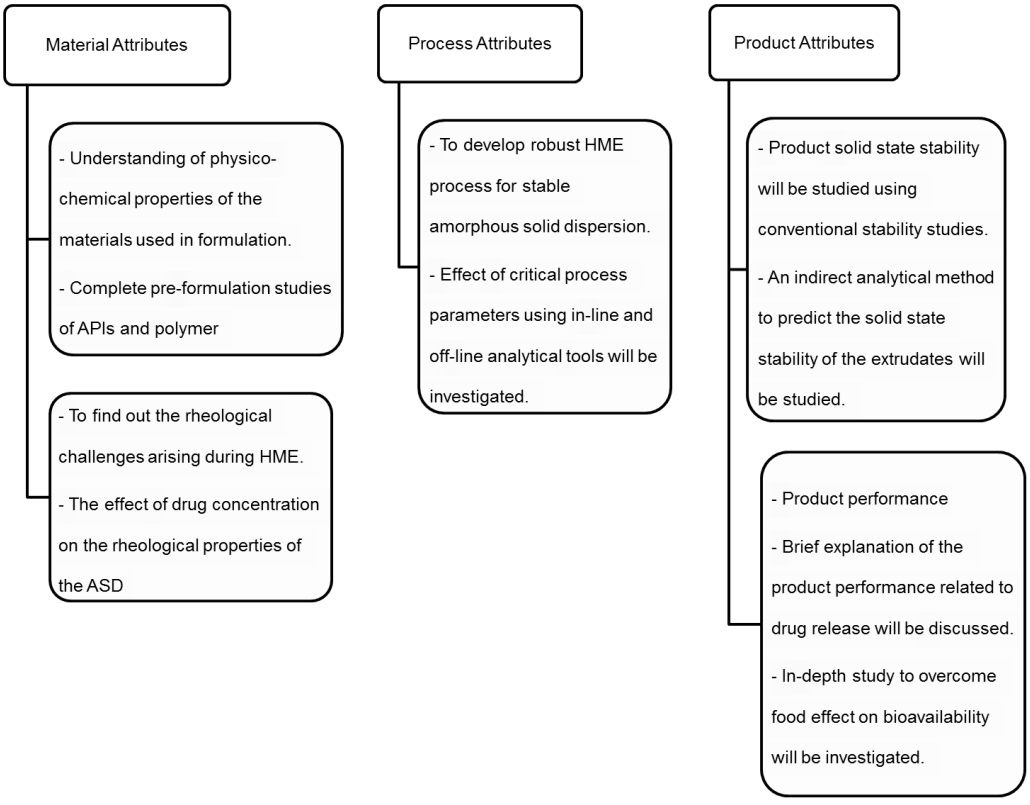

Figure 1.5 Research outline

1.2 Thesis outline

The current report is divided into eight chapters. Chapter 2 provides a background and literature review which is divided into four sections. The first section provides information related to poorly soluble drugs, biopharmaceutical classification system and solubility enhancement techniques. The second section explains the solid state chemistry which is the basis for preparation of amorphous dispersions. The third section explains in brief about the solid dispersion and methods of preparation. The final section provides in-depth information about hot melt extrusion including its background, principle, characterisation tools and their applications in pharma industry. The report structure is provided in Figure 1.6.

Chapter 3 gives detailed information about materials and methods. It provides the rationale for the selection of API and polymer and their advantages and disadvantages. It also describes the processing equipment used and provides rationale and parameters for the analytical instruments used.

Chapter 4 provides a comprehensive study on the material attributes affecting formulation developments of amorphous solid dispersion. Physico-chemical properties of APIs and polymer were studied and analytical methods to characterise the same will be discussed.

Chapter 5 investigates critical quality attributes affecting the formulation development of amorphous solid dispersions using ibuprofen and Affinisol 100cP as API and polymer. Chapter 5 is further divided into three studies which will cover three CQAs of material, process and product attributes.

Chapter 6 focuses on formulation of amorphous solid dispersion using posaconazole and Affinisol 4M as API and polymer. The chapter is further divided into two parts of which 6.1 covers detailed study designs for preparation of amorphous solid dispersion using posaconazole. Chapter 6.2 provides and alternative formulation strategy to overcome food effect on the oral bioavailability of posaconazole.

Chapter 7 covers global conclusions of the studies carried out and provide suggestions for future work.

Chapter 8 provides a list of references used for supporting the research carried out.

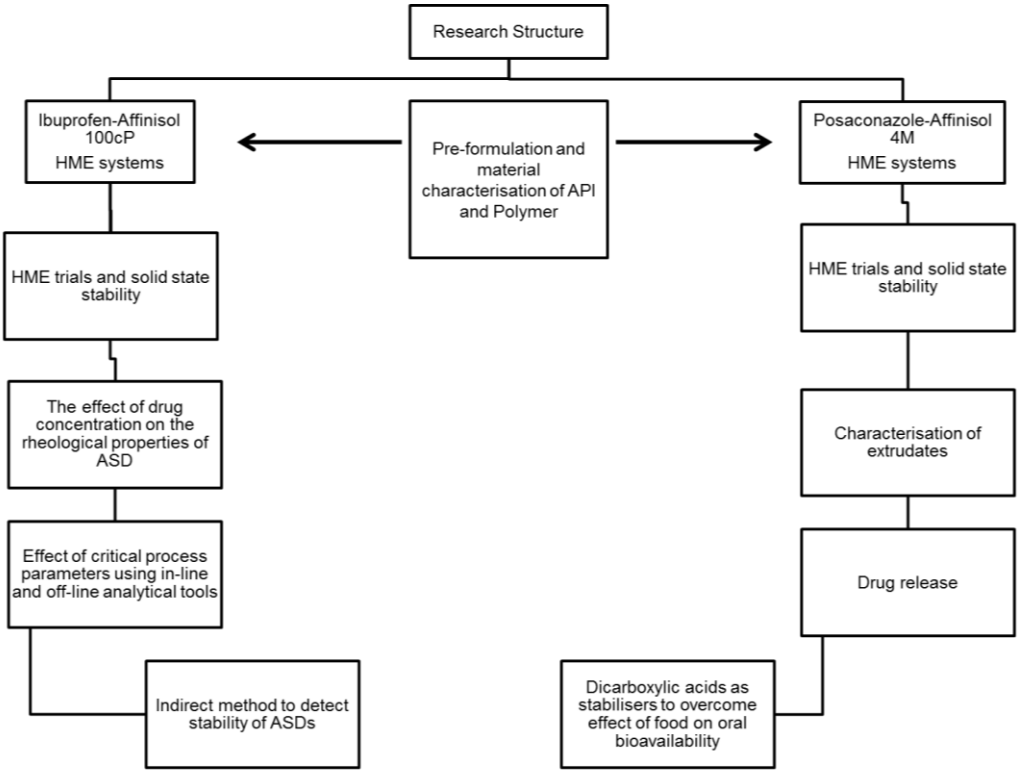

Figure 1.6 Schematic representation of the research structure

Chapter 2: Literature review

The current chapter will provide relevant background of the topic and the literature review on poorly soluble drugs, solid state chemistry, solid dispersions and hot melt extrusion (HME). The main aim of the chapter will be to provide a brief overview of the need of HME and its advances and capabilities.

2.1 Introduction

The poor solubility and bioavailability property of active pharmaceutical ingredients (API) is one of the prevalent challenges faced during the design and development of pharmaceutical dosage forms. Over past two decades, poor solubility has become major issue with the new chemical entities (NCEs) due to implementation of high throughput screening and combinatorial chemistry in the drug discovery process (Baird and Taylor 2012; Vo et al. 2013). About 80% of the drugs are marketed in the form of oral solids (tablets) and around 30-40% of the drugs under development stage have poor solubility. The oral route of administration for drugs is the most commonly used due to its high patient compliance, low sterility constraints, flexibility in the design of dosage forms and low cost (Baghel et al. 2016). Upon administration of the dosage form, drug molecule need to cross barriers like dissolution into gastrointestinal fluids (GIT), passing through gut membranes and first-pass metabolism in order to reach to the site of action through systemic circulation. To categorise the drug moieties based on the solubility and permeability parameters, Biopharmaceutics classification system (BCS)

was generated. According to the BCS classification system, drug moieties are classified into four categories (Figure 2.1). BCS is an indicator of the solubility and permeability of API solely as an aid for post-approval changes based on *in-vitro* data wherever applicable and also during development phase (CDER/FDA 2015).

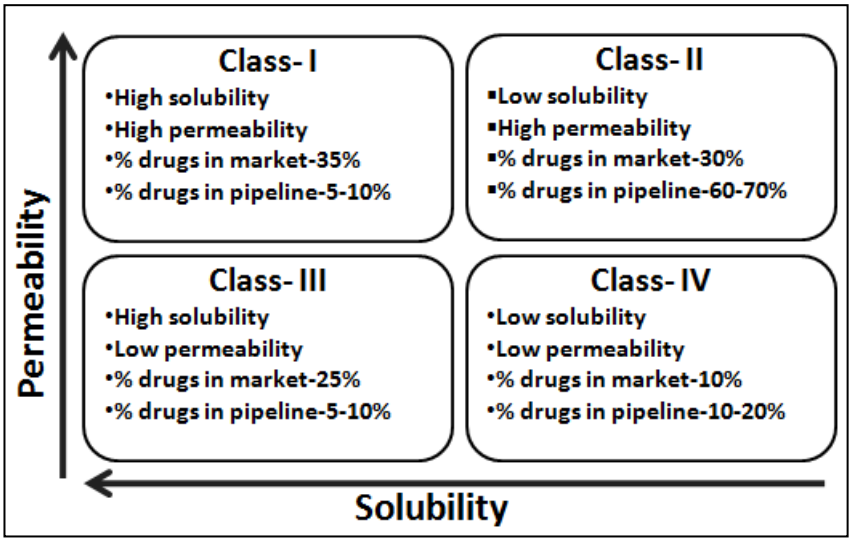

Figure 2.1 Biopharmaceutical classification system

Based on the seminal work, Amidon postulated that the drug absorbtion in the GI tract is controlled by membrane permeability and solubility/dissolution rate. The membrane permeability of a particular drug component is calculated based on the partition coefficient of the uncharged or neutral state of drug molecule between *n*-octanol and water, which is represented as log P and C log P parameters (Dahan et al. 2009). The reference standard for addressing high permeability or low permeability boundaries in the *n*-octanol/water partition coefficient for metoprolol (log P 1.72). The drug components having log P value greater than 1.72 are categorised as high-permeability components because it has been reported that metoprolol undergoes 95% absorbtion in the GI tract. To date only 29 reference drugs have been screened

for human jejunal membrane permeability and all the experimental and calculated values are in good agreement. The permeability of the drug component was determined based on the caculated value of log P or C log P value of drug component. The solubility parameter of the drug component is calculated based on the Dose number (Do), which is the ratio of the highest strength of the drug dose in the administered volume (taken as 250 mL= a glass of water) to the saturation solubility of the drug in water (mg/L). Drug components with Do value <1 are considered as highly soluble drugs where as Do value > 1 are considered as poorly soluble drug components. Based on the Do value the drug components are classified as low, moderate and highly soluble components.

Recently, it is estimated that 80-90% of the drug components in the R&D pipeline may face failure due to low solubility issues (Babu and Nangia 2011).The drugs with low solubility in the aqueous media over pH range (~pH <7.5) at 37°C (however high permeability)come under class II BSC classification system (Babu and Nangia 2011; Dengale et al. 2016). These drugs despite having high permeability display low oral bioavailability due to the slow and delayed release into intestinal fluids (Vasconcelos et al. 2007). A well-known example is Danazol which shows low aqueous solubility (approximately 1µg/mL) and needs to be administered with a daily dose of 600mg/d. Hence to completely dissolve this dose into GI fluids would require approximately 200L of aqueous media (physiological pH) which is practically not possible considering *in vivo* conditions. Hence these poorly soluble APIs may exhibit limited absorption as they pass through their absorption site (Baghel et al. 2016). As a consquence, formulation scientists focusing on the

development of novel, reliable and cost-efficient strategies to enhance the apparent solubility/dissolution rate of poorly soluble drugs. For this purpose, various approaches have been investigated in the drug development process. Most popularly used approaches are salt formation (Baghel et al. 2016), particle size reductions (Rabinow 2004), prodrug approach (Rautio et al. 2008) , complex formation (Loftsson and Duchêne 2007) , micelles (Lavasanifar et al. 2002), micro and nano-emulsions (Mueller et al. 1994; Fatouros et al. 2007), solid-lipid nanoparticles (Potta et al.), co-crystallisation (Babu and Nangia 2011) and solid dispersion. In particular, solid dispersion is gaining significant popularity in the pharmaceutical industry to enhance the solubility and dissolution profile of poorly soluble drugs (Vasconcelos et al. 2007). The choice of preferred strategy depends on the physicochemical properties of the API and its intended application.

2.1.1 Solid State chemistry

Solids are forms of matter which have rigid defined molecular arrangement due to their deifinte shape and volume. Strong interactions are observed in their intermolecular forces and only vibrate upon application of external force and stress. Thus solids are tend to form rigid defined structures called as crystals. A crystal structure is a highly ordered and repeating arrangement of molecules or atoms held together with non-covalent forces. This property of the molecule influences its physicochemical properties.

2.1.2 Classification of Solid forms

Two main classifications of solids are amorphous and crystalline solid forms (Sekhon 2009). Figure 2.2 illustrates the classification of different solid forms

of API into its substituent's based on its chemical structure, composition and molecular arrangements. A solid can exist in two forms either amorphous or crystalline. In crystalline form a solid can exist as polymorph, hydrate, solvate, or co-crystal.

Polymorphs arise when molecules of a compound attain different conformations with differing energies of stabilisation. Although their chemical properties may be the same, they differ in structural orientation. Generally a less stable polymorph converts into its stable polymorph. However, the conversion may take years or just a few seconds to occur as it depends on the activation energy supplied to the polymorph and free energy of that solid. The lowest energy form is more stable. Irreversible transition of one form to another below the melting point are monotorpic while reversible transitions are seen for enantiotropic polymorphs. When the crystal's repeating arrangement unit has a molecule of solvent attached to it then it is called a solvate. When the solvate molecule is replaced by water molecule then it is called a hydrate. A co-crystal is a distinct solid-state material with unique, unpredictable structure and physical property profile.

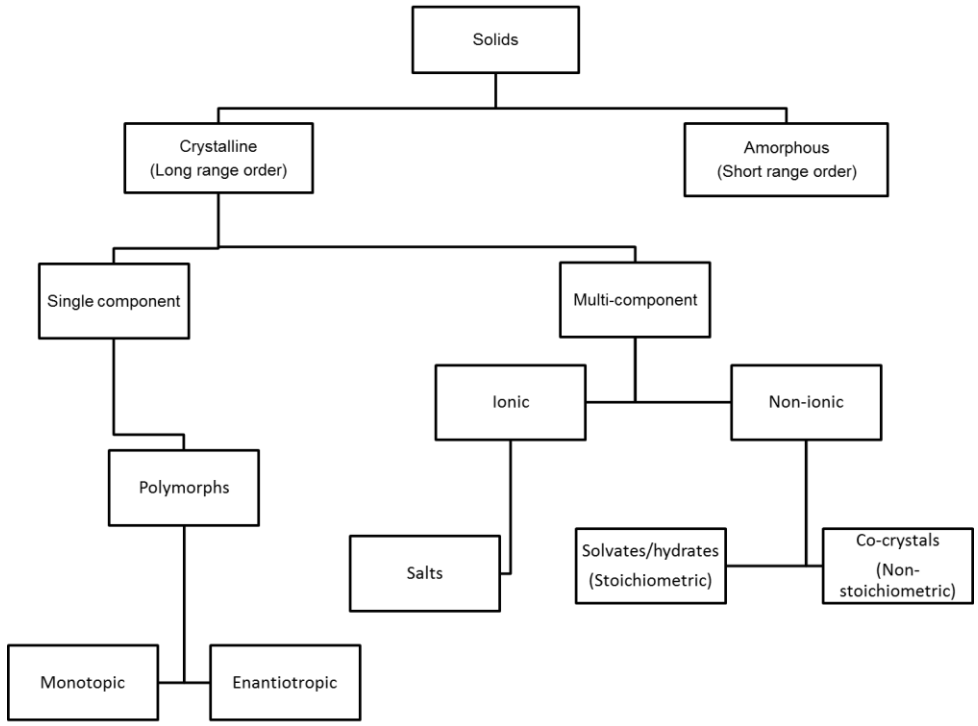

Figure 2.2 Classification of Solid forms based on structure and composition.

2.2 Cocrystals

Intermolecular interaction between multi components due to hydrogen bonding leads to formation of co-crystals. A prominent rise in the commercialisation using co-crystals as a strategy for API stabilisation has gained importance in the pharmaceutical sector. This is due to the ability of co-crystals to improve physicochemical properties such as solubility, chemical and physical stability, dissolution rate and bioavailability without affecting the pharmacological activity of the API. FDA guidelines of 2003 define co-crystals as a molecular association of two or more ingredients in the same chemical crystal lattice (Trask et al. 2006).

From a pharmaceutical perspective, the multicomponent system will consist of an active (API) and excipient (co-former). The co-former is selected on the basis of its ability to form weak non-covalent interactions with an API (Jones

et al. 2011). Selection of co-former depends on various factors like individual component solubility, lattice-free energy, pKa values etc. Several reports are published where different approaches like liquid assisted grinding (Trask et al. 2006), solution crystallisation, spray drying (Mehta 2013), hot melt extrusion (Kelly et al. 2012), ultrasound crystallisation (Aher et al. 2010) and supercritical fluid (Subramaniam et al. 1997) are used as processing techniques to prepare co-crystals.

Cocrystallisation occurs due to competition of molecular association between similar (homomers) or different (heteromers) of functional group of API and co-former. Co-former selection is guided by its chemical nature. It should posses functional moities which can posses the ability to form non-covalent intermolecular interactions such as hydrogen bonds, Van-der-waals forces and π-π interactions (Jampílek 2012). One approach of selection is by the supramolecular synthon approach (Desiraju 1995). Synthon approach is to focus on the functional group present on the API and co-former to form a supramolecular synthon. Carboxylic acid-acid synthon, amide-amide synthon, the acid-pyridine heterosynthon and acid-amide synthon are some of the typical supramolecular synthons (Thakuria et al. 2013) (Figure 2.3).

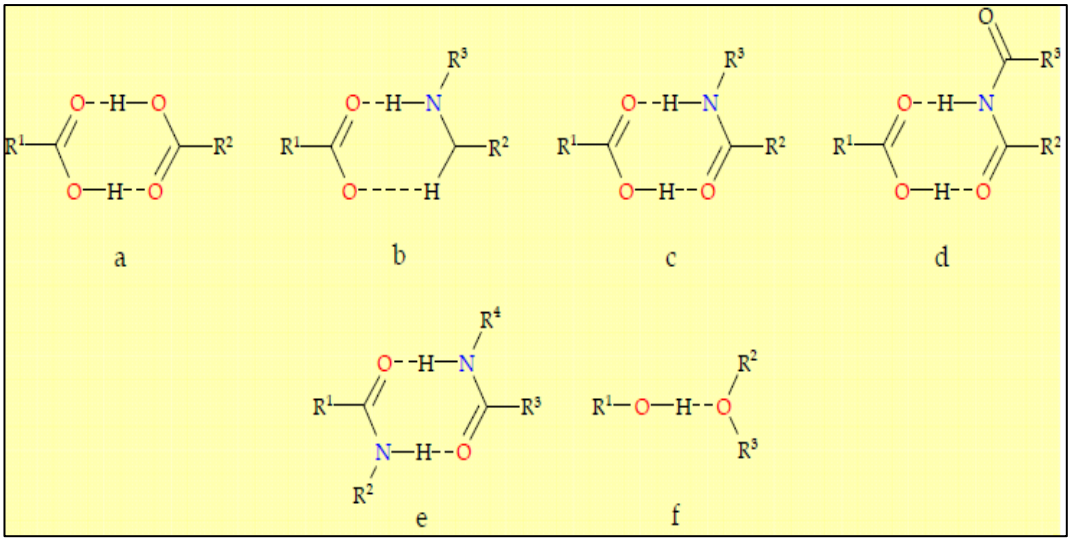

Figure 2.3 Types of hydrogen bonding between two synthons (a) acid-acid, (b) acid-amine, (c) acid-amide, (d) acid-imide, (e) amide-amide and (f) alcohol-ether (Thakuria et al. 2013)

The synthon approach limits itself to only functional group interaction and lacks in consideration of factors such as steric hindrance and density, and molecular arrangement. To overcome this, other approaches such as use of polar density and crystal shape and computational prediction possibilities based on unit cell measurements were also used (Thakuria et al. 2013). Currently FDA proposes to still consider the selection process on the basis of difference in the pKa values which should be less than 3.

Selection of co-former was the first step in prediction of formation of co-crystals. These lead researchers to study the mechanisms of co-crystallisation. Of which, solution state crystallisation, thermal fusion method, eutectic and vapour phase, and deliquescence methods were proposed as the mechanisms for co-crystallisation (Figure 2.4).

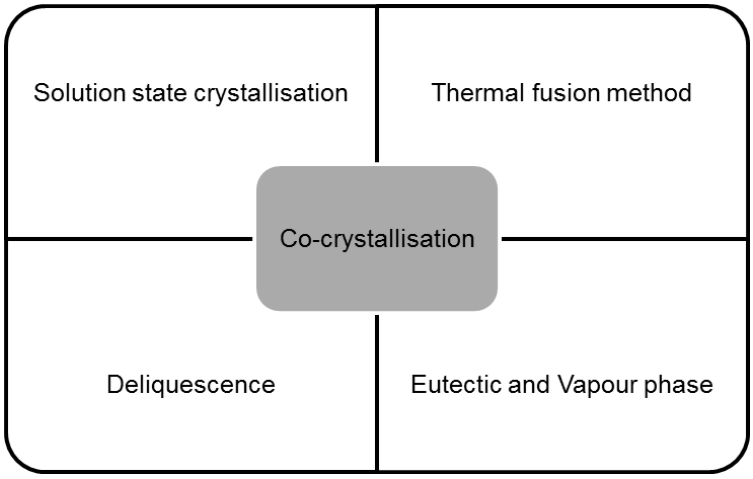

Figure 2.4 Proposed mechanisms of co-crystallisation

Solution state crystallisation is the traditional approach which involves solubilising solute within a solvent. Co-crystallisation is achieved on the principle of supersaturation where molecule will get just about enough energy for molecular rearrangement. This by far is still the preferred choice for scale-up (Nehm et al. 2006).

The heat fusion method involves fusion of API and co-former by application of thermal energy which works on the principle of mixing within thermal depression zone created due to concomitant melting of API and co-former (Berry et al. 2008).

Eutectic or vapour phase mechanism involves generation of co-crystals using mechanical grinding. To assist the eutectic mixing, solvent may be added in small quantities. In such trials co-crystallisation process occurs during vapour evaporation of solvent (Chadwick et al. 2007).

The deliquescence method involves use of hygroscopicity as a mode for achieving co-crystals. Phase transformations between API and co-former are

achieved by exposure to humid conditions and co-crystals are formed due to molecular rearrangement (Jayasankar et al. 2007).

To summarise, co-crystals are one of the emerging strategies used for crystal engineering. Attempts and guidelines are available for co-former selection. Mechanisms are proposed to understand in depth the factors promoting co-crystallisation. Applications of co-crystals range from enhancement of physical as well as chemical properties of drugs (Figure 2.5).

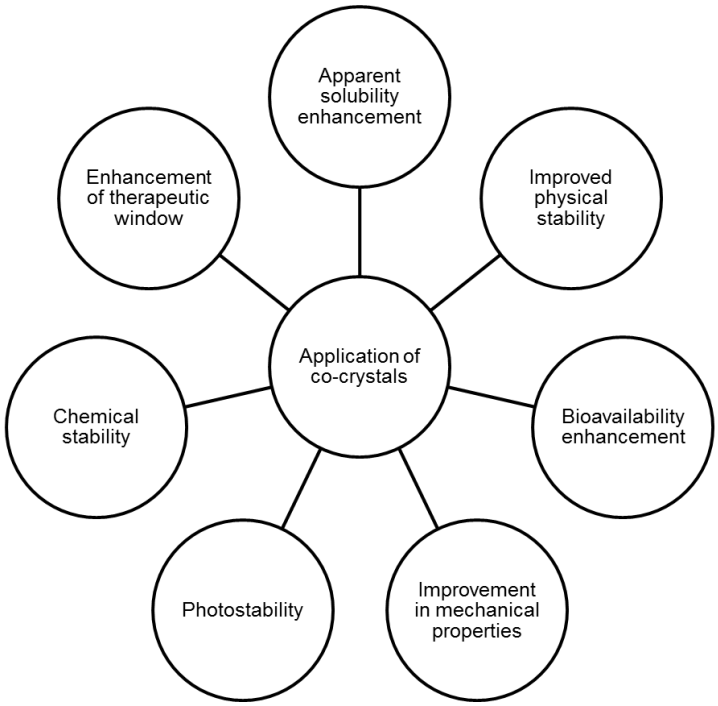

Figure 2.5 Applications of co-crystals

2.3 Amorphous systems

Amorphous means lack of form, and has no long range order of molecular packing or conformations (Yu 2001). An amorphous system thus, is actually fluid but appears to be a solid in the given time scale observation. Amorphous materials play a significant role in different industries ranging from polymers, ceramics, food and pharmaceuticals. Amorphous forms are very common for certain polymers, proteins, peptides and certain sugars, and they can be generated by using certain standard pharmaceutical processes. The amorphous phase in the solid state is referred as the high energy solid state due to increase in the specific volume and intermolecular energy which enhances solubility/dissolution rate.

Amorphous forms can be generated by using four major ways while processing the Pharmaceutical compounds (Figure 2.6) (Hancock and Zografi 1997).

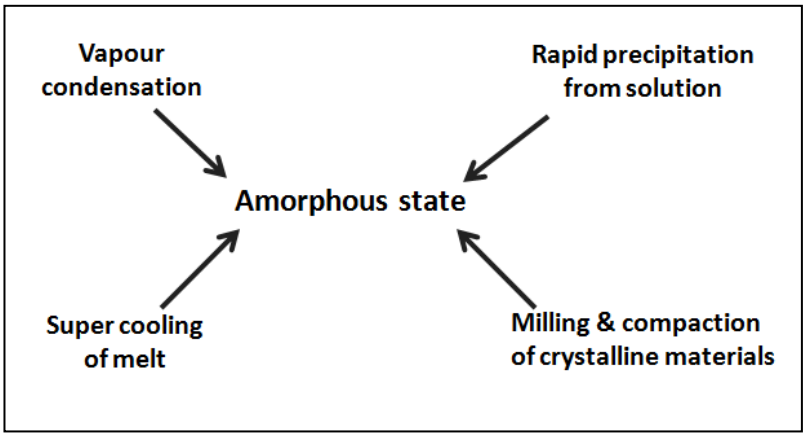

Figure 2.6 Schematic representations of four common pathways to obtain amorphous compounds

Pharmaceutical amorphous dosage forms are multicomponent systems containing drug substances as the active component and polymeric material as an excipient. Figure 2.7 represents the correlation between the enthalpy (ΔH) and specific volume (V) of a material as a function of temperature. In crystalline materials, we may see at very low temperatures a small increase in enthalpy and specific volume with respect to the temperature indicative of a certain heat capacity (C_p) and thermal expansion coefficient (α). When a crystalline material reaches its melting temperature (T_m) discontinuity in both ΔH and ΔV represent a first-order transition to liquid state. Upon rapid cooling beyond its melting temperature values of ΔH and ΔV may follow equilibrium or first order in “super cooled region”. On further cooling, a change in slope is seen at a characteristic temperature called the “glass transition temperature” (T_g) (Figure 2.7).T_g is a significant property for the characterisation of pharmaceutical solids. At T_g, the properties of the glassy material deviate from those of the equilibrium super-cooled liquid to give a non-equilibrium state having even higher H and V than the super-cooled liquid (Kumar and Singh 2013). T_g is a thermodynamic requirement otherwise the system would collapse as it will possess the lower enthalpy than its crystalline phase. The temperature at which it collapses is called the Kauzmann Temperature (T_k).

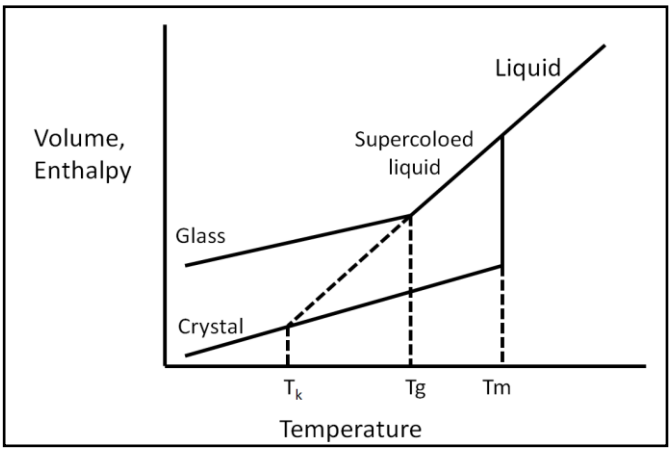

Figure 2.7 Schematic depiction of the variation of enthalpy (or volume) with temperature (Hancock and Zografi 1997)

The high internal energy and specific volume of an amorphous state can lead to an increased dissolution rate and enhanced bioavailability (Randall et al. 1995; Serajuddin 1999). Amorphous forms on the other hand although improve apparent dissolution rate of the poorly soluble drugs but are likely to be unstable and there are more chances of them re-crystallising into the stable crystalline form depending upon various factors like temperature, humidity, pressure and time (Yoshioka et al. 1994). To overcome this drawback, the solid dispersion (SD) approach has gained importance and received wide acceptance in the pharmaceutical industry.

2.3.1 Limitations of amorphous form

Glass transition temperature plays a pivotal role in understanding the stability of the amorphous system. By definition glass transition temperature is the temperature below which the solid form acts like glass, this term was extrapolated from polymer chemistry. Stability issues associated with amorphous systems arise due to the relaxation of the glass transition temperature, this happens due to a decrease in molecular mobility of the

molecules. The amorphous state is not generally preferred by the molecules and will tend to crystallise out the moment they receive the necessary energy to form bonds. Pharmaceutical stability is limited if the glass transition temperature of the API reaches below the environmental conditions due to various extraneous parameters such as temperature, pressure, hygroscopicity etc. This acts as a precursor for the molecules to form bonds and get converted into thermodynamically stable crystalline phase by releasing energy. Thus, the phase conversion remains a limiting factor during the formulation of pure amorphous systems; as there is always risk of conversion of amorphous form to crystalline form over the period of time.

2.3.2 Stabilisation of amorphous form

The dissolution rate of the amorphous form of an API is significantly higher than its crystalline counterpart, and thereby shows increased bioavailability. The amorphous material is easy to formulate into different dosage forms like tablets, capsules, freeze dried powders and gels than the crystalline material due to its high internal energy, increased mobility and compressibility. But the amorphous state is unstable and hence the molecules try to release the energy and recrystallize to a more stable crystalline form. Little change in temperature or humidity may largely affect the stability of the dosage form. Various pharmaceutical processes affect the final form of the drug.

2.4 Solid dispersion

To overcome the limitation of the amorphous state, an alternative strategy of solid dispersions (SD) is generally used. The strategy is to have molecular dispersion of the drug and the polymer (Figure 2.8) (Huang and Dai 2014). Solid dispersions can also be described as products formed by converting a fluid drug-carrier combination to solid state (Craig 2002). One of the key shortcomings of the amorphous forms is the low glass transition temperature. Solid dispersion overcomes this problem by incorporating the drug within an inert carrier with high glass transition temperature. This will in turn increase the glass transition temperature of the binary system and makes the final system more stable. Solid dispersions therefore provide an alternative approach to increase the dissolution rate of the drug in a system stable.

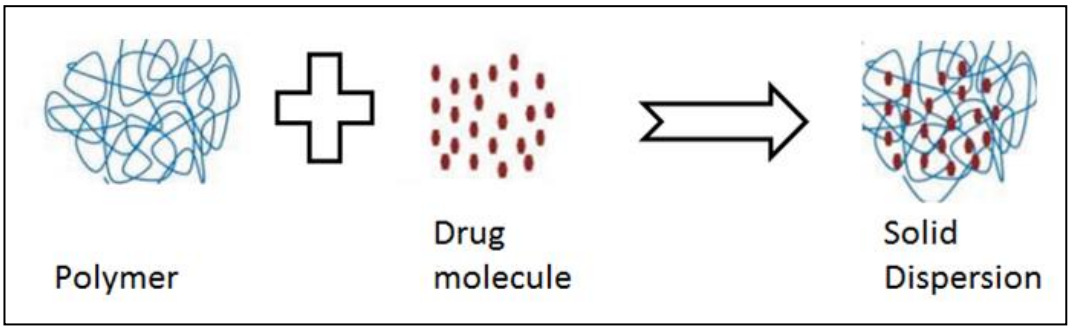

Figure 2.8 Overview of solid dispersion process (Kumar and Gupta 2013)

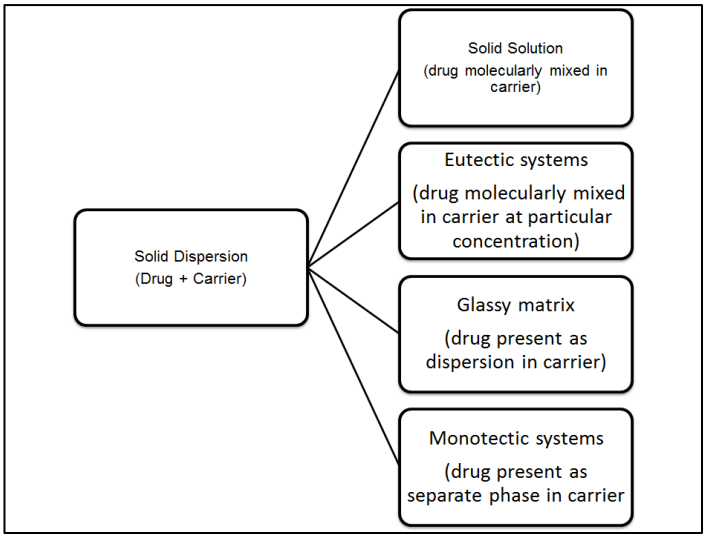

Figure 2.9 Types of solid dispersion (Craig 2002)

Another important aspect related to solid dispersions is the type of system that is formed. There are still some uncertainties regarding mechanism of formation of different types of solid dispersion. Currently, solid dispersions can be divided in to four types which vary in terms of its final product (Figure 2.9) (Craig 2002).

- Solid solutions are the type of solid dispersions where the drug is present as a molecular dispersion with the carrier. This type of solid dispersion is difficult to detect as most of the solid dispersions are molecularly mixed at lower concentrations. Since the drug is molecularly mixed within the polymer the stability of the solid dispersion is highest compared to other types of solid dispersion.
- Eutectic system is the type of solid dispersion in which the drug and carrier are uniformly mixed only at a particular concentration to form a solid dispersion. In this type of the system the melting point of the eutectic is below the melting point of both the drug and carrier alone (Nidhi et al. 2011).

- Glassy matrix systems are those where the drug is in dispersion within the carrier. These types of systems are commonly found in the semi-crystalline or amorphous polymers. It becomes difficult to predict the dispersion of drug whether it is in the crystalline or the amorphous domain of the polymer.
- Monotectic systems are basically those systems where the eutectic point and meting depression point of the solid dispersion is overlapping. In this type of systems the melting point of the carrier is unchanged in presence of the drug moiety

2.4.1 Factors affecting solubility of solid dispersions

Another interesting aspect regarding solid dispersions is the type of drug release through the drug-polymer matrix. Before moving onto the mechanism of drug release it is important to understand the factors affecting the apparent solubility of the drug in the particular form of solid dispersion. Several aspects are responsible for the increase in the apparent solubility of the drug.

1) Particle Size reduction: One of the reason for the increase in the dissolution rate of the API molecule in amorphous or solid dispersion form compared to the crystalline phase is reduction in particle size due to which the surface energy properties are enhanced. Particle size reduction will have a direct impact on the specific surface area exposed during dissolution which will in turn increase the drug release. Additionally, polymers used as carriers act as wetting agents and hence promote dissolution.

2) Increased apparent solubility or dissolution rate: Apparent solubility or dissolution rate increase depends on various reasons. It could be due to the increased solubility of the API solid dispersion because of complex formation as seen in the cyclodextrins type of complexes. Another reason could be the decrease in the degree of crystallinity having direct impact on the dissolution rate of the drug component.

Understanding the drug release mechanism is important while formulating solid dispersions. In binary systems such as solid dispersion, two types of release mechanism are possible namely carrier controlled dissolution and drug-controlled diffusion (Figure 2.10).

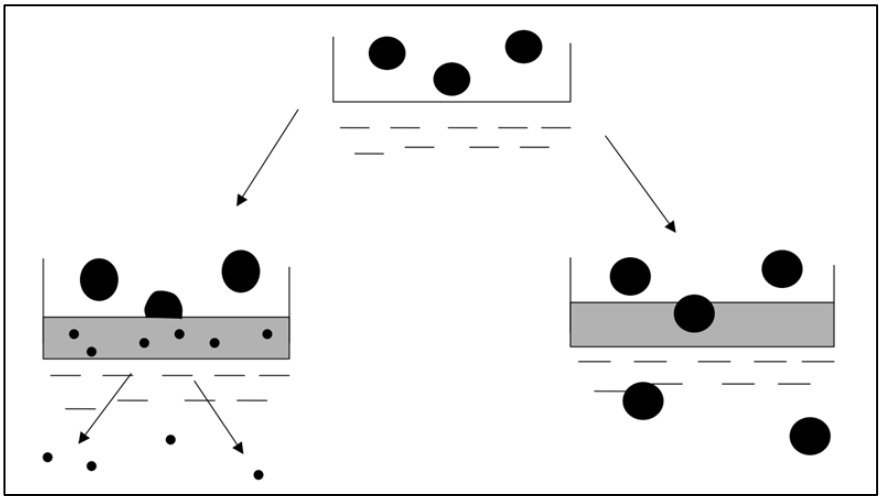

Figure 2.10 Drug release mechanisms during the dissolution process, carrier-controlled dissolution (left) and drug-controlled dissolution (right) (Craig 2002)

In carrier-controlled dissolution, the drug molecules dissolve in the diffusion layer dominated by polymer; and it will be slowly released either through erosion or swelling of the polymer. This type of phenomenon is generally seen in the solid dispersion with low drug loadings as they are molecularly mixed at low concentrations within the polymer.

In drug controlled dissolution, the polymer diffusion layer will be thin and the drug will be released as solid particles. Thus, the rate of the dissolution will be dependent on the physicochemical properties of the drug and not the polymer (Craig et al. 2001). Amorphous solid dispersions are normally considered as thermodynamically unstable but can be formulated and processed to adjust kinetic stability for the desired shelf life of 24-36 months. Ideally, a solid solution type is preferred as there is an absence of any entrapped free crystalline drug which can act as nuclei if the system receives some energy. There are several processes by which solid dispersions can be prepared (as shown in Figure 2.11).

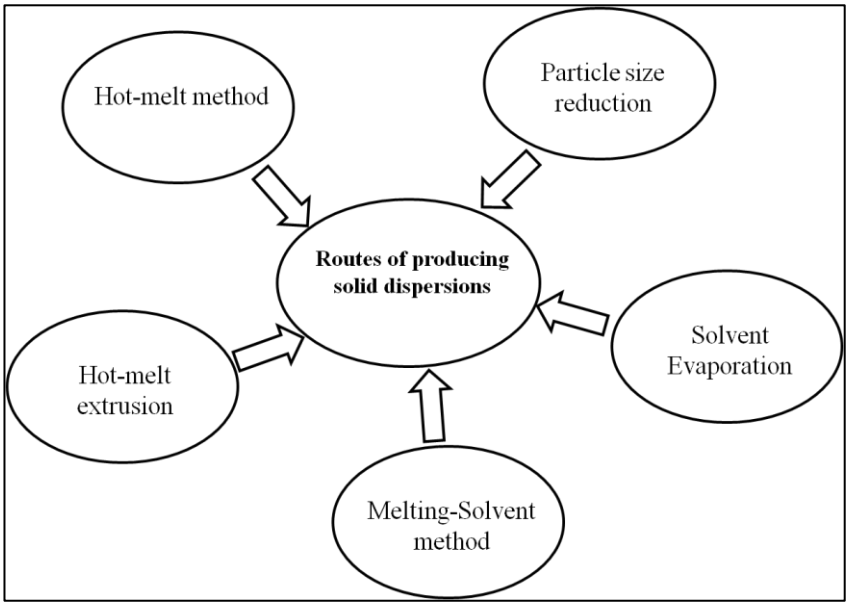

Figure 2.11 Routes of producing solid dispersions

2.4.2 Limitations of solid dispersions

Although Solid dispersions provide an attractive alternative to enhance the solubility/dissolution rate of poorly soluble APIs, however it has few limitations (Vasconcelos et al. 2007):

- Processes development and optimisation: The process to prepare solid dispersion requires stringent controls of temperature; solubility, miscibility etc. hence are not easy to develop and optimise.
- Repeatability and reproducibility: It is possible that products obtained can vary in surface properties and hence it is difficult to obtain a product in a reproducible manner.
- Solid and solution state stability: In the solid dispersion system there is always some change of the drug crystallisation. As drug is entrapped in the amorphous state (high energy state) and as soon as it receives sufficient energy from extraneous factors it crystallises out. However, this process also depends on the kinetics and use of suitable polymers/stabilisers can suppress this process.
- Selectivity: Not all drugs are suitable for solid dispersion technique due to several constraints. Thermo-labile drugs cannot be formulated using hot melt extrusion, and drugs with poor solubility in organic solvents can be processed using solvent evaporation technique.

2.5 Screening techniques for amorphisation

The methods used to convert crystalline forms of drugs into amorphous forms are categorised into two types

In the first type, the stable crystalline API or material is converted into an

unstable noncrystalline material form by quench cooling, melt amorphisation or through the rapid precipitation using spray drying. In the second type, transformation of crystalline material into amorphous form is mechanically performed through molecular disruption such as milling.

In the first type of mechanism, using the solubilisation or melting of API the crystalline properties are completely lost in the intermediate phase (which is a solution or melt phase); while in the second case the crystalline property is not lost completely due to incomplete loss of molecular arrangement. It should also be noted that amorphous material or solid dispersions prepared using different techniques may exhibit different physicochemical properties (Hancock and Zografi 1997). One of the example is of Simvastatin (BCS class II). When this API was cryo-milled it exhibited lower recrystallisation rate and low solubility compared to quench cooled samples (Yu 2001). Karmwar et al., reported that cryo-milled indomethacin exhibited low stability compared to the quench cooled amorphous form (Angell 1995; Saleki-Gerhardt et al. 1995; Dahan et al. 2009). The properties of amorphous material prepared using different techniques can be measured on a molecular level using solid-state NMR (ss-NMR) or tetrahertz spectroscopic tools (Karmwar et al. 2011; Otsuka et al. 2012).

Based on the annealing time and the route used to produce amorphous materials a term called “polyamorphism” has been derived. Polyamorphism is also described as the presence of different amorphous phases which are separated by first-order phase transition, and further investigation is needed to understand the complexity associated with this terminology (Angell 1988; Patterson et al. 2005). Besides, the possibility of the presence of different

phases of amorphous materials (polyamorphs), a new concept of Rigid Amorphous Fraction (RAF) has been derived based on the intermediate phase between crystalline and amorphous stage. The RAF phase in amorphous material is very closely associated with the crystalline phase thus the striking difference between the RAF and pure amorphous material is that, an amorphous material consisting of RAF phase will exhibit a very narrow change in the heat capacity (ΔC_p) and glass transition temperature T_g as compared to the same amorphous material without RAF (Craig et al. 2001).

2.5.1 Amorphisation- solution based techniques

2.5.1.1 Melting and quench cooling

This is a relatively simple and conventionally used technique to prepare amorphous material. In this technique the molten API is suddenly frozen below the freezing point of the materials using liquid nitrogen in a Dewar flask. DSC coupled with a chiller unit is also used to generate amorphous materials using the same principle.

The stability and purity of the amorphous material is based on the time needed to lower the temperature below the freezing point of the material. Sudden decrease in temperature results in the hindering of the molecular motion or rearrangement of the molecules, and hence upon cooling a significantly disordered state is obtained as the process of crystallisation is hindered. Slower rate of cooling provides longer time to the molecules for the configurational changes at a given temperature and hence enthalpy value of the end product varies from the starting material. Hence the rate of cooling should be optimised as material may crystallize out during this cooling step.

Thermal degradation of API and excipients is a major drawback using this approach (Angell 1988). The PXRD pattern of crystalline and amorphous Itraconazole (ITZ) is shown in Figure 2.12 and it highlights the difference in crystalline and amorphous phases of the drug. The crystalline ITZ is represented by characteristic PXRD peaks while the amorphous material domed shaped pattern is observed. Quench cooling or cryo-grinding for 30 min results in the loss of crystalline phase and disruption of the crystal lattice. The loss of peaks in the PXRD confirms the formation of amorphous phase (Engers et al. 2010). This approach has been successfully used to prepare amorphous forms of APIs and excipients (Liu et al. 2002).

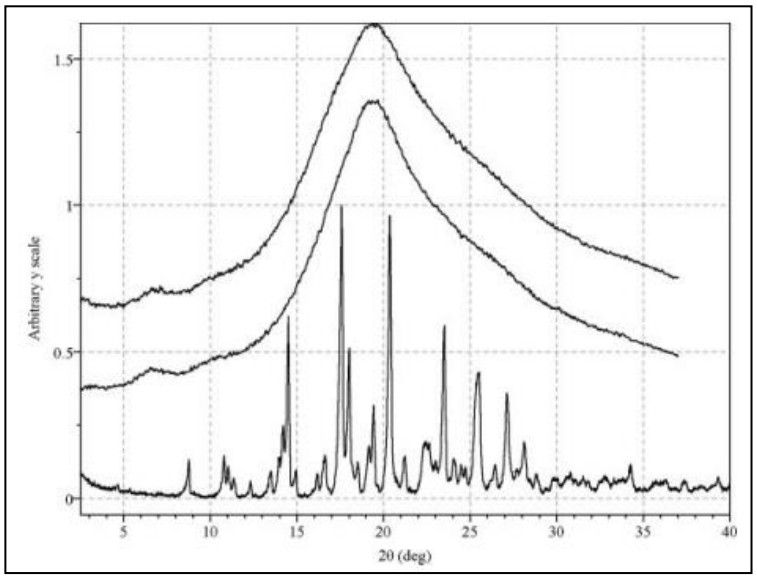

Figure 2.12 Overlay of PXRD pattern (top to bottom) of melt-quenched cooled Itraconazole (ITZ), cryo-ground ITZ and crystalline ITZ (Engers et al. 2010)

2.5.1.2 Spray drying

In this solution based approach, an amorphous material is prepared by solubilisation of an API into a suitable solvent followed by solvent evaporation. Amorphous material is produced either alone or in combination with excipients such as polymers. The important parameters to be considered to obtain stable amorphous material using this approach are feed rate, inlet/outlet temperature, concentration of solution, droplet size (atomiser rate) and drying temperature. Figure 2.13 schematically represents the spray drying setup and lists critical instrumental and process parameters to produce a desired end product (Chiou et al. 2008).

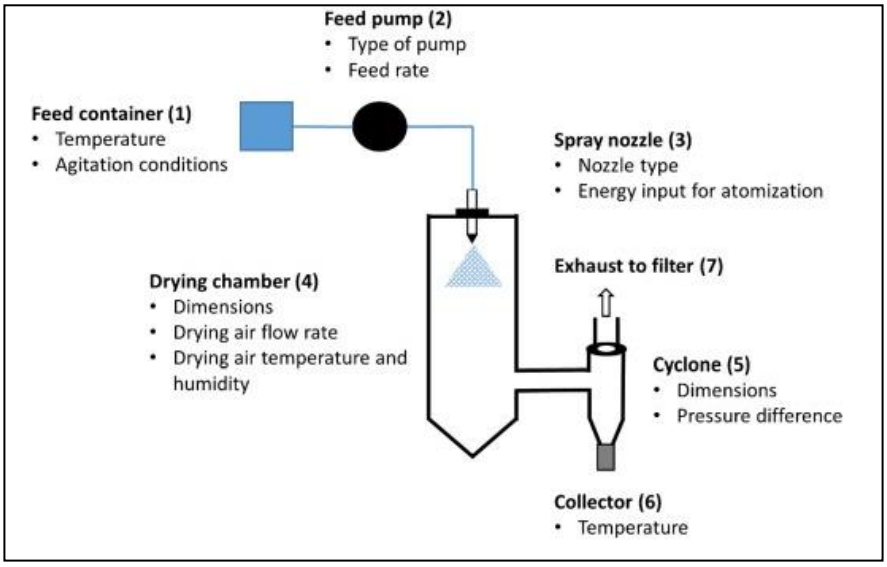

Figure 2.13 Schematic representation of spray drying setup and list of different parameters

In this technology, saturated solution, suspension or emulsion of API alone in combination of polymer/API solution is pumped to the atomiser device which leads to the formation of droplets. The chamber is heated using a hot air stream which leads to evaporation of the solvent when droplets come in

contact with the hot air stream. This results in the formation of dry mass which is suspended in the hot air stream. The crystallisation of the solid dispersion material within the spray dryer may occur in the liquid phase when the droplet is dried leading to an increase in the concentration of solute above its solubility limit, or in a solid amorphous state. The rate of solid-state crystallisation is based on the difference between the particle temperature and its T_g. The rate of solvent evaporation is an important factor which controls the extent of nucleation; higher solvent evaporation implies enhanced transfer of thermal energy per unit time to the solute molecule present in the droplet. Thus at higher solvent evaporation the solute component undergoes turbulent molecular motion and faster diffusion within the particle droplet which can prevent the formation of three-dimensional crystalline phase. Not all spray dried materials display the similar trend, an increase in the inlet air temperature to 134-210°C resulted in a higher degree of crystallinity for spray dried lactose (Chiou et al. 2008). This process could be challenging for drugs with relatively low T_g to obtain a stable amorphous material; as external temperature could be higher than the T_g and in such cases final product obtained may be a partly amorphous, super cooled rubbery mass as this type of rubbery material may be sticky in nature which ultimately affects the product recovery and thereby results in the poor process yield (Takeuchi et al. 1987; Broadhead et al. 1992; Takeuchi et al. 2004; Haque and Roos 2005). Spray drying is widely used in the pharmaceutical industry to produce amorphous materials.

2.5.1.3 Freeze drying

This technique is a sublimation process also called lyophilisation. It is a widely used technique in the pharmaceutical industries for the development of parenteral products where drying at low temperature is preferred (Liu 2006). In this approach, formation of water crystals (ice) occurs at low temperature and it is followed by sublimation of water vapour from the solid state at reduced pressure. Conversion of crystalline to amorphous state involves preparation of concentrated solution which is dried at low temperature and high pressure conditions. Based on the cooling rate, solutes from certain solutions may crystallise out during the freezing step. The solutes which do not crystallise get converted in to the amorphous phase due to a decrease in temperature below the individual transition temperature of maximally concentrated solute (Bhardwaj and Suryanarayanan 2012). At the end of the freeze-drying process the solvent is completely removed through sublimation, amorphous or partially amorphous material is formed. The transition temperature of the end product is determined based on the composition of the formulation and residual water content, which acts like a plasticiser lowering the T_g (O'Donnell and Woodward 2015).

2.5.1.4 Flash evaporation /Rotary evaporation

Solvent evaporation is the key limiting step which governs the stability of products such as solid dispersions. Heating of solvent mixtures may have an impact on the phase separation due to increased molecular mobility. Thus, vacuum dryer and rotary evaporators are preferred for solvent evaporation. These processes are carried out at moderate temperatures to restrict the

thermal degradation of the solid dispersions. A major disadvantage of these processes is that they are time-consuming and can act as precursor to phase separation of solid dispersion and the process is also not scalable (Bennett et al. 2015).

2.5.1.5 Supercritical fluid processing

In this process, supercritical carbon dioxide is used as a solvent system to solubilise the drug/mixture of drugs and excipients. The mixture is sprayed through a nozzle into an expansion vessel where low pressure conditions are maintained. The only difference between supercritical fluid processing and spray drying is the use of supercritical carbon dioxide to replace organic solvents. The rapid expansion and drying of materials leads to formation of amorphous materials or solid dispersions with different particle size distribution (Moneghini et al. 2001). The major drawback of this process is the difficulty in optimization of process parameters and selectivity of the solvent and drug component.

2.5.2 Amorphisation- Solid-state techniques

2.5.2.1 Dehydration of crystalline hydrates

This approach is reported as a simple and feasible route to obtain an amorphous phase of organic molecules (Saleki-Gerhardt et al. 1995). Hang *et al.*, reported the formation of the amorphous raffinose by heating raffinose pentahydrate at 60°C under vacuum conditions., The product obtained by this approach was similar to lyophilised raffinose (Li et al. 2000) They demonstrated the formation of amorphous carbamazepine by heating crystalline carbamazepine dihydrate at 45°C under a nitrogen environment.

The resultant amorphous state of carbamazepine undergoes glass transition at 56°C, which is higher than the drying temperature (45°C). Upon further heating at 86°C, the crystalline phase is crystallized out. Recently Hang Li *et al.*, has investigated the formation of the amorphous phase of crystalline polymorph of trehalose dihydrate upon dehydration (Li et al. 2000). Thus, dehydration of crystalline hydrates can be used as a potential route to amorphisation. Drying of crystalline hydrates of organic materials may impact the physical and chemical stability due to the loss of crystallinity

2.5.2.2 Milling

Milling is a widely used process for particle size reduction in the pharmaceutical industry (G.Cole; Parikh 2005). This process is also named grinding or comminution in the processing industries. Particle size reduction leads to an increase in the surface area of poorly soluble drugs and hence an increase in dissolution rate and bioavailability can be achieved (R.Liu 2008).

Milling instruments used in pharmaceutical processes can be divided into three categories based on the mechanism of energy transfer between the materials as follows: ball milling, shock action milling, and shear action milling. During the milling process, the materials undergo different deformations due to shear and stress conditions. Initially materials undergo elastic deformation followed by plastic and shear deformation and finally partially or completely amorphous materials can be obtained. Figure 2.14 below represents the milling process.

In the ball milling process, the energy transfer to the material subjected to micronization occurs through balls (milling bodies or impellers) where the materials are exposed to normal shear and stress conditions. In shear action

milling the material is ground by directly crushing with mechanical crushing elements. On the other hand, in case of shock action milling the energy is directly transferred to the materials; this occurs through collision of materials which leads to generation of heat and stress energy between the particles and enables them to undergo structural and configurational deformation.

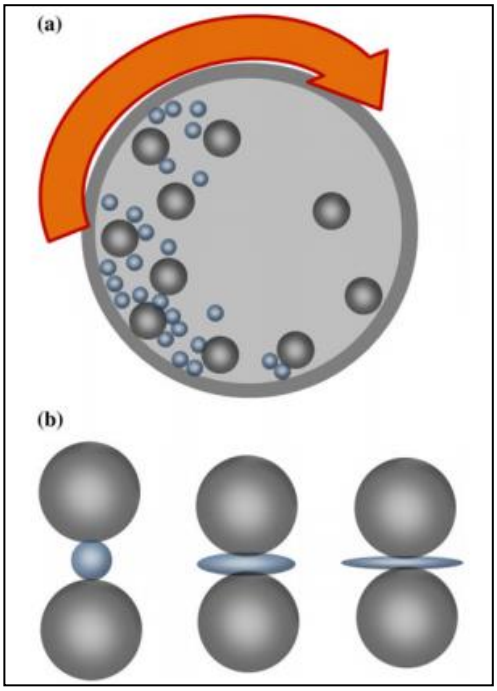

Figure 2.14 Schematic presentation of (a)milling process, (b)effect of milling on spherical particles (Jung et al. 2013)

Although the milling process is a widely used approach to reduce particle size, it is also accompanied by certain drawbacks. Milling results in unintended changes in morphology or crystal habit and crystallinity of materials (R.Liu 2008; Jung et al. 2013). It can also impact polymorphism and glass transition temperature as well as chemical stability of the milled material. Researchers have investigated the effect of temperature on milling, especially the relationship between the temperature of milling and T_g of the corresponding materials. It is postulated that, when cryo-milling is performed below the T_g of

the materials that the amorphous form is generated while operation at temperatures above the T_g results in polymorphic transformation (Willart et al. 2004; Willart et al. 2006; Descamps et al. 2007).

Co-milling:- In order to accelerate amorphization and solid state stability, drug and excipients are employed together in the co-milling process. Stable solid dispersions of indomethacin were produced by this process using polyvinylpyrrolidone or silica as an excipient (Dong et al. 2010).

2.5.2.3 Vacuum compression moulding

Film casting is one of the easiest methods used to prepare amorphous materials/solid dispersions. Film casting involves melting of the API-polymer mixtures above their eutectic point to form a solid dispersion upon cooling. API-polymer mixtures are fused together to form a miscible hot liquid, which is cooled down or solidified using different techniques.

This method benefits from being solvent free and is a quick way of preparing amorphous materials. A hot-press coupled with a vacuum chamber is used for this approach; amorphous materials are produced by varying temperature and pressure conditions as required. Samples are placed between a separating foil (PTFE coated glass fibre foil) and further subjected to temperature and pressure cycles where the sample material is melted and compressed to form an amorphous material. This technique is often implemented in the pharmaceutical industry to control the rheological properties of the amorphous material.

MeltPrep is an advanced version of the film casting process, where vacuum compression moulding (VCM) is used to prepare amorphous thermoplastic

specimens. This technique minimises heat pressure and mechanical stress to the solid materials and chances of degradation are lower. Figure 2.15 describes different settings and assembly of MeltPrep process (Treffer et al. 2015). Film casting is a method of choice for the feasibility studies; however it has some limitations as it could adversely affect the stability of the material. The major limitation of the technique is its suitability only for the drug-polymer combinations with acceptable solid state miscibility and solubility. It is not suitable for polymers with high melting point and molecular weight. Furthermore, solid state mixing of the blends is not easy and can result in phase separation.

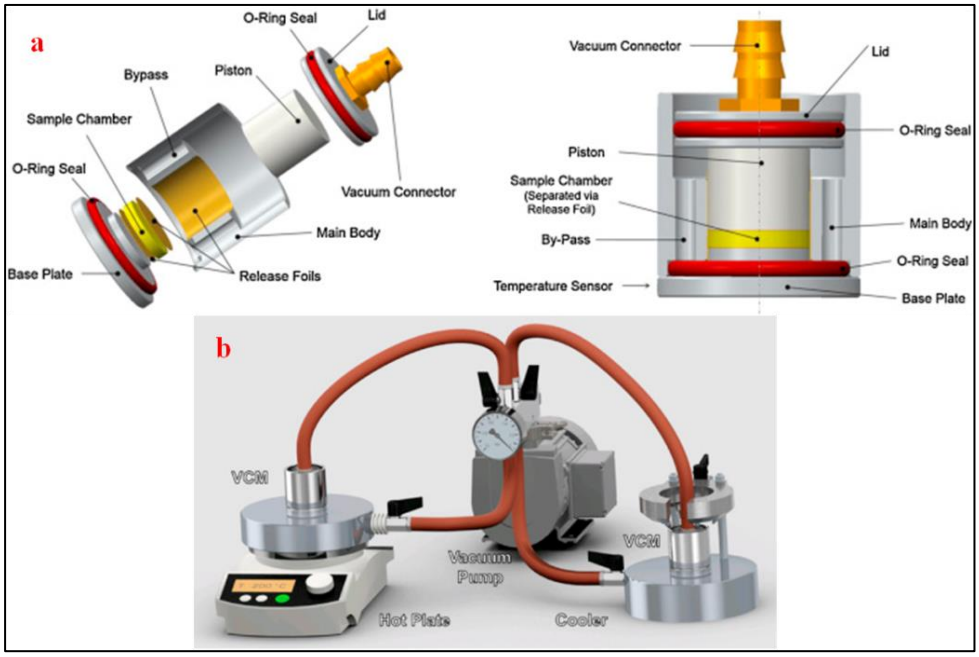

Figure 2.15 Description of different components of vacuum compression moulding VCM, b: Setup design of vacuum compression moulding -MeltPrep (Treffer et al. 2015)

2.6 Hot melt extrusion (HME)

Hot-melt extrusion (HME) is another widely used process for the amorphisation of the APIs. This technique is extensively used in plastics industry and gaining importance in the pharmaceutical industry to obtain different solid phases of drugs such as cocrystals, polymorphs, and amorphous solid dispersions. The hot melt extrusion process involves feeding the material (API or API/excipient) into the feeder using a rotating screw at high temperature to force the material through a die to form amorphous product (Qi et al. 2008). This process offers many advantages over other technologies, as it is a continuous, solvent free and scalable. In this process, drug moiety alone or in combination with excipients (especially polymer matrix) can be used to generate amorphous materials. In the HME process, the polymer acts as a solid solvent for the drug molecules to become miscible in the polymer matrix and generate amorphous solid dispersions. During the extrusion process, the molten polymer acts as a drug-depot or thermal binder to lower the transition temperature so that the process takes place at lower temperature and shear conditions (Crowley et al. 2007). Solid state mixing of the two or more ingredients may impact the success of the process significantly. In an ideal case, the drug should be molecularly dissolved within the polymer matrix to produce a solid solution. Often plasticisers are added to aid in the mixing process and to lower the T_g of the drug-polymer blend; this can also result in raising the softening temperature of the drug-polymer blend.

Two types of the extruders are used in the HME process ram extruders and screw extruders. In case of screw extrusion, rotating screws (single and twin screw) are placed inside a heated barrel; while in case of the latter extruder a

positive displacement capable of generating high pressure to push the material through the die is used. Figure 2.16 shows the schematic representation of twin screw extrusion process.

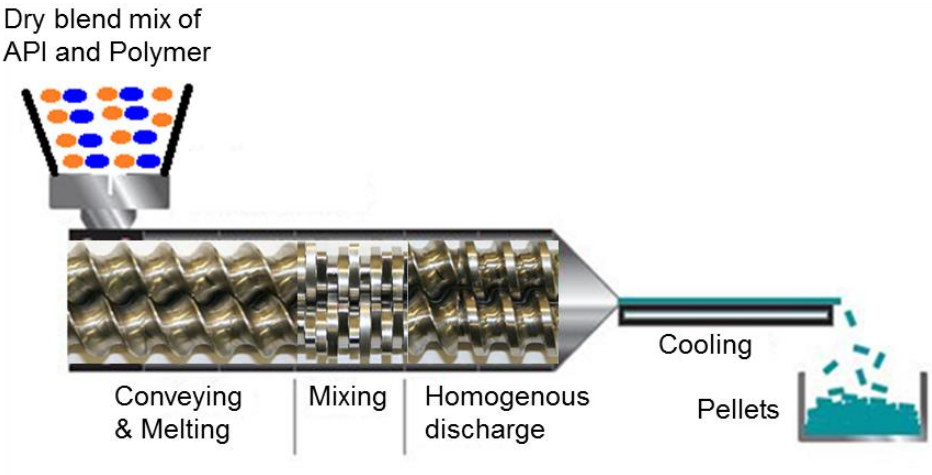

Figure 2.16 Schematic presentation of extrusion process in rotating screw extruder

2.6.1 Background and need in pharma

There is a long history of extrusion in the food and plastics industries. The first ram extruder was developed in 1845 in England by Henry Brewley and Richar Brooman for wire coating. Ram extruders are batch extruders and with growing demand for continuous processing, the single screw extruder was first patented by Mathew Grey in 1879 (Crowley et al. 2007). This lead to increase in the use of single screw extruders and by 1881 multiple extruders appeared in the market. The first counter rotating twin screw extruder appeared in 1916 (Herrmann 1972).

While using the ram extruder, material is placed in a heated cylinder; and once the material softens a ram (piston) pressurises the soft material through a die to produce materials with a desired shape (Perdikoulias and Dobbie 2003).

Major drawbacks of ram extrusion are lack of material homogeneity and poor temperature uniformity due to the limited melting capacity of the instrument.

Twin screw extrusion is most widely used design in pharmaceutical processing; it has several advantages over single screw extrusion such as easy material feeding, high kneading and dispersing capacities.

The extrusion process however was first applied in 1969 in pharmaceuticals by Rippie and Johnson (Rippie and Johnson 1969) where drug release was studied with respect to the effect of pellet geometry. Since then, there have been numerous studies reporting the use of HME in pharmaceutical formulations (Forster et al. 2001; Patterson et al. 2005; Dong et al. 2008; Maniruzzaman et al. 2012).

Many conventional pharmaceutical processing techniques had major drawback of increased solvent use. Solvents are prone to be harmful for the human consumption hence most of the regulatory bodies have set limits for commonly used solvents. Especially for amorphous formulations, solvent entrapped during processing can act as a precursor for recrystallisation of the API. Hot melt extrusion provides an attractive alternative single-step green technology for pharmaceutical development. The versatility of HME is explained in Figure 2.17. Solubility enhancement is achieved by using HME for preparation of solid dispersion.

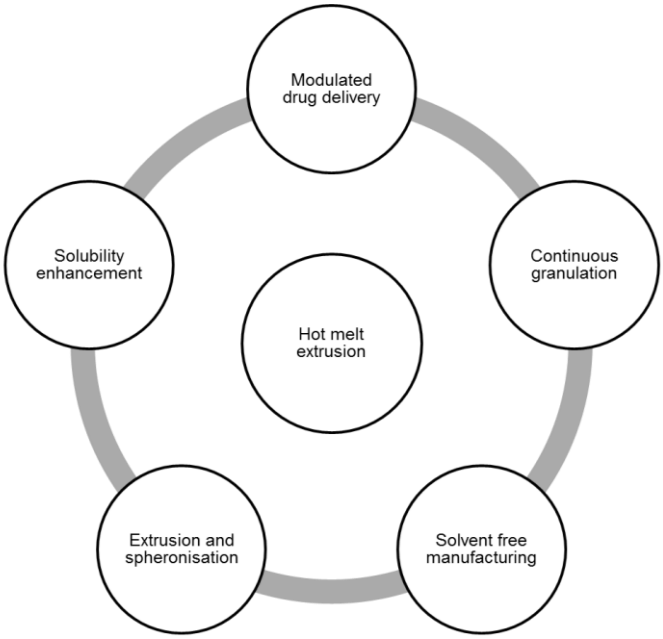

Figure 2.17 Applications for HME in pharma industry

Although first use of HME in pharma was reported in 1969, it took many years to consider HME as a viable process for product development. This can be correlated with the slow emergence of solid dispersion as strategy and linked to the lack of approved polymers suitable for HME. This is highlighted by the relative lack of approved products in the market prepared by HME. A few commercially marketed products can be seen in Table 2.1 (Shah et al. 2013; Patil et al. 2016).

Product name	**Treatment**	**HME purpose**	**Company**
Lacrisert® (Opthalmic Insert)	Dry eye syndrome	Shaped system	Merck
Resulin®	Hyperglycemia	Oral IR tablet	Parke-Davis
Zoladex™ (Goserelin Acetate Injectable Implant)	Prostate cancer	Shaped system	AstraZeneca
Implanon® (Etonogestrel Implant)	Contraceptive	Shaped system	Organon

Gris-PEG (Griseofulvin)	Anti-fungal	Crystalline dispersion	Pedinol Pharmacal Inc.
NuvaRing® (Etonogestrel, Ethinyl Estradiol depot system)	Contraceptive	Shaped system	Merck
Norvir® (Ritonavir)	Anti-viral (HIV)	Amorphous dispersion	Abbott Laboratories
Kaletra® (Ritonavir/Lopinavir)	Anti-viral (HIV)	Amorphous dispersion	Abbott Laboratories
Eucreas® (Vildagliptin/Metformin HCl)	Diabetes	Melt granulation	Novartis
Zithromax® (Azythromycin enteric-coated multiparticulates)	Anti-biotic	Melt congeal	Pfizer
Orzurdex® (Dexamethasone Implantable Device)	Macular edema	Shaped system	Allergan
Fenoglide™ (Fenofibrate)	Dyslipidemia	MeltDose® (solid dispersion)	Life Cycle Pharma
Anacetrapib (Discontinued)	Atherosclerosis	Amorphous dispersion	Merck
Posaconazole	Antifungal	Amorphous dispersion	Merck

Table 2.1 Marketed products of HME

Lacrisert® was one of the first marketed ophthalmic insert prepared using HME. It was prepared and manufactured by Merck in 1981 using hydrophilic polymer hydroxypropyl cellulose (HPC). Although, the first insert was approved in 1981, it took pharmaceutical industry sixteen years to come up with conventional solid tablet using HME. In 1997, Parke-Davis prepared and manufactured Resulin®. It is an oral immediate release tablet where troglitazone API used to lower insulin level was used along povidone as

polymer of choice. Since then, a lot of pharmaceutical companies started evaluating HME as an alternate process for preparation of solid dispersions. A contraceptive vaginal ring was with ethinyl estradiol and etonorgestrel was prepared and manufactured by Merck. Coaxial fibres were prepared using hot melt extrusion using ethylene vinylacetate as polymer. Abbott laboratories came up with first drug combination tablets prepared using HME. Kaletra® which contained lopinavir and ritonavir as APIs was prepared and manufactured using copovidone as polymer to make an immediate release oral tablet. Pfizer came up with targeted enteric coated multi particulates Zithromax®. Azythromycin was the API used as an antibiotic was extruded using hydrophilic polymer HPMC. In 2013, Merck prepared and manufactured Noxafil. Noxafil® contains posaconazole and uses hypromellose acetate succinate (HPMCAS) to form amorphous solid dispersion using HME. The extrudates formed are further milled and other excipients were added to form oral tablets which were enteric coated for immediate drug release in small intestine. Detailed history about Noxafil® will be discussed in chapter 6.

Although, with shrinkage of NCE market and growing generic competition pharmaceutical companies have finally started acknowledging HME as an alternate choice. More drug candidates in pipeline are checked for its feasibility with HME. Additionally, polymer companies are conducting extensive research with already pharmaceutical approved polymers and preparing similar monomer analogues which would be suitable for HME processing.

2.6.2 Mechanism of Hot Melt Extrusion

In HME, the drug/API is homogenously mixed with the polymer and melted in eutectic proportions to form a uniform dissolved state or softened phase which is then passed through a die to form extrudes (Qi et al. 2008).

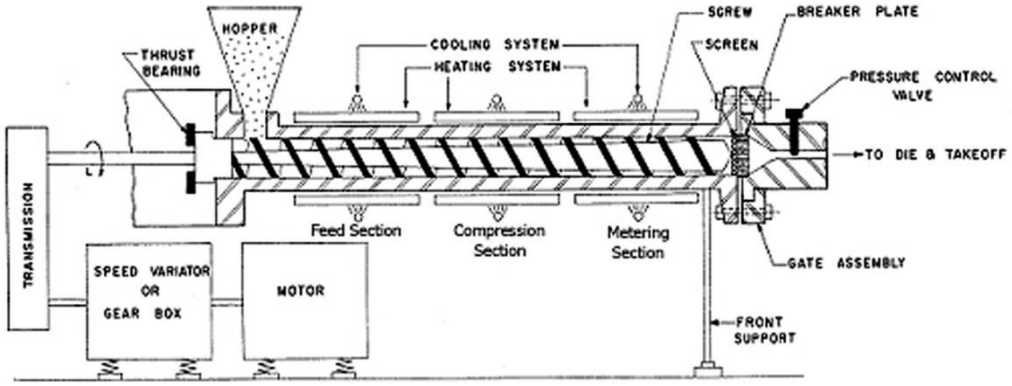

Figure 2.18 Typical Hot Melt Extrusion Process (Michael M. Crowley 2007).

Solid state mixing is pre-requisite for a robust HME process. In HME, polymer acts as a solid solvent for the drug molecules. In an ideal case, the drug should be molecularly dissolved within the polymer matrix to give rise to solid dispersion solution. Sometimes to aid this mixing, plasticisers are used. Alternatively, plasticisers are used to lower the glass transition temperature of the drug-polymer blend and/or raise the softening temperature of the drug-polymer blend. The crystal lattice energy of the crystalline material must be exceeded to form a stable amorphous material. Furthermore, the drug and excipients (polymer component) must be blended and co-dispersed subsequently. This step is performed in the extrusion process by applying shear stress to both the components. The crystal lattice energy is exceeded because of the temperature and energy generated due to the friction through

shear stress ; it further leads to softening of the polymer matrices. Rotating screws and various kneading elements lead to the desired amorphisation; and precise selection of process parameters as well as drug-excipient combination leads to formation of the stable amorphous solid dispersion (K.Kolter 2012).

A typical extruder can either have a single screw or twin screw conveyor (Figure 2.18 and 2.19). Twin-screw extruder have several advantages like easier material feeding, high kneading, dispersing capacities, less tendency to over-heat and decrease in residence time over single screw extruder. Depending on the orientation of the screws, shear and mixing can be varied. The screws are the main components of HME and along with temperature are responsible for formulation of solid dispersion in a single continuous process. Generally, dimensions of screws are given by L/D ratio i.e. length of the screw divided by the diameter. Typically, the screw configuration ranges from 20 to 40:1 in L/D ratio (Michael M. Crowley 2007). Screw configuration is assembled using various elements of the screw which are responsible for feeding, mixing, compression and metering. The screws are thus further classified into two types of elements; conveying and kneading elements (Figure 2.20) (Dhumal et al. 2010). Typically, kneading elements are responsible for adding more shears to the process and are further classified as 30°, 60° and 90°. Conveying elements are responsible for pushing the mixture ahead towards the discharge. Orientation of the kneading elements governs the shear rate and uniform mixing of the melt (Dhumal et al. 2010). Table 2.2 outlines the application of the screw elements. A combination of the conveying and kneading elements is one of the critical parameters for HME. Each screw element has certain advantages either in conveying or mixing. A certain

combination of these can help serve the purpose of shear and mixing depending on the need for the drug-polymer blend mixing for the HME.

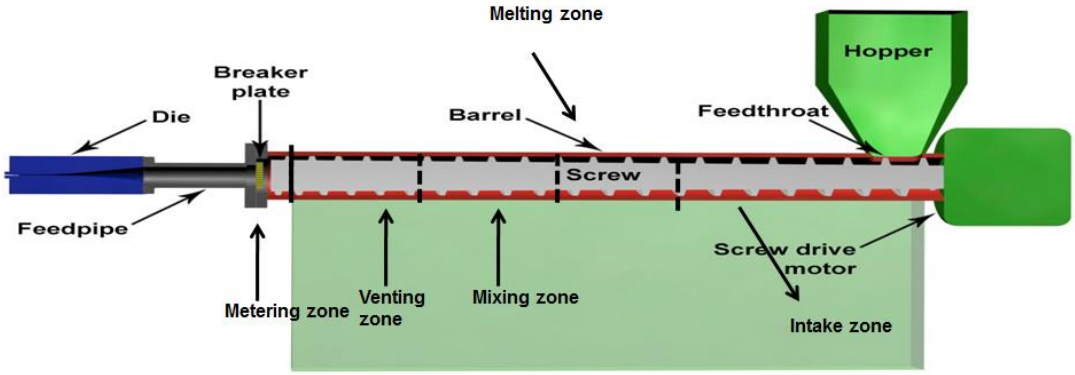

Figure 2.19 Schematic Diagram of twin screw extruder

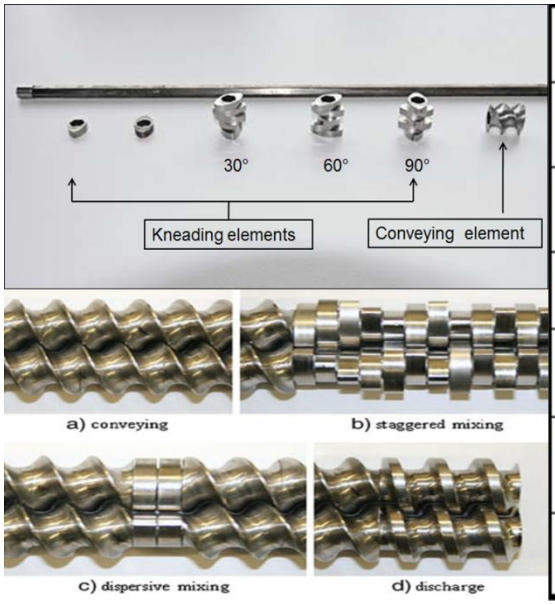

	CONVEYING	MIXING
Feed Screws	++++++++	+
30 deg Forward	+++++	++
60 deg Forward	++++	+++++
90 deg Alternate	zero	++++++++
60 deg Reverse	- - - -	++++++
Reverse Feed Screw	- - - - - - - -	++

Figure 2.20 Configuration of Twin screws (Top left), screw elements (Right), and mixing zones (Bottom left) (Dhumal et al. 2010)

Conveying elements	Kneading elements
	
Profiles with open chambers ➢ In the feeding sections ➢ For melt exchange ➢ For degassing (venting)	➢To introduce shear energy to the extruded materials
Profiles with closed chambers ➢For high pressure build-up	➢The elements are arranged in different offset angles (30°, 60° and 90°) used for ➢ Plasticizing ➢ Mixing ➢ Dispersing

Table 2.2 Application of screw elements (Daurio et al. 2014)

The hot melt extruder can be divided into four zones viz. (Daurio et al. 2014)

1. Feed: Input materials are placed in the feed either as a physical mixture of the drug and polymer or are placed separately in the feed.

2. Melting zone: Predominately, this screw orientation in the zone is made up of only conveying elements. Temperature for this zone should be kept according to the melt of the physical mixture of the drug and polymer.

3. Mixing Zone: This is the most important zone. The type of solid dispersion formed is dependent on the uniform mixing of the melt. Screw configuration of this zone consists of only kneading element (Figure 2.20). Orientation of the kneading elements governs the type and texture of the solid dispersion product.

4. Homogeneous Discharge: If a uniform solid dispersion melt mix or eutectic mix is formed in the mixing zone then discharge zone is responsible for conveying of the melt. The screw configuration of this zone consists of only metering elements. Additionally, this zone is responsible for uniformly passing the mix through die to produce the extrudates.

2.6.3 Selection of drug candidate

Despite the various advantages offered by HME, it still remains a niche technique for certain type of drugs. There are certain aspects related to the drug properties which need to be taken in to consideration before proceeding with the HME formulation strategy. Figure 2.21 outlines the typical properties which the drug candidate must have to be considered for HME.

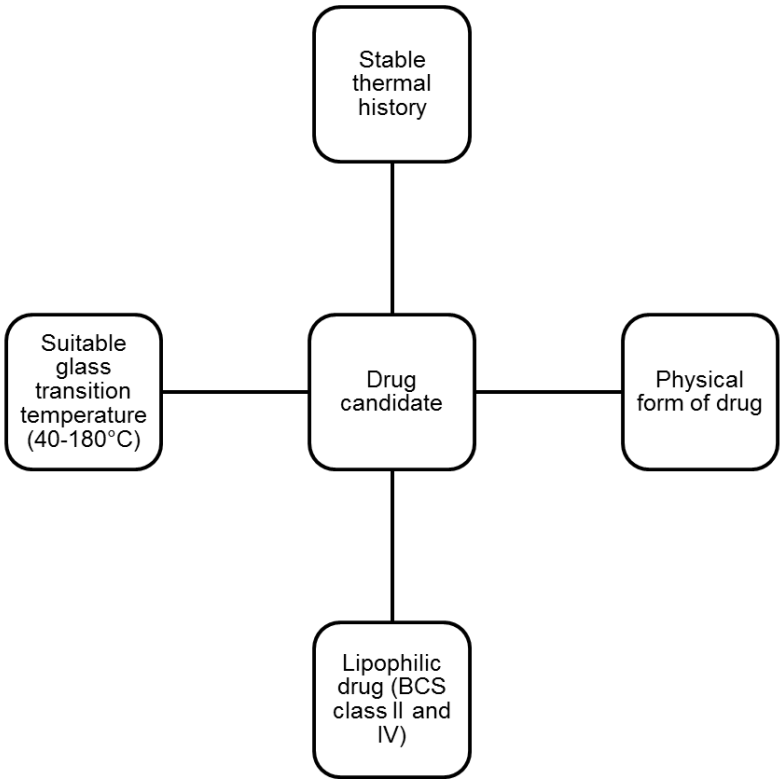

Figure 2.21 Selection of drug candidate for HME (Michael M. Crowley 2007)

Hence, HME can be selected as a formulation strategy provided the drug candidate does not melt with degradation, have suitable glass transition temperature, is not a pseudo-polymorph and is lipophilic in nature.

2.6.4 Polymer selection for HME

One of the main reasons for the slow uptake of HME in the pharmaceutical industry is the selection of polymer. Not many polymers typically used in the

Pharma industry were specifically developed for HME. Most them were prepared for the conventional process like granulation, roller compaction etc. The role of polymer as excipients can be outlined as follows:

1. Polymer needs to act as a solvent or co-solvent.
2. They should have a solubilising or wetting effect.
3. Should exhibit thermoplastic behaviour.
4. Should have weak to strong interactions with the API.
5. Should offer wide range of glass transition temperatures.
6. Offer a broad range of dissolution behaviours.

Thermoplastic properties for the polymer are summarised in table 2.3

Suitable Tg	45 – 180°C.
High thermal stability	45 – 180°C
Low hygroscopicity	prevents crystallization
No toxicity	application of large amounts possible
High or no solubilization capability	thermodynamically stable formulation

Table 2.3 Selection of Polymer for HME

2.6.5 Pre-formulation and characterisation

Due to its selectivity, there is a need for deeper understanding of drug and polymer of choice. Thus this makes pre-formulation studies for HME important. There are two main challenges for extrusion chemical stability of the drug substance and physical stability of the drug substance.

1. Chemical stability of drug substance:

Stability of the drug in consideration should be closely monitored during HME as it is typically carried out at elevated temperatures. Degradation of the drug thus poses a serious threat in consideration of HME as a formulation strategy. Degradation can occur by three mechanism hydrolysis, solvolysis and oxidation (Michael M. Crowley 2007). For hydrolysis and solvolysis to take place, the presence of water or solvent is needed. Since HME is a solvent free technology, hydrolysis and solvolysis generally are not the most likely mechanisms for degradation. On the other hand, oxidation which is a free-radical chain reaction is reported to cause significant degradation during HME. Formation of peroxides of the drug and polymer during extrusion can have a direct effect on the chemical stability of the product and thus decrease its potency. Addition of antioxidants have been shown to significantly decrease the oxidation phenomenon but that means inclusion of an excipient in the binary solid system to make it ternary which can affect the miscibility and solubility of the product.

2. Physical stability of drug substance

In HME the drug and polymer are subjected to elevated temperatures, which increase solubility between the drug and polymer. The drug either melts and

mixes with the polymer or solubilises within the polymer matrix to for solid dispersion. Re-crystallisation of the drug can occur upon cooling of the extrudate. Thus, studying solid state solubility and miscibility becomes important for prediction of the stability of the solid dispersion. DSC and DMA are the techniques of choice which are proven to detect glass transition temperature of the solid dispersion and help in determination and confirmation of the miscibility of the drug within the polymer. Confirmation of the concentration of the drug within the solid dispersion can be carried out by chromatographic techniques. Table 2.4 provides an overview of the pre-formulation studies along with characterisation techniques needed for HME (Sarode et al. 2013; Tian et al. 2013):

Parameters	**Characterisation technique**	**Potential Outcome**
Glass Transition	DSC, DMA	Miscibility determination and type of solid dispersion prediction
Solubility Parameter	Van Krevelen and Hoftyzer's solubility parameters	Solubility predictions for eutectic mixture.
Fragility index	DSC	Understanding the type of glass formed by the drug
Solid State Characterisation	DSC,TGA, XRD, Raman, FTIR, Viscometers, SEM and Solid State NMR	Form confirmation, Raw materials characterisations and solid dispersion confirmations
Miscibility Predictions	Fox Equation or Gordon-Taylor Equation	Miscibility prediction of the solid dispersion
Related substance	HPLC, UPLC and TGA	Determination of Impurity levels
In-vitro Dissolution	Dissolution Apparatus	Dissolution profiling

Table 2.4 Pre-formulation studies along with characterisation techniques needed for HME

2.6.7 Process analytical technology (PAT)

According to the revised FDA's process analytical technology (PAT) guidance, ICH Q8, Q8 (R2), Q9 and Q10 guidelines, it is mandatory to provide the robustness of the process by providing a design space according to the Quality by Design (QbD) concept (Wu et al. 2011). In QbD concept, the impact of the raw materials and processing parameters on the critical quality attributes (CQA) of the products needs to be studied and demonstrated (Wu et al. 2011). Pharmaceutical processes are generally not univariate in nature and hence have a lot of critical factors/variables for consideration (Wu et al. 2011). For formation of a robust design space, understanding the impact of all the critical factors affecting the critical quality attributes (CQA) is of utmost importance. Following Fig 2.22 lists down the typical variables in HME process which have a significant impact on the critical quality attributes (CQA) of the HME products.

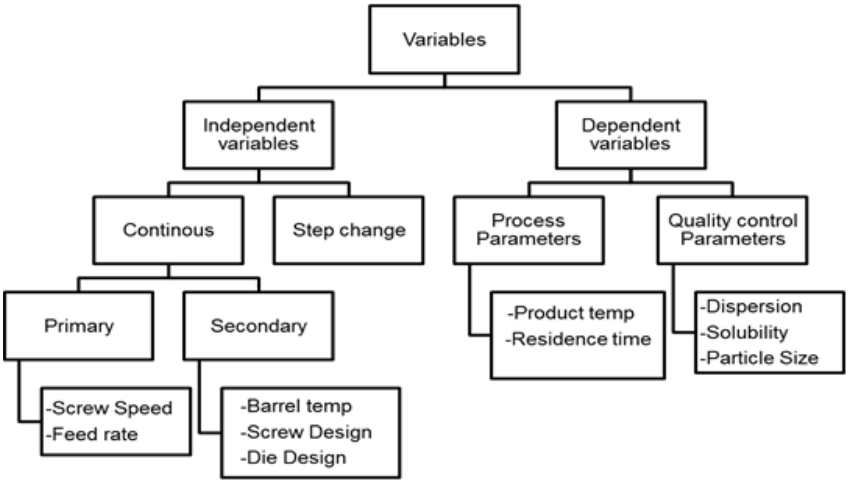

Figure 2.22 Typical process variables of HME affecting Critical Quality Attributes (Vigh et al. 2014)

Independent variables are those which have a direct impact on the critical quality attributes of the product. Dependent variables are those which can be considered as responses to the independent variables (Montgomery 2000). For understanding the effect of critical process parameters on the critical quality attributes, design of experiments or multivariate analysis is carried out. Depending on the criticality, level of the factorial design is fixed (Montgomery 2000). A full factorial design provides insight on effect of single parameter as well as interaction between parameters.

Process analytical technology (PAT) is defined by US FDA as mechanism to design, analyse, and control pharmaceutical manufacturing processes via measurement of critical process parameters that affect critical quality attributes (Patil et al. 2016). Ultimate goal of PAT is to select and develop methods which will help in complete understanding of the HME process and provide data to track consistent quality of the product. For determination of the design space, on-line, in-line and at-line monitoring of the process using non-destructive tools like spectroscopic probes are used which helps in understanding the uniformity of the process by providing data for statistical evaluation (Wu et al. 2011). This helps in understanding the critical process parameters (CPP) and forming of a robust design space. At-line measurements are the ones where sample is removed from the process and analysed. On-line measurements are those where sample is removed for analysis and re-circulated back in the manufacturing process after analysis. In-line measurements provide near-real time data and sample is analysed by invasive or non-invasive techniques within the process.

Due to recent advances and stringent regulations PAT has gained much attention and application in pharmaceutical industry (Wahl et al. 2013; Hitzer et al. 2017; Repka et al. 2018). Kelly et al. studied real time measurement of melt rheology to track the API within polymer matrix during HME (Kelly et al. 2018). Critical process parameters of HME were investigated using in-line responses of torque, shear and extensional rheometry (Kelly 1997; Köster and Thommes 2010; Aho et al. 2015; Aho et al. 2016). However, these PAT tools are important when there is solid state insolubility between drug and polymer.

Drug degradation and solid state purity are two main critical quality attributes during HME which can have a direct impact on the product performance. Hence, tracking of these attributes through non-invasive spectroscopic tools is on the rise (Troup and Georgakis 2013; Wahl et al. 2013). Several studies have been reported about use of NIR and Raman spectroscopy as PAT tools of choice for HME (Tumuluri et al. 2008; De Beer et al. 2011). Non-invasive spectroscopic studies were also used for investigation of drug-polymer interactions and quantifications (Saerens et al. 2011; Saerens et al. 2012; Martínez et al. 2013). API quantification, solid state tracking and purity were also monitored using NIR and Raman spectroscopy (Saerens et al. 2014; Vigh et al. 2014; Netchacovitch et al. 2015; Netchacovitch et al. 2017; Park et al. 2017). Apart from the conventional uses, non-invasive spectroscopic techniques were also used for confirmation of co-crystals and solid-state transformation (Kelly et al. 2012; Islam et al. 2015; Van Renterghem et al. 2017a). Another important process variable is mean residence time (MRT) which will be discussed in chapter 5.2.

2.6.7 Advantages of HME

HME provides an attractive alternative green technology process for formulation of poorly soluble drugs. Advantages include:

1. Improved solubility of many drug substances (BCS class II and IV).
2. Drug release retardation possible.
3. Uniform mixing.
4. Fewer processing steps.
5. Continuous processing/ High throughput.
6. No solvents required-no drying step required.
7. Short residence time.

2.6.8 Challenges and Shortcomings

Although there are a lot of positives for formulating poorly soluble drugs using HME, there are some shortcomings as well (Shah et al. 2013):

1. Not viable for thermolabile materials (drug/polymer).
2. Limited number of polymers available.
3. Typically limited to drug loading NMT 40 %.
4. Thermodynamically unstable.
5. Potential for polymorphic transition (conversion of forms of drug).

2.6.9 Summary

Hot Melt Extrusion (HME) provides an attractive alternative single-step green technology for pharmaceutical development. However, the process is selective in nature and requires a lot of process optimisation. To overcome this, there is a great need for profound understanding of the drug and polymer of interest. Recent advances in its suitability have led a lot of major pharmaceutical drug makers to invest heavily in its research and development with currently more than 10 pharmaceutical products in the market. This process also benefits from being PAT enabled with use of invasive and non-invasive analytical tools and products can be manufactured with QbD approach. However, HME has its fair share of shortcomings of elevated processing temperatures, drug loading, degradation, thermolabile drugs and availability of limited number of suitable approved polymers. Products obtained by HME are generally intermediate products and requires downstream processing to form into final product. Additionally, processing parameters will have a direct effect on the properties of the finished products. Therefore, HME was selected to study the impact of the material and process attributes on critical quality attributes of amorphous solid dispersion products obtained using hot melt extrusion.

Chapter 3: Materials and Methods

A detailed explanation of materials and methods is provided in this chapter. The rationale for selection of the materials is explained. Methods will be further classified according to pre-formulation, processing, and characterisation techniques. The section also includes brief details about the principles and software of the different characterisation instruments used.

3.1 Materials

Ibuprofen was procured from Medex UK. Affinisol^{TM}HPMC 100cP and 4M were provided as gift samples by DOW chemicals. Posaconazole was supplied by the funding partner Merck & Co., Inc. as a gift sample.

3.2 Methods

3.2.1 Preformulation and characterisation of polymer, API and co-former properties

This section briefly describes the applicative principles of the analytical instruments used in Preformulation. Preformulation studies provide a deep understanding of the physicochemical properties of materials used during formulation and try to provide an overview of the challenges arising during the actual formulation process.

3.2.1.1 Thermo-analytical instruments

3.2.1.1.1 Differential Scanning Calorimetry (DSC)

Thermal analysis is one of the prominent approaches to characterise pharmaceutical solids, semisolids, amorphous material, crystalline solids etc. DSC is one of the thermal tools which is used to investigate phase behaviour

of pharmaceutical solids including the quantification of amorphous solid materials (Newman et al. 2008). Based on the design of the instrument, experimental conditions and measuring parameters, varied range of methodologies can be implemented to analyse the sample. Among them are DSC, modulated temperature DSC (MTDSC) and high-speed DSC (HSDSC) (Nollenberger et al. 2009). Conventional DSC works on the principle of linear temperature heating rate. In MTDSC apart from the temperature heating rate, a small temperature modulation is done to enhance the sensitivity of detecting a small amorphous fraction of crystalline materials. In newly developed, hyper or high-speed DSC the temperature modulation can be controlled by fast heating and cooling rates of 50-500° min^{-1}. Hyper-DSC due to increasing the heating scan rate leads to higher heat flux which makes easy to analyse most of the amorphous materials by displaying glass transition temperature with increased sensitivity and less time. This property is lacking in conventional DSC instrument.

DSC runs were performed using TA Q.2000 and TA discovery DSC. Standard aluminum pans were used. Around 2-5mg of the sample was weighed in the standard aluminum pans and was crimped with a pinhole aluminum lid. Samples were run at the heating rate of 10°C/min up to just before the reported degradation of the samples. Additionally, samples were run from -60°C up to melting for detection of glass transition events. Modulated DSC was run to confirm the events observed and to affirm the same. For fragility studies, samples were run with varying heating rate in a Heat-Cool-Heat cycle. Melting point depression studies were carried out at a heating rate of 2°C/min. Thermograms generated was analysed using TA universal software. Both TA

Q.2000 and TA discovery DSC are typical Heat flux DSC (Figure 3.1). These consist of a sample and a reference disc respectively. Standard aluminum pans crimped with aluminum lids containing the sample are placed on the sample disc whilst an empty pan is placed on the reference disc. Both the discs are connected to the thermocouples which are connected to a power unit. Any deflection observed due to solid state changes in the sample pan provides a change in the baseline which is recorded as a function of temperature.

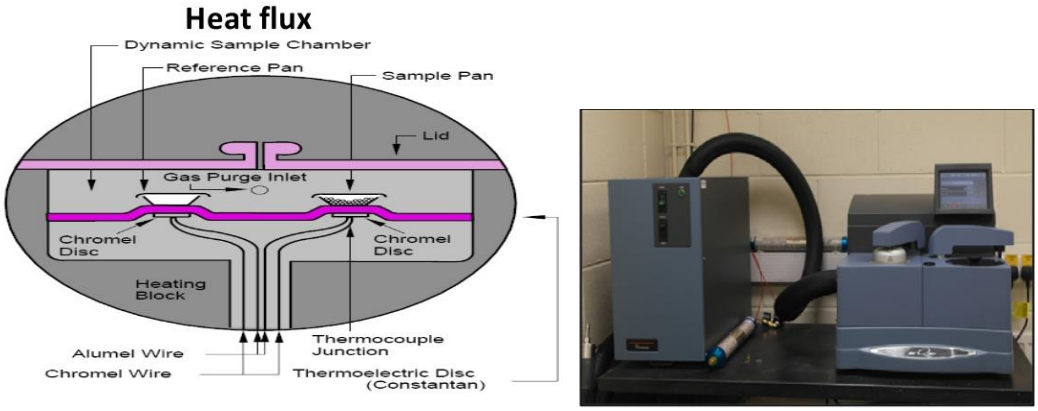

Figure 3.1 Typical Heat Flux DSC (left) and TA Q2000 DSC (right)

One of the key parameters in DSC is the heating rate. A slow heating rate is advised for increasing the resolution while faster heating rates can aid in separation of events or can help to skim any re-crystallisation events. In this study, a heating rate of 10°C/min was used as melting of the compound was of interest and that would not vary with respect to heating rate.

Typically, events observed in DSC are either exothermic or endothermic in nature. For this study, the interest will be for the glass transition temperature and melting temperature events.

3.2.1.1.2 Thermo Gravimetric Analyser (TGA)

TGA runs were carried out using TA Q.5000 TGA and Discovery TGA (Figure 3.2). Samples were placed in platinum pans which were previously tared in TGA. Samples were run up to 500°C with a heating rate of 10°C/min. TGA runs were analysed using TA universal analysis software. TGA works on the principle of recording change in mass as a function of temperature. The reference and sample platinum pans are connected to a microbalance which records changes in the sample. Mass loss occurs either due to water/solvent loss and/or degradation. These two events are typically seen in pharmaceutical powders. The focus for this study was to find out the degradation temperature of polymers used so as to fine-tune them for hot melt extrusion.

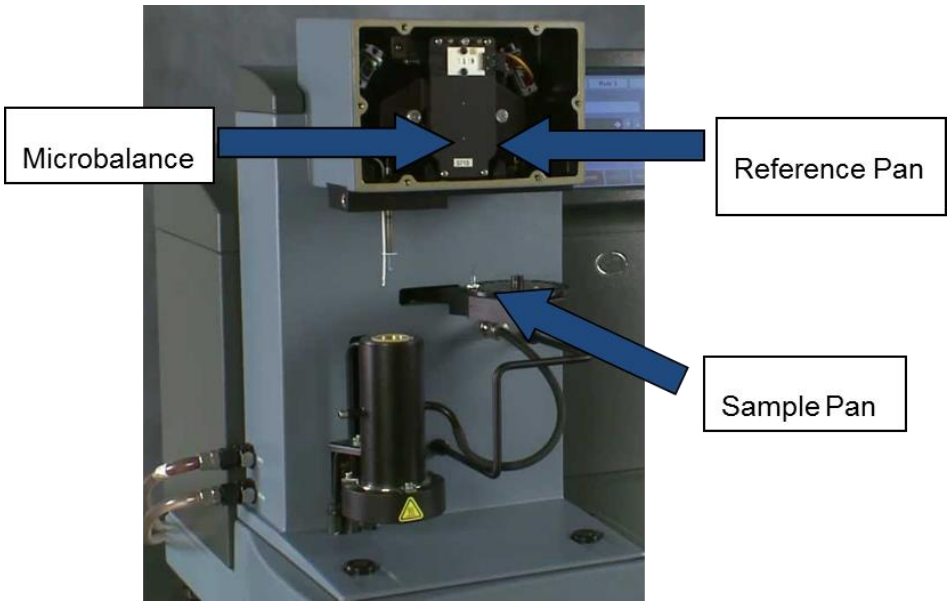

Figure 3.2 TA Q.5000 TGA

3.2.1.2 Vibrational Spectroscopy

Unlike crystalline materials, amorphous solids do not exhibit orientation and positional long-range crystal order in all three-dimensional space. However, molecular association characterised by the short-range order can occur in amorphous materials. Vibrational spectroscopy techniques like Raman spectroscopy, near-infrared (NIR), mid-Infra-red (IR) and recently Terahertz pulsed spectroscopy (TPS) have exhibited promising results in characterising pharmaceutical amorphous materials in pharmaceutical settings. These techniques have gained importance as they can investigate molecular assemblies of amorphous solids; it is non-destructive, fast and require little sample preparation.

3.2.1.2.1 Mid-infrared spectroscopy

Based on the type of pharmaceutical solids analysed, MID-IR spectroscopy can show significant spectral variation between crystalline and amorphous phases of the sample, thus this technique is also used for quantification of crystalline content, as the intensity of the vibrational bands correlates directly with the presence of the concentration of concerned phase. The amorphous phase of pharmaceutical solids exhibit different IR spectra in comparison with the crystalline phase of the similar sample. The difference in the IR spectra can be attributed to the presence of a wider range of conformations typically in amorphous solids, which normally leads to the presence of different intermolecular interactions and broader peaks compared to crystalline solid. When performing quantification studies, firstly identification of characteristic crystalline peaks which is independent of crystal state of the sample needs to

be identifed and then based on the intensity compared with the reference peak, degree of crystallinity can be determined.

Fourier transform infrared (FTIR) spectra of the samples were acquired using a Thermo-Scientific Nicolet iS50 FTIR spectrophotometer equipped with a single reflection diamond attenuated total reflection (ATR) module. Around 2-5mg of the sample was placed on the ATR and clamped to avoid spaces between holder and sample. Spectra were recorded in absorbance mode from 4000 cm^{-1} to 400 cm^{-1} at 4 cm^{-1} resolution, and averaged over 64 scans. Total scan time was 1 min 35 secs.

3.2.1.2.2 Raman spectroscopy

The process of inelastic light scattering is referred as Raman radiations and was first reported by Raman and Krishnan in 1928. When samples are irradiated with a beam of monochromatic light, most of the scattered energy consists of energy derived from the incident frequency (Rayleigh scattering). In addition, minor amount of photons accompanied with shift is observed. The fraction of photon energy scattered from the center of the sample which consists of less energy before interaction is called Stokes scattering. Both IR and Raman spectroscopy works on the principle of measurement of molecular rotational and vibrational energy. However, in case of Raman, the requirement of vibrational energy is not related to change in the dipole moment (in case of IR) but it is associated with the change in polarisation of molecules (Vankeirsbilck et al. 2002). It probes the molecular property, and changes in the solid phase of the material are inferred by a change in the molecular environment and molecular conformation. The difference in the solid-state

properties can be seen by the subtle changes in the spectral position and intensity.

Two types of Raman spectrometers were primarily used namely Dispersive Raman & Raman Mapping.

Figure 3.3 DXR Dispersive Raman (left) and DXRi Raman Microscope (right)

In Dispersive Raman, DXR Dispersive Raman of Thermo Scientific was used (Figure 3.3). The laser of 780nm wavelength and 50mW power was used. Aperture was 50μm slit to get the estimated area spot size of 3.1μm. Samples were either placed in glass vials (for powder samples) or were placed as it is (for extrudates) on the sampling plate. Samples were exposed for 30 sec to the laser and 64 scans were collected within the spectral range of 50-3360 cm^{-1}. Total time of collection was 33 mins.

For Raman Mapping, DXRi Raman Microscope of Thermo Scientific was used (Figure 3.3). The laser of 780nm wavelength and 24mW power was used. Aperture was 50μm slit to get the estimated image pixel size of 70μm using 10X objective lens. Fine flat sections of samples were placed on aluminum slide. Samples were exposed for 3 sec to the laser and 5 scans were collected within the spectral range of 50-3360 cm^{-1}. Total time of collection varied from 16mins to 1 hr 7mins.

Spectra and images were analysed for both Dispersive Raman and Raman Mapping using TQ Analyst and OMNICXi software respectively.

To confirm the spectral regions for amorphous ibuprofen and posaconazole, DSC coupled with Raman probe was used (Figure 3.4). A Renishaw Raman probe of the laser of 780nm wavelength and 17.8mW power was used. Aperture was 25μm slit to get the estimated image pixel size of 70μm using 10X objective lens. Samples were exposed for 2 sec to the laser and 3 scans were collected within the spectral range of 100-2000 cm^{-1}.

Figure 3.4 DSC-coupled with Raman probe

3.2.1.3 Hygroscopicity Studies

DVS experiments were carried out using DVS intrinsic from SMS (Figure 3.5). Samples were weighed in the previously tared aluminum pan and were enclosed in the DVS chamber within the instrument. A humidity cycle from

0%RH to 90%RH with a step change of 10% was set. Desorption cycle from with similar parameters was carried out. Step change to next humidity condition happens when the difference between ratios of change in mass with time was less than 0.002%.

Figure 3.5 DVS intrinsic

DVS works on a similar principle as TGA but the main difference is that the change in mass is recorded as a function of humidity. The experiment is run at isothermal temperatures typically 25°C. For humidity generation a mixture of water vapour and nitrogen gas is used. DVS was used to provide an overview of the water uptake capability of the polymers, API and the extrudates prepared.

3.2.1.4 X-Ray Diffraction

X-ray powder diffraction is a powerful non-destructive technique for analysis of the crystalline structure and atomic spacing of different materials. In 1912, Max Von Laue and Co. proposed that a crystalline substance is made up of a three-dimensional structure which is diffracted by the X-ray wavelength according to the arrangement of the crystal planes or crystal lattice (Bunaciu

et al. 2015). In this XRD technique, a cathode source is used to generate monochromatic radiations, scattered to concentrate and focus towards the particular sample material. These X-ray diffractions are generated by the constructive interference of monochromatic X-rays and crystalline samples. The X-ray radiations are directed towards the sample region the interactions of the incident rays with the sample materials generate interference when Bragg's Law is satisfied. Below figure 3.6 represents a schematic representation of Bragg's Law reflection (Bunaciu et al. 2015).

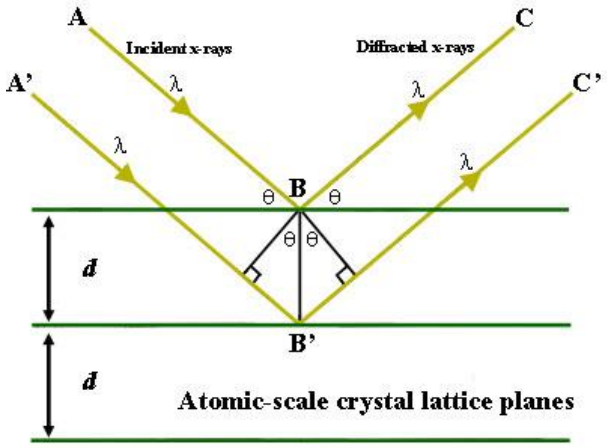

Figure 3.6 *Bragg's Law: X-ray diffraction path exhibit an interference when the distance between path ABC and A'B'C' differs by an integer wavelength number* (Eby 2004).

X-ray diffractometer consists of three basic components, X-ray cathode tube, sample holder, and detector. To understand the working of XRD, consider the crystal lattice planar distance of a crystal sample is d, where the difference between the path length between the path ABC and A'B'C' is an integer multiple of wavelength (λ). When X-ray is incident on the crystalline sample then each planar phase of the sample will undergo individual refraction with a unique angle (θ), constructive interference takes place in a combination of

particular wavelength, lattice spacing (d) and angle of incidence (θ) (Eby 2004). The general relationship between wavelength of X-rays, planar distance and angle of incidence is known as Bragg's Law, expressed as : ($n\lambda = 2dsin\theta$), where n is an integer, λ- wavelength of X-rays, d- is the interplanar spacing produced due to diffraction and θ is the interplanar diffraction angle. By analysing the sample through a particular angle 2θ, the sample will undergo diffraction in all possible directions based on the planar phase arrangement of solid material and conversion of these diffracted peaks to d-spacing allows us to investigate the crystalline properties of the unknown sample. Basically more finely ground samples will display all the possible orientations when analysed as most of the planes come in contact with the rays. According to Smith, the powder X-ray diffraction experiments can be conducted in two different ways: automated X-ray diffraction analysis yielding digital computer output and Debye-Sherer diffractometer providing analogue film output. Both these instruments provide the diffraction intensities beam as a function of angle of diffraction. The collected theta degree is processed using the Rietveld method to minimise the bad signals or function by using non-linear algorithms.

X-ray scattering of the samples was acquired using a SAXSspace from Anton Paar Austria. The samples were placed on the stainless steel sample holder and sealed with transparent film. The distance between sample and detector was 112mm and the intensity I (q) was monitored at a wavelength of 0.15418nm. An XYZ stage was used for auto-recognition of the sample stages. A fast read-out detector (Pilatus 100K-S) was used with the total acquisition of 20 frames with an exposure time of 60 secs and data was analyzed using

SAXSdrive™ software. The scattering vector q range was used to calculate 2Θ values ($q = 4\pi/\lambda \sin\theta$, where $\lambda = 0.15418nm$) (Pauw 2014; Kimanius et al. 2015; Li et al. 2016a).

3.2.1.5 Theoretical considerations

3.2.1.5.1 Solubility Parameters

The term solubility corresponds to the dissolution of one component into another to form a single phase. The term solubility, when extended to solid state solubility of a compound within a polymer purely, depends on the chemical structures of both compounds and their cohesive properties. Thus solid state solubility of these materials can be predicted based on their similarity of the solubility parameters (Tian et al. 2013) (P. Sakellariou 1986).

The concept of solubility parameter basically works on two principle properties cohesive energy density and molar volume. Cohesive energy density is the energy required for any molecule to free it up from its neighbouring molecule (Cowie 1968). Molar volume refers to the volume occupied by the fragments of the compound in contention.

Hildebrand and Hansen were considered pioneers in this area. Hildebrand's method focused on the dispersion forces between two solutions while Hansen's method along with the dispersion forces took into considerations the interactions between polar groups and hydrogen bond capacity (Hansen 1999).

Thus, solubility parameter (δ) is the first initial step of theoretically predicting the miscibility between drug and the polymer based on the measurement of the cohesive energy density (David J. Greenhalgh 1999) (Verhoeven et al.

2008). Cohesive energy density comprises of all the inter-intra-atomic and molecular interactions and types of bonds with the molecules. The method chosen was the Van Krevelen and Hoftyzer's group contribution method (δ MPa1/2) (Adamska and Voelkel 2005).

$$\delta^2 = (\delta_d)^2 + (\delta_p)^2 + (\delta_h)^2 \qquad \text{Equation 3.1}$$

Where

$$\delta_d = \Sigma F_{di}/V \quad \delta_p = (\sqrt{\Sigma F^2_{pi}})/V \quad \delta_h = \sqrt{(\Sigma E_{di}/V)} \qquad \text{Equation 3.2}$$

δ is the total solubility parameter, δd is the contribution from dispersion forces, δp is the contribution from polar forces, δh is the contribution from hydrogen bonding, Fdi is the molar attraction constant due to the dispersion component, Fpi is the molar attraction constant due to the polar component, Ehi is the hydrogen bonding energy, and V is the molar volume (Van Krevelen 1990). The solubility parameter is measured in $MPa^{1/2}$. When the difference between the total solubility of drug and polymer i.e. Δδ is less than 7 $MPa^{1/2}$ then they are considered to be miscible whereas above 10 $MPa^{1/2}$ predicts immiscibility (Forster et al. 2001) (David J. Greenhalgh 1999); (Garekani et al. 2001).

Solubility parameters were calculated using Van Krevelen and Hoftzyer's group contribution method. Molecular weight and density of the API and polymers were calculated using ACD Chemsketch software. Since the Affinisol monomer structure was unavailable, HPMC structure was used.

3.2.1.5.2 Fragility Index

One of the critical parameters from the viewpoint of stabilisation of the amorphous form is the glass transition temperature (T_g). T_g is considered as the most important factor in prediction of the stability of the ASDs and provides

an indication of its molecular mobility. Below T_g the molecule behaves like a glass which in turn suggests a decrease in its molecular mobility and thus protects molecular conformation from collapsing.

Thus glasses can be explained as a combination of mechanistic strength of crystals and spatial uniformity of liquids in amorphous materials. These are formed by cooling of liquids and considered as non-equilibrium solids (Angell 1988; Angell 1991). Glasses of small molecules typically used in pharmaceutical industries as APIs are brittle in nature and easily fractured. This can lead to free surfaces which promote crystallisation. From HME point of view, identification of glass transition temperature (T_g) is one of the critical parameters for consideration for the selection of the drug/polymer candidates. T_g plays a significant role in the stability of the products of solid dispersions. Hence, it is important to understand the ability and type of glass formed by the drug/polymers of interest. This will in turn help in understanding the molecular mobility offered by the drugs/polymer of choice in its amorphous state.

The glass is obtained due to the structural relaxation within the molecule of an amorphous or a crystalline material. This structural relaxation is a direct function of its cooling rates and kinetics (Baird and Taylor 2012). The ability of the compound to form a glass is determined by a factor called as the fragility parameter which is calculated by determining the glass transition temperature (T_g) as a function of cooling rate. This concept of fragility parameter and categorising them into different types of glasses was first conceived by Angell in 1991. The classification of types of glasses was further divided into fragile or strong glasses (Angell 1991). It is proven to an extent that the fragility parameter can be co-related to its molecular mobility.

The fragility of a compound is considered to be the energy during the structural relaxation of the material when cooled under its glass transition temperature. For a generation of glass transition of Ibuprofen with varying cooling rates, DSC was used. The activation energy (ΔH) of the materials can be correlated with the glass transition temperature obtained by varying the cooling rates. The activation energy (ΔH) for the material in consideration is the one near or at its T_g value (Borde et al.). For the current study, the following equations were used for calculation of the fragility parameter

m= ΔH / (2.303$*R*Tg$) Equation 3.3

$d$ln (Q) / d (1/Tg) = ΔH / R Equation 3.4

Where R is the ideal gas constant, and Q is the cooling rate from DSC.

The fragility parameters for IBU and POSA was quantified using DSC at cooling rates of 1, 2, 5, 10, 12 16, 18 and 20 °C/min respectively. Equation 2 was utilised and a plot of ln (Q) against 1/Tg was produced – the slope of the line being utilised to calculate ΔH/ R for the crystalline components. ΔH/ R value obtained was replaced by the equation 3.3 to calculate the fragility parameter (m). If the fragility parameter values of m is < 70 and m is> 100 indicates formation of strong and fragile glass respectively (Borde et al.).

3.2.1.5.2 Theoretical Binary Phase Diagram

Melting point depression approach

Flory-Huggins polymer solution theory proposes the drug-polymer temperature-composition phase diagram by understanding the interaction parameter χ between the drug-polymer and its change with temperature (Tian

et al. 2015). This can be achieved by using melting point depression data to predict χ by using Equation 3.5: (Lin and Huang 2010; Huang et al. 2016)

$$\frac{1}{T_m} - \frac{1}{T_{mo}} = -\frac{R}{\Delta H}[log\ \phi_{drug} + \phi_{poly}\left(1 - \frac{1}{m}\right) + \chi\phi_{poly}^{2}] \qquad \text{Equation 3.5}$$

Where $m = [(\text{Mol wt\_poly}/\text{Density\_poly})/(\text{Mol wt\_drug}/\text{Density\_drug})]$

T_m and T_{mo} are the melting points of the drug-polymer blend and pure drug respectively, ϕ is the volume fraction of the components. ΔH and R denote enthalpy of fusion and the gas constant respectively.

χ is a function of temperature which can be empirically described by Equation 3.6:

$$\chi = A + B/T \qquad \text{Equation 3.6}$$

Where A is the entropic contribution and B is enthalpy contribution of the system.(Lin and Huang 2010; Huang et al. 2016)

Prediction of spinodal curve

According to the Flory–Huggins theory, the free energy of mixing for a drug-polymer solid dispersion can be described by Equation 3.7:

$$\Delta G_{mix} = RT[\phi_{\text{drug}} \log \phi_{drug} + \frac{\phi_{\text{poly}}}{\text{m}} \log \phi_{poly} + \chi\, \phi_{\text{drug}}\phi_{\text{poly}}] \qquad \text{Equation 3.7}$$

The second derivative of ΔG_{mix} for at different temperature will give the spinodal curve.

Theoretical glass transition temperature calculation by Fox equation

Researchers often co-relate the extent of plasticisation based on T_g values of polymeric blends. Generally, values of T_g reduce with increase in plasticiser concentration and a plot of T_g of polymeric blend against concentration of

plasticiser yields a relationship which determines the plasticisation efficiency. Such a relationship can also be obtained theoretically by use of the Fox equation.(Lin and Huang 2010)

$$1/T_g mixture = \left(w_1/T_{g1}\right) + \left(w_2/T_{g2}\right) \quad \text{Equation 3.8}$$

where w_1 & w_2 are weight fractions while T_{g1} & T_{g2} are the glass transition temperatures of drug and polymer respectively.

3.2.1.6 Melt Rheology

3.2.1.6.1 Rotational rheometer

All rotational rheological testing was carried out using a Physica MCR 501 rheometer (Anton Paar, Austria) with parallel plate geometry (diameter 25mm) and gap size of 1mm. For each test, polymeric sample films were used. Three sets of oscillatory tests: a strain amplitude test, frequency sweep test, and time sweep tests were carried out.

• Amplitude Sweep (AS)

For the identification of Linear Visco-elastic region (LVR) amplitude sweep was carried out at a constant angular frequency of 10 rad/sec. The prepared films were subjected to the extrusion temperature used to generate the extrudates for determination of LVR. The samples were subjected to % strains from 0.01%-100%. The linear viscoelastic regions (LVER) was calculated from the straight line of G' and G'' until it deviates and taken into consideration for frequency sweep tests.

• Frequency sweep (FS)

Frequency sweep (FS) was carried out at constant %strain of 0.1% for all the samples. To check the G' & G'' over a range of frequency at a constant temperature, the samples were subjected to angular frequency ranges of 100 rad/sec to 0.1 rad/sec respectively. All the %IBU-Affinisol^{TM}HPMC 100cP films were carried out at the temperature at which these blends were extruded and two temperatures below. The aim was to have common temperatures between the varying samples of %IBU-Affinisol^{TM}HPMC 100cP for comparison.

• Time sweep (TS)

The degradation of samples as a function of time was measured using time sweep tests at low shear rates. This test was performed to study the viscosity of polymers over 30mins at a specific temperature, at fixed strain (0.1%) and at a fixed frequency (10 Hz). All the %IBU-Affinisol^{TM}HPMC 100cP films were carried out at the temperature at which these blends were extruded and two temperatures below.

3.2.1.6.2 Capillary rheometer

A constant shear rate test using twin-bore capillary rheometer was employed. Pellets of the extrudates were dried in an oven at 30°C for 24 hours prior to testing. Rosand RH10 capillary rheometer, Malvern Instruments Ltd, was used for the capillary rheometer studies. It was mounted with 30,000 psi (Long die) and 10,000 psi (short die) pressure transducers and were calibrated and allowed to stabilize before every run. Temperatures were controlled within ± 0.5 °C of the set values and monitored by platinum resistance thermometers fitted in the three (top, middle, and bottom) zones of the barrel. The pellets

were fed into both barrels and manually compressed before the test was started. They were subjected to two-stage of the pre-compression pressure of 0.6 & 0.3 MPa, for a total pre-heating time of 540 seconds. The experiment was run in an 8-stage discrete speed program (Table 3.1) and the material was passed through 2 dies having dimensions of 2.0 mm diameter with 20.0 mm (long die) and 0.25mm (zero length die, short die) of length. The shear rate values mentioned were calculated by software upon fixing the 8-stage discrete speed program.

Stage number	Piston speed (mm/min)	Wall shear rate (/s)
1	5.31	19.90
2	8.39	31.47
3	13.37	50.13
4	21.19	79.47
5	33.54	125.78
6	53.15	199.30
7	84.17	315.65
8	133.35	500.05

Table 3.1 Steady shear rate test stages

3.2.2 Processing studies

3.2.2.1 Ibuprofen-Affinisol^{TM}HPMC HME studies

For extrusion experiments, Pharma Lab 16mm of Thermo Scientific UK with screw length to diameter ratio of 40:1 was used (Figure 3.7). Gravimetric twin-screw feeder (Brabender, Germany) was used for the auto-feeding of the blends. Feeder calibration for all the IBU-Affinisol^{TM}HPMC blends was carried out. A feed rate of 0.4Kg/hr was kept constant for all the studies except for the

DOE study. Residence time was recorded using an in-line UV-vis spectrophotometer probe and data was recorded using LabVIEW program. Extrudates from the extruder were air-cooled and were either pelletised or were kept as such for storage.

Figure 3.7 Pharmalab 16 HME

3.2.2.1.1 Screw configuration and screw speeds

One of the critical process factors in formulation development using HME is the residence time. Residence time depends mainly on the feed rate, screw configuration, and speed. All the IBU-Affinisol^{TM}HPMC trials except for the DOE study were carried out at one single type of screw configuration having an increased mixing zone which imparts high mixing and kneading (Figure 3.8 and table 3.2). Screw speed for all the trials apart from the DOE study was kept constant at 100rpm.

Length (D)*	Element type
28	Forwarding
2.25	30°
1.25	60°
1	90°
6	Forwarding
1.5	Discharge

Table 3.2 Type 4 Screw configuration used for extrusion

Figure 3.8 Screw configuration used for extrusion

3.2.2.1.2 Temperature profile and zones

IBU-Affinisol^{TM}HPMC 100cP blends with varying drug loadings were processed at different temperatures profiles. The Pharmalab 16mm extruder has 10 different zones starting from zone 1 till zone 10. The mixing section is located from zone 7 till 9 and was followed by discharge elements in zone 10 and die. Typical temperature profile zones for all the trials are shown in table 3.3:

Temperature profile	Zones								
	2	3	4	5	6	7	8	9	Die
Affinisol^{TM}HPMC 100cP	40	60	90	110	180	180	180	180	180
10% IBU load	40	60	90	110	170	170	170	170	170
15% IBU load	40	60	90	110	170	170	170	170	170
20% IBU load	40	60	90	110	160	160	160	160	160
30% IBU load	40	60	90	110	150	150	150	150	150
40% IBU load	40	60	90	110	130	130	130	130	130

Table 3.3 Temperature profile used for extrusion

3.2.2.2 Ibuprofen-Affinisol^{TM}HPMC partial factorial DOE

As stated above, residence time is one of the critical process attributes in formulation development using HME. Factors affecting the residence time include feed rate, screw speed, and screw configurations. The direct response effect of residence time was calculated by incorporation of a marker pellet made by 30%w/w load of fluorescent optical brightener called UVITEX with Affinisol^{TM}HPMC 100cP using HME. 20mg of tracer pellet was put at regular intervals during the HME process and was tracked using an in-line high-temperature UV-vis probe. The tracer pellet excites at 500nm wavelength and the amplitude was recorded as a function of time. A partial factorial DOE consisting of 3 levels of feed rate, screw speed and configuration was randomised using Minitab software keeping temperature profile constant. 40% IBU drug load with Affinisol^{TM}HPMC 100cP blend was used for all the studies. Along with residence time, in line monitoring of %torque and pressure was used as a response. Off-line monitoring was done using DSC and dissolution which was also used as a response.

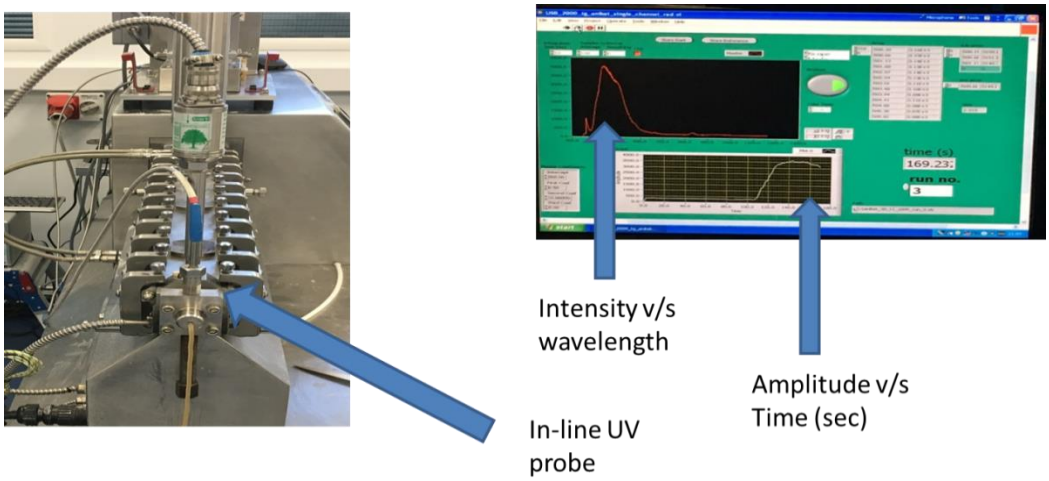

Figure 3.9 In-line UV measurement during extrusion

No	Processing Parameters		
	Screw configuration	Screw speed (rpm)	Feed rate (Kg/hr)
1	-1	100	0.4
2	-1	300	0.5
3	-1	500	0.6
4	0	100	0.5
5	0	300	0.6
6	0	500	0.4
7	1	100	0.6
8	1	300	0.4
9	1	500	0.5

Table 3.4 Design of experiment for process parameter study

No Mixing Screw configuration (-1) conveying only

Less Mixing Screw configuration (0) single mixing zone

High Mixing Screw configuration (1) double mixing zone

Figure 3.10 Screw configuration for process parameter study

Three types of screw configuration used were:

1. With only conveying elements (-1)
2. With one mixing zone (0)
3. With two mixing zones (1)

3.2.2.3 Ibuprofen-Affinisol^{TM}HPMC compression moulding

For rheological studies, one of the key requirements is to have minimal sample variation. A significant variation of thickness uniformity was observed within the pelletised HME pellets. Affinisol^{TM}HPMC is an amorphous polymer which only softens at elevated temperatures. Hence, it is difficult to form uniform extrudates/film without incorporating shear into the process. To overcome this, compression moulding (CM) was done to obtain flat square sheets which were further cut into circular discs. Compression moulding experiments were carried out using equipment provided by MOORE UK. Top and bottom plate were kept

at a constant temperature just below or above the temperature at which the blends were subjected during extrusion (Figure 3.11). Square sheets of thickness 0.3 and 0.9mm were used alternatively for the constant thickness of the film. The samples were placed on two larger metal plates with the center of the square bar for proper and uniform distribution. The hot plate was subject to variable pressure and cooling was carried out using water circulation through the outer parts of the plates.

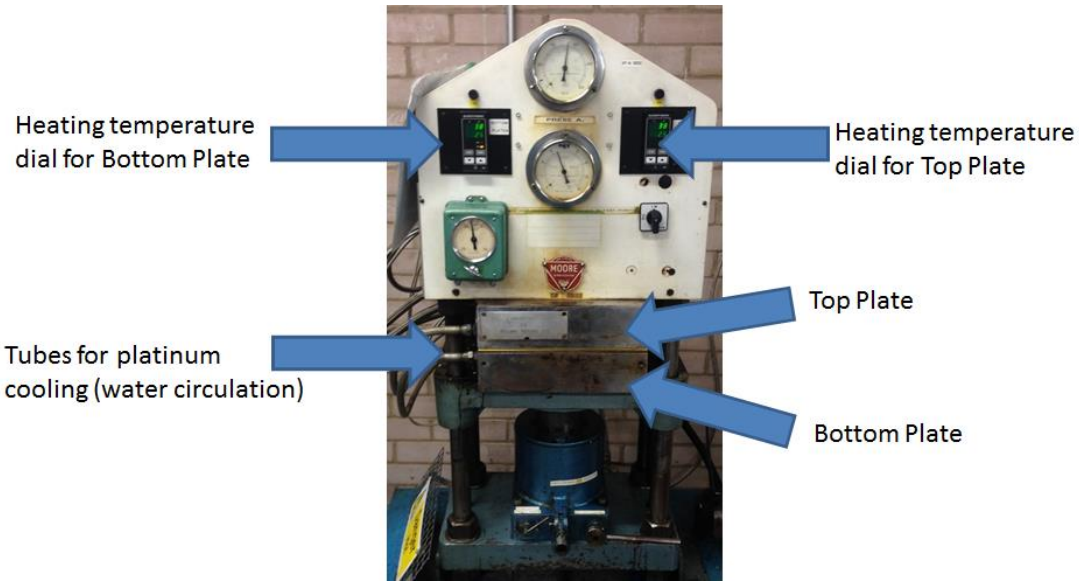

Figure 3.11 Compression Moulding equipment by MOORE UK

Properties	Affinisol 100cP	10%IBU	20%IBU	30%IBU	40%IBU
Process temp (°C)	200°C	180°C	160°C	150°C	130°C
Film Thickness (mm)	0.6mm	0.6mm	0.6mm	0.6mm	0.6mm
Weight of extrudates per batch (g)	10g	10g	10g	10g	10g

Table 3.5 Compression moulding trials

3.2.2.4 Posaconazole-Dicarboxylic acids solid-state screening trials

Solid state screening trials were carried out using a solvent assisted ball mill MM 200 from Retsch (Figure 3.12). Two stainless steel jars of 10ml volume were used. Two stainless steel balls of 7mm in diameter were used for milling. All the experiments were carried at vibrating frequency of 25Hz for 30mins. Molar ratios of 1:1 and 2:1 of Posaconazole and Dicarboxylic acids with 5ml of Acetonitrile solvent were used. Trials for binary phase diagram were plotted for Posaconazole-Succinic Acid and L-Malic Acid trials respectively. All samples were air dried and were analysed using DSC, XRD, Raman, and ATR-FTIR for solid-state stability.

Figure 3.12 Ball mill

3.2.2.5 Posaconazole-Affinisol^{TM}HPMC HME studies

Extrusion trails were carried out using a Pharma Lab 16mm of Thermo Scientific UK with screw length to diameter ratio of 40:1. A gravimetric twin-screw feeder (Brabender, Germany) was used for the auto-feeding of the blends. Posa-Affinisol^{TM}HPMC 4M blends with varying drug percent w/w were processed at different temperatures profiles. Pharmalab 16mm extruder has 10 different zones starting from zone 1 till zone 10 with zone one being the auto-feeder zone. The mixing section comprised from zone 7 till 9 and was followed by discharge elements in zone 10 and die. Typical temperature profiles for all trials are shown in the table 3.6:

Temperature profile	Zones								
	2	3	4	5	6	7	8	9	Die
Affinisol^{TM}HPMC 4M	40	60	100	120	180	180	180	180	180
10% Posa load	40	60	100	120	180	180	180	180	180
20% Posa load	40	60	100	120	180	180	180	180	180
30% Posa load	40	60	100	120	180	180	180	180	180
40% Posa load	40	60	100	120	180	180	180	180	180
50% Posa load	40	60	100	120	180	180	180	180	180
60% Posa load	40	60	100	120	180	180	180	180	180
70% Posa load	40	60	100	120	180	180	180	180	180
40%Posa+Maleic Acid+Aff 4M (1-1)	40	60	100	120	170	170	170	170	170
40%Posa+Succinic Acid+Aff 4M (2-1)	40	60	100	120	180	180	180	180	180
40%Posa+Malic Acid+Aff 4M (2-1)	40	60	100	120	160	160	160	160	160
40%Posa+Succinic Acid+Aff 4M (1-1)	40	60	100	120	150	150	150	150	150
40%Posa+Malic Acid+Aff 4M (1-1)	40	60	100	120	160	160	160	160	160
30%Posa+Succinic Acid+Aff 4M (1-1)	40	60	100	120	150	150	150	150	150
30%Posa+Succinic Acid+Aff 4M (1-1)	40	60	100	120	160	160	160	160	160
3.37%Succinic Acid+Aff 4M	40	60	100	120	180	180	180	180	180
3.83%Malic Acid+Aff 4M	40	60	100	120	180	180	180	180	180

Table 3.6 HME trials with posaconazole, Affinisol 4M and dicarboxylic acids

The screw configuration described in Ibuprofen-Affinisol^{TM}HPMC 100cP studies was used in the Posaconazole-Affinisol^{TM}HPMC 4M studies. The screw speed for all the experiments was kept constant at 100rpm.

3.2.3 Characterisation of extrudates

3.2.3.1 Accelerated stability conditions

To check the long-term solid-state stability, the ASDs were stationed at three stability conditions 40°C/75% RH, 25°C/60% RH and room temperature. Samples were removed at regular intervals and analysed using ATR-FTIR, Raman microscopy, XRD, and DSC.

3.2.3.2 Solid state characterisation of extrudates

All extrudates were analysed using DSC, XRD, ATR-FTIR, and Raman to check for solid state stability. The protocol used was same as described in the earlier section of 3.2.1.

3.2.3.3 Dynamic Mechanical Analyser (DMA)

DMA analysis was carried out using TA Q 800 DMA. Extrudates and films were characterised using dual cantilever sample holder. The frequency was set at 1Hz at a temperature ramp was applied out from 20°C to just before the extrudates degrade at a rate of 1°C/min. Experiments were carried out using controlled strain thermal scan. A constant % stain of 0.1% was applied for all the experiments. Analysis of data was performed using TA Universal Analysis Software. Experiments were carried out with and without relative humidity chamber head. Outline of the DMA studies is summarised in Figure 3.13.

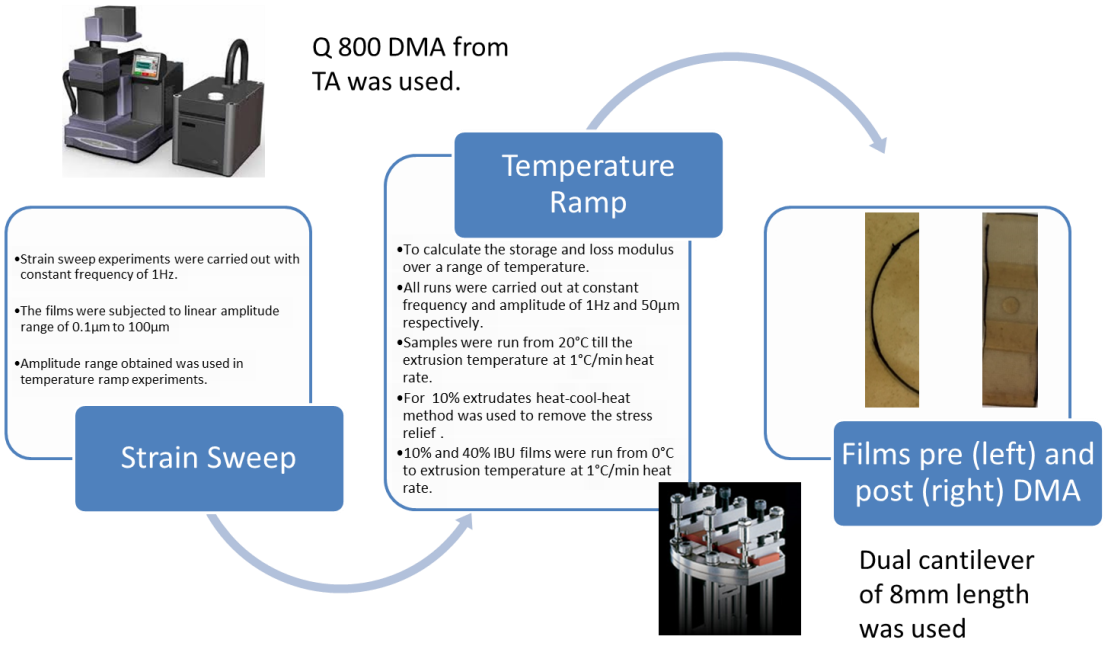

Figure 3.13 Outline of DMA Studies

3.2.3.4 Dissolution

Drug release studies were carried out using DS 8000 with auto-sampler from Lab India (Figure 3.14). USP apparatus II paddle type was used. Pellets or milled samples were placed directly within the dissolution vessels containing phosphate buffer pH 7.2 of 900ml.Paddle speed was set at 50-100 rpm and the dissolution test was carried out at 37.5°C. 5ml of sample volume was removed at various fixed time points and the samples removed were analysed using UV-Vis spectrometer at a fixed wavelength of 221 and 263nm by dilutions. The dissolution test was carried out under sink conditions. A calibration curve for Ibuprofen and Posaconazole was plotted by preparing serial dilutions of concentrations ranging from 1-10 µg/ml and taking UV readings at a fixed wavelength of 221 and 263nm using UV-vis spectrometer.

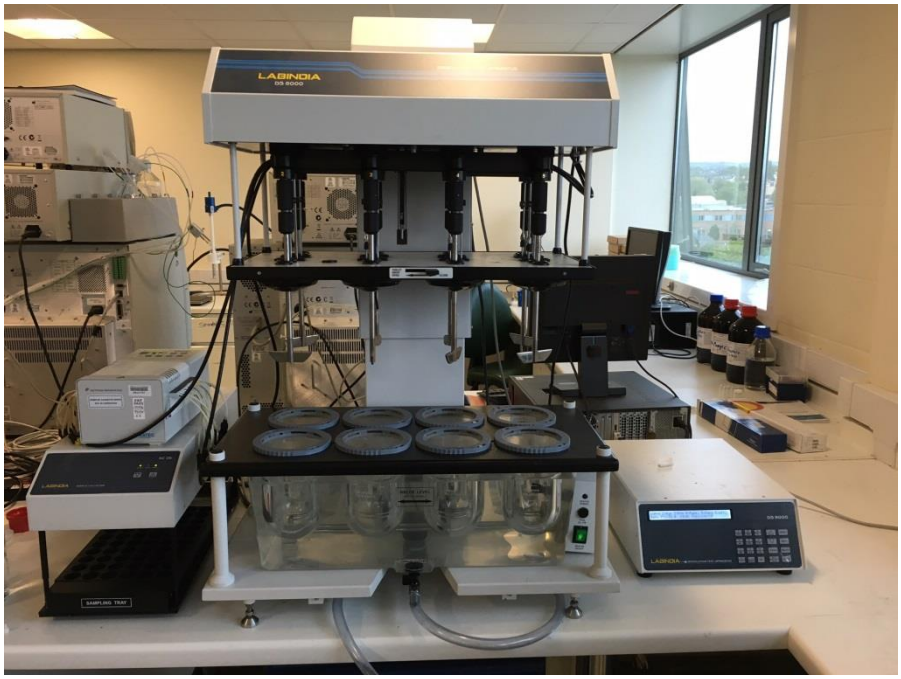

Figure 3.14 DS 8000 Dissolution apparatus with autosampler (paddle type)

Chapter 4: Material characterisation and feasibility studies

The aim of this chapter is to provide an in-depth understanding of the material attributes affecting the formulation development of the ASDs. It will provide a detailed investigation of the physicochemical properties of IBU, Posa, and Affinisol^{TM}HPMC. Further, it will detail the theoretical parameters like solubility parameter, fragility and binary phase diagram by Flory-Huggins theory using the depression of melting point approach. The rationale for selection of analytical instruments for detection of solid state stability of ASDs will also be discussed.

4.1 Thermal properties of the materials

Thermal history of API and polymer of choice is an important attribute in formulation development of ASDs using HME. Thermal history of the material will supplement physicochemical properties like glass transition temperature, melting temperature, degradation and water/solvent loss events. Understanding of thermal history will help foresee gaps during process development.

Degradation temperature of the IBU, Posa, and Affinisol^{TM}HPMC was measured using TGA. Affinisol 100cP and 4M showed three events of weight loss at 150°C, 210°C, and 380°C respectively. The first weight loss could be due to water/solvent loss as the weight loss was gradual and over a temperature range. The second and third weight losses could be due to two-step thermal degradation. DSC thermogram showed a change in baseline which could be due to glass transition temperature at 104.65°C and 106.64°C respectively (Figure 4.1). Thus, it was noted that Affinisol 100cP and 4M had a tendency to pick up surface moisture although reversible in nature can have an effect during HME. Either a vent needs to be provided during extrusion for the release of surface moisture or Affinisol should be dried in a preheated oven to remove surface moisture. Affinisol 100cP & 4M were dried in pre-heated vacuum oven at 50°C for 2hrs prior to use. Additionally, from TGA it was noted that all extrusion experiments involving Affinisol 100cP & 4M need to be carried out below 210°C to avoid solid state thermal degradation.

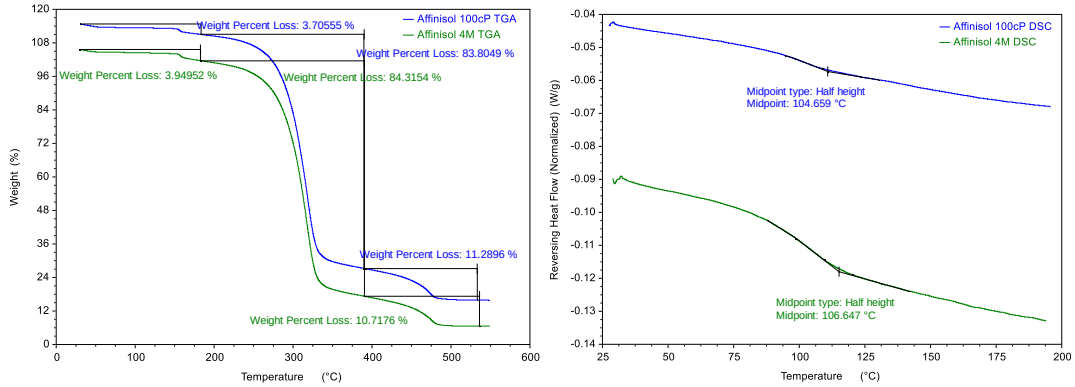

Figure 4.1 TGA (left) and DSC (right) thermograms of Affinisol 100cP and 4M

Thermal degradation temperature of ibuprofen was found to be around 100°C. DSC thermogram of a heat-cool-heat method for ibuprofen showed a sharp endothermic event corresponding to melting of ibuprofen at a peak of 75.53°C (Lerdkanchanaporn and Dollimore 1997). In the second heat cycle, a change in baseline corresponding to glass transition temperature at -44.34°C was observed (Figure 4.2). It was observed that ibuprofen can be made amorphous using quench cooling method within DSC (Heat-Cool-Heat) and it stays amorphous as no recrystallisation or second melting event was observed. Despite this, T_g of the IBU is low and hence incorporating it within a high T_g polymer to form ASD proves to be a correct rationale.

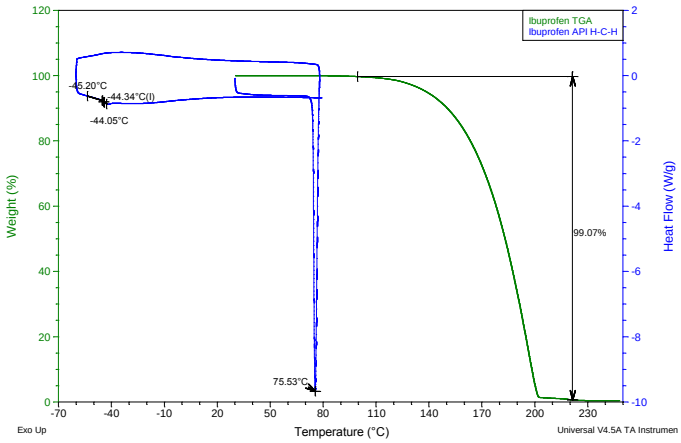

Figure 4.2 Thermal analysis of ibuprofen

DSC thermogram of posaconazole showed one broad endothermic event with a peak temperature at 135.44°C which is due to solid-solid impurity and sharp endothermic event with a peak temperature at 168.85°C which is due to the melting of posaconazole form I (Andrews et al. 2004; Andrews et al. 2005) (Figure 4.3).

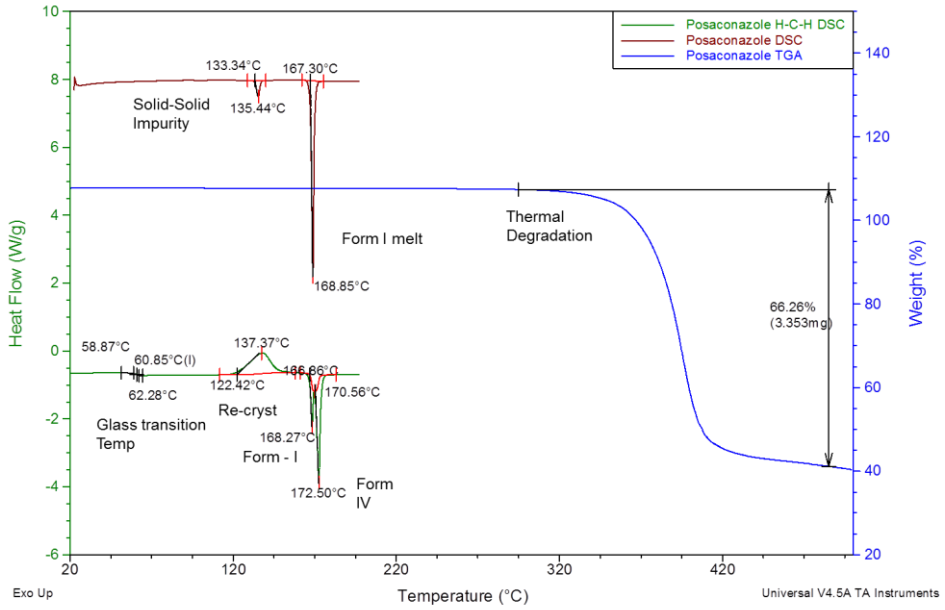

Figure 4.3 Thermal analysis of posaconazole

DSC thermogram of heat-cool-heat cycle showed the presence of a change in baseline which could be due to a glass transition at 60.85°C followed by an exothermic event which could be due to recrystallisation with a peak at 137.37°C and lastly two sharp endothermic events with peak temperatures at 168.27°C and 172.50°C which could be due to melting of form I and IV respectively (Andrews et al. 2004; Andrews et al. 2005; Wieser et al. 2008). Thermal degradation of posaconazole was found to be around 300°C.

4.2 Theoretical considerations

4.2.1 Solubility parameters

The solubility parameter is a quick first step in predicting the miscibility between materials based on their chemical structure. The theoretical calculation can help in the selection of materials to form ASDs. Of the various methods available to calculate solubility parameter to predict miscibility, Van Krevelen and Hoftyzer's group contribution method was used. A detailed calculation of group contribution for ibuprofen, posaconazole, and Affinisol^{TM}HPMC is provided in Table 4.1. According to the van Krevelen method, the values of δ for ibuprofen, posaconazole, and Affinisol^{TM}HPMC were found to be 19.66, 20.02 and 23.9 MPa$^{1/2}$respectively. Moreover, the δ difference between ibuprofen and Affinisol^{TM}HPMC was noted to be 4.24 MPa$^{1/2}$ (Table 4.2)

Group	**F**R_{di}	**F** R_{pi}	**E**R_{hi}	**Repeating units**	∑**F**R_{di}	**F**P^2PR_{pi}	∑**E**R_{hi}
-CH3-	420	0	0	3	1260	0	0
-CH2-	270	0	0	1	270	0	0
-CH-	80	0	0	2	160	0	0
Benzene ring	1430	110	0	1	1430	12100	0
-COOH	530	420	10000	1	530	176400	10000
Total ∑				-	3650	188500	10000
					δR_dR = 18.22	$\delta R_{pi}R$ =2.17	δR_hR =7.06
Ibuprofen δ = 19.66 MPa$P^{1/2}P$							

Group	**F**R_{di}	**F** R_{pi}	**E**R_{hi}	**Repeating units**	∑**F**R_{di}	**F**P^2PR_{pi}	∑**E**R_{hi}
-CH3-	420	0	0	2	840	0	0
-CH2-	270	0	0	3	810	0	0
-CH-	80	0	0	2	160	0	0
C (TETRAVALENT)	-70	0	0	1	-70	0	0
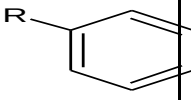	1430	110	0	2	2860	48400	0
-F	220	0	0	1	220	0	0
-OH	210	500	20000	1	210	250000	20000
-O-	100	400	3000	2	200	640000	6000
-CO-	290	770	2000	1	290	592900	2000
NH	160	210	3100	2	320	176400	6200
N trivalent	20	800	5000	6	120	23040000	30000
Ring	190	0	0	3	570	0	0
Total ∑				-	3650	188500	10000
					δR_dR = 13.12	$\delta R_{pi}R$ =9.99	δR_hR =11.35
Posaconazole δ = 20.02 $MPaP^{1/2}P$							

Group	**F**R_{di}	**F** R_{pi}	**E**R_{hi}	**Repeating units**	∑**F**R_{di}	**F**P^2PR_{pi}	∑**E**R_{hi}
-CH3-	420	0	0	2	840	0	0
-CH2-	270	0	0	4	1080	0	0
-CH-	80	0	0	5	400	0	0
-0-	100	400	3000	3	300	1440000	9000
COH	470	800	4500	2	940	2560000	9000

Total ∑				-	3560	4000000	18000
					$\delta R_d R$ = 19.01	$\delta R_{pi} R$ =10.68	$\delta R_h R$ =9.80
Affinisol^{TM}HPMC δ = 23.90 MPa$^{P1/2P}$							

Table 4.1 Calculation of group contribution for ibuprofen, posaconazole, and Affinisol^{TM}HPMC

No	Materials	δ of materials (MPa1/2)	Δδ (MPa1/2)
1	Ibuprofen	19.66	-
2	Posaconazole	20.02	-
3	Affinisol^{TM}HPMC *	23.9	4.24 for IBU and 3.88 for Posa

***Affinisol monomer Structure has not been released hence HPMC monomer structure was considered.**

Table 4.2 The solubility parameter (δ) of Ibuprofen and polymers

The difference between the total solubility of drug and polymer i.e. Δδ is less than 7 MPa$^{1/2}$ and hence are considered to be miscible (Greenhalgh et al. 1999; Forster et al. 2001); (Garekani et al. 2001).

4.2.2 Fragility parameter

The fragility parameters for IBU and Posa were quantified using DSC at cooling rates of 1, 2, 5, 10, 12 16, 18 and 20 °C/min (Figure 4.4). A plot of ln (Q) against 1/Tg was produced – the slope of the line being utilised to calculate ΔH/ R for the crystalline components (Figure 4.4). ΔH/ R value obtained was

utilised to calculate the fragility parameter (m). If the fragility parameter values of m are < 70 and m are> 100 indicates the formation of strong and fragile glass respectively (Borde et al.). Fragility index for IBU was found to be 60.47 hence it forms a strong glass. This can be supported by the DSC thermogram by using the heat-cool-heat method where ibuprofen exhibited no recrystallisation or second melting event. Fragility index for posaconazole was found to be 76.98 and hence forms a weak glass. However, fragility index only provides an indication about the type of glass and its ability to form glass but fails to provide direct relevance to the stability and its role in the stability of the solid dispersion is still unclear.

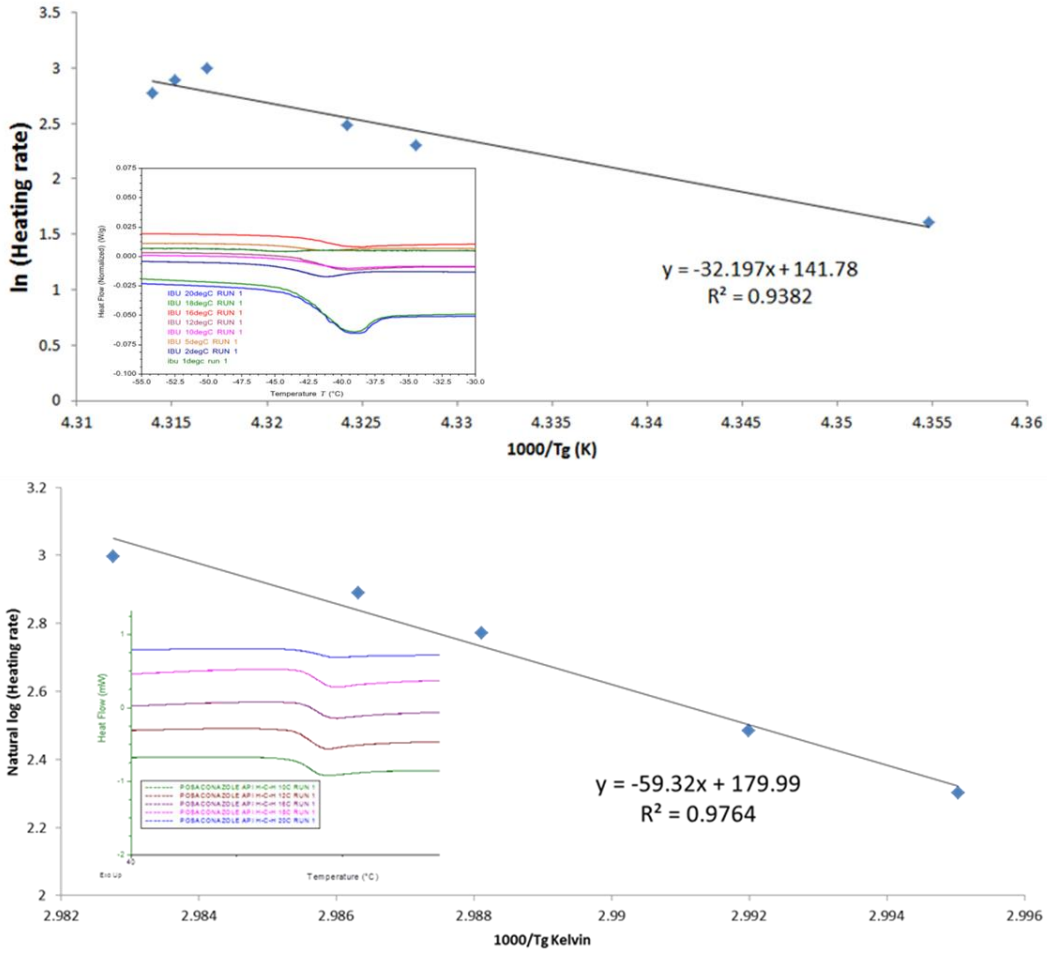

Figure 4.4 Fragility parameter for IBU and POSA

4.2.3 Binary Phase Diagram

Thermodynamics state that every solid solute will possess some solubility in the polymer. Before, going ahead to explain binary phase diagram, it is important to define the terms solid state solubility and miscibility. Solid state solubility is generally considered when a solid solute dissolves in the liquid/melt state of the polymer. This leads to a single phase consisting of solute and polymer to be molecularly mixed (also known as a solid solution). Solid state miscibility, on the other hand, is considered when a solid solute and polymer blend form a single phase system. This single phase system does not necessarily mean the molecular mixing between the solid solute and polymer. A single phase in this context will be the API-polymer blend with a single glass transition temperature (Olabisi et al. 1979).

Construction of binary phase diagram and its limitations:

Phase separation in ASD could be either due to the liquid-solid boundary or liquid-liquid boundary. Phase separation in the liquid-solid boundary occurs either by vitrification or crystallisation of the API. The mechanism for crystallisation is well defined and occurs in two stages of nucleation and growth. Liquid-liquid boundary separates due to the combined effects of thermodynamics or melt flow properties (Olabisi et al. 1979). Mostly, during extrusion, API-polymer immiscibility will be due to its liquid-liquid boundary as melt API solubilises in the softened polymer. However, over stability, the phase separation occurs due to the liquid-solid boundary. Hence for this main reason, the focus in the solid-state miscibility will be on the spinodal curve of decomposition. Solubility curve will not be studied for both ibuprofen-Affinisol 100cP and posaconazole-Affinisol 4M blends.

Spinodal decomposition curve is a phase formed due to a kinetic process governed by crystal nucleation and growth. Amorphous phase separation also has a metastable separation line called the binodal curve (Chen et al. 2016). Kinetics of spinodal decomposition governs the miscibility between API-polymer solution bends (Lin and Huang 2010). Thus, thermodynamic stability of the API-polymer solution blends is provided by the binodal and spinodal curve.

A glass transition temperature curve is not a phase separation curve. It in principle provides information about the ability of a API-polymer blend to form a glass according to its molecular mobility. This, in turn, can be useful in predicting the phase separation kinetics and structure information (Lin and Huang 2010).

A typical binary phase diagram based on the polymer solution theory is shown in figure 4.5. Solubility curve or liquid-solid transition boundary denotes the solubility of API within polymer matrix at different temperatures. The spinodal curve represents the metastable miscibility phase between API-polymer solution blend. The glass transition temperature line provides an overview of phase separation kinetics and molecular mobility within the glassy matrix (Qian et al. 2010).

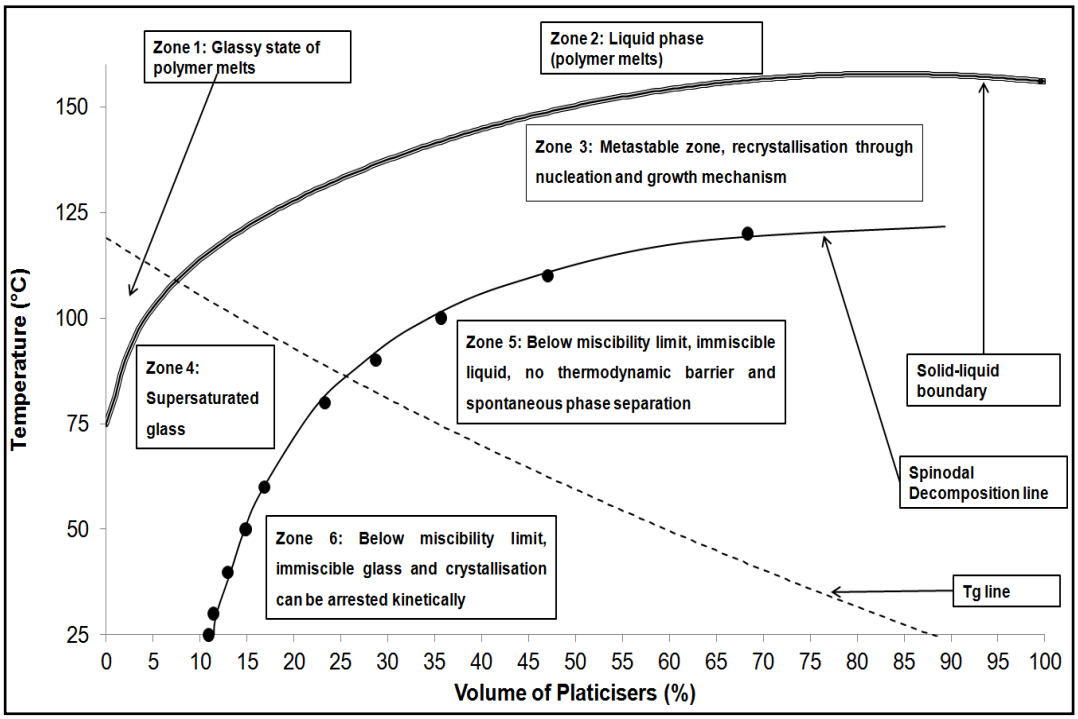

Figure 4.5 Typical binary phase diagram (Karandikar 2015)

The single value solubility parameter approach was not successful in prediction of solid-state miscibility and new methods with more promise gained importance. The application of the Flory-Huggins solid-state solution theory assumes the drug solubilises within the polymer with a similar principle as for a solid solute dissolving in a solvent to form a solution (Tian et al. 2013). Two approaches of lattice theory and non-athermal mixing (interaction parameter approach) are used to confirm Flory-Huggins theory (Lin and Huang 2010). The current study will be utilising the non-athermal approach to predict the same. Flory-Huggins theory works on the principle of free energy of mixing. Free energy of mixing can be explained by understanding the Gibbs free energy. Gibbs free energy for mixing consists of entropy which energy of the system required for mixing and enthalpy which energy needed to break down the stable system. A negative value of Gibbs free energy promotes stability of the phase and vice-versa. According to the theory, the binary phase diagram

can be predicted by studying the drug-polymer interaction parameter χ as a function of temperature range (Lin and Huang 2010; Qian et al. 2010; Knopp et al. 2015). The mathematical equations are well defined in the chapter 3.

Measurement methods used for Flory-Huggins polymer solution theory are well documented (Knopp et al. 2015; Rask et al. 2018). For the current study, melting point depression was chosen as the method of choice. The amorphous polymer in question is not easy to soften and for the formation of single-phase system with APIs, high shear is required which is generally generated in HME. From the feasibility point of view, melting point depression works best with minimal method error. Physical mixtures were pre-mixed for 30mins and were analysed in DSC for melting point depression of the APIs. For calculation of glass transition curve, direct measurement of glass transition temperature is the best method. However, it's not feasible to produce single phase API-polymer blends using heat-cool-heat cycle. Hence, theoretical methods like Gordon-Taylor equation, Fox equation, Couchman-Karaszor, and Kwei are used in prediction of glass transition temperature of API-polymer solution blend (Prudic et al. 2015; Song et al. 2015; Tian et al. 2015; Van Duong et al. 2018). In the current study, the Fox equation was utilised for the prediction of glass transition temperature of API-polymer blends.

Table 4.3 provides the parameters used to calculate the interaction parameter and free energy of mixing.

Parameter	Ibuprofen	Posaconazole	Affinisol 100cP	Affinisol 4M
M_w (g/mole)	206.29	686.75	231708	552800
Density (g/cm^3)	1.03	1.38	1.326	1.326
Glass transition temperature (°C)	-44°C	60.85°C	128°C	128°C

Table 4.3 Calculated parameters for ibuprofen, posaconazole, and Affinisol

The parameters for ibuprofen and posaconazole were obtained by ChemDraw software while experimental values obtained were used for affinisol 100cP and 4M. Glass transition temperature values for ibuprofen and posaconazole were obtained using DSC while, DMA was used for affinisol 100cP and 4M. The values generated using DSC were found to be lower than the DMA values for affinisol 100cP and 4M. The values also matched with values provided by the vendor. The degree of polymerization m was calculated to be 872.48 & 837.73 for ibuprofen and posaconazole. The interaction parameter χ at the melting point was calculated by a melting point depression method using DSC and was found out to be -0.6353 and -0.6337 for ibuprofen and posaconazole (Figure 4.6).(Lin and Huang 2010; Tian et al. 2013; Tian et al. 2014; Huang et al. 2016)

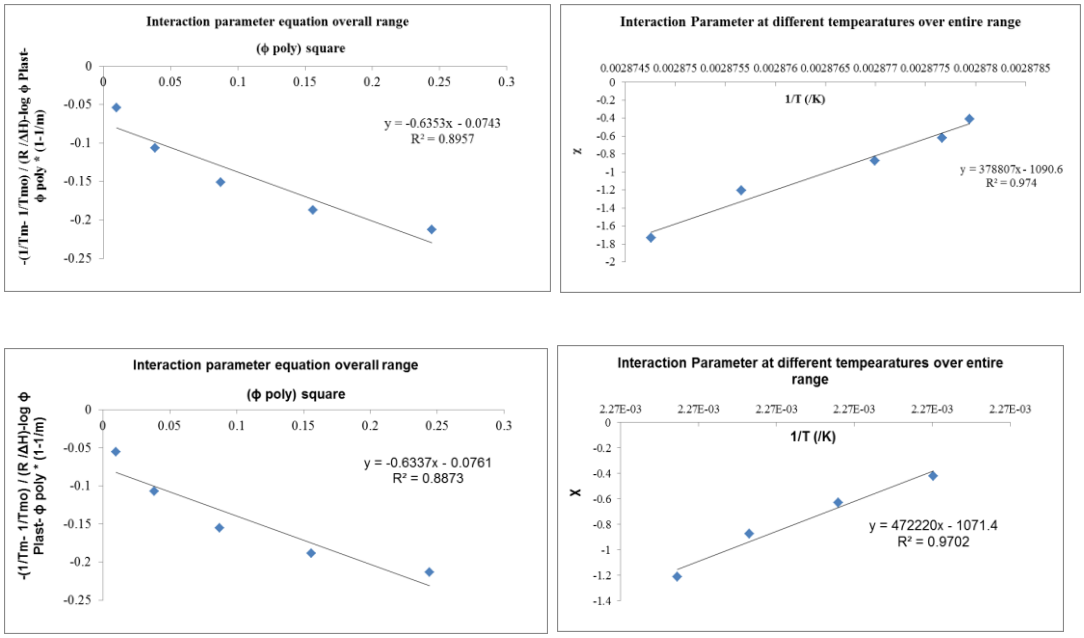

Figure 4.6 Calculation of interaction parameter χ at melting point by Flory-Huggins equation

For the spinodal curve, the interaction parameter was plotted as a function of inverse temperature to get components A and B (Figure 4.6).

According to theory, at the melting temperature, the interaction parameter tends to infinity hence subtle changes in temperatures near the melting point will have a significant impact on the interaction parameter. Using values A and B obtained by plotting figure 4.6, the free energy of mixing $\Delta Gmix$ at different temperature was theoretically calculated (Figure 4.7).

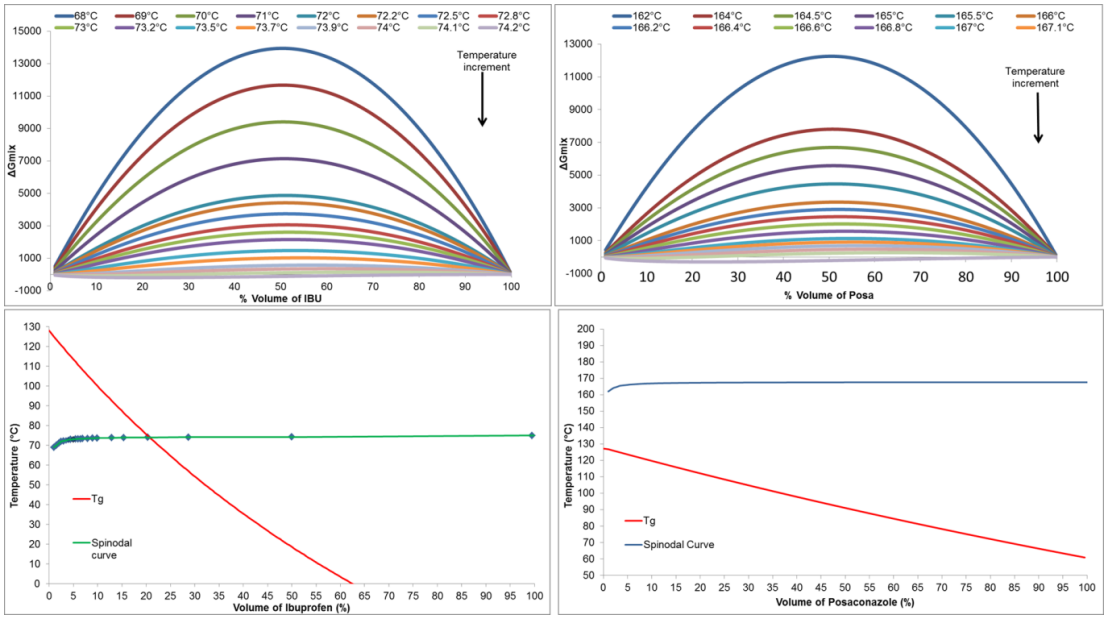

Figure 4.7 The plot of free energy of mixing (top) and phase diagram (bottom) of IBU (left) and Posa (right)

$\Delta Gmix$ values were found to be positive for temperatures below 74°C and 162°C for ibuprofen and posaconazole respectively which indicates de-mixing. The spinodal curve was obtained by calculating the second derivate of $\Delta Gmix$ at various temperatures close to the melting temperature. The theoretical glass transition temperature profile for ibuprofen-Affinisol 100cP and posaconazole-Affinisol 4M was calculated using the Fox equation (Figure 4.7). Table 4.4 summarises the calculated parameters for both the API-polymer blends.

Parameter	Ibuprofen-Affinisol 100cP	Posaconazole-Affinisol 4M
The degree of polymerisation (m)	872.48	837.73
Interaction parameter at melting point (χ)	-0.6353	-0.6337
Entropic contribution (A)	-1090.6	378807
Enthalpy contribution (B)	-1071.4	472220

Table 4.4 Calculated parameters for ibuprofen and posaconazole trials

Affinisol 100cP molecular weight is more than 1000 times of that of ibuprofen. Due to which spinodal curve predicts complete solid-state miscibility between all the drug-polymer compositions and thus the binary phase diagram fails to predict solid-state miscibility between ibuprofen and Affinisol 100cP (Huang et al. 2016). A similar result was observed for the posaconazole-Affinisol 4M binary phase diagram. Hence, it can be inferred that theoretical binary phase diagram by Flory-Huggins theory fails to predict the stability of the ASD formed using ibuprofen and Affinisol 100cP.

4.3 Water uptake capability

The presence of water can pose an issue during hot melt extrusion and can cause extrudates to swell. Thus studying water uptake capability of the materials can help in identifying the precautions needed during extrusion. Dynamic Vapour Sorption (DVS) provides a complete overview of water uptake capability of API and polymers. Furthermore, it also highlights the ability of materials to hold onto surface water. DVS isotherm plots can also help in distinguishing whether water uptake is reversible (surface moisture) or

irreversible (hydrate) in nature (Aubuchon 2011). The absorption plots of ibuprofen, posaconazole, Affinisol 100cP and 4M are shown in figure 4.8. It was observed that ibuprofen and posaconazole are not at all hygroscopic in nature and exhibited saturated mass gain of 0.1% wt gain at 90%RH. Mass weight gain is also reversible in nature. Hence, both APIs showed no tendency to form irreversible hydrates.

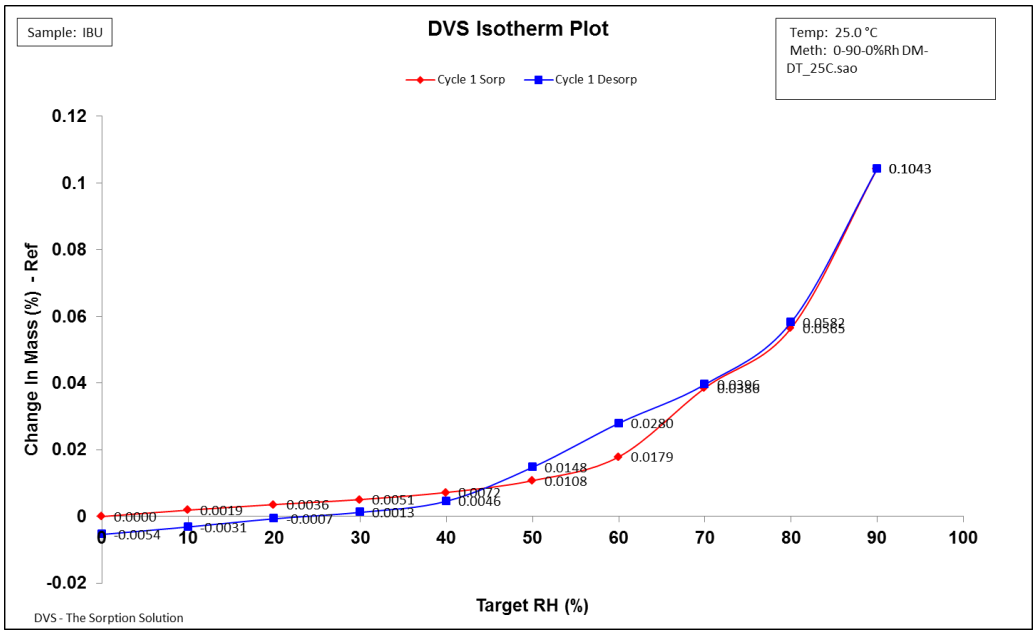

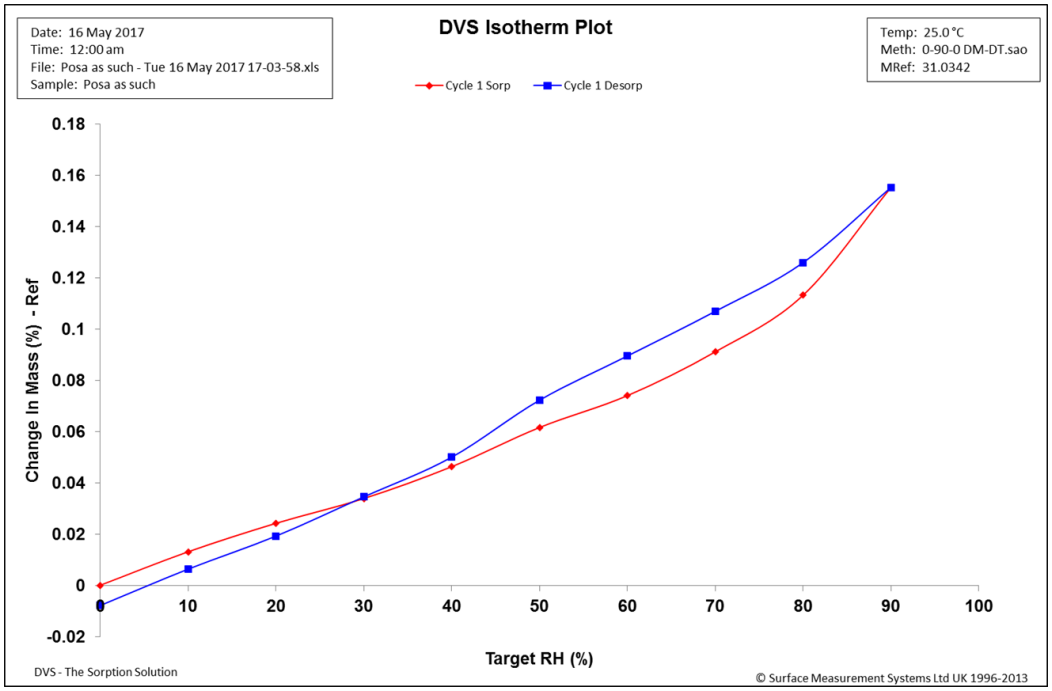

Figure 4.8 DVS isotherms of ibuprofen (top) and posaconazole (bottom)

In the case of Affinisol^{TM}HPMC grades, no significant difference in their water uptake ability was observed, however, a saturated mass gain of 18% and 16% at 90%RH was observed for affinisol 100cP and affinisol 4M respectively (Table 4.5). One important thing to note was that the water uptake capability of Affinisol^{TM}HPMC grades was found to be less than the commercially available grades of HPMC as shown in figure 4.9 (Gupta et al. 2016). This clearly affirms the advantage it offers over traditional HPMC available in terms of its water uptake capability. For extrudates, DVS study was not carried out as they need to be milled in order to check for its hygroscopicity. The tensile strength of the extrudates varies with the increasing amount of drug load and thus extrudates need to be cryo-milled for further studies.

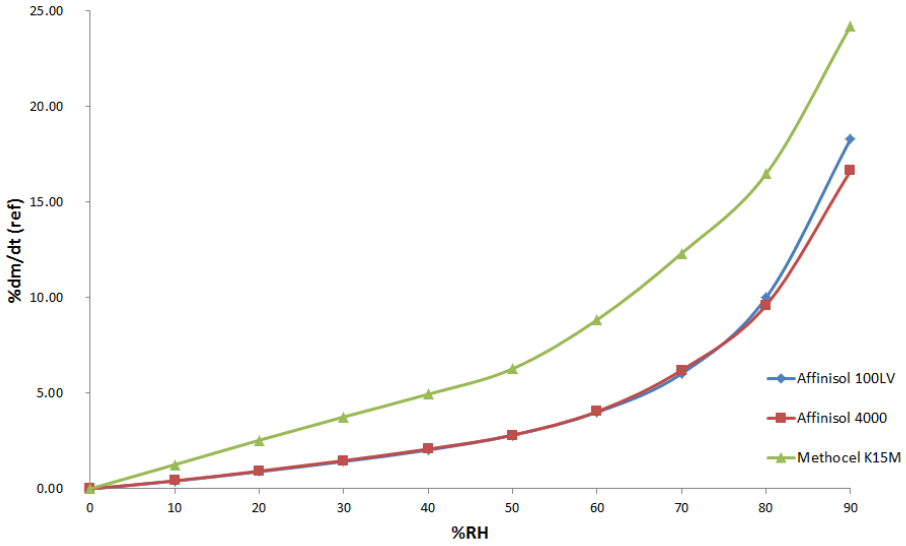

Figure 4.9 DVS data for Affinisol™HPMC 100cP, Affinisol™HPMC 4M and Methocel K15M

%RH	Affinisol 100LV	Affinisol 4000	Methocel K15M
0	0.00	0.00	0.00
10	0.41	0.42	1.26
20	0.90	0.93	2.54
30	1.43	1.48	3.76
40	2.03	2.08	4.95
50	2.81	2.81	6.28
60	4.01	4.05	8.84
70	6.03	6.21	12.32
80	10.01	9.61	16.48
90	18.32	16.64	24.22

Table 4.5 Summary of dm/dt at a particular humidity

4.4 Spectroscopic evaluation

As explained in chapter 3, spectroscopic methods can be used in the identification of the solid state of the API and can be utilised to study the solid state stability of the ASD. Spectroscopic methods provide a quick, easy and non-invasive way of identification of the solid state of the material. Since the

stability of the ASD solely depends on the solid state of the drug within it, the current section will provide a detailed investigation of the spectral evaluations of the various states of ibuprofen and posaconazole. Crystalline, amorphous and melt form of ibuprofen and posaconazole were studied and qualitative methods were developed for detection of the solid state of ibuprofen and posaconazole.

4.4.1 FTIR spectroscopy

Ibuprofen exists as a dimer in its crystalline and melts state (Lerdkanchanaporn and Dollimore 1997; Ryabenkova et al. 2017). However, ibuprofen was made amorphous within DSC by heat-cool-heat cycles but, quench cooling experiments failed to produce pure amorphous ibuprofen. This could be due to its low T_g and tendency to exist as a crystalline dimer. ATR-FTIR spectra of melt ibuprofen, crystalline ibuprofen, and Affinisol 100cP are shown in figure 4.10. It is evident from ATR-FTIR spectra, that active bands between 1800-1700 cm^{-1} can be considered as a non-interfering region for the detection of IBU within ASD. Use of ATR-FTIR method will be detailed more in chapter 5.3.

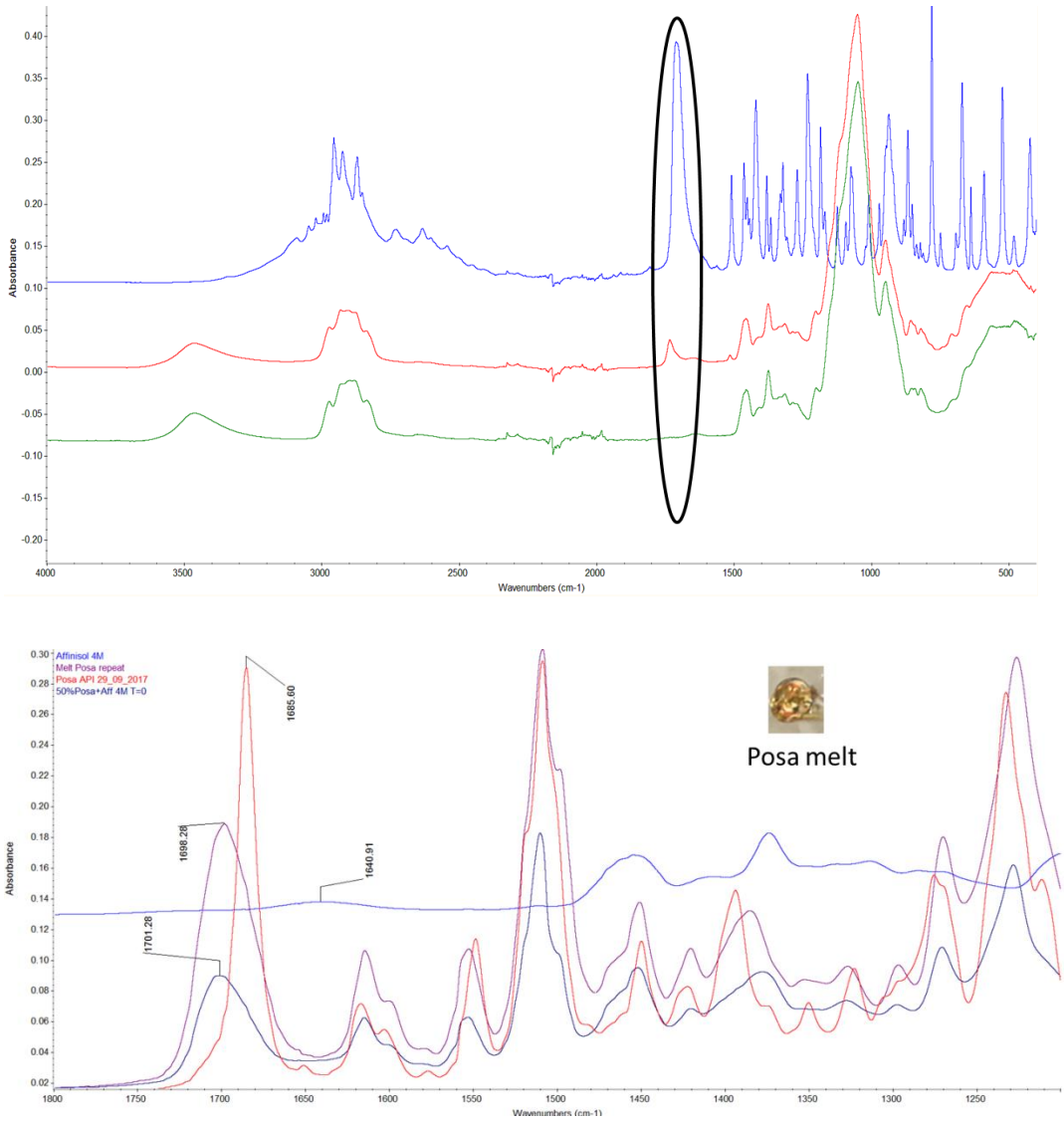

Figure 4.10 ATR-FTIR spectra of ibuprofen (above) and posaconazole (below)

ATR-FTIR spectra of Affinisol 4M, crystalline and melt posaconazole are seen in figure 4.10. All peaks observed are similar to the peaks observed in the posaconazole form I (Andrews et al. 2004). The spectral region of 1650-1710 cm^{-1} was found to be non-interfering between posaconazole and affinisol 4M. A distinct peak at 1685 cm^{-1} in crystalline Posa which is due to the carbonyl group was found to shift to 1698cm^{-1} in the melt form of posaconazole.

4.4.2 Raman spectroscopy

Several studies have reported the Raman spectra for crystalline ibuprofen and posaconazole (Breitenbach J 1999; Hedoux et al. 2011) (Andrews et al. 2004; Andrews et al. 2005). As reported in the FTIR section, quench cooling experiments had failed and hence an in-line technique was needed to confirm the Raman spectral fingerprint of amorphous ibuprofen and posaconazole. DSC coupled with a Raman probe was used to confirm the same. It is important to separate the exact temperature range within DSC to track the Raman spectra (Figure 4.2). Raman spectra for ibuprofen were collected at 20°C & 80°C in the first heating cycle and -70°C and 80°C in the second heating cycle. Raman spectra of ibuprofen melt and amorphous ibuprofen were found to be similar. Amorphous and crystalline ibuprofen Raman spectra were found to be different at 1600-1650 and 750-850 cm^{-1} regions (Figure 4.11). Overlay of Raman spectra of crystalline and amorphous ibuprofen with Affinisol 100cP confirmed the region of 1600-1650 cm^{-1} as a non-interfering region. Raman spectra exhibited a peak shift from 1607cm^{-1} to 1612-1617cm^{-1}, attributed to aryl chain deformation and C-H stretching and bending which occurs due to disorder within the structure and is characteristic of the amorphous state of ibuprofen (Liu and Gao 2012).

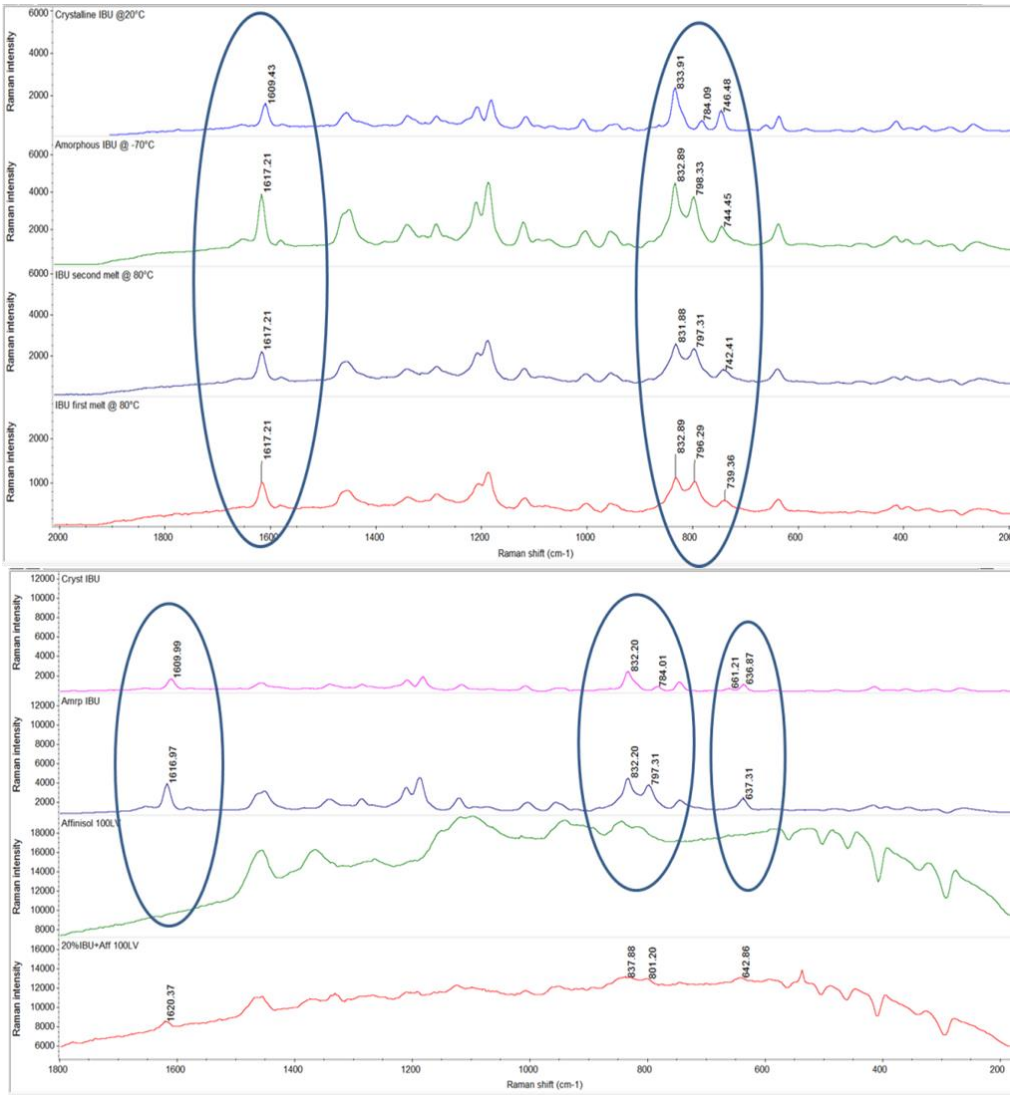

Figure 4.11 DSC-Raman of IBU and Affinisol 100cP

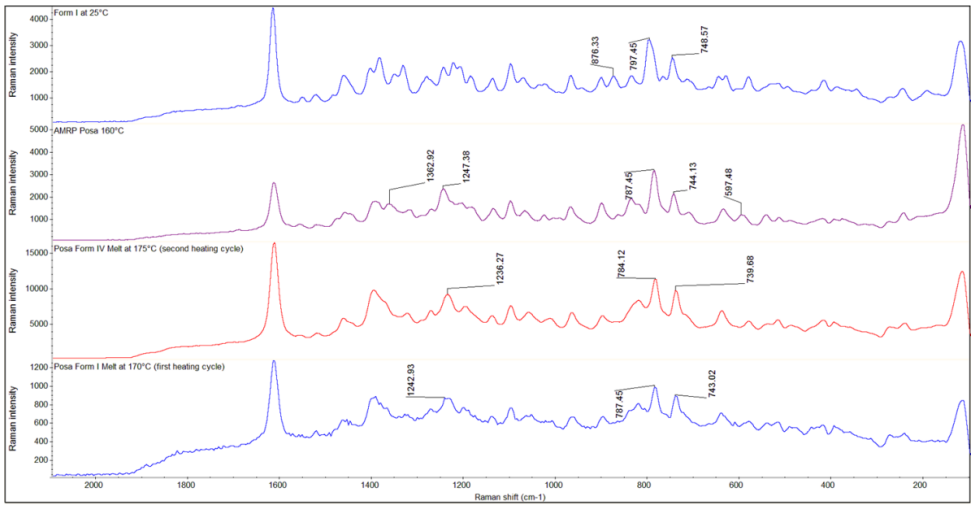

Figure 4.12 DSC-Raman of posaconazole

Raman spectra for posaconazole were collected at 25°, 110°C, 170°C, and 175°C. Raman spectra of the form I melt and amorphous posa were found to be similar. Subtle changes in the spectra were observed in the regions of 700-900 cm^{-1} between crystalline and amorphous posa. These changes are due to the relaxation of the aryl chains of posaconazole. However, the distinct peak of carbonyl group at 1600 cm^{-1} remained unchanged for all the solid forms (Figure 4.12).

4.4.3 Diffraction studies

X-ray diffraction is a simple, non-destructive tool for identification of crystalline materials. Amorphous materials are characterised by the absence of diffracted peaks due to lack of unit cell. Hence, any peaks observed upon stability can be easily picked up by X-ray and can be a useful tool in detection of solid state solubility of the ASDs. Figure 4.13 show overlay of ibuprofen and Affinisol 100cP. Characteristic peaks for ibuprofen confirmed its crystalline nature while Affinisol 100cP showed a halo region predominant for amorphous materials.

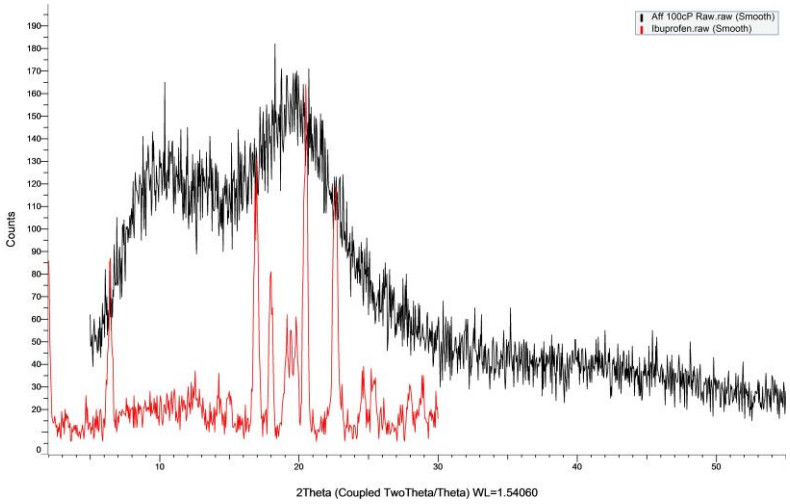

Figure 4.13 XRD diffractogram of ibuprofen (red) and Affinisol 100cP (black)

Posaconazole characteristic peaks match with the peaks observed for the form I (Andrews et al. 2004; Andrews et al. 2005). Affinisol 4M showed a halo region due to its amorphous nature. Dicarboxylic acids used as additives and for co-crystal/eutectic screening showed characteristic peaks which confirmed their crystalline nature (Shevchenko et al. 2012; Shevchenko et al. 2013) (Figure 4.14).

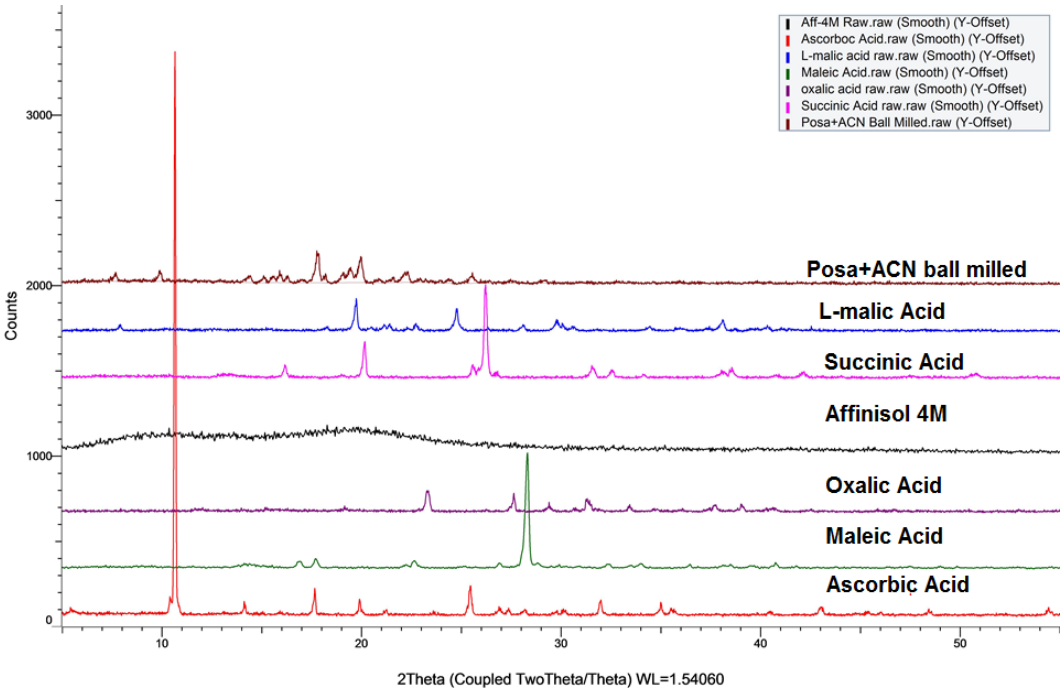

Figure 4.14 XRD diffractogram of posaconazole, Affinisol 4M and dicarboxylic acids

4.5 Conclusion

Thermal history of IBU, Posa and Affinisol^{TM}HPMC provided information like the glass transition temperature, bound and unbound water/solvent ability, decomposition and melting temperatures. Glass transition and decomposition temperatures gave an insight in the likely processing temperature window during HME. Irreversible water/solvent event within Affinisol^{TM}HPMC confirmed the tendency to pick up surface moisture. Surface moisture uptake capability was further confirmed by hygroscopic studies by DVS. Either a vent needs to be provided during extrusion or Affinisol should be dried in a preheated oven to remove surface moisture.

Rationale for selection of APIs and polymer was supported by solubility parameters approach which showed miscibility between APIs and polymer. Fragility index for IBU and Posa confirmed formation of strong and weak glasses respectively. This observation was supported by DSC thermograms where no recrystallisation event was observed for IBU and was observed for Posa. Additionally in open pan DSC experiments it took time for IBU to recrystallise.

Region of non-interference between APIs and polymer were established using ATR-FTIR and Raman spectroscopy. Carbonyl bond was found to shift for both amorphous and crystalline domains of ibuprofen in ATR-FTIR and Raman while for Posa the shift was observed only in ATR-FTIR.

Chapter 5: Ibuprofen-Affinisol

The aim of the current chapter is to focus on the critical attributes affecting the formulation development of the ASDs. These critical attributes were studied using IBU and Affinisol 100cP as API and polymer of choice to form ASD. The chapter is further subdivided into three studies. The objective of section 5.1 is to study the effect of drug concentration on the mechanical properties of the IBU-Affinisol 100cP ASD. Section 5.2 investigates the effect of critical process parameters on the product performance of IBU-Affinisol 100cP ASD using in-line and off-line analytical tools. Lastly, Ibuprofen dimer in the solid dispersion as an early indicator of solid-state stability will be discussed in section 5.3. A schematic representation of the chapter is provided in figure 5.1.

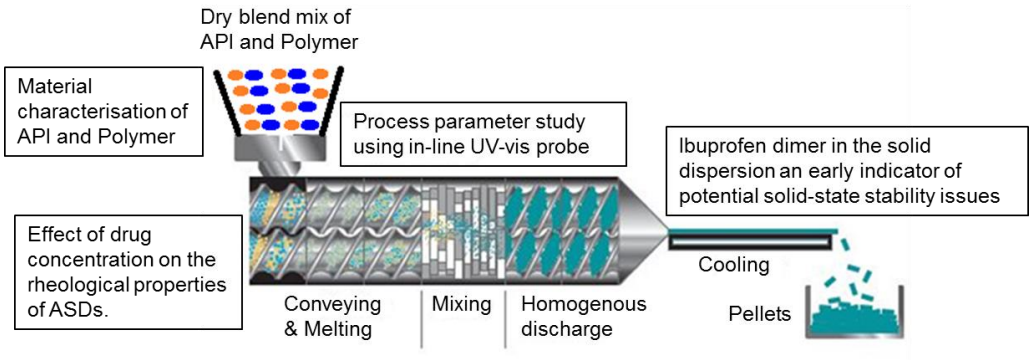

Figure 5.1 Schematic representation of ibuprofen-Affinisol 100cP studies

5.1 Effect of concentration of Ibuprofen on the mechanical properties of Ibuprofen-Affinisol^{TM}HPMC extrudates

Hot melt extrusion (HME) provides an attractive continuous green technology for formulation development of amorphous solid dispersions (ASD). Polymeric excipients comprise an integral part of the development of ASD using HME. Melt based processability of the API-polymer mixtures is highly dependent on the rheological properties of the system. Hence, understanding the melt rheology becomes a critical parameter in the formulation development of the ASD. Additionally, the polymeric excipients used are visco-elastic in nature and thus studying their mechanical properties will provide an insight into HME process development and stability. Effects of ibuprofen concentration on the rheological and mechanical properties of the extrudates with Affinisol 100cP were studied. A thorough investigation of melt rheology and mechanical properties of the extrudates is provided with the aim of examining links between the same. An attempt is also made to correlate the tan delta values obtained by mechanical studies and theoretical glass transition values obtained for the ibuprofen-Affinisol 100cP blends using the Fox equation. Off-line tracking of the crystallisation kinetics of 40% drug load of ibuprofen was studied using Raman microscopy. Dissolution studies of all the ibuprofen-Affinisol 100cP pellets were conducted. Model fitting for dissolution kinetics of all extrudates was carried out (Figure 5.2).

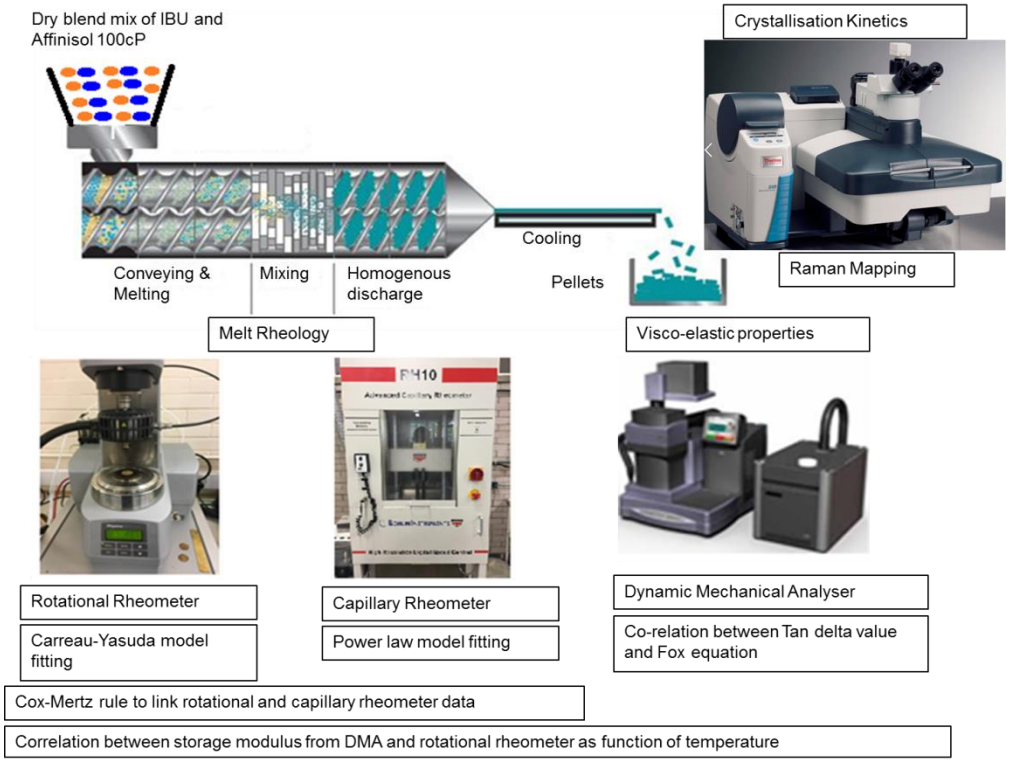

Figure 5.2 Schematic representation of ibuprofen-Affinisol 100cP mechanical study

5.1.1 Introduction

Melt rheology is one of the critical material attributes in the processing of ASDs using HME. It is important to understand the melt rheology of the API-polymer blends to gauge the challenges that may arise during HME. Furthermore, mechanical properties of the extrudates might provide an insight into downstream processing and stability challenges. Linking melt rheology and mechanical properties of extrudates will thus provide a detailed understanding of the shortcomings during formulation development of ASD using HME.

Various processing stages like, solid state conveying, melting, mixing, melt conveying and shaping occur during HME. To aid this, suitable temperature profiles and pressure is required. Thus, investigating melt flow rheology becomes critical in minimising HME trails and optimisation.

Rheology is the study of flow and deformation and is generally studied by measuring effects generated by an applied force. Applied force per unit area is stress while deformation is a strain. The most important parameter describing melt rheology is viscosity. Viscosity is resistance to flow and is due to the relationship between applied stress and deformed strain (Aho et al. 2015). Materials are broadly classified as Newtonian or non-Newtonian fluids. Melt flow behaviour to an applied stress can be categorised as viscous flow, elastic deformation or viscoelasticity. Elastic deformation means the material continues to deform as a function of stress but retards to its original form upon removal. Viscous flow works the exact opposite and does not retard upon removal of stress. Viscoelastic materials exhibit a mixture of both elastic and viscous flow. Most polymers are viscoelastic in nature and behave as non-Newtonian fluids. The viscosity of non-Newtonian materials is not constant and the relationship between stress and strain can be non-linear (Mezger 2011). Polymer melts also show shear thinning behaviour as the melt viscosity decreases with increase in shear. This behaviour is of critical importance in terms of HME processing.

During HME, processing parameters like torque, pressure and die swell will be impacted if appropriate temperature profiles are not used and a direct implication on the melt flow of the API-polymer blend will be observed. Further, surface roughness or shark skin effect can be observed due to less shear thinning (Mezger 2011). Hence, studying of melt rheology is important in HME process development. Similarly, understanding the effect of shear and strain on the extrudates will provide an insight into the selection of downstream processes and stability.

Another aspect impacting HME is the plasticisation effect imparted due to solubilisation of the API within the polymer. Solid state miscibility and solubility between API-polymer blends will impact the individual glass transition temperature to give mostly a single glass transition temperature to the system. This will have a huge impact on the processability of the materials as HME is carried out above the T_g or T_m of the blends and hence the impact of drug concentration on melt rheology in respect to plasticisation needs to be investigated in detail. Plasticisation will also have an impact on the mechanical properties of the extrudates which will have a direct effect on the choice of downstream processes (Van Renterghem et al. 2017b). The current work will focus on three aspects, material characterisation, melt processability and impact of plasticisation.

Rheology of the materials can be characterised by the viscosity and modulus of the material. The slope of stress and strain depicts a measure of material stiffness which is the modulus of the materials. Storage modulus (elastic modulus) represents the amount of energy stored per cycle whereas loss modulus (viscous modulus) represents the portion of strain which is 90° out of phase (Jones et al. 2012). The storage modulus and loss modulus are symbolised as G', G'' and E', E'' for melt and solid phase. The ratio of loss modulus to storage modulus is the tangent of the phase angle between the stress and strain is called Tan delta (δ) (Cogswell 1981; Menard 2008; Mezger 2011).

Rheological measurements can be carried out using a time-temperature superimposition principle also called the Boltzmann superposition principle. The effect of modulus as a function of time or temperature at the constant time,

temperature, strain, stress, and amplitude is studied (Menard 2008; Jones et al. 2015). Rotational rheometer and DMA experiments are conducted in the linear viscoelastic region where applied stress is proportional to deformed strain. Measurement of melt rheology is done using rotational rheometry (low shear rates) and capillary rheometry (high shear rates).

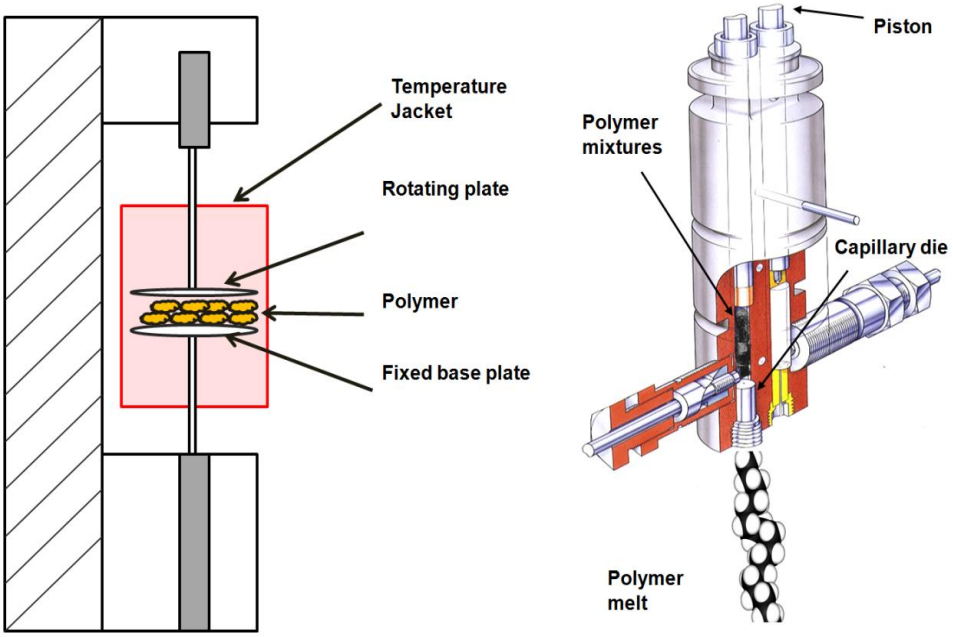

Figure 5.3 Schematic representation of rotational (left) and capillary (right) rheometer (Kelly 1997)

Capillary rheometry mimics the melt flow through an extruder die by subjecting the samples in a pre-heated barrel through various shear rates (Figure 5.3). Capillary rheometers are used to determine shear and extensional properties of the fluid under a range of shear strain rates and temperatures. Capillary rheometers can measure shear rates from 10 to $10^6 s^{-1}$. Melt viscosity is significantly affected by temperature, pressure and flow rate. In capillary rheometry, a sample is melted before being extruded by a piston through a capillary die. Pressure drop through the die is measured at a known flow rate,

defined by piston velocity. Shear stress across the wall is measured by the drop in pressure through the capillary die. Capillary rheometer typically generates shear rates similar to HME and thus mimics the process except mixing element. The values of wall shear stress (τw) and the apparent shear strain rate (γ° app) for Newtonian fluids is obtained using the following equation (Paradkar et al. 2009):

$$\tau w = \frac{D\Delta P}{4L} \qquad \gamma^{\circ} app = \frac{4Q}{\pi R3}$$ Equation 5.1

Where,

ΔP Pressure drop (Pa)

L Length of the die (m)

D Diameter of the die (m)

Q Volumetric flow rate (m^3/s)

R Radius (m)

As stated before, most of the polymers used in pharma are non-Newtonian fluids hence a correction is needed. Slip at the die wall and end pressure drop was corrected by using a zero die (orifice die) and Bagley correction. The revised equation for shear stress is:

$$\tau w = \frac{(\Delta P_L - \Delta P_o) \times R}{2L}$$ Equation 5.2

The complex viscosity is calculated by:

$$\eta = \frac{\tau w}{\gamma app}$$ Equation 5.3

Rotational rheometry is used to study the shear dependent behaviour of the materials. The effect of temperature and viscous and elastic behaviour can be studied using this rheometer. Rotational rheometry is useful in studying melt rheology between shear rates of 0.001 to $100s^{-1}$. A parallel plate rotational rheometer was used to decrease the equilibrium time between internal and external stress which is useful for viscoelastic polymers. This type of geometry is recommended for viscous polymers. Gap size between the plates is typically 1mm. Stress was applied in an oscillatory mode which was generated with one bottom stationary plate and an upper moving plate (Figure 5.3). To understand at what strain the material can undergo without damage, amplitude sweeps were carried out where the samples was oscillated at a low frequency at increasing strains to find out the linear viscoelastic region (LVE) and yield point which point after which stress and strain are not directly proportional to each other. The samples were then held at constant strain with varying shear rates to calculate modulus and viscosity. The complex viscosity is calculated by:

$$\eta = \frac{2MH}{\pi R^4 \omega} \qquad \text{Equation 5.4}$$

Where, η is the viscosity, M is the torque, ω is the angular frequency, R is the radius, H is the gap size (Mezger 2011).

DMA is used to study the mechanical properties of the extrudates. Modulus is generated by applying an oscillating force to materials and analysing its response. DMA can be used to understand the following (Jones et al. 2012):

1. The tendency to flow i.e. Dynamic viscosity in its solid state
2. Stiffness within the material i.e. Storage and Loss modulus
3. Ability to lose energy as a function of temperature i.e. damping

4. Ability to recover after release of energy i.e. Elasticity.

The storage (elastic) modulus E' and loss (viscous) modulus E'' is defined as follows (Jones et al. 2012):

$$E' = \left(\frac{\sigma_0}{\gamma_0}\right)\cos\delta \qquad E'' = \left(\frac{\sigma_0}{\gamma_0}\right)\sin\delta \qquad \text{Equation 5.5}$$

Understanding rheology as stated not only will help in process development but also provide an insight into challenges during downstream processing and stability. Depending on the viscosity, tensile strength, and modulus of the extrudates, downstream process can be selected. Stability plays an important in formulation development of the ASD. Tracing of crystallisation of API is one of the key parameters during product development of ASD. The objective of the present study is to understand the effect of ibuprofen concentration on the mechanical and rheological properties of IBU-Aff^{TM}HPMC extrudates by HME. The extrudates were pelletised and compressed into films for rheological studies. Detailed investigation of extrudates include (1) effect of % IBU load on the extrusion temperature and torque along with tracking of of-line crystallisation kinetics for 40% drug load extrudates, (2) complex viscosity variation using capillary and rotational rheometers (3) effect of the G',G'', E' and E'' with increase in % ibuprofen concentration within the extrudates. Additionally, correlation of tan delta values with theoretical glass transition values obtained using Fox equation. Dissolution of all the pellets was compared. Type of release mechanisms were studied by model fitting to calculate the rate of release constant using different models.

5.1.2 Results and Discussion

Preparation of the extrudates and films with HME and CM (Figure 5.4) was briefly described in chapter 3. Confirmation of solid state stability of the extrudates is explained in chapter 5.3.

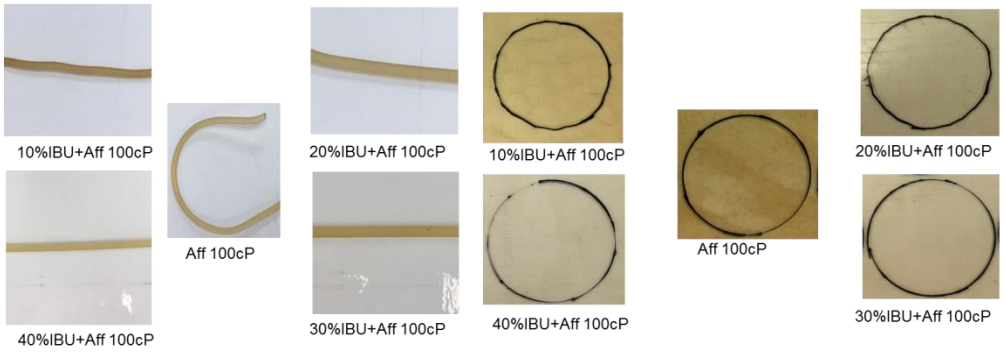

Figure 5.4 Ibuprofen-Affinisol 100cP extrudates and films

5.1.2.1 Effect of drug concentration on the extrusion temperature and torque

Set temperature profile for HME is an important parameter for consideration. The temperature profile will have a direct impact on the torque and pressure generated during HME. Torque is generated by the resistance provided by the twin screws on the molten material blends at the processing parameter. Maximum torque generated by the Pharmalab 16mm extruder is 32Nm i.e. 16Nm by each screw. For data equality, the higher range of extrusion temperature window for each ibuprofen-Affinisol 100cP blend was selected. To ensure similar conditions for each blend, screw configuration, screw speed and feed rate were kept constant. A linear decrease in torque was observed with an increase in the concentration of IBU in the extrudates (Figure 5.5). This affirms the plasticisation effect of ibuprofen on the ibuprofen-Affinisol 100cP blends which decreased the T_g of the ASDs.

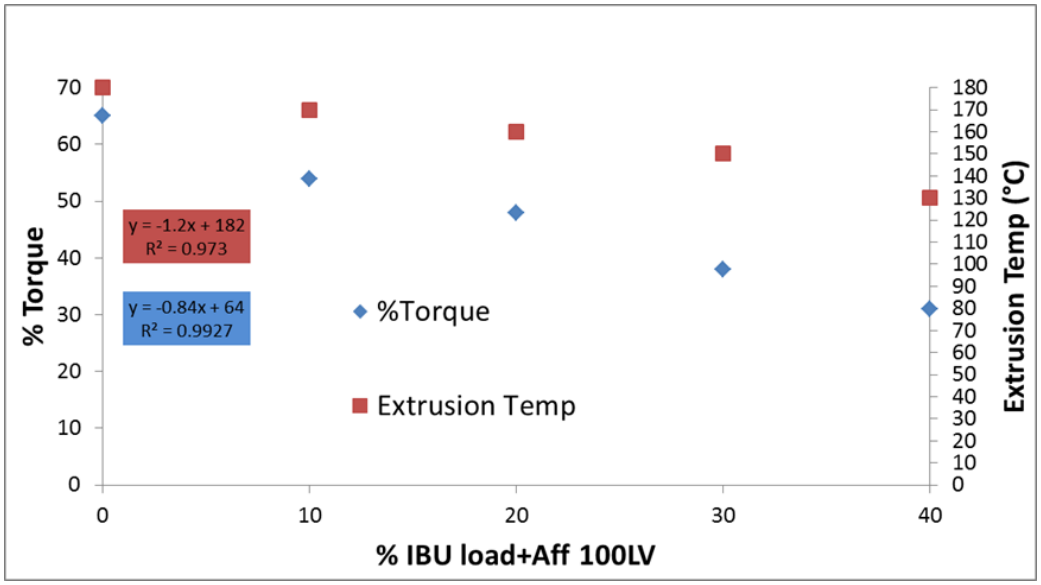

Figure 5.5 Torque analysis for ibuprofen-Affinisol 100cP blends

5.1.2.2 Melt Rheology

5.1.2.2.1 Effect of IBU concentration on complex viscosity at different temperatures

Shear rates affect the melt viscosity of the material and hence their effect should be studied in detail. Figure 5.6 shows an overlay of shear viscosity vs shear rate for Affinisol 100cP and ibuprofen-Affinisol 100cP extrudates. The correlation was established for at least one common temperature between each % IBU load except for 40% IBU load. An increase in shear viscosity was observed for each blend with a decrease in temperature. Additionally, shear viscosity at the extrusion temperature for each blend was observed to decrease with increase in % IBU load. This affirms the decrease in torque observed during extrusion of all the blends.

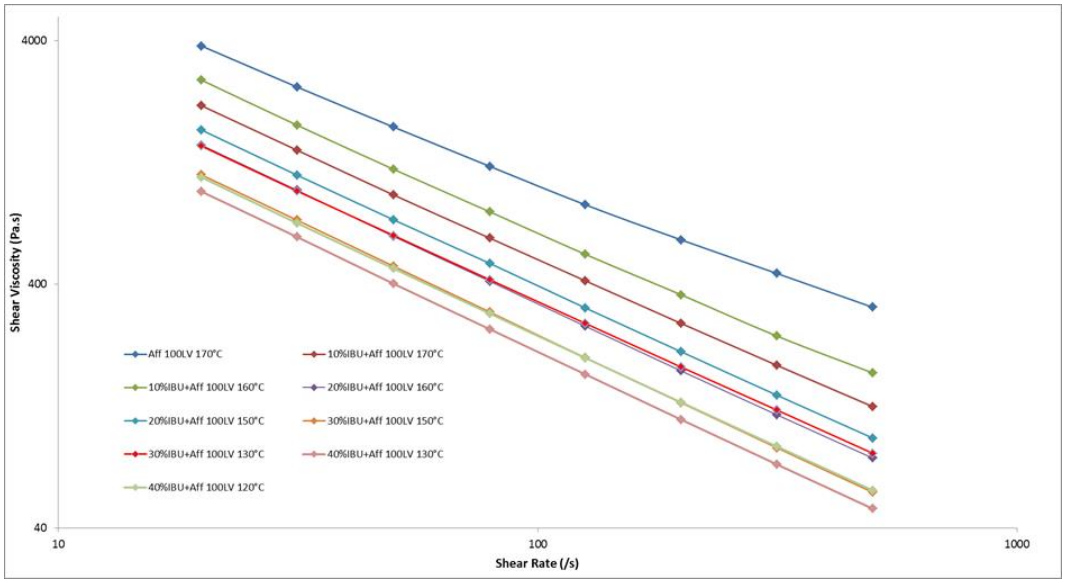

Figure 5.6 Overlay of capillary data for ibuprofen and Affinisol 100cP blends

The data obtained from capillary rheometry was using the Power law equation (Paradkar et al. 2009):

$$\eta = K * (\sigma)^{n-1} \qquad \text{Equation 5.5}$$

Whereby, σ is shear rate, n is the power law index and K is consistency index. They both are obtained by plotting log shear stress vs log shear rate. The slope of the line provides the power law index where the consistency index is the intercept.

Power law index indicates whether the blends depict shear thinning or thickening capability, n < 1 indicates shear thinning. Table 5.1 provides the power law index and consistency index for the ibuprofen-Affinisol 100cP blends.

% IBU-Affinisol 100cP extrudates	Shear Thinning index (n)	Consistency index (k)	Temperature (°C)	R^2
Affinisol 100cP	0.2026	134.66	180	0.94
	0.3202	151.03	170	0.96
	0.2525	208.58	160	0.54
10%IBU	0.115	128.59	170	0.93
	0.1631	143.66	160	0.96
	0.2441	162.55	150	0.96
20%IBU	0.0683	117.42	160	0.92
	0.0841	118.32	150	0.91
	0.0965	136.02	140	0.93
30%IBU	0.0481	102.56	150	0.90
	0.0564	98.202	140	0.93
	0.0719	99.685	130	0.90
40%IBU	0.0416	85.778	130	0.91
	0.05	85.121	120	0.91
	0.0541	89.66	110	0.84

Table 5.1 Power law and consistency index of ibuprofen and Affinisol 100cP blends

All the blends showed shear thinning and an increase in the shear thinning index was observed with decrease in temperature with an exception of Affinisol 100cP at 160°C which also showed lower regression value. However, the shear thinning ability of extrudates increased with an increase in % IBU load within the extrudates.

5.1.2.2.2 Effect of Angular Frequency/Time sweep on Complex Viscosity of different % drug load extrudates

Shear thinning was observed in all ibuprofen-Affinisol 100cP blends. Hence a detailed investigation of the effect shear rate on viscosity is important. Rotational rheometry was used to study the viscosity with respect to angular frequency. Additionally, shear rheology provides storage modulus (G') and

loss modulus (G'') which provide information on the elastic and viscous behaviour of the polymer respectively. As stated previously, polymers used for Pharma are viscoelastic in nature hence, G' and complex viscosity will be used for correlation with other rheometry. All experiments on the rotational rheometer were carried out at 0.1% strain. Figure 5.8 shows an overlay of G' vs angular frequency for Affinisol 100cP and ibuprofen-Affinisol 100cP blends. For similar comparison purposes correlation was established for at least one common temperature between each % IBU load except for 40% IBU load. A decrease in storage modulus was noted with a decrease in temperature within the particular blend. However, storage modulus decreased with increase in ibuprofen concentration of the films. Time sweep experiments for all the blends showed no variation in G' and G'' which indicated that the extrudates showed no thermal degradation for 30 mins thus confirming no solid state degradation (Figure 5.7).

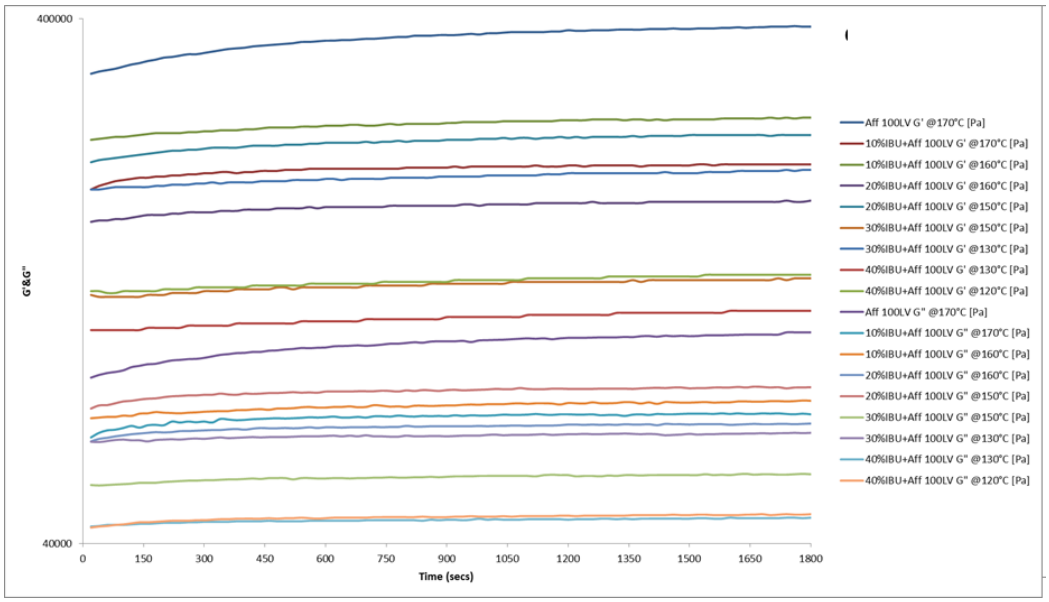

Figure 5.7 Time sweep experiments of ibuprofen and Affinisol 100cP blends

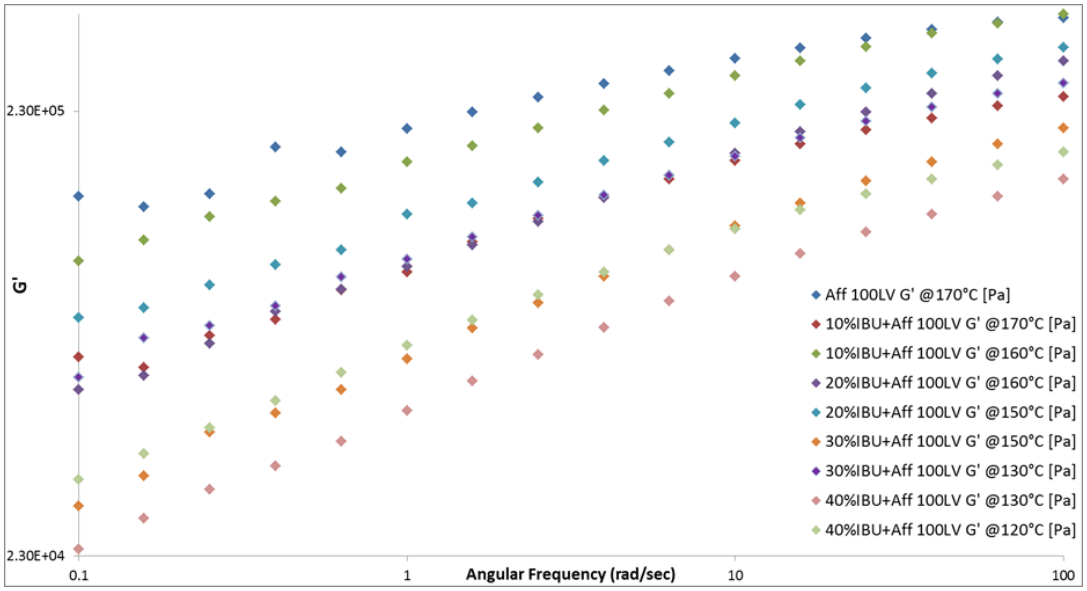

Figure 5.8 Frequency sweep experiments of ibuprofen and Affinisol 100cP blends

Complex viscosity at given measuring point can be calculated by using values of shear stress, strain, time and temperature. For comparison and to provide a better understanding of the rotational rheometer data, various mathematical models functions are available for curve fitting (Aho et al. 2016). These can be utilised to calculate complex viscosity which can further determine important parameters like yield point and zero shear viscosities. For the following study, a Carreau-Yasuda model was used to calculate complex viscosities and correlate the same with experimental values. The model predicts the complex viscosity by using material time constant ʎ, power law index ɳ which denotes shear thinning capability and Yasuda constant p which provides a transition region between zero shear-rate and power law.

Experimental results and model fitting results were found to be in accordance with all the blends. Figure 5.9 shows the overlay of complex viscosity obtained from Carreau-Yasuda model vs angular frequency.

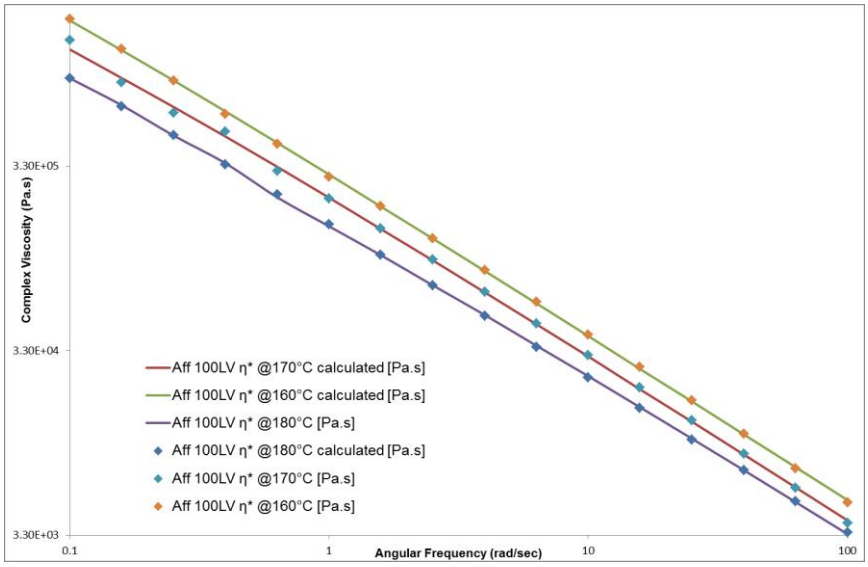

Figure 5.9 Complex viscosity obtained using Carreau-Yasuda model fit for Affinisol 100cP

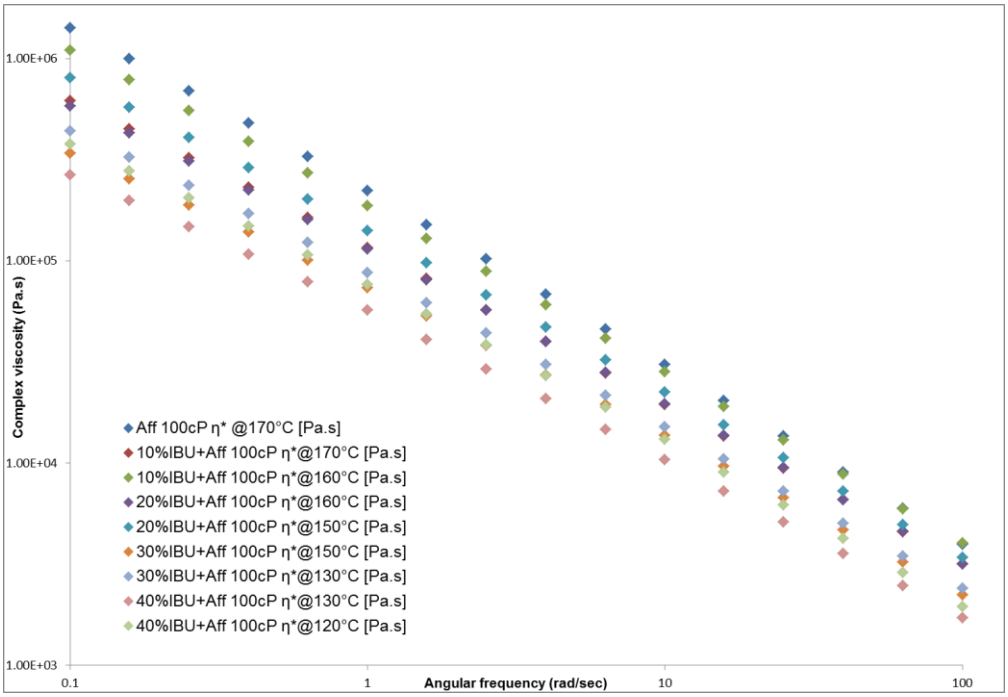

Figure 5.10 Complex viscosity obtained using Carreau-Yasuda model fit for ibuprofen and Affinisol 100cP blends

A similar trend was observed for complex viscosity. Complex viscosity increased with a decrease in temperature within the same blend whereas it increased with decrease in %IBU (Figure 5.10).

The focus of the study was to understand the melt behaviour of the API-polymer blends over a range of temperature and shear rates. Linking rotational rheometer data over a range of angular frequencies with capillary rheometer data over a range of shear rates can help map and track complex melt viscosity behaviour over a range of shear rates. These effects can be studied by using Cox-Mertz rule.

Cox and Merz (Cox and Merz, 1958) derived an equation which links complex viscosity obtained from rotational to steady shear rate-viscosity obtained from capillary rheometers:

$$\lim_{\omega \to 0} (\eta^* \omega) = \lim_{\gamma \to 0} \eta(\gamma) \qquad \text{Equation 5.6}$$

Data obtained from capillary and rotational rheometer were fitted together using Cox-Mertz equation. Figure 5.11 shows an overlay of Cox-Mertz rule for all ibuprofen-Affinisol 100cP blends.

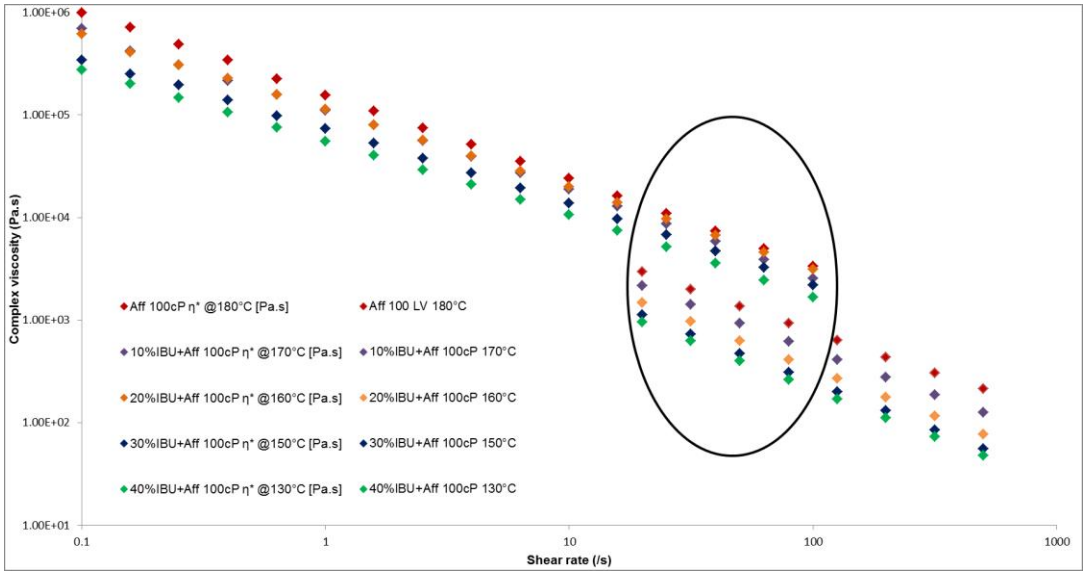

Figure 5.11 Cox-Mertz rule for ibuprofen and Affinisol 100cP blends

All blends did not follow the Cox-Mertz rule as rotational data and capillary data were found not to overlap. Generally, Cox-Mertz holds true for polymeric blends which melt and dilute and is generally seen in polymers with linear branching. Also, G' data was higher than G'' data for all the blends which indicated the visco-elastic nature and thus does not follow the rule. However, the difference was found to be less for Affinisol 100cP and 10% IBU-Affinisol 100cP blends compared to other blends. This can attributed to the sudden decrease in the viscosity of the extrudates with increase in ibuprofen content. Generally, the Cox-Mertz rule is not followed when the polymer has more than one phase or have additives added.

5.1.2.2.3 Effect of mechanical force and modulus generated by DMA on different % drug load extrudates

Understanding melt rheology has gained importance and detailed studies have been increasingly carried out. However, less attention has been given to understanding the rheology of the extrudates in its solid state. This is of importance as different drug loads have an effect on the tensile strength of the extrudates and can provide an insight into understanding the crystallisation of the extrudates. Additionally, storage and loss modulus can highlight the challenges arising during downstream process like milling.

The current focus is on mechanical studies carried out using a Dynamic Mechanical Analyser (DMA). Modulus is generated within DMA by applying an oscillating force to a sample and analysing its response (Jones et al. 2012). It is predominantly done to study the viscoelastic properties of the extrudates which are primarily contributed to by the polymer used in the physical mixture. % strain for the current studies was found to be 0.1% which was calculated by

performing strain sweep experiments at an isothermal temperature of 25°C and at a constant frequency of 1Hz. Storage modulus or elastic modulus E' represents the amount of energy stored per cycle. Loss modulus (viscous modulus) E'' represents the portion of strain that is 90° out of phase. The ratio of loss modulus to storage modulus is the tangent of the phase angle between the stress and strain is called Tan delta (δ). Effect of temperature ramp on both moduli was studied using DMA.

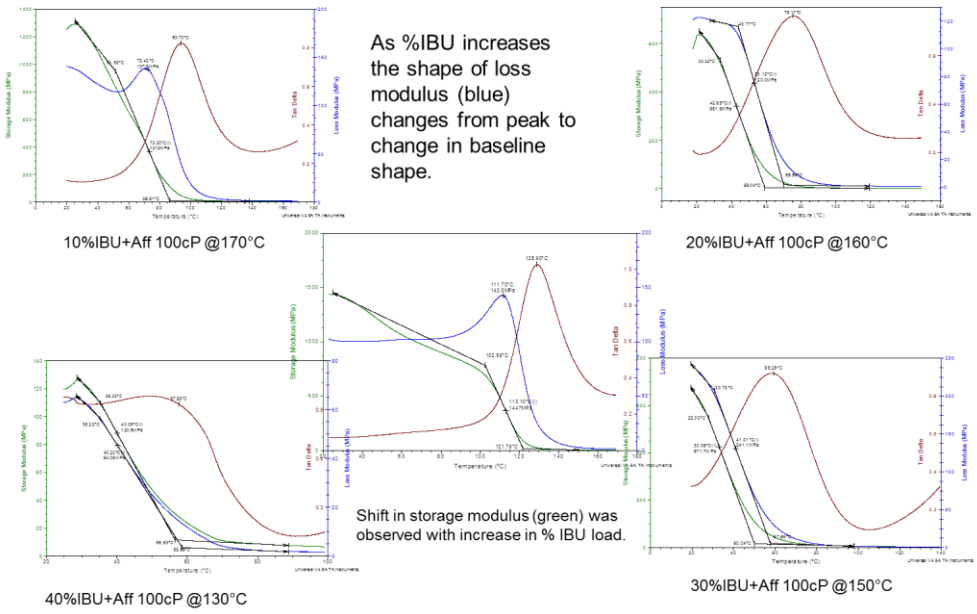

Figure 5.12 DMA thermograms for ibuprofen and Affinisol 100cP blends

Figure 5.12 shows an overlay of Temperature ramp DMA runs at a controlled strain of 0.1% for all the ibuprofen-Affinisol 100cP blends. Interestingly, the viscous modulus (E'') drastically decreased with an increase in % IBU load. A similar decrease in Storage modulus (E') and Tan delta (Δ) values was observed with increase in % IBU load. This could be due to plasticity imparted by increased ibuprofen content. Thus, high ibuprofen content increases the elasticity of the extrudates which could be detrimental to a downstream process like milling. Extrudates above 20% ibuprofen load are prone to provide

a challenge during milling and therefore cryo-milling of those extrudates should be considered. Hence viscosity of the extrudates decreased with increase in ibuprofen content which showed a similar trend to melt rheology values.

%IBU load	Storage Modulus °C (mid-point)	Storage Modulus Mpa	Loss Modulus °C (peak)	Loss Modulus Mpa	Max Tan delta (°C) (peak)	Fox Eqt predicted values (°C)
0	113.19	1372	112.03	145.20	128.67	120
10	73.58	1377	74.06	151.23	93.77	93
20	41.77	703.33	53.99	131.83	73.60	71
30	36.02	455.6	40.22	189.67	59.32	53
40	34.73	191.57	34.39	99.46	45.03	34.91

Table 5.2 DMA data of ibuprofen and Affinisol 100cP blends

Glass transition temperature for API-polymer blends represents the kinetic boundary of molecular mobility (Qian et al. 2010). Below glass transition temperature molecules have less molecular mobility and thus decrease chances of recrystallisation and thus are more stable. Of various techniques available DSC and DMA are commonly used for detection of glass transition temperature (Lin and Huang 2010). For the current ibuprofen-Affinisol 100cP blends, no glass transition event was observed in DSC. This could be due to the viscous nature of the Affinisol 100cP. DMA was also used to detect T_g. The peak observed in Tan delta is considered as the glass transition temperature of the blend due to the crossing over of E' and E''. This point signifies relaxation within the extrudates.

Predictive equation models for determination of glass transition temperature of solid dispersion blends are available (Jayachandra Babu et al. 2009). Of

these, the Fox equation is the simplest and assumes random mixing between two components and equal heat capacity value contribution (Kalogeras and Brostow 2009). It is the only equation which calculates the glass transition from pure components only and does not involve any fitting parameters (Jayachandra Babu et al. 2009; Kalogeras and Brostow 2009). Thus, it can be inferred that ASDs formed purely due to solid-state miscibility should follow values generated using the Fox equation.

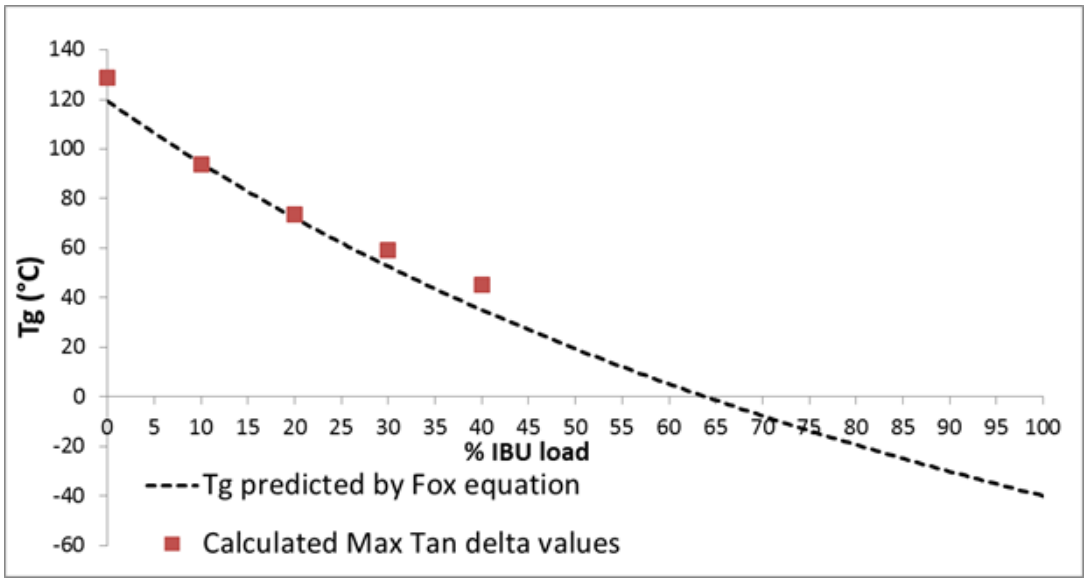

Figure 5.13 Experimental and theoretical glass transition temperature values of ibuprofen and Affinisol 100cP blends

The Tan delta values obtained were found to correlate with the theoretical values obtained by the Fox equation (Table 5.2 and Figure 5.13). Also, co-relation was seen more for 10 and 20%w/w drug loading. Fox equation as stated, assumes random kinetic mixing between API and polymer and hence slight deviation will be due to insolubility. Thus, the deviation suggests the supersaturation of IBU within Affinisol 100cP above 20%w/w.

Formation of amorphous solid dispersions between ibuprofen and Affinisol 100cP thus could be purely due to solid-state miscibility of the two. Correlation between values obtained by the Fox equation and DMA confirm the absence of inter-component interaction in the melt and glassy state of the ibuprofen-Affinisol 100cP mixture. Along with an overview of the visco-elastic nature of extrudates, the DMA was also helpful to identify the absence of inter-component interaction between ibuprofen-Affinisol 100cP blends.

The main aim of the study was to understand and track the rheology of the API-polymer blends from the melt phase to an amorphous solid dispersion phase. Rotational and capillary rheometers were able to provide an overview of the complex viscosity over a range of shear rates. Time sweep data from rotational rheometry confirmed the absence of solid state degradation with the ibuprofen-Affinisol 100cP blends for 30mins. Confidence in data was confirmed by applying a model fit using the power law model (capillary rheometer) and Carreau-Yasuda model (rotational rheometer). Model fit data were found to correlate with experimental values.

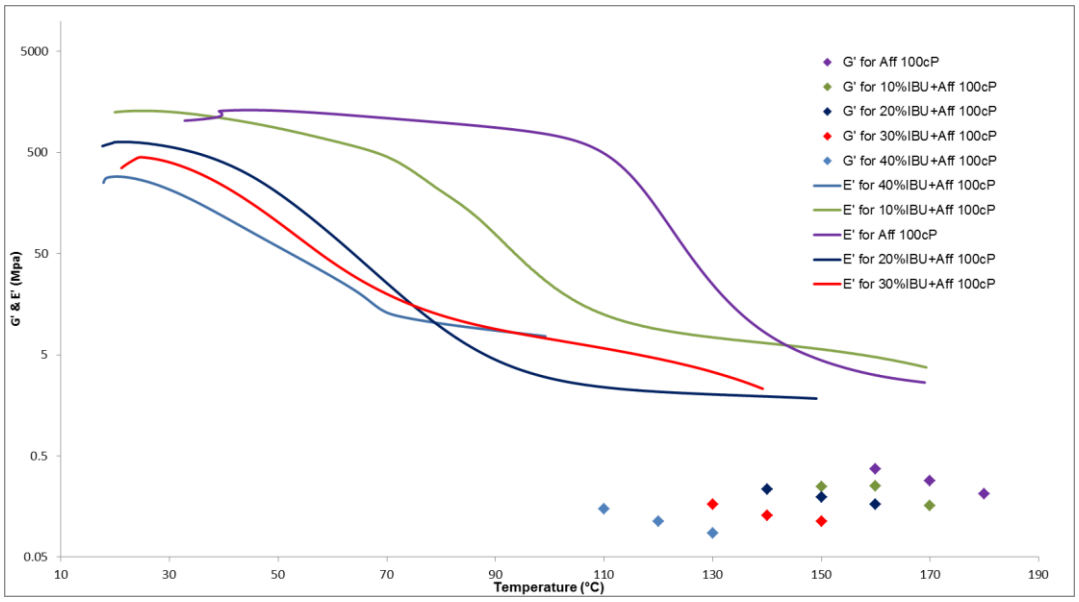

Figure 5.14 Rotational and DMA data for ibuprofen and Affinisol 100cP blends

Visco-elastic properties of extrudates were confirmed using DMA. A similar trend of decrease in viscosity was observed with increase in ibuprofen content. It also provided an insight ibuprofen drug loads which can provide a challenge during milling. Tan delta values from DMA overlapped with theoretical values obtained from Fox equation and thus confirmed the absence of inter-component interaction between ibuprofen and Affinisol 100cP in ASD. An attempt to map the storage modulus E' & G' obtained from DMA and rotational rheometry over a range of temperature can be seen in figure 5.14. A large difference was observed between the moduli of melt and a solid phase for all the ibuprofen-Affinisol 100cP blends. Thus, understanding shear thinning behaviour and visco-elastic nature of extrudates provide a platform for optimisation of process for amorphous solid dispersion using HME.

5.1.2.2.4 Crystallisation kinetics using an ortho-analytical approach

Solid state stability of amorphous solid dispersions is one of the limiting steps in its development. A detailed investigation of the rheology of ibuprofen and Affinisol 100cP from its melt phase to the solid phase was conducted. In-line tracking of crystallisation of extrudates of 40% ibuprofen load was carried out. Off-line tracking of extrudates were carried out at three different stability conditions and recrystallisation analysed with an ortho-analytical approach using XRD, DSC and Raman spectroscopy. These studies are discussed in detail in chapter 5.3.

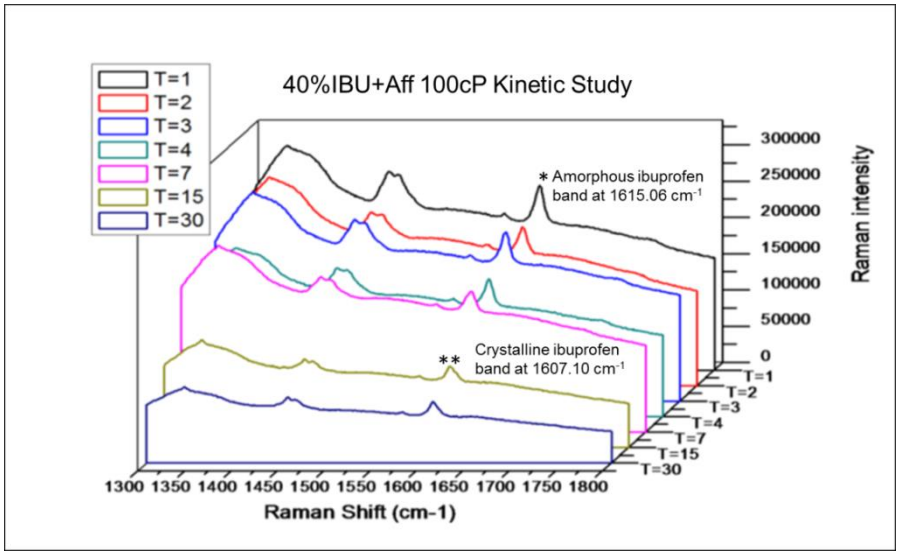

Figure 5.15 In-line Raman studies of 40% ibuprofen and Affinisol 100cP blend

40%ibuprofen-Affinisol 100cP extrudates took 15 days for recrystallisation on open exposure (Figure 5.15). A decrease in a shift of the Raman band of 1615cm^{-1} to 1607cm^{-1} was observed. This shift is attributed to aryl chain deformation and C-H stretching and bending which occurs due to disorder within the structure and is characteristic of the amorphous state of ibuprofen (Liu and Gao 2012). The recrystallisation of the extrudates was quicker due to its low glass transition temperature of 45°C which was calculated using DMA. Raman spectroscopy was able to track the recrystallisation of the 40% ibuprofen loaded extrudates.

5.1.2.2.4 Drug release

Drug release mechanisms of solid dispersions were described in chapter 2. In ASDs, the release of the drug primarily depends on the drug entrapment within the polymer matrix. However, physicochemical properties of the product and thermal processing history can also have an effect on dissolution (Yang et al. 2016; Chen et al. 2017a; Chen et al. 2017b). Dissolution of the product follows the Noyes-Whitney equation where the rate of dissolution (dc/dt) is directly

proportional to surface area and inversely proportional to the drug-polymer layer thickness (Siepmann and Siepmann 2013).

$$\frac{dc}{dt} = \frac{\mathbf{D\,A}}{\mathbf{d}}\ (\mathbf{Cs} - \mathbf{C}) \qquad \text{Equation 5.7}$$

Where $\frac{dc}{dt}$ is the rate of dissolution, $\mathbf{D}$ is the diffusion co-efficient, $\mathbf{d}$ is boundary layer thickness, $\mathbf{Cs}$ is the saturation solubility, $\mathbf{C}$ amount of drug dissolved at time T.

Visual observations of the pellets at the start and end of dissolution time can be seen in Figure 5.16. Visual observations show that the release of ibuprofen through the matrix is dual in nature. The polymer boundary swells but drug releases through erosion. More studies need to be performed to confirm these mechanisms.

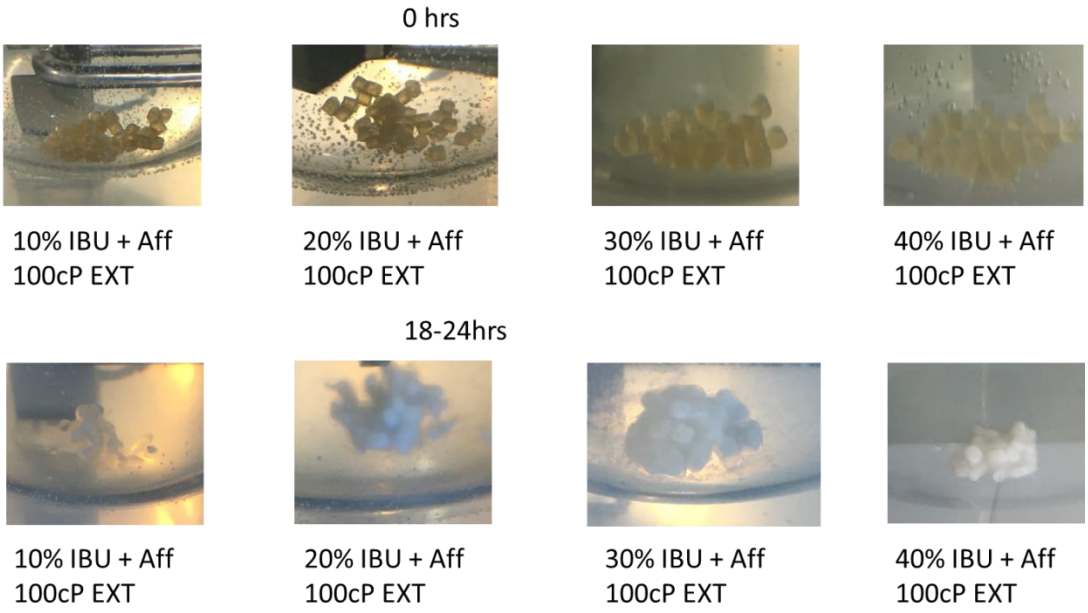

Figure 5.16 Dissolution of ibuprofen and Affinisol 100cP pellets

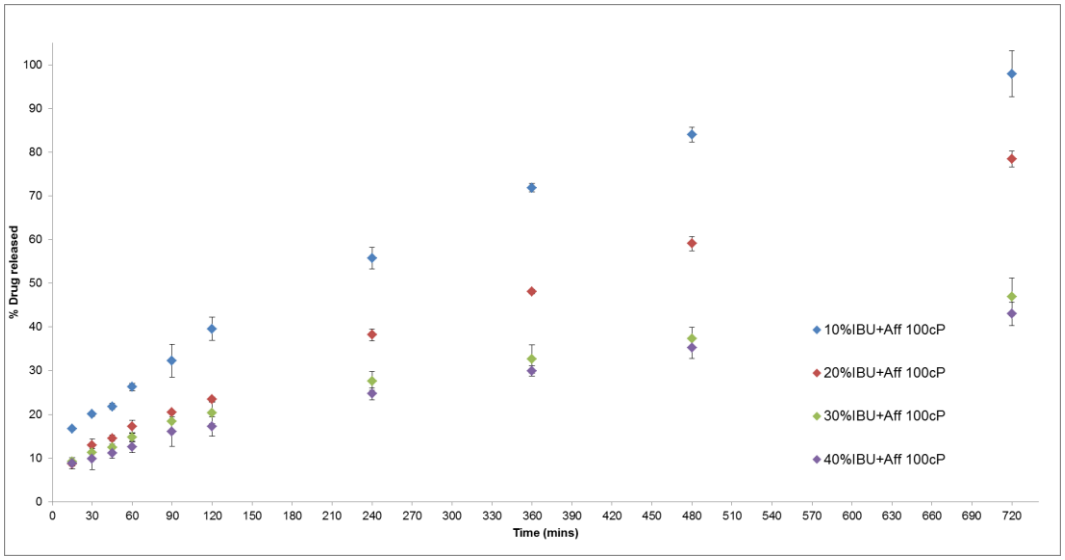

Figure 5.17 Drug release of ibuprofen and Affinisol 100cP pellets

All the ibuprofen-Affinisol 100cP pellets showed sustained release. Drug release reduced with increased ibuprofen concentration in the extrudates. This could be due to recrystallisation of ibuprofen within the matrix which will act as a barrier to the boundary layer and thus decrease drug release (Costa et al. 2003). Also, ibuprofen dose was not kept constant across all the %drug load extrudates.

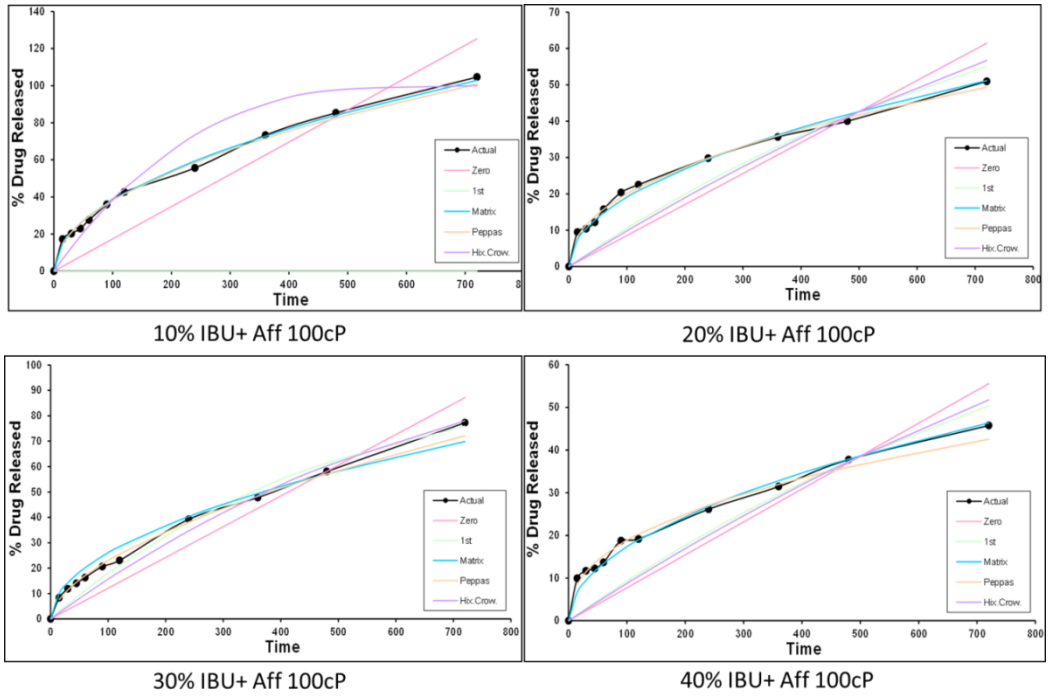

Figure 5.18 Dissolution kinetic model fitting for ibuprofen and Affinisol 100cP pellets

Drug-polymer system	Model fitting					Release mechanism
	Zero-order	1st Order	Higuchi	Hix. Crow	Peppas	
10%Ibuprofen-Affinisol 100cP pellets	R^2 = 0.8665 k = 0.1740	*	R^2 = 0.9982 k = 3.8343	R^2 = 0.9938 k = -0.0015	R^2 = 0.9938 n = 0.4943 k = 3.9002	Peppas
20%Ibuprofen-Affinisol 100cP pellets	R^2 = 0.9408 k = 0.1211	R^2 = 0.9916 k = -0.002	R^2 = 0.9875 k = 2.6049	R^2 = 0.9861 k = -0.0006	R^2 = 0.9970 n = 0.580 k = 1.5896	Peppas

30%Ibuprofen-Affinisol 100cP pellets	R^2 = 0.7975 k = 0.0854	R^2 = 0.9082 k = -0.0011	R^2 = 0.9963 k = 1.9076	R^2 = 0.8780 k = -0.0003	R^2 = 0.9963 n = 0.4586 K = 2.4154	Peppas
40%Ibuprofen-Affinisol 100cP pellets	R^2 = 0.7739 k = 0.0772	R^2 = 0.8873 k = -0.001	R^2 = 0.9934 k = 1.7285	R^2 = 0.8559 k = -0.0003	R^2 = 0.9888 n = 0.4128 k = 2.8131	Peppas

Table 5.3 Model fit parameters for ibuprofen and Affinisol 100cP pellets *Insignificant

To obtain a detailed understanding of the drug release of all blends, release kinetics with different model fitting was carried out. Mathematical models are well established and extensively used for release kinetic prediction (Costa et al. 2003; Baishya et al. 2017; Hirai et al. 2017). The current study involves the use of Zero order, 1st order, Higuchi, Hixson-Crowell and Korsmeyer-Peppas model to study release kinetics. These models were specifically developed for drug-polymer diffusion systems.

Zero-order release kinetics is one of the simplest where constant drug release is achieved at all given time points. If the drug dissolution follows zero order kinetics then the release is found to be controlled release.

First order kinetics depends on the concentration of the drug within the polymer matrix.

The Higuchi or Matrix model was the first model developed for drug-polymeric diffusion systems. Drug diffusion through a polymer matrix can either be

Fickian or non-Fickian. Fickian diffusion is when the rate of drug release is independent of the drug concentration. The Higuchi model assumes the drug diffusion to be Fickian in nature and assumes both dissolution and diffusion happening at same time.

The Korsmeyer-Peppas model builds upon Higuchi model. Once, drug diffusion is established by the Higuchi model, the Korsmeyer-Peppas model focuses on the mechanisms of dissolution from the matrix. It also considers swelling of polymer which is not considered in Higuchi model. Along with kinetic constant k ,it also calculates the release component n. Depending on the value of n, one can predict the type of diffusion (Costa et al. 2003).

The Hixson-Croswell model takes into consideration the surface area and diameter of the particles. Thus, it is a strong model for the understanding of drug-diffusion within polymer matrix by an erosion mechanism. However, this model is used for powders and thus is not applicable for pellets. An overview of the models used is provided in table 5.4.

Release models	Type of release mechanism
Zero-order	Constant release rate
First order	Dependent on the concentration of the drug
Higuchi	Fickian diffusion mechanism
Krosmeyer-Peppas model	Diffusion based mechanism n<0.45 = Fickian Diffusion, 0.45<n<0.89 = Non Fickian Diffusion, n>0.89 = Zero order release
Hixson-Croswell	Erosion based mechanism

Table 5.4 Overview of dissolution kinetic model fitting (Costa et al. 2003; Baishya et al. 2017)

The entire model fit graph and calculated release constant with a regression coefficient for all the extrudates can be seen in Figures 5.17 and 5.18 and Table 5.3 and 5.4.

All the ibuprofen-Affinisol 100cP pellets showed best fit for Korsmeyer-Peppas models. The release rate constant was also highest for the Korsmeyer-Peppas model. The release component n was higher than 0.45 for all the pellets hence, drug diffusion follows a non-Fickian mechanism. This could be due to a solid barrier formed due to crystallisation of extrudates for higher drug loading of 30 and 40%w/w. Thus, dissolution kinetics is dependent on ibuprofen concentration for all pellets.

To summarise, model fitting of dissolution data for the extrudates confirmed that the drug release for all pellets was sustained release. Drug diffusion through the polymer matrix was due to a dual mechanism of swelling and erosion. The decrease in dissolution rate with increase in ibuprofen concentration was due to recrystallisation of ibuprofen within the polymer matrix.

5.2 Effect of process parameters on the product performance if IBU-Affinisol 100cP solid dispersion

The current study focusses on the effect of process parameters on the product performance using hot melt extrusion. Taguchi method was used to analyse the effect of process variables, feed rate, screw speed and configuration. Mean residence time, torque and pressure were used as in-line responses while DSC and dissolution were used as responses for the extrudates generated. A detailed description about process parameters and responses used was provided in chapter 3.

5.2.1 Introduction

To understand the effect of critical process parameters on the critical quality attributes, a design of experiments or multivariate analysis can be carried out. Depending on the criticality, level of the factorial design is fixed (Montgomery 2000). A full factorial design provides insight on effect of a single parameter as well as interactions between parameters.

As discussed in chapter 5.1, the HME process window was set for all drug loadings of ibuprofen and Affinisol 100cP blends. The aim was to focus on process parameters apart from temperature profiles, hence independent parameters like feed rate, screw speed and screw design were selected. In-line response data was collected using residence time, torque and pressure while offline response data was collected using DSC and dissolution. The entire design was carried out using a Taguchi method as the focus was on finding the robustness of the ibuprofen-Affinisol 100cP blends. Hence, interactions between the parameters was not investigated.

A typical stage of conducting design of experiments involves a clearly defined design space and selection of critical process parameters. After design of the experimental space, processing runs are carried out and data is generated using in-line and off-line responses. Data generated may be refined or data treatment carried out to compensate for any personal or analytical errors. Multiple regression analysis is carried out using different responses and a model developed to establish the relationship between the dependent and independent variables. Lastly, to confirm the predictive model, Annova is applied.

The current study investigates process parameters in terms of process robustness but a full factorial design should be carried out to study the deep impact of interaction of process parameters. Responses were analysed using Taguchi method. Furthermore, multiple regression analysis using analysis of variance (ANOVA) was carried out to statistically find critical impacts by the single parameters using P-value. Non-significant variables were eliminated using backward elimination method. For the current study, 40% drug load of ibuprofen was selected. The process temperature window was wide for this drug load and viscosity of the extrudates is low due to plasticity imparted by the ibuprofen. Additionally, for offline studies the extrudates crystallise out within 3 day and a good correlation of the crystallisation kinetics can be observed at 15 days on 40°C/75%RH conditions.

5.2.2 Residence time measurement

HME consists of feeding, degassing and extruding in a continuous phase (Wesholowski et al. 2018). This process can be further broken down into solid state conveying, melting, mixing, melt conveying and shaping which are heavily impacted by different critical process parameters like feed, temperature, screw speed and configuration. A common parameter linking them all is residence time distribution.

Residence time during HME is important to determine the extent of solid state miscibility and solubility between the API and polymer to produce single phase solid dispersion. Higher residence times have a direct impact on the thermal degradation of the material. This may result in decreasing the purity of the API and increase of impurities with the extrudates (Karandikar et al. 2015). Lower residence time will impact the mixing and kneading of the blend and may in turn not produce a single phase extrudate (Ziegler and Aguilar 2003). Hence optimising residence time plays a crucial role in process optimisation using HME.

Very few studies have been reported in literature about residence time distribution. Residence time distribution (RTD) can be calculated either by a formulation/step change (Ziegler and Aguilar 2003) or by placing a tracer within the process (Reitz et al. 2013; Engisch and Muzzio 2016; Wesholowski et al. 2018). Wahl et al. calculated residence time distribution using in-line video analysis, however, analysis was performed off-line (Wahl et al. 2018). Although, residence time distribution is important factor, very few studies have been reported highlighting its importance.

A typical residence time distribution plot looks similar to a normal distribution plot (Figure 5.19). T_{onset} represents the minimum time required for molten mass to reach the die and extrude out. This parameter denotes duration time required for the process and is critical if solid state impurity is one of the critical product performances. $T_{50\%}$ represents time required for the 50%w/w of marker to extrude out from the process. This parameter is more robust and provides an average transit and mean processing time (Wesholowski et al. 2018).

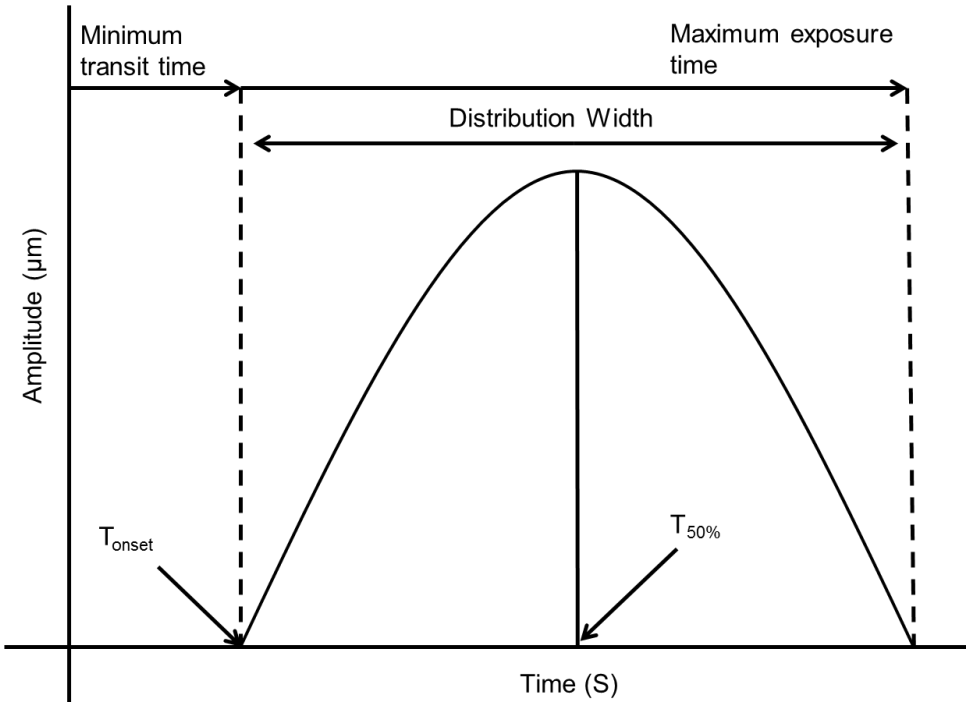

Figure 5. 19 Typical residence time distribution curve

For determination of RTD of HME, various PAT tools are available. Off-line techniques like intensity of colour (Mu and Thompson 2012), UV absorption (Reitz et al. 2013) or radioactive radiation (Janssen et al. 1979) are reported for determination of RTD. However, these techniques do not provide a true representation of the process and loss of material will be significant as compared to in-line measurements. In-line tools using magnetic susceptibility

(Puaux 2000), light scattering (Wahl et al. 2018) and UV-fluorescence spectroscopy (Wesholowski et al. 2018) are reported in calculating RTD in HME.

This study utilises an in-line high temperature UV-vis probe in continuous mode and uses a UV tracer to calculate the RTD. The method for residence time measurement was explained in chapter 3. For the DOE study, only 40% drug load was selected. However, a mono variate experiment to calculate the mean residence time was conducted for all the drug loads of ibuprofen and Affinisol 100cP blends (Figure 5.20). Screw configuration for the blends had one mixing and kneading zone and feed rate was kept constant at 0.4 kg/hr (Figure 5.21)

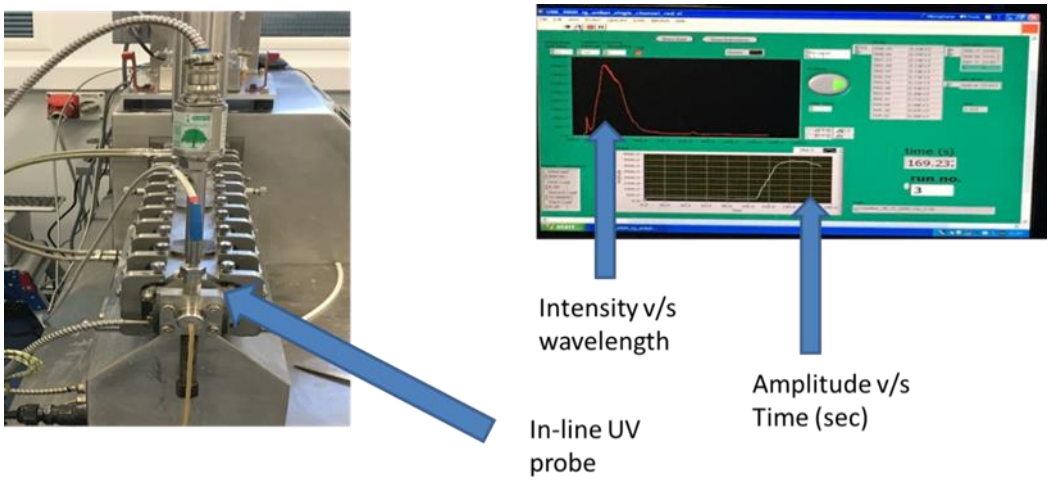

Figure 5.20 In-line UV measurement during extrusion

Figure 5.21 Screw configuration used for extrusion

For all drug loads the total batch size was 0.8kg. Duplicate runs were obtained for average and standard deviation. Data obtained is variation with respect to time (Figure 5.22). Good correlation was observed within the duplicate runs.

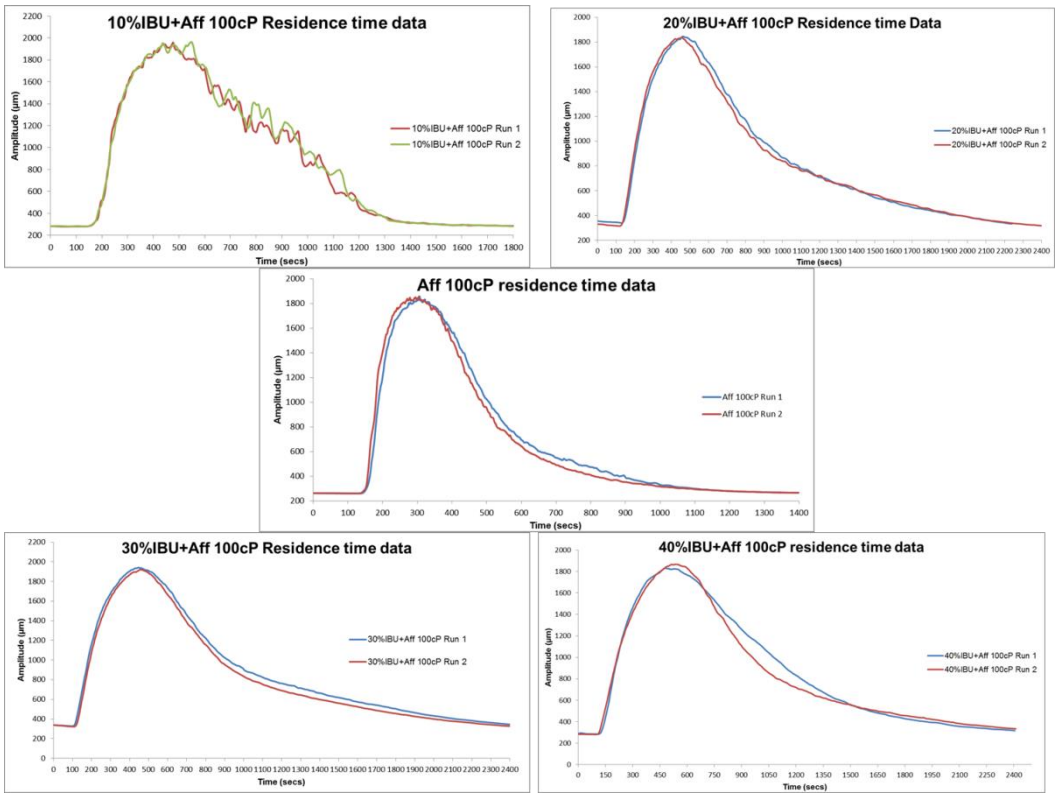

Figure 5.22 Residence time data for all ibuprofen and Affinisol 100cP blends

The data was further normalised to calculate mean residence time (MRT) (Figure 5.23).

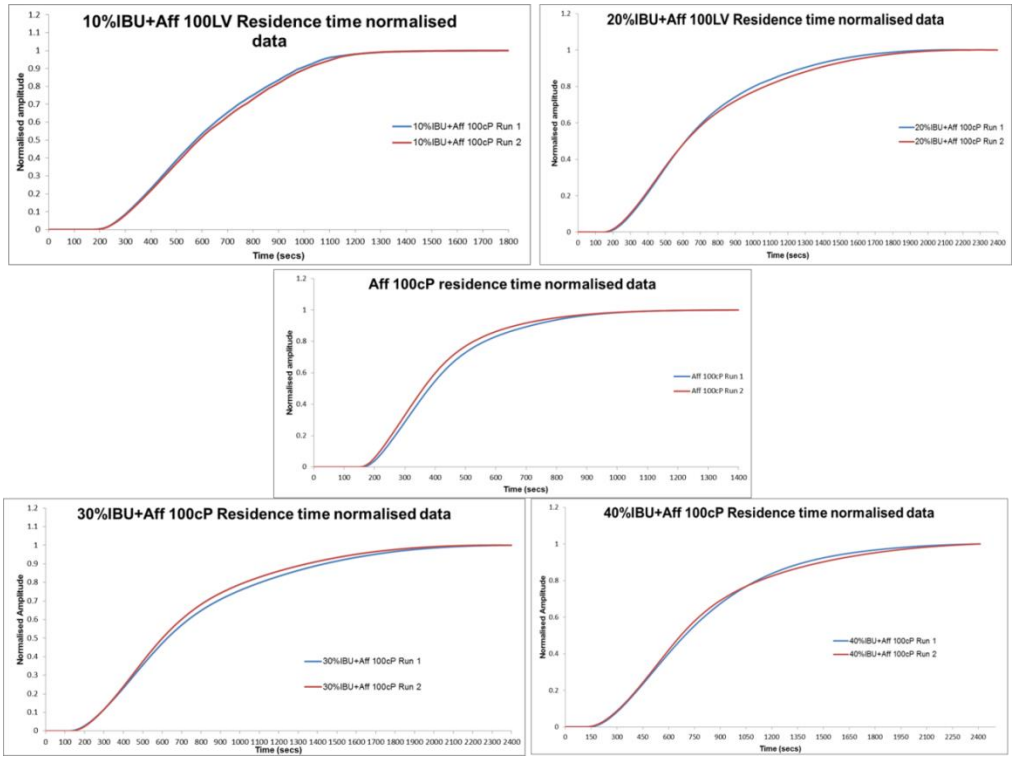

Figure 5.23 Normalised cumulative residence time data for all ibuprofen and Affinisol 100cP blends

Table 5.5 provides MRT for all the ibuprofen and Affinisol 100cP blends.

%Drug load	Mean Residence Time (secs)			
	Run 1	Run 2	Avg	SD
Affinisol 100cP	380.22	362.00	371.11	12.89
10% IBU	576.91	586.61	581.76	6.86
20% IBU	615.58	617.57	616.58	1.41
30% IBU	627.46	611.51	619.49	11.28
40% IBU	694.11	672.00	683.06	15.63

Table 5.5 Mean residence time for ibuprofen and Affinisol 100cP blends

MRT for Affinisol 100cP was found to be the lowest. This could be due to its decreased particle size and good flow properties. As ibuprofen concentration increased, an increase in mean residence time was observed at same feed rate. This confirms that the viscosity of the blend decrease with increase in ibuprofen concentration.

5.2.3 Results and Discussion

Preparation of extrudates using HME was detailed in chapter 3. Pressure and Torque was recorded in-line by the instrument, while residence time measurements were carried out using a tracer and in-line UV probe. Extrudates were further pelletised and used for dissolution studies. Duplicate runs were carried out for dissolution. Additionally, extrudates were stationed at 40°C/75%RH and analysed for recrystallisation on 15th day using DSC in duplicates.

Run order	Processing Parameters			Response				
	Screw configuration	Screw speed (rpm)	Feed rate (kg/hr)	Residence time (secs)	% Torque	Pressure (bar)	DSC (J/g)	%Drug release at 720 mins
1	-1	100	0.4	533.42	13	12	20.64	34.92
2	-1	300	0.5	411.06	14	9	10.89	31.33
3	-1	500	0.6	297.24	10	6	11.03	39.32
4	0	100	0.5	705.41	20	12	13.67	30.34
5	0	300	0.6	345.62	15	8	16.55	29.19
6	0	500	0.4	603.84	13	4	11.29	27.40
7	1	100	0.6	318.43	24	15	11.23	45.26

8	1	300	0.4	554.22	18	9	11.14	45.47
9	1	500	0.5	597.60	17	4	10.86	39.31

Table 5.6 Taguchi method with response for 40%IBU-Affinisol 100cP blend

Table 5.6 provides taguchi design with responses observed during and after extrusion.

5.2.3.1 Residence time measurement

The main effects and residual plots for means of the response generated were calculated using Minitab software. Larger the better option was selected for signal to noise ratio. Since it is a Taguchi design, interaction parameters were not selected. Figure 5.24 shows the main effects and residual plot for residence time response.

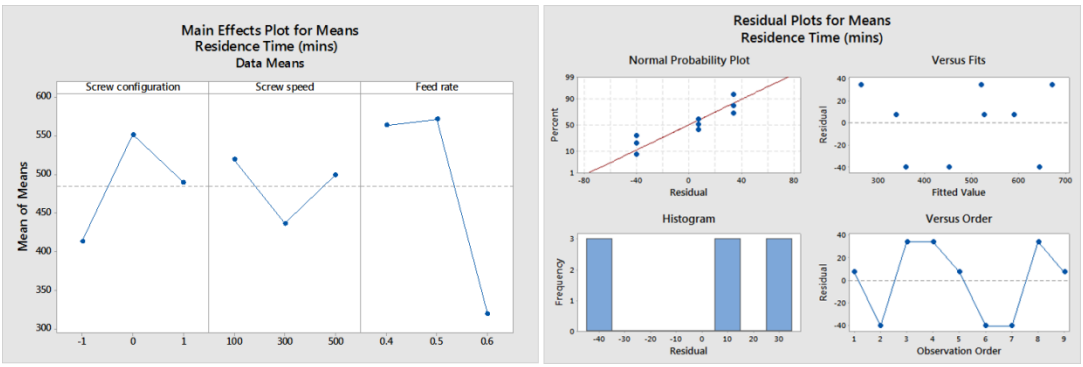

Figure 5.24 Main effects and residual plot for residence time measurement response

For the main effects plot it can be noted that feed rate is the only parameter which had effect on the residence compared to screw configuration and speed. To confirm the same, a regression analysis was carried out by applying ANOVA to find out P-values of the process parameters (Table 5.8).

Analysis of Variance for residence time					
Source	DF	Seq SS	Adjusted MS	F-Value	p-Value
Regression		117993	29498.3	2.25	0.226
Screw speed	2	572	572	0.04	0.845
Feed rate	2	88864	88864.1	6.78	0.06
Screw Configuration	2	28557	14278.5	1.09	0.419
Error	2	52421	13105.3		
Total	8	170414			

Model Summary					
S	R-sq	R-sq (adj)			
114.478	69.24%	38.48%			

Regression Equation
Screw configuration
-1 Residence time = 1037 - 0.049 Screw speed - 1217 Feed rate
0 Residence time = 1175 - 0.049 Screw speed - 1217 Feed rate
1 Residence time = 1113 - 0.049 Screw speed - 1217 Feed rate

Table 5.7 Analysis of variance for residence time response.

Thus, only feed rate was found to be a critical factor affecting residence time measurement. This confirms the observations of the model fitted for main effects plot using the Taguchi method. It can be inferred that residence time measurement for 40%IBU-Affinisol 100cP blend is only affected by feed rate for the current DOE. Higher feed rate will significantly lower the residence time of the 40%IBU-Affinisol 100cP blend.

5.2.3.2 Torque

Torque as explained before, is one of the critical parameters in process optimisation. An increase in torque can have a significant impact on the stability of the end product. Detailed investigation of the melt rheology of the

API-Polymer blends will provides an insight to challenges to expect during HME process. This was explained in chapter 5.1 for all drug loads. Current focus was only on the 40% drug load of ibuprofen-Affinisol 100cP blend.

Main effects and residual plot for % torque as response was analysed using Minitab software (Figure 5.25). It was observed that screw configuration and screw speed had a significant impact on the torque compared to feed rate.

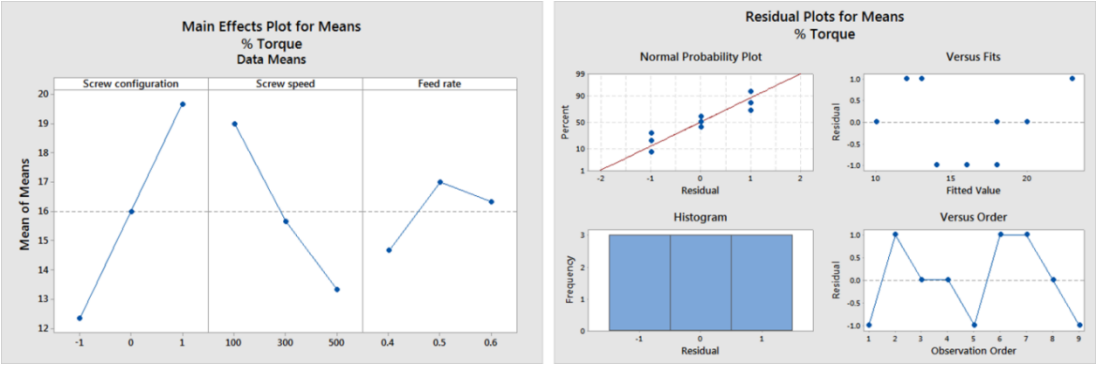

Figure 5.25 Main effects and residual plot for % torque response

Torque was highest for the screw configuration with two mixing elements and low screw speed. To confirm the model fit a multiple regression analysis using ANOVA was carried out. P-values for screw configuration and screw speeds were found to be significant (5.9).

Analysis of Variance for Torque					
Source	DF	Seq SS	Adjusted MS	F-Value	p-Value
Regression	4	133	33.25	12.09	0.017
Screw speed	1	48.167	48.167	17.52	0.014
Feed rate	1	4.167	4.167	1.52	0.286
Screw configuration	2	80.667	40.333	14.67	0.014
Error	4	11	2.75		
Total	8	144			
Model Summary					

S	R-sq	R-sq (adj)	R-sq(pred)		
1.65831	92.36%	84.72%	63.18%		
Regression Equation					
Screw configuration -1 Torque = 12.42 - 0.01417 Screw speed + 8.33 Feed rate 0 Torque = 16.08 - 0.01417 Screw speed + 8.33 Feed rate 1 Torque = 19.75 - 0.01417 Screw speed + 8.33 Feed rate					

Table 5.8 Analysis of variance for % torque response

By using a back elimination method a response surface plot was plot using screw configuration and screw speed as variables (Figure 5.26).

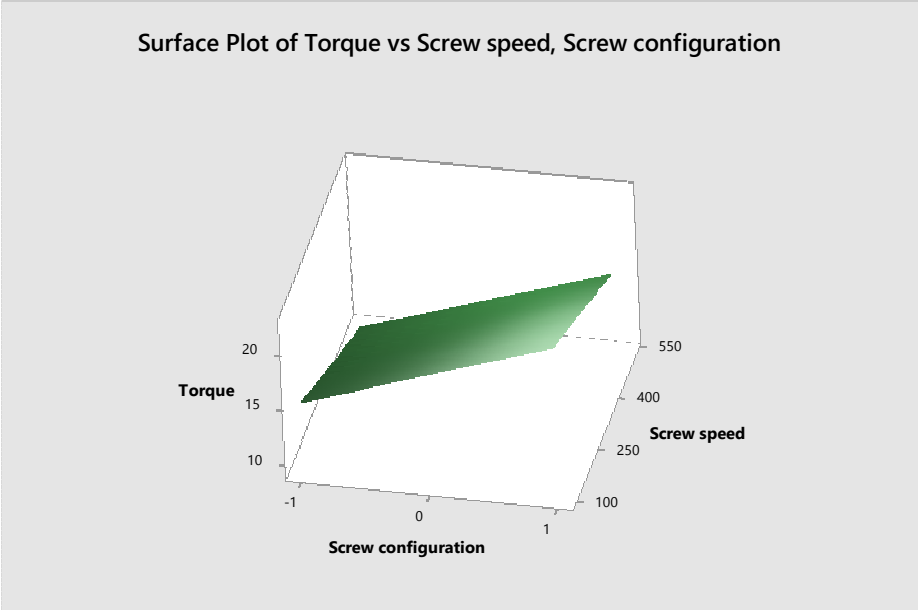

Figure 5.26 Response surface plot for %torque as response

Higher screw speed and no mixing elements resulted in the lowest % torque. This will hold true if solid state solubility and miscibility remains the same

irrespective mixing element contribution. This needs to be cross-checked with off-line responses of DSC and Dissolution.

5.2.3.3 Pressure

Pressure generation during HME occurs due to resistance in melt flow of API-polymer blend. From a safety perspective, this can have a significant impact and is a critical parameter for consideration during FMEA analysis.

Main effects and residual plots for pressure as a response are shown in figure 5.27. It was observed that screw speed was the only parameter which had a huge impact on the pressure generated. However, it is worth noting that the highest pressure generated was below the limit of 80bar which is a safety cut off for the extruder.

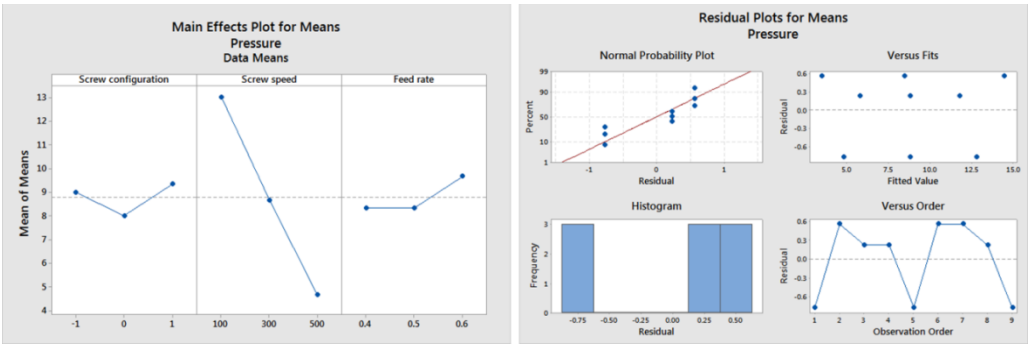

Figure 5.27 Main effects and residual plot for pressure response

Anova for confirming the model fit showed only screw speed as parameter affecting pressure (Table 5.10). An assumption was that the screw configuration will also have an impact on the pressure but was found to be insignificant for the 40%IBU-Affinisol 100cP blend.

Analysis of Variance for Pressure					
Source	DF	Seq SS	Adjusted MS	F-Value	p-Value
Regression	4	109.722	27.431	28.62	0.003
Screw speed	1	104.167	104.167	108.7	0
Feed rate	1	2.667	2.667	2.78	0.171
Screw configuration	2	2.889	1.444	1.51	0.325
Error	4	3.833	0.958		
Total	8	113.556			

Model Summary					
S	R-sq	R-sq (adj)	R-sq(pred)		
0.978945	96.62%	93.25%	78.8		

Regression Equation	
Screw configuration	
-1	Pressure = 11.92 - 0.02083 Screw speed + 6.67 Feed rate
0	Pressure = 10.92 - 0.02083 Screw speed + 6.67 Feed rate
1	Pressure = 12.25 - 0.02083 Screw speed + 6.67 Feed rate

Table 5.9 Analysis of variance for pressure response

A higher screw speed resulted in lower pressure generation. Thus for process optimisation, highest screw speed of 500rpm was found to optimum for minimisation of %torque, residence time and pressure.

5.2.3.4 DSC

DSC was used as response to determine the effect of process parameters on the crystallisation kinetics of the blend. Tracking of stability of the extrudates over stability conditions was explained in chapter 5.3. It was understood that 40%IBU-Affinisol 100cP extrudates recrystallised within 15 days on 40°C/75%RH and hence DSC analysis were carried out on all runs to find out the melting enthalpy of the recrystallised ibuprofen. This was then used as a comparative response of percent crystallinity. However, for data integrity only enthalpy values were used as a response.

Main effects and residual plot using DSC as a response is depicted in figure 5.28. Screw configuration and screw speed were found to have a slight effect on the enthalpy values of ibuprofen. Screw configuration with two mixing zones and screw speed of 500rpm were found to result in lowest enthalpy of ibuprofen. However, enthalpy values were found to be close to each other and p-values generated by the model fit showed screw configuration and screw speed to be insignificant.

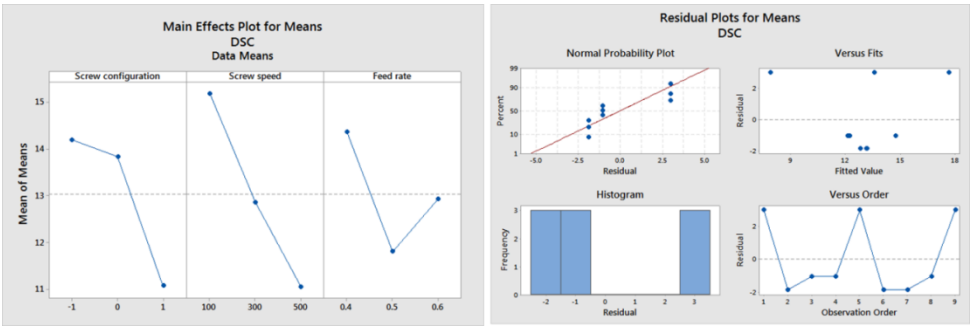

Figure 5.28 Main effect and residual plot for DSC response

Anova applied using screw configuration and screw speed proved the same and can be seen in table 5.11.

Analysis of Variance for DSC					
Source	DF	Seq SS	Adjusted MS	F-Value	p-Value
Regression	4	45.948	11.487	0.96	0.516
Screw speed	1	25.508	25.508	2.13	0.218
Feed rate	1	3.03	3.03	0.25	0.641
Screw configuration	2	17.411	8.705	0.73	0.538
Error	4	47.902	11.976		
Total	8	93.85			
Model Summary					
S	R-sq	R-sq (adj)	R-sq(pred)		
3.46057	48.96%	0.00%	0%		
Regression Equation					
Screw configuration					
-1	DSC = 20.83 - 0.01031 Screw speed - 7.1 Feed rate				
0	DSC = 20.48 - 0.01031 Screw speed - 7.1 Feed rate				
1	DSC = 17.72 - 0.01031 Screw speed - 7.1 Feed rate				

Table 5.10 Analysis of variance for DSC response

Thus, screw configuration and screw speed were found to have minimal impact on the crystallisation process of the 40%IBU-Affinisol 100cP extrudates. However, an increase in mixing zones and screw speed will slightly lower the crystallisation of the ibuprofen.

5.2.3.4 Dissolution

Drug release of ibuprofen-Affinisol 100cP blends across all drug loads was detailed in chapter 5.1. Drug release plays the most important role in formulation development using any process. It has direct impact on the critical target profile for and is part of release specifications for any formulated product. In this study, only the drug release at 720mins was used as response.

Main effects and residual plots for dissolution as a response was analysed using Minitab software. Screw configuration was seen to have significant impact on the drug release compared to screw speed and feed rate (Figure 5.29).

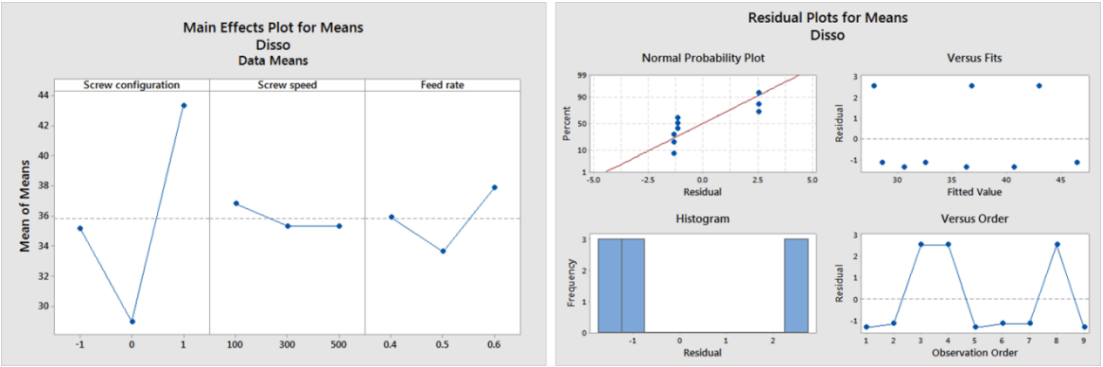

Figure 5.29 Main effect and residual plot for dissolution response

Anova was used to confirm the model fit. Screw configuration had a p-value less than 0.05 while other two parameters were found to have higher p-values (Table 5.12).

Analysis of Variance for Disso					
Source	DF	Seq SS	Adjusted MS	F-Value	p-Value
Regression	4	320.825	80.206	6.23	0.052
Screw speed	1	3.351	3.351	0.26	0.637
Feed rate	1	5.959	5.959	0.46	0.534
Screw configuration	2	311.516	155.758	12.11	0.02
Error	4	51.462	12.865		
Total	8	372.287			
Model Summary					
S	R-sq	R-sq (adj)	R-sq(pred)		
3.68683	86.18%	72.35%	31.43%		
Regression Equation					
Screw configuration					
-1	Disso = 31.33 - 0.00374 Screw speed + 10.0 Feed rate				
0	Disso = 25.11 - 0.00374 Screw speed + 10.0 Feed rate				
1	Disso = 39.48 - 0.00374 Screw speed + 10.0 Feed rate				

Table 5.11 Analysis of variance for dissolution response

Increase in the number of mixing elements had a significant impact on the drug release. Higher drug release was achieved in screw configurations with two mixing zones. A stark decrease was observed in the screw configuration with one mixing zone and it was lower compared to screw configuration with no mixing elements. Hence, elongation of mixing zone will increase the solid state solubility and miscibility of the ibuprofen-Affinisol 100cP blends and will in turn have a significant increase in drug release of the product. This result overlaps with the observations of DSC although these were insignificant.

5.2.4 Summary

A Taguchi method was used to optimise the HME process of 40%IBU-Affinisol 100cP blend. Feed rate, screw configuration and screw speed were chosen as process parameters of interest. Temperature profiles across all HME zones and batch size were kept constant for all the runs. Impact of the process parameters was studied using in process responses like mean residence time, %torque and pressure. Off-line responses of DSC and dissolution were studied to link the effect of process parameters to stability and product performance of the extrudates. All data collected were run in duplicate and a Taguchi method was analysed using Minitab software. To cross check the model fit generated, multiple regression analysis using ANOVA was calculated and a response surface plot was generated where needed.

Mean residence time was calculated using a UV tracer which was tracked using an in-line UV probe placed at the die. %torque and pressure was detected by extruder software. The pressure probe was calibrated before every run at extruder temperature. Extrudates generated were air cooled and pelletised for dissolution. Additionally, extrudates were stationed at 40°C/75% RH for stability and samples were taken out on the 15th Day and analysed using DSC.

Feed rate was found to be the only significant parameter to affect residence time measurement. Higher feed rate reduced residence time measurement by half. Torque was found to be affected by screw configuration and screw speed while pressure was affected only by screw speed. Higher screw speed of 500rpm was found to be ideal for generating lower torque and pressure. Increase in mixing intensity increased the torque while pressure remained

unaffected. Thus from a processing perspective a screw configuration with no mixing element, screw speed of 500rpm and feed rate of 0.6Kg/hr were found to be ideal for generation of low torque, pressure and residence time.

Off-line measurement of DSC showed that the set extrusion variables had little impact on the crystallisation kinetics. Ibuprofen crystallised out of all samples. Thus, the process parameters selected had negligible impact on the stability of the extrudates. Although insignificant, screw configuration with two mixing zones at a screw speed of 500rpm was found ideal to decrease in ibuprofen crystallisation. For dissolution, screw configuration with two mixing zones had a positive effect on the drug release and was the only significant factor. DSC and dissolution response confirm the assumption of higher mixing zone favouring the increase in solid state solubility and miscibility between 40%IBU-Affinisol 100cP extrudates. Thus, from stability and product performance perspective screw configuration with two mixing elements and higher screw speed of 500rpm is preferred with no significant impact due to feed rate.

To summarise, for process optimisation of 40%IBU-Affinisol 100cP blends, feed rate should be kept the highest at 0.6kg/hr. Screw speed for the blend should be 500rpm. Screw configuration with no mixing elements produced less torque, but still below the process capability and hence screw configuration with two mixing zones should be preferred. The latter, had a significant positive effect on the drug release and a slightly significant effect on the stability. Hence screw configuration with two mixing zones, screw speed of 500rpm and feed rate of 0.6kg/hr were found to be ideal parameters for optimisation of 40%IBU-Affinisol 100cP blends.

5.3 Ibuprofen dimer in the solid dispersion as an early indicator of solid-state stability

Achieving high drug load while maintaining stability of amorphous solid dispersions (ASD) is one of the critical formulation challenge during the developmental phase. Here the early detection of ibuprofen dimer in the ASD was investigated as an indicator of potential physical destabilisation of the ASD. Conventional approaches to determine this parameter involve exposure of prepared ASDs to different stress conditions in order to observe drug recrystallisation. The approaches are time-consuming and often considered as a limiting factor in the use of ASD. Attenuated total reflection fourier transform infrared spectroscopy (ATR-FTIR) has been used as a tool to detect ibuprofen dimer in the ibuprofen and hydroxypropyl methylcellulose (HPMC) ASD prepared using hot melt extrusion (HME). X-ray diffractometry (XRD), differential scanning calorimetry (DSC) and Raman spectrometry were used to support the investigation. Ibuprofen dimerisation in the ASD was found to correlate well with the solid-state stability of ASDs. Results confirmed that 15%w/w drug loading of ibuprofen within HPMC ASD was the maximum drug concentration to produce a stable ASD.

5.3.1 Introduction

Poor water solubility of Active Pharmaceutical Ingredients (APIs) is a major challenge for the pharmaceutical industry (Serajuddin 1999). One approach to address low solubility is to produce an amorphous solid dispersion (ASD), which is formed when the drug is molecularly dispersed and stabilised in a polymer matrix. The polymer matrix retards the molecular mobility of the API and stabilises the API in an amorphous state (Craig 2002). Solid dispersions

are obtained either by solvent evaporation or melt fusion methods (Limbachiya 2012). Melt based processing involves melting a physical mixture of API and polymer to obtain a homogeneous molten phase, for example by application of shear and heat in a twin screw extruder (Michael A. Repka 2007; Michael M. Crowley 2007). This is followed by cooling to ambient temperature to lock the API in its amorphous form. The concentration of the API in the solid dispersion is a critical factor affecting stability which depends on the miscibility of the API in the polymer.(Yang et al. 2013) The glass transition temperature (T_g) of the solid dispersion related to temperature and humidity during storage will affect the stability of the solid dispersion. It is generally desirable to incorporate the highest possible concentration of the API in ASD to control size and weight and to minimise the cost of the final dosage form. High drug loading is the preferred choice but has the drawback of solid-state stability (Yang et al. 2013). Drug entrapped within the polymer, if not molecularly mixed, may recrystallise thus affecting the stability of the drug.

The objective of this work was to study the relationship between molecular association of the drug within an ASD and its long-term stability. Molecular associations like dimerisation can provide an insight into drug aggregation within ASDs which can be further used as an indirect measure to study solid state stability. Current understanding of the stability of ASDs is predominantly based on theoretical predictions of drug-polymer miscibility (Lin and Huang 2010; Thakral and Thakral 2013; Tian et al. 2015; Wang et al. 2017), analytical measurements of molecular mobility and dynamics (Mistry and Suryanarayanan 2016; Sibik and Zeitler 2016; Kissi et al. 2018), onset of crystallisation, crystal growth kinetics (Weuts et al. 2011; Nurzynska et al.

2015; Schram et al. 2016) and intermolecular interactions between the drug and polymer (Kothari et al. 2015; Maniruzzaman et al. 2015; Nie et al. 2016).

One common approach for the prediction of the solid-state stability is to use the Flory-Huggins polymer solution theory as a function of temperature (Zhao et al. 2011; Tian et al. 2013; Tian et al. 2014; Tian et al. 2015; Rask et al. 2018). However, the method fails to provide a link between molecular distributions of the drug within the polymer matrix and stability of the ASD. Hence, a basic practical screening tool is needed for early detection of the solid state stability of amorphous solid dispersions.

Currently, the stability of an ASD is determined empirically then estimated by exposing it to different temperature and humidity conditions while monitoring it for the appearance of crystalline API using suitable analytical tools such as powder XRD and DSC (Baird and Taylor 2012; Thakral et al. 2015). Various studies using in-line and off-line spectroscopic techniques have reported the monitoring of the crystalline phase (Breitenbach J 1999; Wu et al. 2012; Rehder et al. 2013; Korang-Yeboah et al. 2016). Suryanarayanan et al. used dielectric spectroscopy (DES) to predict stability based on molecular mobility and studied the effect of hygroscopicity (Bhardwaj et al. 2014; O'Donnell and Woodward 2015; Mehta and Suryanarayanan 2016). Findings from these works are selective and moreover, the approaches involved studying either the glass forming ability or crystal growth mechanism and not the molecular association of drug within the polymer matrix. Additionally, analytical techniques available for solid state detection are limited and require that samples be exposed to different time-consuming stability conditions. The difficulties in proving long term stability during storage can restrict use of

amorphous solid dispersions for solubility enhancement of poorly soluble drugs (Serajuddin 1999; Sarode et al. 2013).

Several studies have also reported the use of a solid dispersion of IBU with polymers to increase its oral bioavailability (Ryabenkova et al. 2017; Varghese and Ghoroi 2017). The main focus of those studies was to enhance the product performance and investigate the relationship between ibuprofen and polymers. However, none have studied systematically the identification of the molecular association of ibuprofen within the polymer matrix and attempted its correlation with the solid state stability of the ASD.

In the current study, solid dispersions of ibuprofen and Affinisol^{TM}HPMC 100cP (Affinisol 100cP) of varying drug concentrations (10, 15, 20, 30 and 40%w/w) were prepared using HME. The extrudates were characterised using attenuated total reflection fourier transform infrared spectroscopy (ATR-FTIR) to identify the IBU aggregation and Raman spectroscopy, X-ray diffraction (XRD) and differential scanning calorimetry (DSC) to provide an ortho-analytical approach to monitor recrystallisation of the extrudates. Prepared extrudates were subjected to conditions of 40°C/75% RH, 25°C/60% RH and room temperature (RT) to investigate stability. Attempts were also made to understand the solid state solubility and miscibility using the Flory-Huggins polymer solution theory.

5.3.2 Results and Discussion

Construction of binary phase diagram and its limitations:

The binary phase diagram was explained in detail in chapter 4.

The molecular weight of Affinisol 100cP is more than 1000 times of that of ibuprofen. Due to which spinodal curve predicts complete solid-state miscibility between all the drug-polymer compositions and thus binary phase diagram fails to predict solid-state miscibility between ibuprofen and affinisol 100cP (Huang et al. 2016). Hence, it can be inferred that the theoretical binary phase diagram by Flory-Huggins theory fails to predict the stability of the ASD formed using ibuprofen and Affinisol 100cP.

Confirmation of Solid dispersion prepared by Hot Melt Extrusion:

The formation of an ASD was confirmed through analysis by DSC, XRD, and Raman spectroscopy. The absence of any crystalline IBU melting endothermic peak in DSC confirmed the amorphous solid state of solid dispersions (Lerdkanchanaporn and Dollimore 1997). No distinct crystalline ibuprofen peaks were observed in XRD diffractograms and a halo region confirmed the amorphous nature of the extrudates at all concentrations of ibuprofen (Figure 5.31) (Xu et al. 2009; Thakral et al. 2015; Ryabenkova et al. 2017). Raman spectra exhibited a peak shift from 1607cm^{-1} to 1612-1617cm^{-1}, attributed to aryl chain deformation and C-H stretching and bending which occurs due to disorder within the structure and is characteristic of the amorphous state of ibuprofen (Liu and Gao 2012). Thus, the peak shift affirmed the amorphous nature of the solid dispersions for all ibuprofen-Affinisol 100cP extrudates at varying drug concentrations (Figure 5.30).

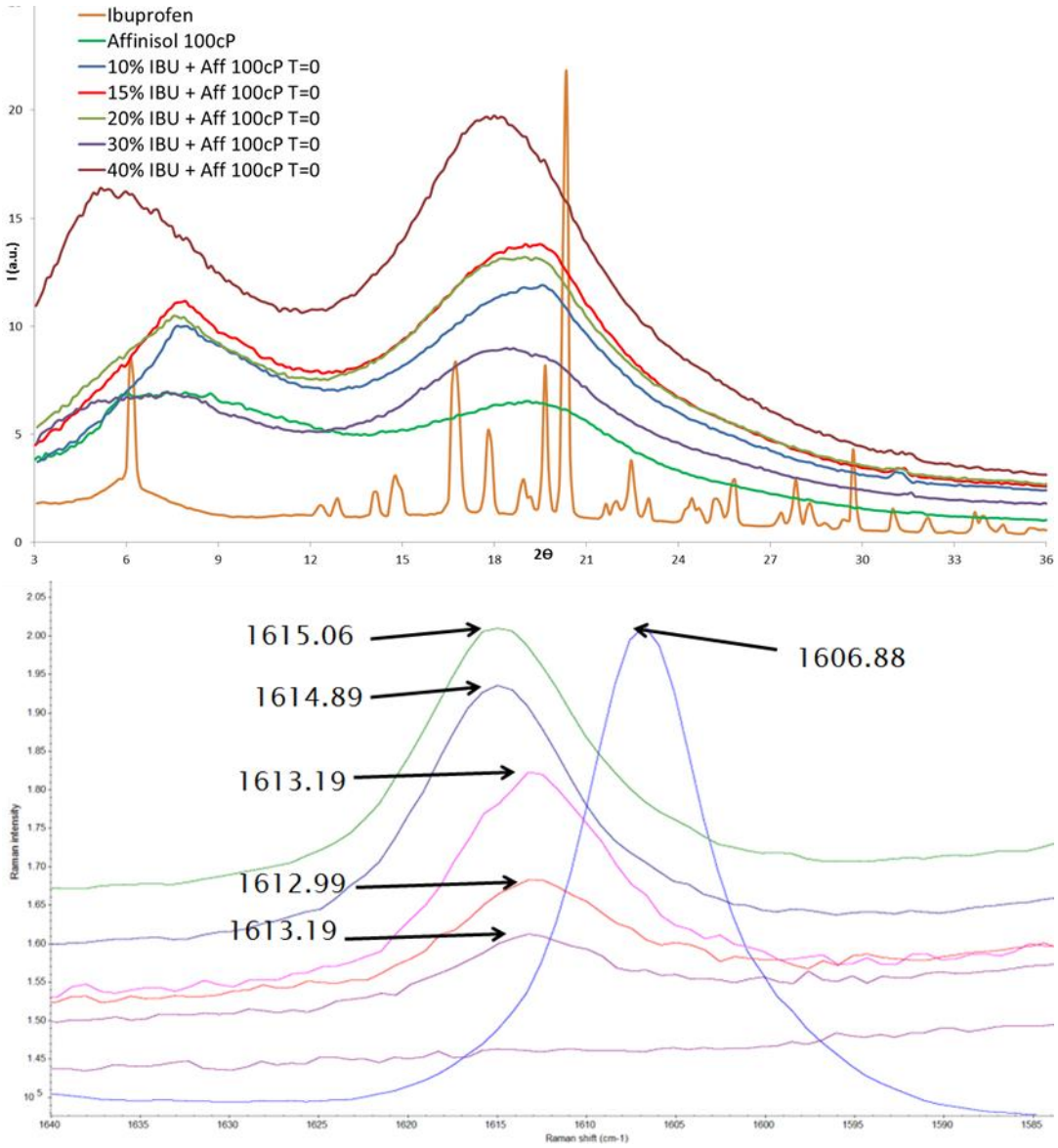

Figure 5.30 XRD spectra (top) and Raman spectra (zoomed view) of ibuprofen powder (blue), affinisol 100cP (purple), 10 (purple), 15 (red), 20 (pink), 30 (dark blue) and 40%w/w (green) ibuprofen-affinisol 100cP extrudates

Ibuprofen Dimer as an early indicator of solid-state stability by ATR-FTIR:

Ibuprofen exists as a dimer in both its crystalline and melt states (Ryabenkova et al. 2017). However, when IBU solubilises within Affinisol 100cP, the dimer of IBU is broken down into its monomeric form either due to shear-induced or by the effect of temperature during the process and is entrapped within the

polymer resulting in an amorphous solid dispersion. A single phase ASD affirmed uniform mixing between IBU and Affinisol 100cP. No chemical interaction was observed between the spectral bands of the drug and polymer which confirms the formation of a solid dispersion due to its solid state solubility and miscibility.

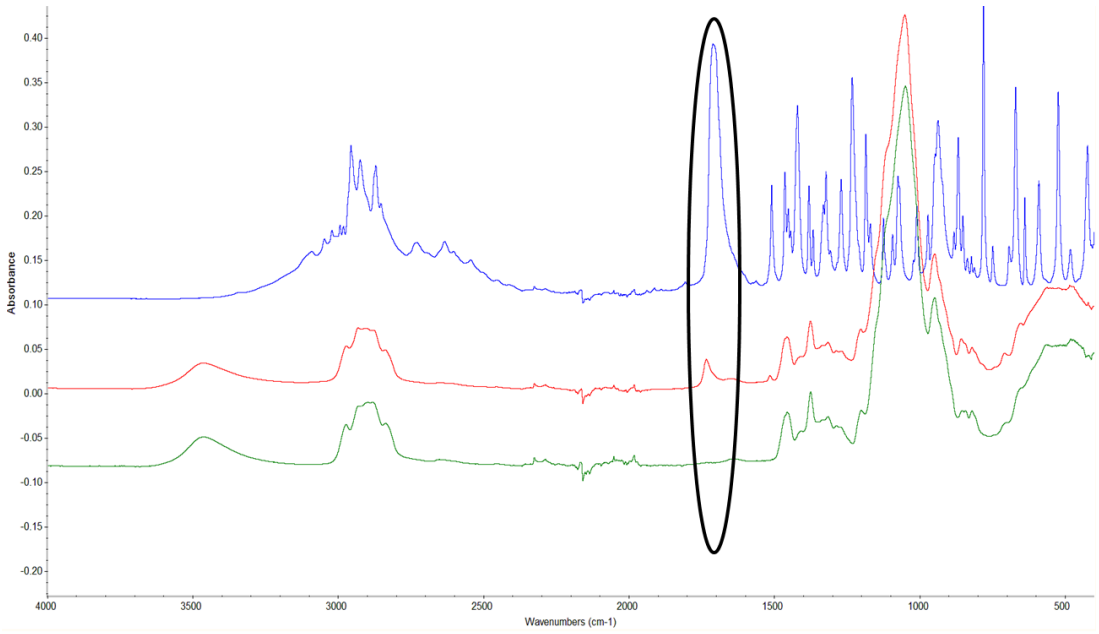

Figure 5.31 ATR-FTIR of IBU powder (blue), 10% IBU-Affinisol 100cP extrudate (red) and Affinisol 100cP powder (green)

It is evident from ATR-FTIR spectra, that active bands between 1800-1700 cm^{-1} can be considered as a non-interfering region for the detection of IBU within ASD (circled in figure 5.31). A distinct shift in the 1707 cm^{-1} band of IBU powder which is attributed to the carbonyl bond to 1732 cm^{-1} in the solid dispersion was observed. Several studies have reported similar shifts which have been attributed to the breaking of hydrogen bonding of the IBU with other polymers within ASD (Lerdkanchanaporn and Dollimore 1997; Ryabenkova et al. 2017). Thus, the shift in the carbonyl bond of the ibuprofen to 1732 cm^{-1} was due to the formation of monomeric form within the ASD.

Using this as a reference indirect measurement to understand the IBU solid state within the ASD, ASDs with different percent drug loading of IBU were prepared. It was observed that all ASDs above 15% drug loading showed the presence of the dimer along with some monomeric form (Figure 5.32). This suggests that presence of ibuprofen dimer can be used as a measure in predicting the solid state stability of the ASDs.

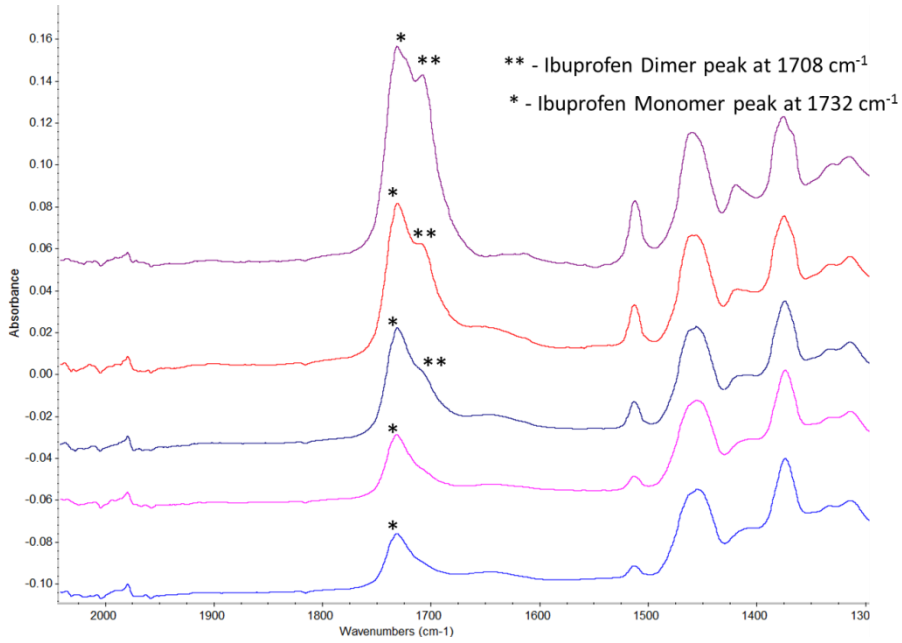

Figure 5.32 ATR-FTIR spectra (zoomed view) of 10 (blue), 15 (pink), 20 (dark blue), 30 (red) and 40%w/w (purple) ibuprofen-Affinisol 100cP extrudates

Although all the extrudates above 15% IBU load showed some presence of the dimer form of IBU, the traditional analytical techniques like XRD, DSC, and Raman which are predominantly used in the detection of the crystalline phase of API within ASD showed the absence of crystalline domains (figures 5.30).

To confirm the approach of ibuprofen dimer detection by ATR-FTIR studies, ASDs of different IBU concentration were stationed for accelerated stability studies. All the samples were stationed at three different stability conditions of

40°C/75% RH, 25°C/60% RH and room temperature. Extrudates were analysed off-line using ATR-FTIR, Raman, XRD, and DSC to check for recrystallisation of ibuprofen. Table 5.12 provides a summary of these stability studies. It was observed that 40% IBU loaded extrudates recrystallised within a week at 40°C/75% RH whereas 30% IBU loaded extrudates took 30 days to recrystallise (Figure 5.33). Lower IBU concentration extrudates at 20, 15 and 10% loadings were stable at all three stability conditions measured up to 8 months. The 20% IBU concentration extrudates were predicted to recrystallise due to the presence of ibuprofen dimer domains but this was not observed with 8 months of the study.

IBU-Affinisol 100cP extrudates	Day 15	Day 30	Day 120	Day 180	Day 240	Ibuprofen dimer at Day 0
40% IBU	+	+	+	+	+	Yes
30% IBU	-	+	+	+	+	Yes
20%IBU	-	-	-	-	-	Yes
15%IBU	-	-	-	-	-	No
10%IBU	-	-	-	-	-	No

Table 5.12 Summary of stability studies. (-) & (+) denotes amorphous and crystalline extrudates respectively.

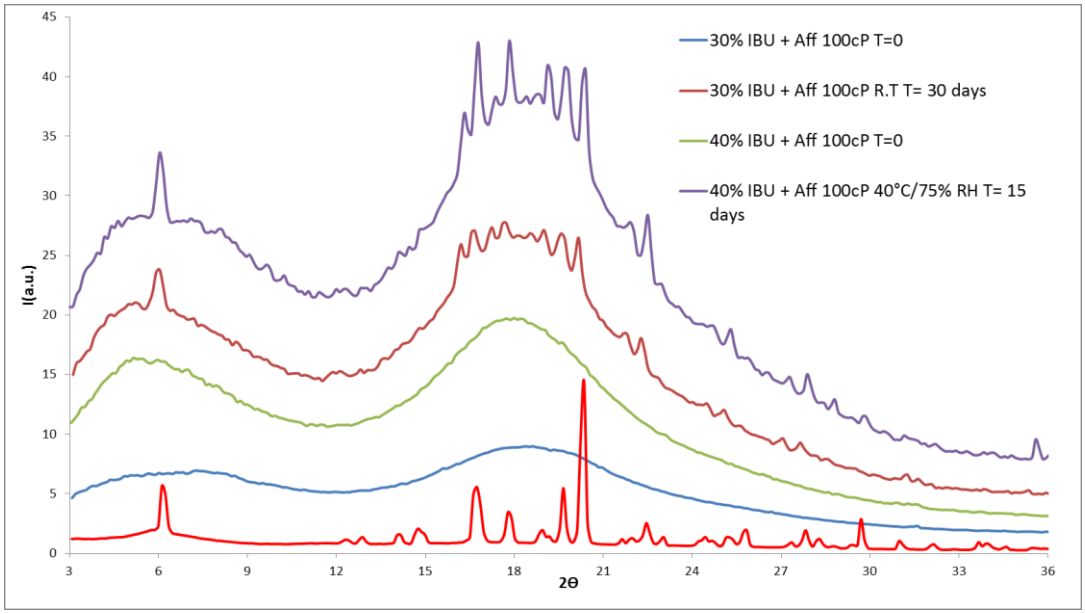

Figure 5.33 XRD diffractogram of ibuprofen powder (red), 30% T=0 day (blue), 30% R.T T=30 days (maroon), 40% T=0 day (green), and 40% 40°C/74% RH T=15 days (purple) of Ibuprofen-Affinisol 100cP extrudates

ATR-FTIR was able to provide an early indication of the presence of the dimer form of ibuprofen within the ibuprofen—Affinisol 100cP ASDs. Detection of this dimer form within ASDs represents free IBU domains either in crystalline or melt form within the extrudates which appeared to correlate with IBU recrystallisation. Thus, ATR-FTIR provided a quick and simple pre-formulation tool for detection of drug-drug interaction within the extrudates which could be used to predict solid state stability of the ASDs.

5.3.3 Summary

The above results suggest that ATR-FTIR can be used as a predictive tool to indicate long-term stability of ASDs by providing a mechanistic understanding of the drug-drug molecular association within the polymer matrix. This approach has significant advantages over conventional methods such as theoretical binary phase diagrams by Flory-Huggins polymer solution theory, or by subjecting samples to accelerated stability tests. The use of advanced analytical tools can help identify molecular level interaction within ASDs at the initial stage and provide a simple, rapid and robust prediction technique to identify solid-state stability of the ASDs. Identification of molecular level interaction led to significant reduction of time required to confirm solid state solubility of the ASDs using conventional approaches of monitoring crystallisation by charging to accelerated stability conditions.

Chapter 6: Novel dosage form of Posaconazole

This chapter will detail investigation of process and product attributes affecting the formulated ASD products. For this, posaconazole (POSA) and Affinisol 4M were selected as API and polymer of choice. The objective of section 6.1 will be a complete investigation of preparation of ASD using HME with aim to determine the maximum drug concentration that can be incorporated within the polymer. section 6.2 will discuss the use of dicarboxylic acids as a strategy to overcome food effects on oral bioavailability of POSA (Figure 6.1).

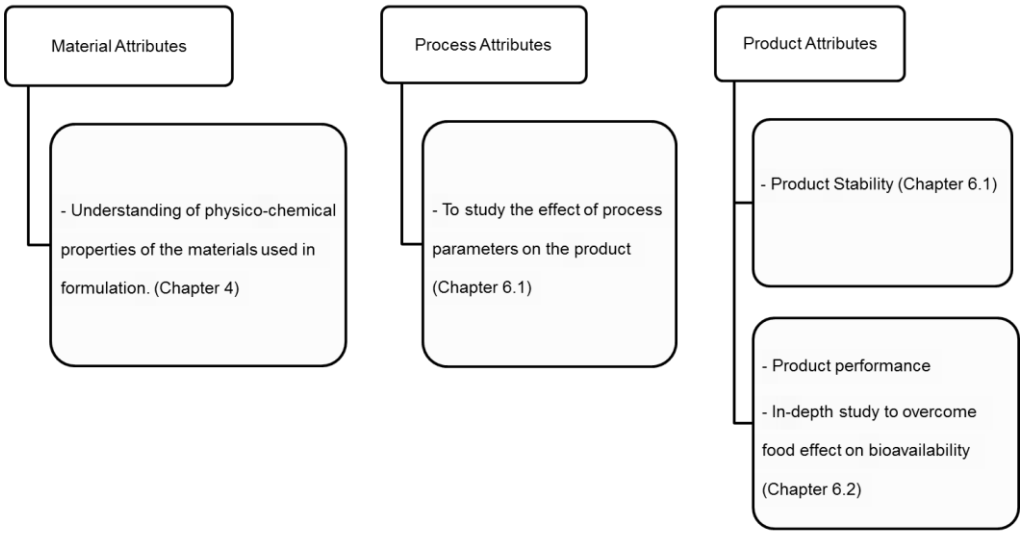

Figure 6.1 Schematic representation of Posaconazole study

6.1 Posaconazole-Affinisol

As discussed in the chapter 5.3, from a formulation perspective it is desirable to incorporate the maximum possible concentration of drug within polymer for a stable ASD. This will control size and weight and also minimise the cost and dose frequency of the final dosage form. Hence, determining the API maximum concentration is one of the key critical attributes during product development.

6.1.1 HME trials and solid state stability

Parameters for HME have been detailed in chapter 3. Systematic HME trials with increasing posaconazole content were carried out to check the maximum concentration for drug loading within polymer to form stable amorphous solid dispersions. Table 6.1 summarises the HME trials taken.

Properties	Affinisol 4M	10%w/w Posa	20%w/w Posa	30%w/w Posa	40%w/w Posa	50%w/w Posa	60%w/w Posa	70%w/w Posa
Tg at day 0	110°C	80.364°C	70.17°C	64.68°C	60.16 °C	57.1°C	54.07°C	Melt observed
Solvent loss in DSC	Yes	Yes	Yes	Yes	Yes	Yes	Yes	Yes
Feed rate	0.65 Kg/hr	0.71 Kg/hr	0.54 Kg/hr	0.34 Kg/hr	0.28 Kg/hr	0.27 Kg/hr	0.24 Kg/hr	0.23 Kg/hr
Pressure (bar)	NA	41-42	37-38	23-24	16-17	15-16	10-12	7-8
% Torque	NA	41-46	36-39	34-36	22-23	22-23	13-15	5-6

Table 6.1 Posaconazole and Affinisol 4M HME trials at screw speed of 100 rpm and extrusion temperature of 180°C

A decrease in glass transition temperature of the ASDs was observed with an increase in Posa content. However, the observed glass transition temperature was lower than the theoretically calculated glass transition temperatures using the Fox equation. A key observation noted was the decrease in pressure and % torque with increase Posa content even though, the temperature profiles were same for all drug loadings. Thus, Posa had plasticisation effect which is typical of low T_g APIs on the ASDs.

Temperature profiles were kept constant for all the drug loadings due to the high melting point of posaconazole. Additionally, the temperature window for processing is small as Affinisol 4M degradation temperature is around 210°C respectively. Hence, all the drug loadings were extruded at a temperature of 180°C.

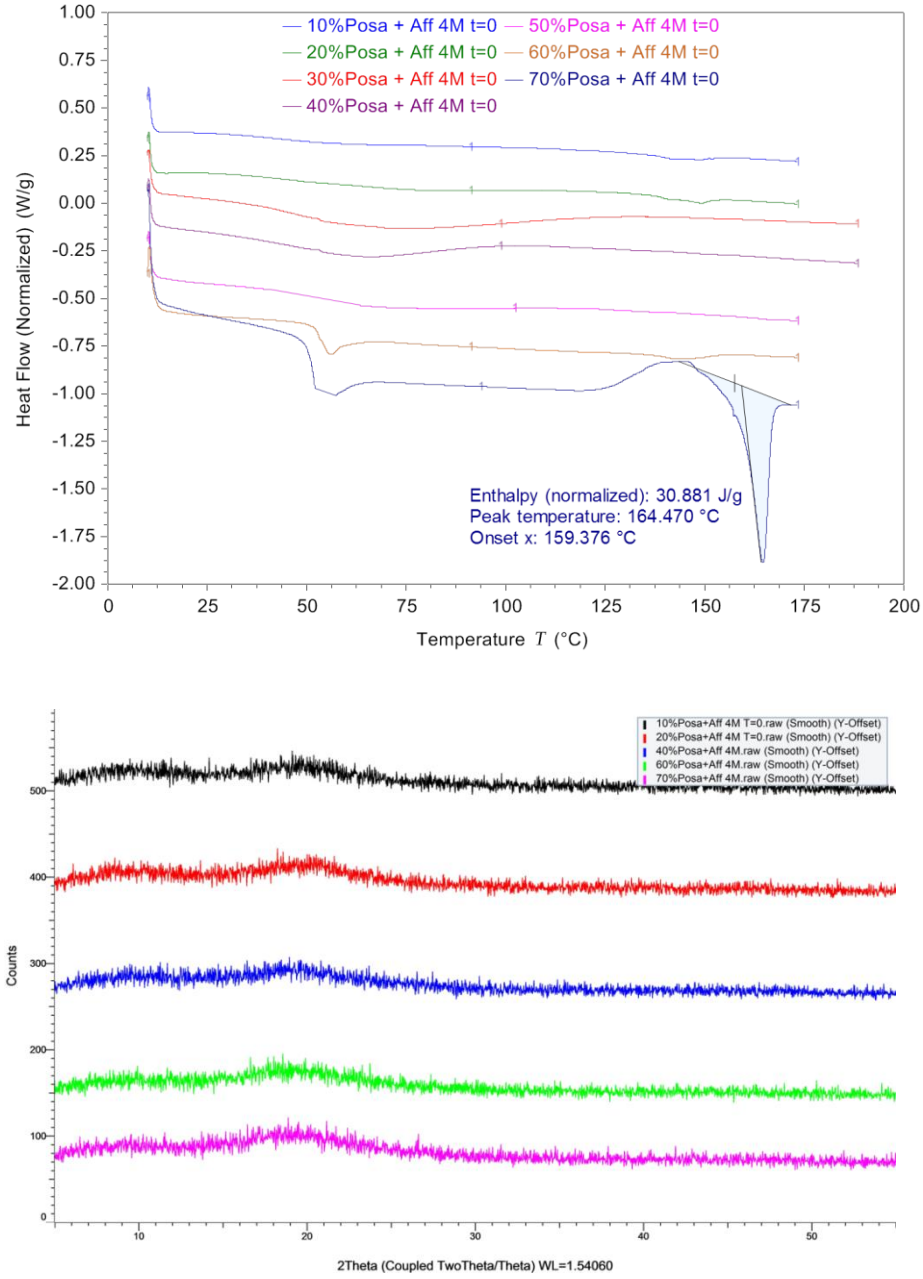

Figure 6.2 DSC thermogram (above) and XRD diffractogram (below) for Posa-Affinisol 4M trials

Confirmation of the solid state of the ASDs was carried out using DSC and XRD. All the extrudates were pelletised and milled to form a fine powder which was then used for DSC and XRD. DSC of the extrudates and milled samples showed similar results confirming the amorphous state of ASDs in its milled state (Figure 6.2). XRD complimented the DSC results with showing a halo

region with absence of any distinct diffractive peaks in the powder XRD pattern.

Posa-Affinisol 4M extrudates	Day 60	Day 90	Day 120	Day 180	Day 240
10% Posa	-	-	-	-	-
20% Posa	-	-	-	-	-
30% Posa	-	-	-	-	-
40% Posa	-	-	-	-	-
50% Posa	-	+	+	+	+
60% Posa	+	+	+	+	+

Table 6.2 Summary of stability studies. (-) & (+) denotes amorphous and crystalline extrudates respectively

40%w/w drug loading of Posa with Affinisol 4M was found to be the maximum stable concentration for ASD (Table 6.2). Higher drug loadings of 60% and 50%w/w were found to be stable for 2 and 3 months respectively on 40°C/75%RH conditions (Figure 6.3). 70%w/w extrudates are possible but recrystallise within 24hrs. Hence, 40%w/w drug loading was used for further analysis in chapter 6.2.

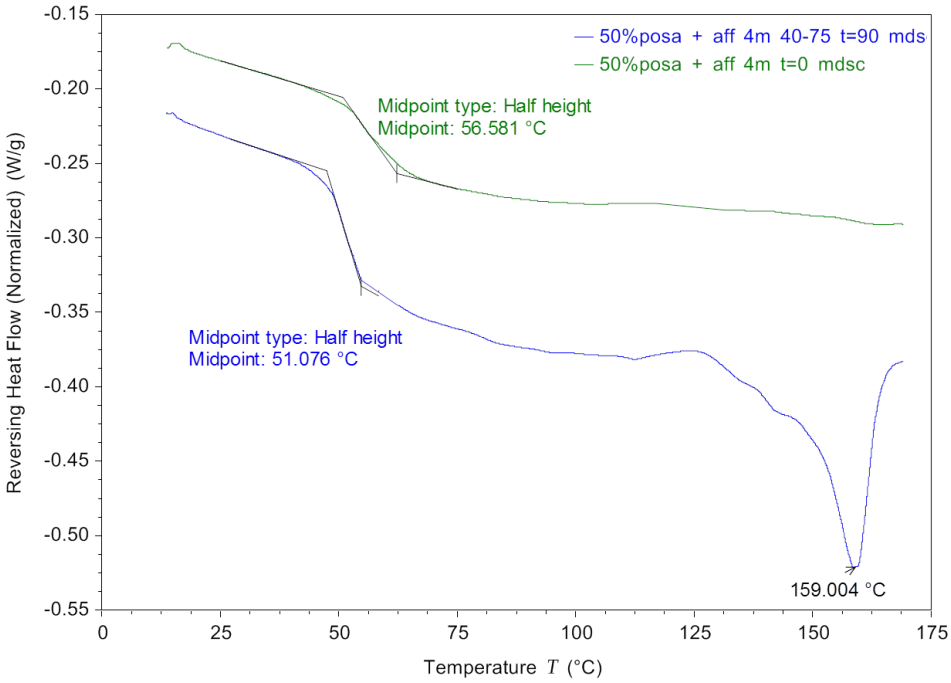

Figure 6.3 DSC thermogram of 50%Posa+ Affinisol 4M on day 0 and day 90

6.1.2 Drug release

Drug release mechanism and dissolution model fitting was described in chapter 2 and 5 respectively. Dissolution was carried out on the milled samples using 0.1N HCL (Figure 6.4).

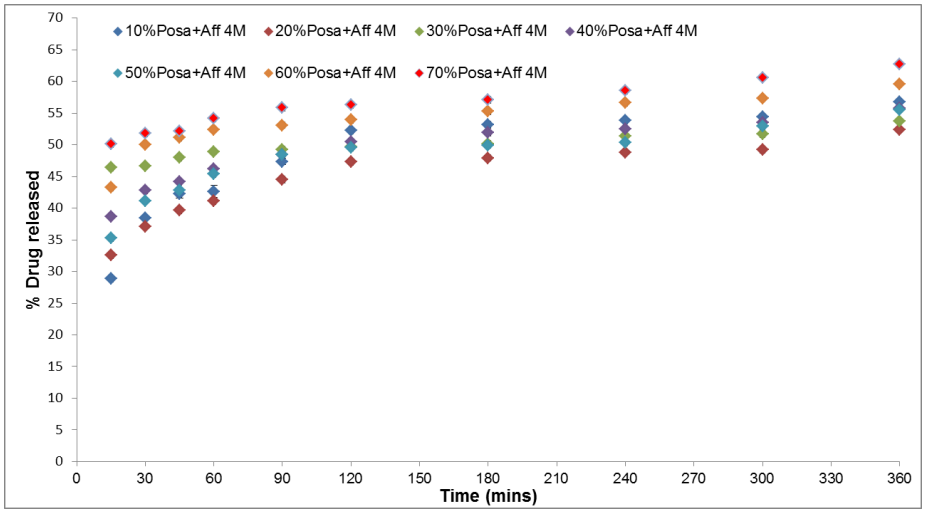

Figure 6.4 Dissolution studies of Posa and Affinisol 4M extrudates

Maximum release for all the batches was observed within 120 mins followed by plateau region. A slight increase in dissolution release profile was observed with increase in posaconazole content.

Dissolution strategy used for POSA-Affinisol 4M extrudates will be explained in detail in chapter 6.2.

6.2 Dicarboxylic acid study

The current study will provide an overview of the evolution of marketed products containing posaconazole and their shortcomings. Furthermore, it will highlight the importance to study effect of food on the oral bioavailability of the formulated products. A detailed investigation on use of dicarboxylic acids as a formulation strategy to enhance bioavailability to avoid effect of food will be discussed.

6.2.1 Introduction

To understand the shortcomings of in-vitro dissolution of Posa-Affinisol 4M extrudates, it is important to study the formulation strategies used for marketed products containing posaconazole.

Noxafil is the trade name for the marketed products containing posaconazole and is developed by MSD US. Initially, it was developed as a suspension with dose of 40mg/ml. Also, a concentrate for solution for IV infusion was developed for critical patients. According to the EMEA application by the company, the oral suspension is administered 3-4 times daily and was to be taken with food (high fat meal) to ensure adequate systemic exposure (MSD 2014).

To overcome the food effect and to maximise systemic absorption, a gastro resistant tablet was developed. The product was developed using the pH sensitive polymer (HPMCAS) by HME and coated to limit its dissolution in the stomach whilst maximising dissolution and absorption in the small intestine (Fang et al. 2011).

Thus, studying the bioavailability problems of drug formulation becomes one of the critical quality attribute in product development. Based on in-vitro dissolution results, several models are available to predict in-vivo performance of the drug formulations.

6.2.2 Effect of food and the role of biorelevant media

Failure to identify bioavailability issues is one important shortcoming during formulation development. This may arise if proper attention is not given to the robust method development of the dissolution study (Klein 2010). Drug dissolution is achieved through its solubility and dissolution rate. Kinetics of dissolution were explained by use of the Nernst-Brumer and Levich model equations which build upon the Noyes-Whitney equation (Kostewicz 2002). A brief explanation about dissolution and its kinetic models is detailed in chapter 5.1.

A drug's ability to diffuse and dissolve is governed by its physicochemical properties like pKa, solubility, lattice energy, particle size and shape and, partition coefficient and surface area (Kostewicz 2002; Klein 2010; Kostewicz et al. 2014). Physiological parameters might also hinder the drugs ability to dissolve within the GI tract (Kostewicz et al. 2014). Choice of excipients also plays an important role in affecting a drug's dissolution (Chen et al. 2015; Elkhabaz et al. 2018). Thus, the scope of in-vitro dissolution testing has expanded to prediction of in-vivo performance of the drug formulations. This is of prime importance if the choice of drug is poorly soluble in nature.

Most of the poorly soluble drugs are weakly acidic or basic in nature. The presence or absence of food can have a huge impact on the bioavailability of

the drug in the formulation. Presence of food can affect bioavailability of the drug and give rise to pharmacokinetic variability (Mathias et al. 2015). This is affirmed by FDA guidance on bioavailability/bioequivalence studies to be conducted in both fast and fed state. Presence of food in the stomach can delay gastric emptying, change pH, affect solubilisation of bile salts present and food components can interact with the drug and affect its physicochemical properties which in turn affect dissolution and diffusion. Due to this, it becomes imperative to study the effect of food on a drug's bioavailability.

A key drawback of fed state studies is its cost and selection of the type of food chosen during clinical trials. Type of dosing, thus has a huge impact on studying food effects. To prepare better, it is vital to develop in-vitro models which can closely resemble in vivo performance. This has led to an increase in the use of biorelevant media for dissolution testing. The choice of biorelevant media however, is critical for predicting effect of food on the formulations. Figure 6.5 gives an overview of the types of media available.

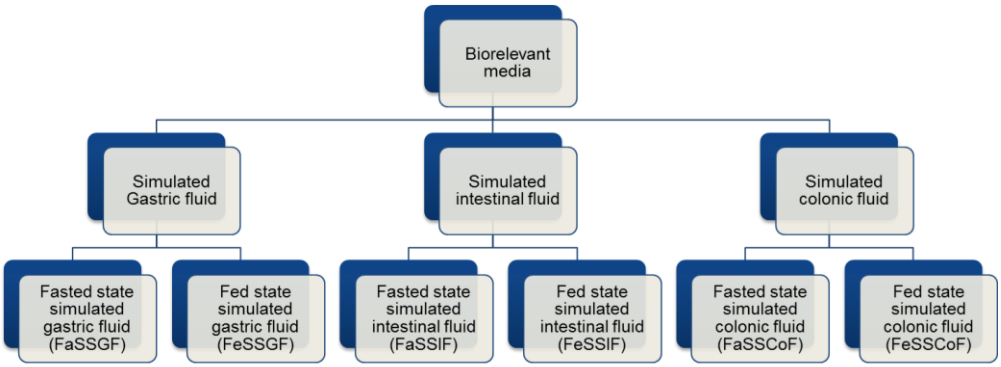

Figure 6.5 Biorelevant media available for in-vitro dissolution studies

USP describes traditional medium to simulate gastric and intestinal fluids. Simulated gastric fluid (SGF) contains hydrochloric acid, sodium chloride, pepsin and water. The pH is around 1-1.3. Simulated intestinal fluid (SIF) consists of potassium phosphate and sodium hydroxide with pH around 6.5-6.8. Certain key parameters like presence of bile salts, pepsin concentration and surface tension are not taken into consideration in the traditional simulated fluid (Klein 2010). Several studies have reported the role of bile salts and their shortcomings in affecting bioavailability of poorly soluble drugs (Chen et al. 2015; Li et al. 2016b; Lu et al. 2017a; Lu et al. 2017b; Lu et al. 2017c). Also, there are no recommendations and guidance over preparation of media to simulated fed states. Studies using milk and other fatty and lipophilic foods to simulate the fed states have been reported (Vertzoni et al. 2005; Klein 2010; Kostewicz et al. 2014; Dey et al. 2015; Baxevanis et al. 2016; Zaheer and Langguth 2018).

Thus to summarise, use of biorelevant medias is necessary to highlight food effect on oral bioavailability. Traditional simulated medium does not necessarily provide an exact representation of GI and intestinal physiology and should be altered according to the drug formulation in contention. Use of in-vitro dissolution with biorelevant medias can be helpful in predicting its in-vivo performance and to reduce the cost of clinical trials.

6.2.3 Formulation strategies to overcome food effects

It is well established that food can cause pharmacokinetic variability of drug dissolution by affecting stomach pH, delaying gastric emptying time and interacting with drug. Hence, identification of food effect in the early development phase plays a key role in developing formulation products. A change in pH can have a huge impact on the dissolution of poorly soluble drugs which are weak acids and bases in nature. Additionally, it may impair dissolution of drugs which have a high partition coefficient due to presence of lipophilic meal.

Poorly soluble drugs which are weak acids generally will dissolve in the small intestine where pH is about 6.8-7. Weak bases are likely to dissolve more in the acidic pH of the stomach whereas neutral molecules are shown to open in gastric as well as small intestine (Dressman et al. 2007). Fig 6.6 provides examples of poorly soluble drugs which show food effect on the oral bioavailability. A positive food effect was seen in neutral compound-Danazol and weak acid-Phenytoin. For weak bases, itraconzole and ketoconazole higher release was observed in acidic pH of gastric fluid compared to fast and fed state of simulated intestinal fluid. Thus identification of food effect and type of dosing is important during pre-clinical stages to develop the formulation accordingly.

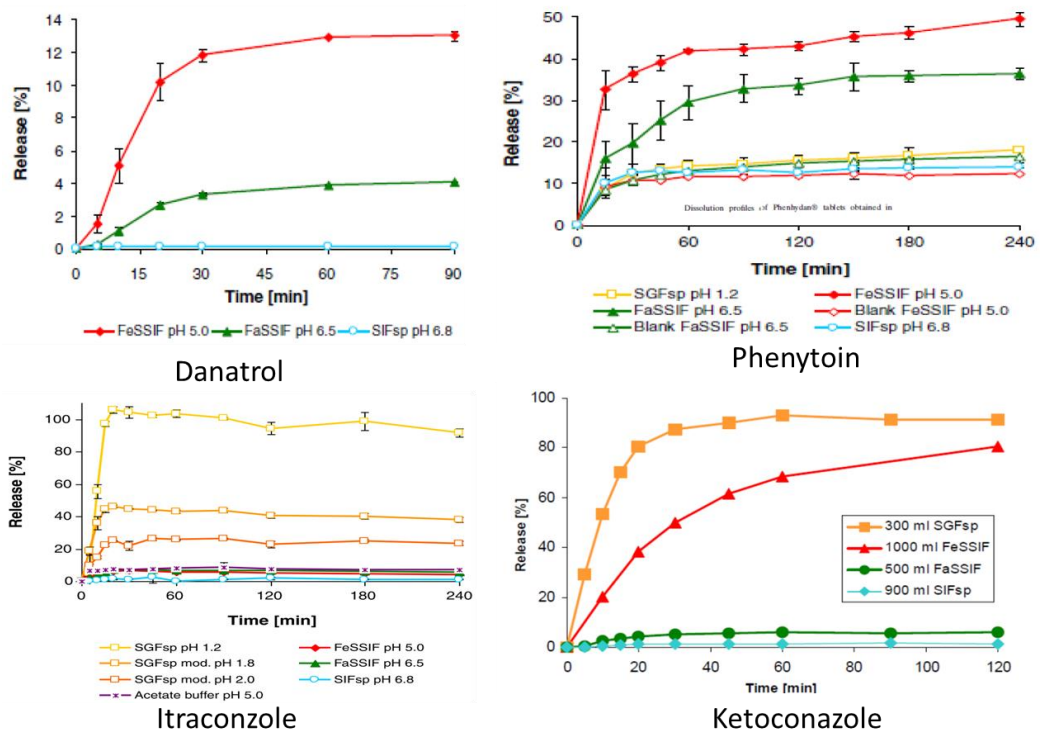

Figure 6.6 Food effect on oral bioavailability (Klein 2010)

Identification of food effect using adequate in-vitro dissolution trials with biorelevant media and formulation development should seamlessly overlap with each other. Figure 6.7 shows the type of formulation strategies employed by researchers with the aim of overcoming oral bioavailability issues. Apart from physicochemical properties of drug, type of drug release, gastric emptying rate, circadian difference, interaction with food, individual variation of GI tract and disease state are major factors contributing to oral bioavailability variation. Poor bioavailability could be due to solubility, partition coefficient, first pass metabolism, degradation in the GI tract and drug-food interaction (Thakkar 2010).

Formulation strategies should be developed according to the factors responsible for affecting oral bioavailability. Formulation strategies are broken down into three strategies (Figure 6.7).

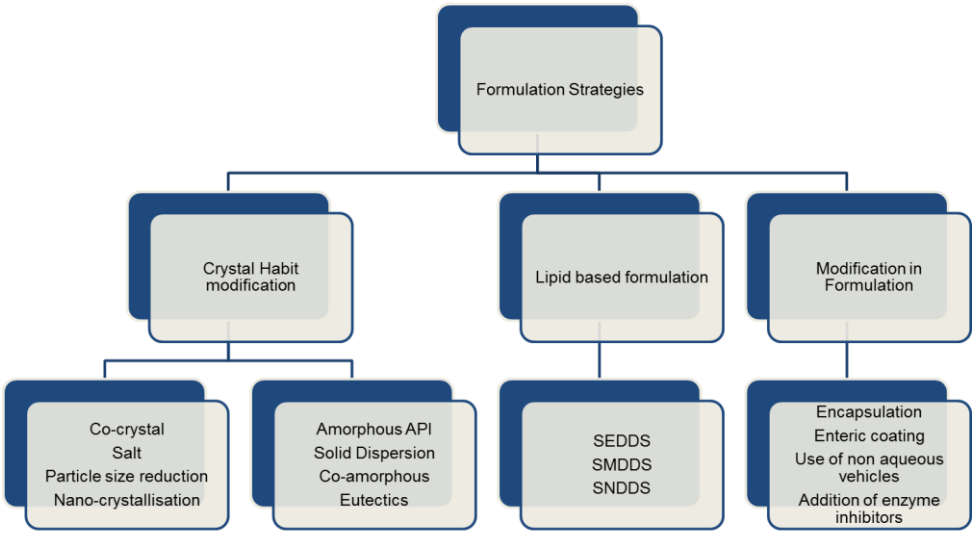

Figure 6.7 Formulation strategies to overcome food effects (Thakkar 2010)

Crystal habit modifications are utilised in cases where oral bioavailability is affected due to the drug's poor solubility (Ghule 2018). A detailed discussion on the crystal habit modification is discussed in chapter 2.

Lipid based formulations are utilised by incorporating drug in the lipid based carrier system. This will increase the drug's diffusion within the body which in turn increases dissolution (Gupta et al. 2013).

Alternative strategies involve modification within the formulation. To protect the drug from stomach variation, encapsulation or enteric coating strategies can be utilised to bypass first pass metabolism. Enzyme inhibitors can be incorporated within the formulation to neutralise the drug's interaction with enzymes (Thakkar 2010; Borbas et al. 2018).

6.2.4 Novel formulation strategy for oral bioavailability of Posaconazole

Dissolution of drugs depends on its solubility and diffusion rate. For a weak base like Posaconazole, the solubility should be higher in stomach but maximum systemic absorption was observed in the small intestine. Due to which, the market suspension was suggested to be taken on a fatty meal which will increase the pH of stomach to 6-7 {Fang, 2011 #653}. Orally administered tablet was enteric coated to limit its release in stomach and a pH sensitive polymer HPMCAS was used which released the drug in small intestine where pH is 6.8. Posaconazole thus behaves differently from similar analogues like itraconzole which has a maximum systemic release in acidic pH.

Although maximum systemic release for posaconazole was observed in the small intestine, there are several studies which concluded that this was not solely due to the change in pH (Hens et al. 2016; Kourentas et al. 2016; Hens et al. 2017). Hence, a formulation strategy to enhance dissolution in acidic pH can be investigated. Use of di-carboxylic acids as additives to posaconazole-affinisol extrudates can be employed as a strategy to enhance dissolution of posaconazole in acidic pH to avoid food effects.

6.2.4.1 Selection and characterisation of additives and posaconazole

Addition of dicarboxylic acids as additives will impart a slight acidity to the solid dispersion of posaconazole and Affinisol 4M and thus enhance dissolution in acidic media.

A literature search revealed the ability of posaconazole and itraconazole to form co-crystals and eutectics with aliphatic dicarboxylic acids. Several studies reported detailed investigation of co-crystal formation of itraconazole with

aliphatic dicarboxylic acids (Nonappa et al. 2012; Shevchenko et al. 2012; Shevchenko et al. 2013). Itraconazole-amino acid co-crystals have also been well investigated (Shete et al. 2015). It was found that itraconazole forms co-crystals with succinic acid and L-malic acid in a 2:1 ratio. Different methods to generate the itraconazole co-crystals are also reported (Ober and Gupta 2012; Ober et al. 2013). It would be vital to screen posaconazole which is structurally similar to itraconazole to check its affinity with aliphatic dicarboxylic acids.

With posaconazole being a poorly water soluble compound, the co-crystal strategy may not be attractive to achieve the desired dissolution. On the other hand, a eutectic which is multicomponent solid mixed in stoichiometry to form a solid solution can be a more viable option to resolve dissolution issues (Cherukuvada and Nangia 2014). Eutectics have recently gained importance as an alternative formulation strategy (Cherukuvada and Nangia 2012; Cherukuvada and Guru Row 2014; Cherukuvada and Nangia 2014). Positive dissolution enhancement was investigated in the case of eutectic formed by posaconazole and benznidazole (Figueiredo et al. 2017).

It becomes important to check the interaction of posaconazole with aliphatic dicarboxylic acids used as additives in the solid dispersion. Screening of posaconazole with aliphatic dicarboxylic acid was done using solvent mediated ball milling using acetonitrile. Details of the method and characterisation techniques were provided in chapter 3. Figure 6.8 shows an overview of the trials of posaconazole with selected aliphatic dicarboxylic acids.

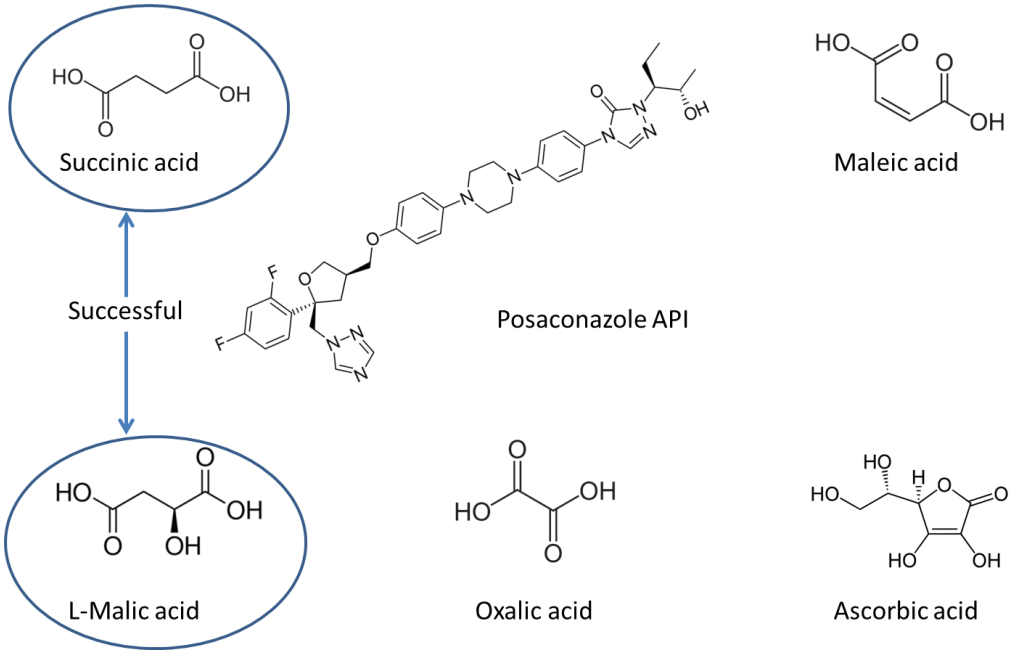

Figure 6.8 Posaconazole and dicarboxylic acid primary screening plan

To overcome the solvent effect of acetonitrile, trials were taken using the same method parameters on the posaconazole and co-formers (succinic acid and L-malic acid). No change in solid form was observed for all the trials and these were thus used as reference for comparison with trials with posaconazole and co-formers.

No interaction was observed in trials with oxalic acid, ascorbic acid and maleic acid. Trials with succinic acid and L-malic acid showed different DSC and ATR-FTIR patterns (Figure 6.9). DSC thermograms of Posa-Succinic acid trials showed a broad endothermic event which could be due to solvent loss at 108°C and an endothermic event at 150°C. Melting endothermic events of Posa and succinic acid were not observed. In ATR-FTIR spectra, an additional new peak shoulder was observed at 1710 cm^{-1} which could be due to an interaction between posaconazole and succinic acid. Initial conclusion for Posa-succinic acid trial suggested formation of eutectic as XRD patterns were

crystalline with no shift and Raman pattern showed no change. Also, melting endotherm of Posa-Succinic acid was found to be lower than its starting materials.

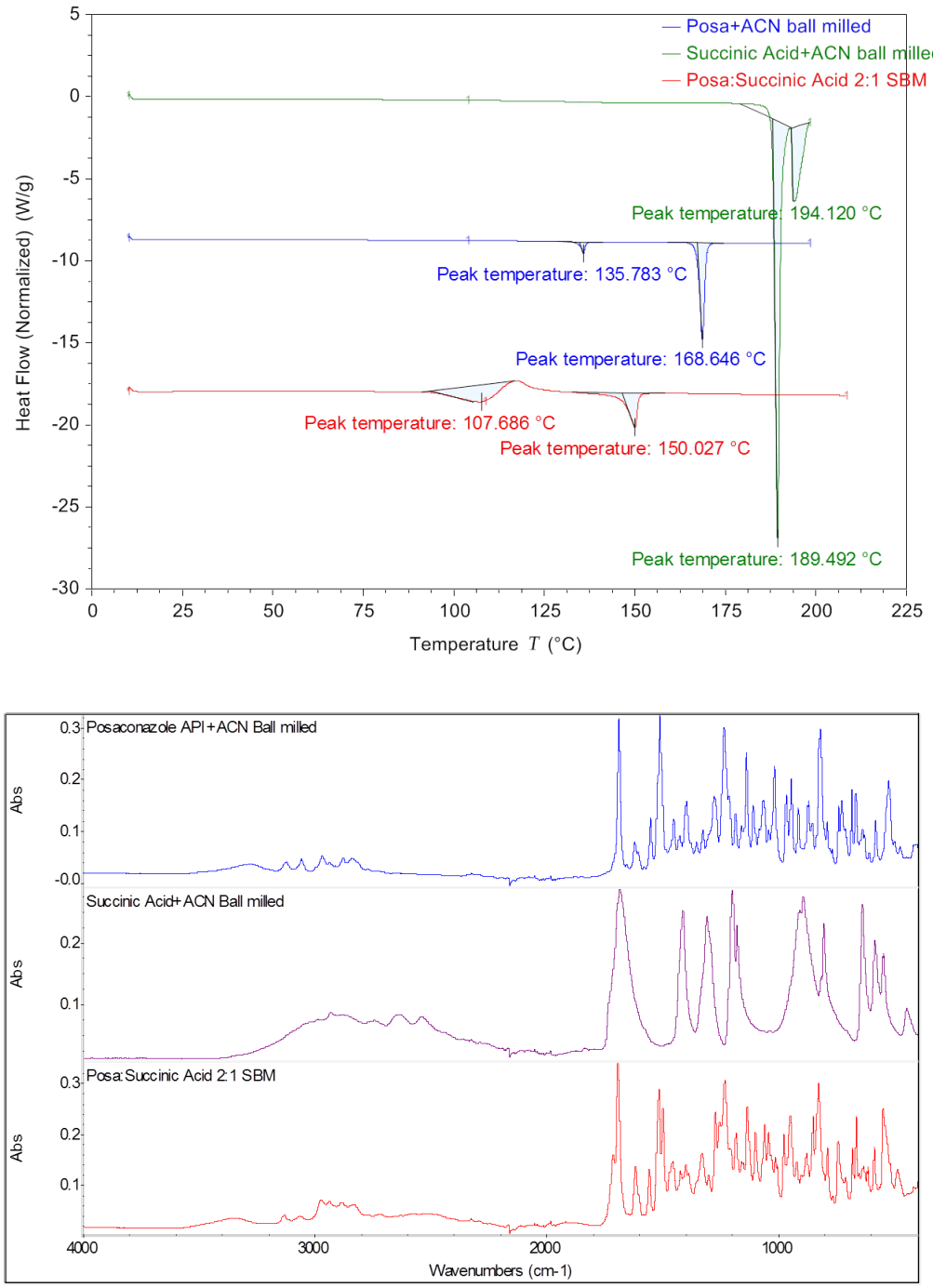

Figure 6.9 DSC thermogram (above) and ATR-FTIR (below) of Posa and succinic acid trials

DSC thermogram of Posa-Malic acid showed a sharp melting endothermic peak at 149°C and absence of a melting endothermic event of starting materials. ATR-FTIR spectra showed a broad shoulder 1732 cm^{-1} which could be due to interaction between Posa and L-malic acid. XRD and Raman showed no distinct change. Results suggested it be a co-crystal and was only based of DSC result as the melting was observed within melting range of the starting materials (Figure 6.10).

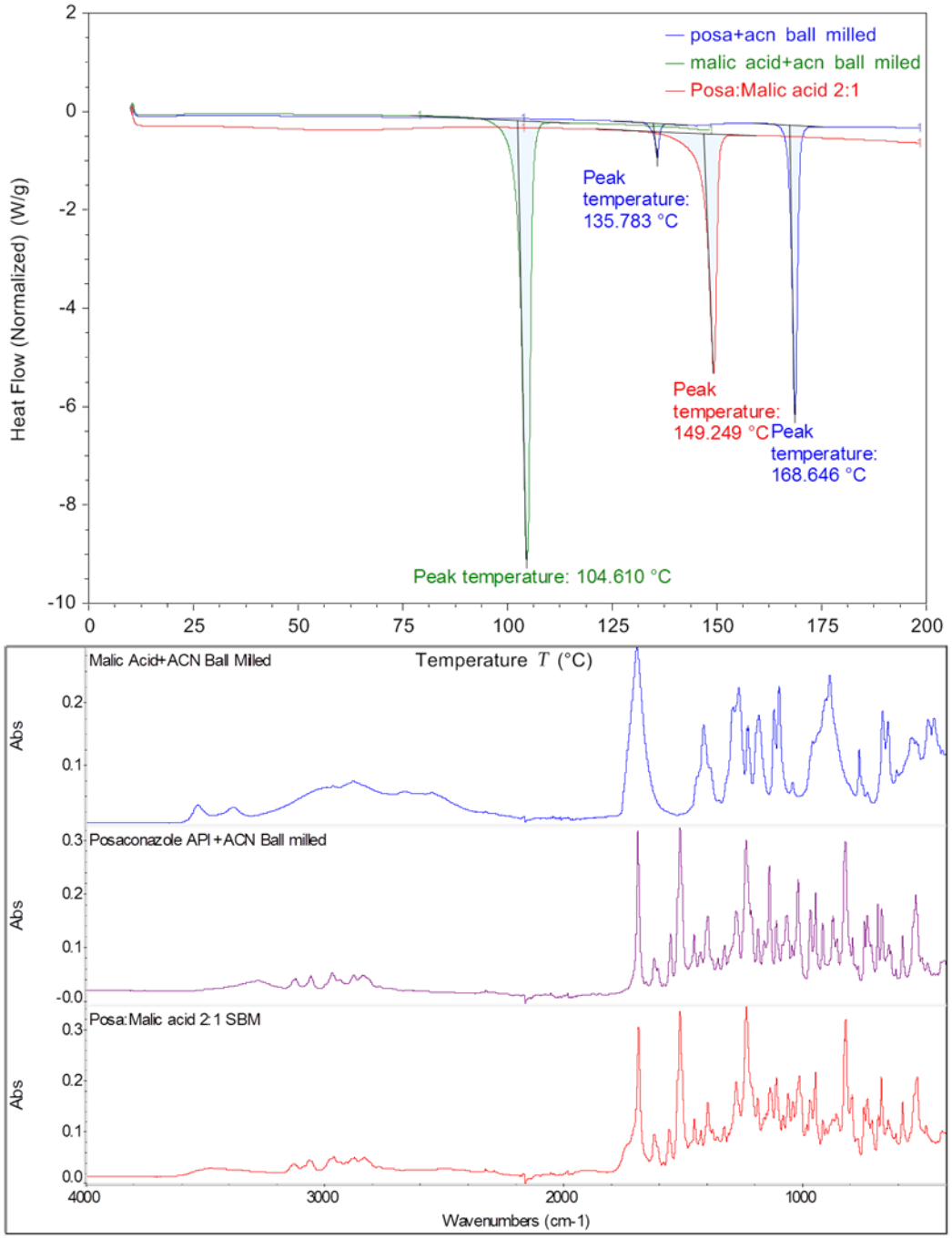

Figure 6.10 DSC thermogram (above) and ATR-FTIR (below) of Posa and L-malic acid trials

Primary screening trials were carried out in the ratio of 2:1 of the molecular weight of posaconazole and co-formers. To confirm the stoichiometry between posaconazole and co-formers (succinic acid and L-Malic acid), binary phase diagrams were constructed for the systems.

DSC thermogram of all the Posa-Succinic acid mixtures showed the presence of an endothermic event at 150°C which could be due to eutectic from 50:50 to 90:10 ratios of Posa and succinic acid. For mixture between 60:40 and 70:30, no other endothermic events of the starting materials was observed (Figure 6.11). Similar shift in spectra were observed for ATR-FTIR (Figure 6.14). A slight shift was observed in XRD patterns for 60:40 and 70:30 mixtures (Figure 6.13). Thus, Posa and succinic acid form eutectic in 2:1 ratio (Figure 6.12).

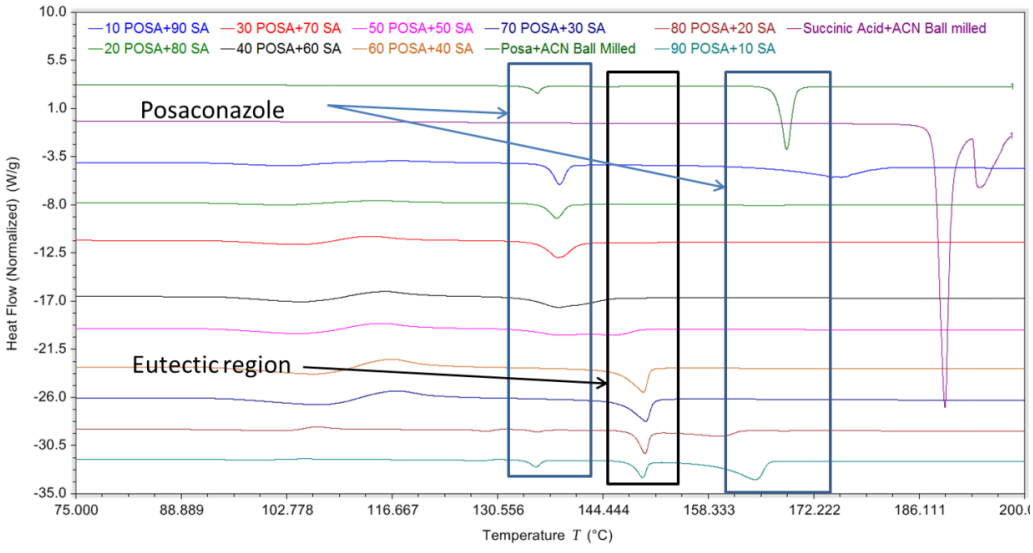

Figure 6.11 DSC thermogram of Posa and Succinic acid binary mixtures

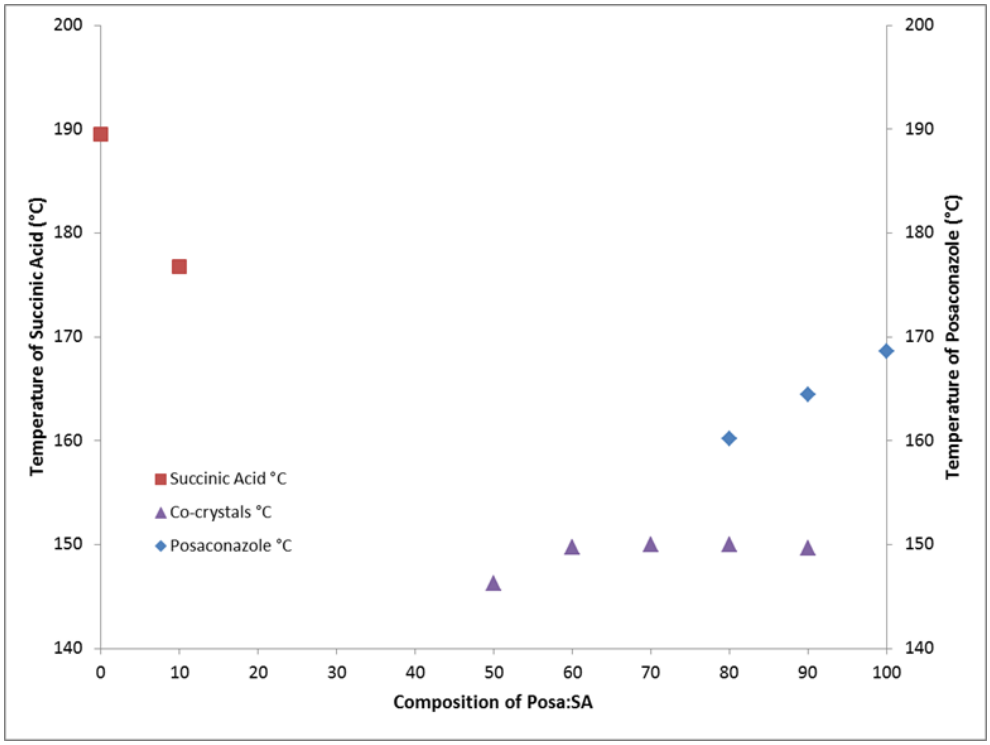

Figure 6.12 Binary phase diagram of Posa and succinic acid

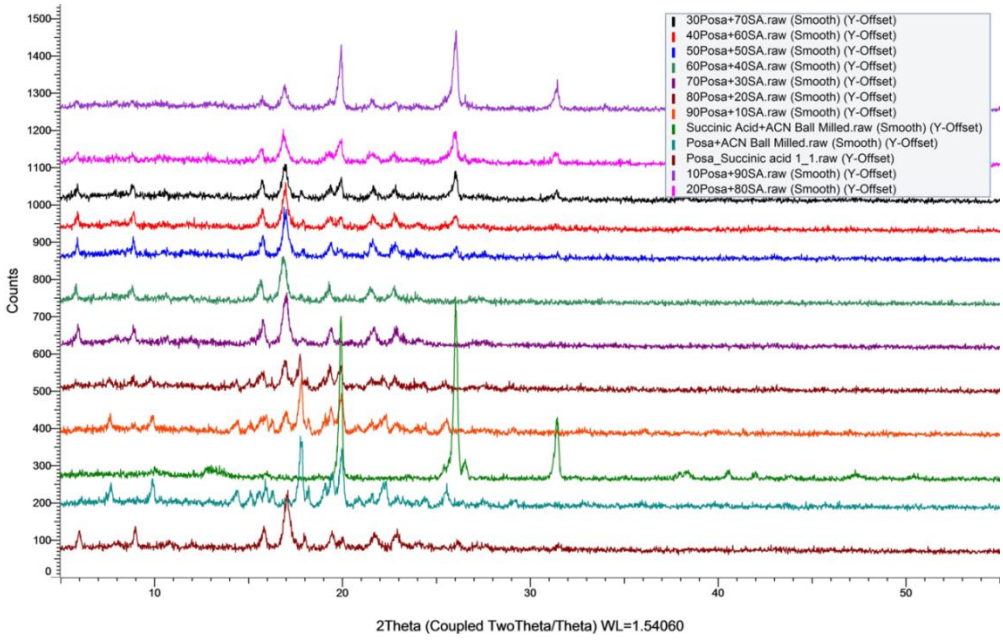

Figure 6.13 XRD diffractogram of Posa and Succinic acid binary mixtures

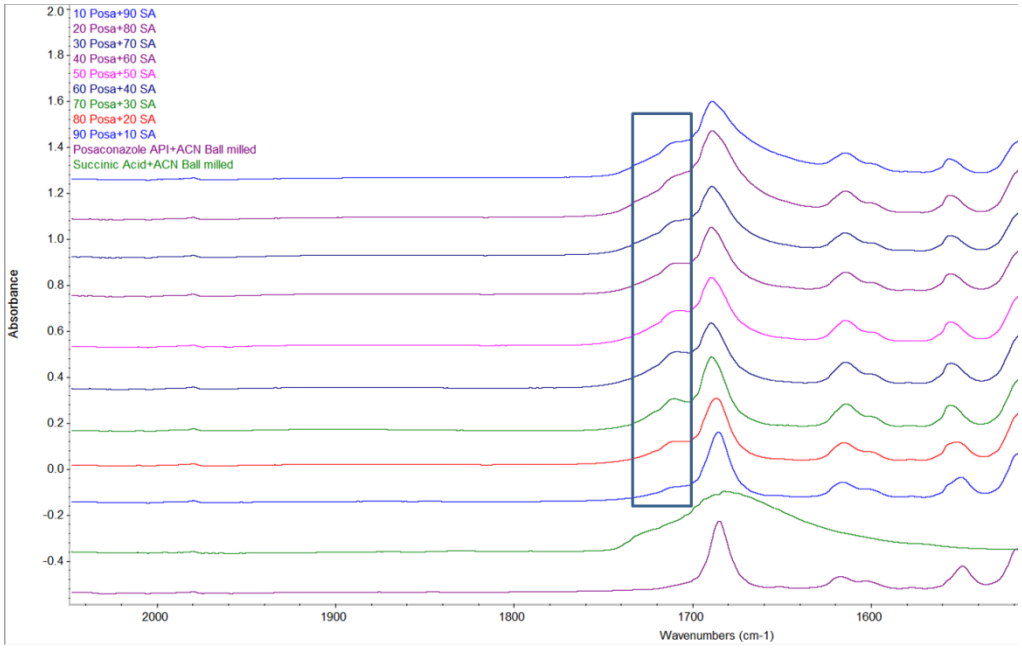

Figure 6.14 ATR-FTIR spectra of Posa and Succinic acid binary mixtures

Similar results were observed in Posa-Malic acid trials. The absence of melting endotherms of starting material was observed in 60:40 mixtures. Thus, Posa and malic acid form co-crystal in 2:1 ratio (Figures 6.15, 6.16, 6.17 and 6.18).

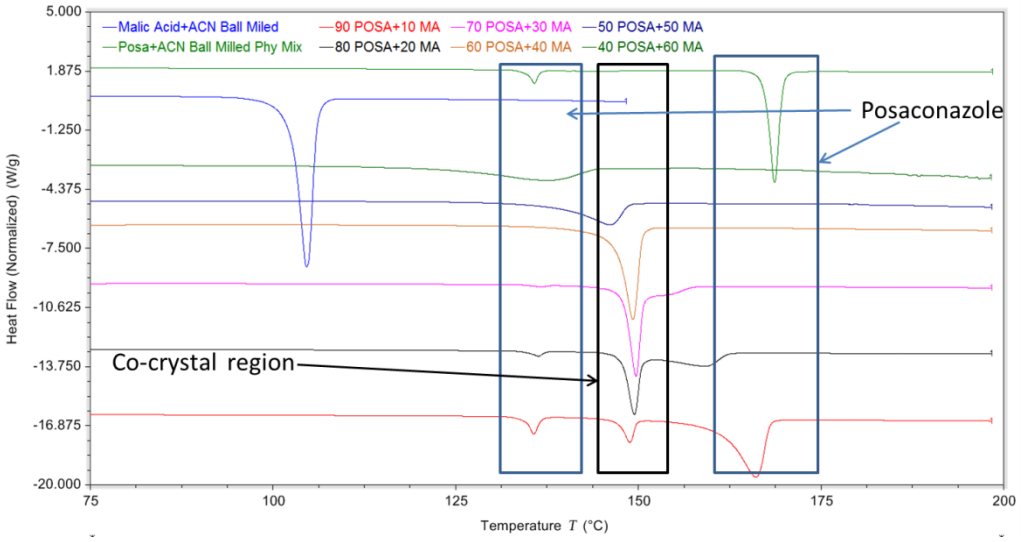

Figure 6.15 DSC thermogram of Posa and L-malic acid binary mixtures

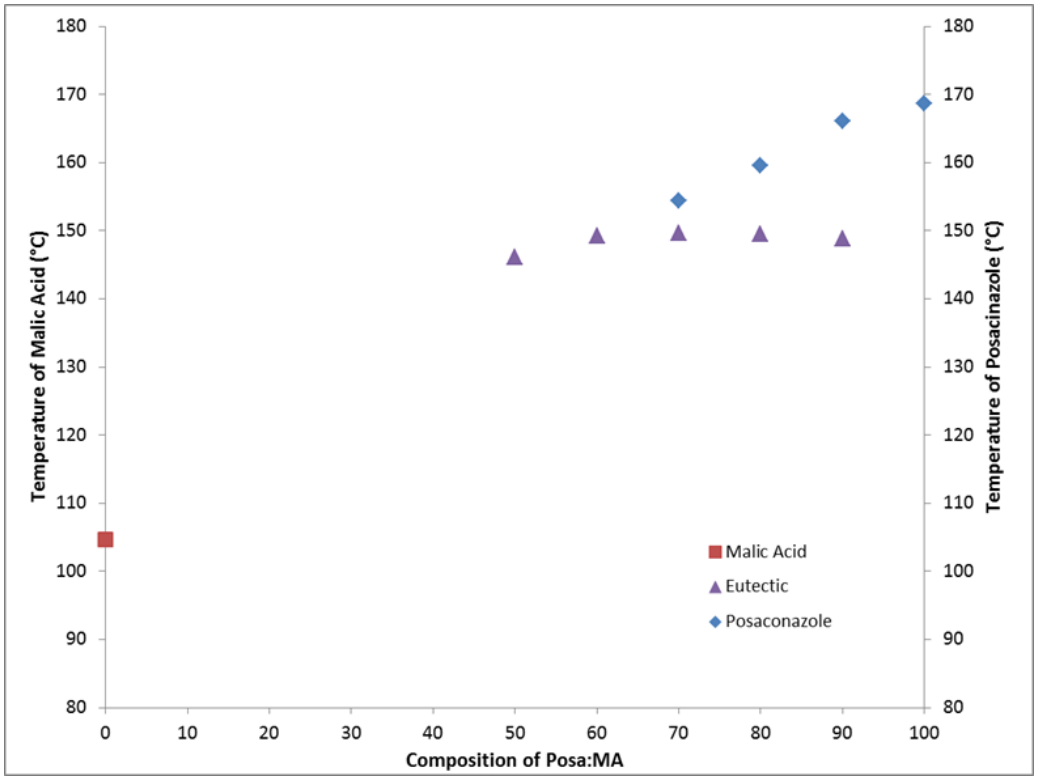

Figure 6.16 Binary phase diagram of Posa and L-malic acid

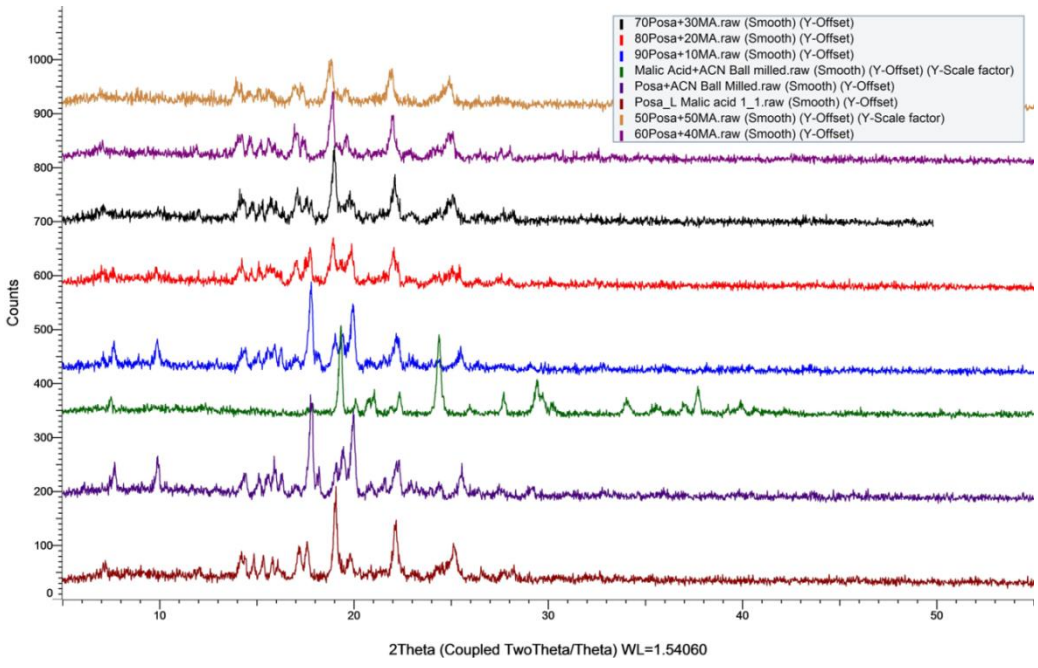

Figure 6.17 XRD diffractogram of Posa and L-malic acid binary mixtures

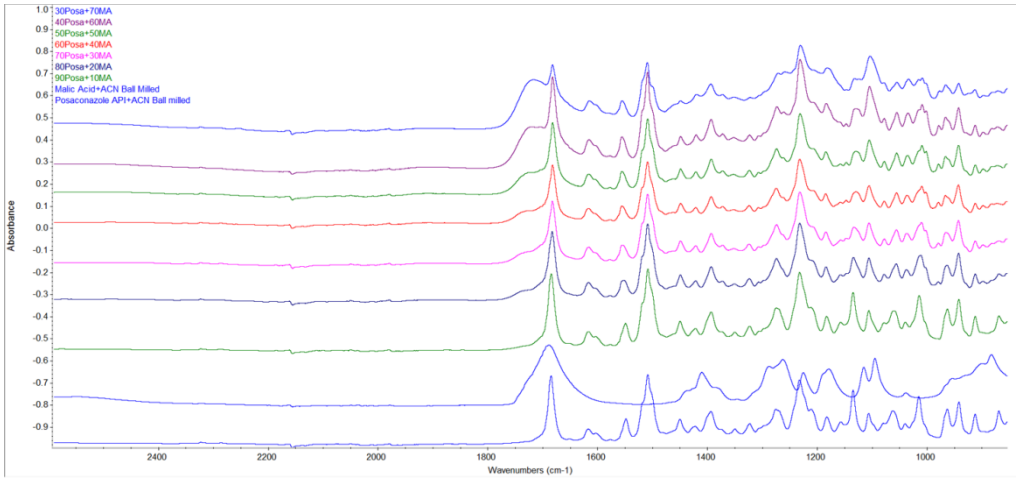

Figure 6.18 ATR-FTIR spectra of Posa and L-malic acid binary mixtures

Posaconazole thus forms a eutectic with succinic acid and a co-crystal with L-malic acid in 2:1 molecular ratio. This interaction however needs to be further proven by either single crystal XRD or solid state NMR studies.

Incorporation of dicarboxylic acid within posaconazole will have an impact on its solubility and dissolution. To investigate dissolution performance, intrinsic dissolution studies were carried out. In intrinsic dissolution rate the diffusion and dissolution is carried out with controlled specific surface area. Dissolution parameters were kept constant as used for Posa-Affinisol 4M extrudates. Physical mixtures of 2:1 Posa-succinic acid and 2:1 Posa-malic acid were found to show similar drug release as that of posaconazole alone.

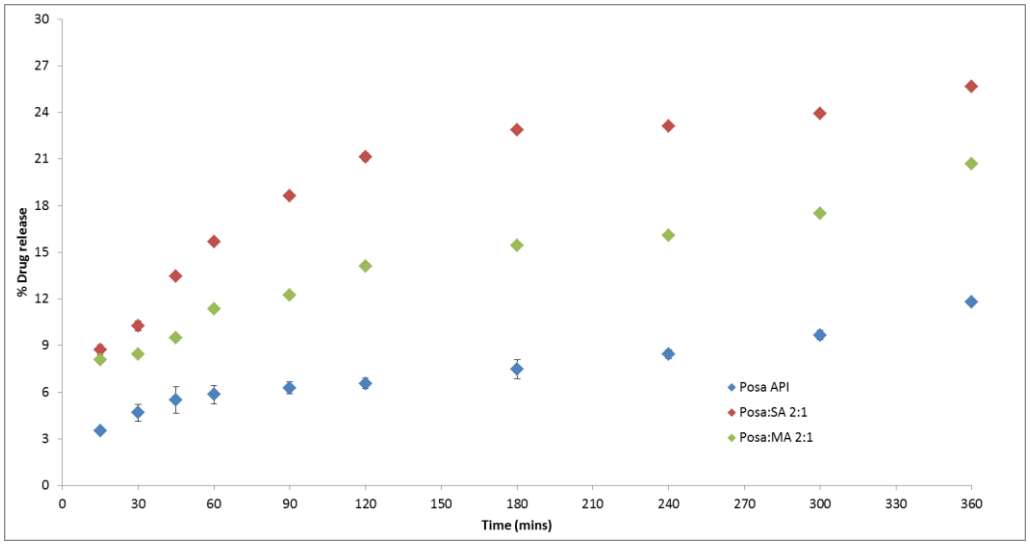

Figure 6.19 Intrinsic dissolution studies of Posa and dicarboxylic trials

2:1 Posa-succinic acid and 2:1 Posa-malic acid showed higher drug release compared to posaconazole alone. 2:1 Posa-succinic acid showed the highest drug release compared to all the other trials (Figure 6.19). Posa: SA 2:1 > Posa: MA 2:1 > Posa. Eutectics generally show higher and faster dissolution compared to co-crystal since its high energy state compared to co-crystals. A t-Test paired two samples for means was applied to the % drug released at 360 mins. P-value for all the means was found to be significant and thus the difference in % drug release is significant (Table 6.3). Linear regression was applied to the first initial solubilisation phase in the dissolution to check for significance in the rate of reaction. Data till 120 mins was selected for correlation. A clear difference in slope was observed which agreed with the trend and Posa: SA 2:1 > Posa: MA 2:1 > Posa (Figure 6.20).

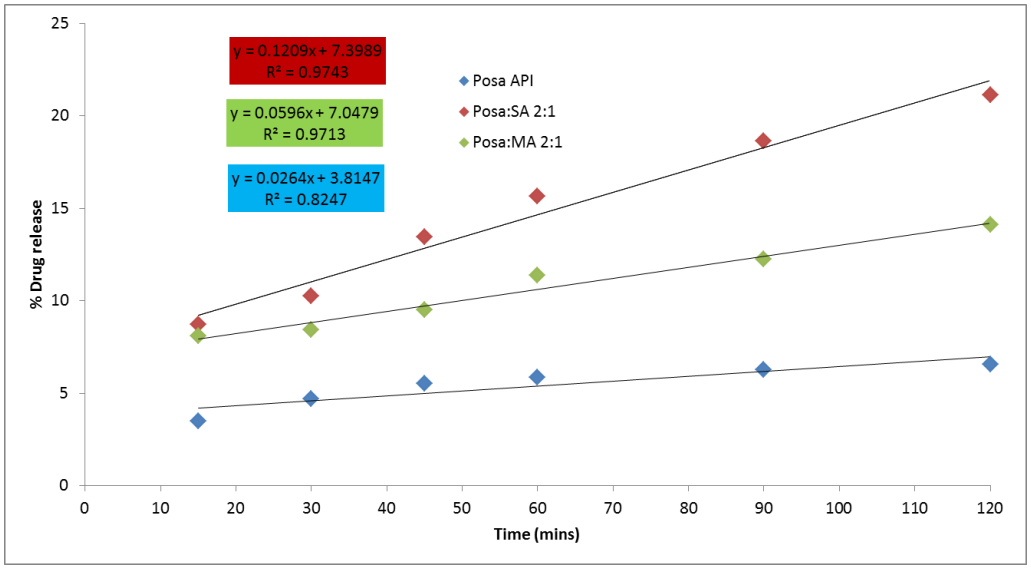

Figure 6.20 Intrinsic dissolution studies of Posa and dicarboxylic trials for 120mins

t-Test: Paired Two Sample for Means	Posa API	Posa:SA 2:1
Mean	11.8150575	25.65
Variance	0.56039924	0.045
Observations	2	2
Pearson Correlation	-1	
Hypothesized Mean Difference	0	
df	1	
t Stat	-20.3653044	
P(T<=t) one-tail	0.01561746	
t Critical one-tail	6.31375151	
P(T<=t) two-tail	0.03123493	
t Critical two-tail	12.7062047	

t-Test: Paired Two Sample for Means	Posa API	Posa:MA 2:1
Mean	11.8150575	20.7078
Variance	0.56039924	0.08635
Observations	2	2
Pearson Correlation	1	
Hypothesized Mean Difference	0	
df	1	
t Stat	-27.6556454	
P(T<=t) one-tail	0.01150475	
t Critical one-tail	6.31375151	
P(T<=t) two-tail	0.0230095	
t Critical two-tail	12.7062047	

t-Test: Paired Two Sample for Means	Posa:SA 2:1	Posa:MA 2:1
Mean	25.65	20.7078
Variance	0.045	0.08635
Observations	2	2
Pearson Correlation	-1	
Hypothesized Mean Difference	0	
df	1	
t Stat	13.81329	
P(T<=t) one-tail	0.023004	
t Critical one-tail	6.313752	
P(T<=t) two-tail	0.046007	
t Critical two-tail	12.7062	

Table 6. 3 t-Test paired to sample for means of Posa and dicarboxylic trials

Thus, posaconazole was screened with five dicarboxylic acids as co-formers. Of which posaconazole interacted with succinic acid and malic acid to form eutectic and co-crystal in 2:1 ratio respectively. Posa: SA 2:1 was proven to have higher drug release compared to Posa: MA 2:1 and posaconazole. Hence, these dicarboxylic acids when used as additives could interact with posaconazole in Posa-Affinisol 4M mixtures to prepare ASD using HME.

6.2.4.2 Formulation strategy to enhance posaconazole dissolution

Aim of the study was to enhance dissolution of posaconazole in acidic pH by the addition of di-carboxylic acids. This strategy is designed for higher dissolution of posaconazole in an empty stomach. Primary screening of posaconazole and dicarboxylic acids, showed interaction only with succinic acid and L-malic acid and in 2:1 stoichiometry. Posaconazole formed eutectic with succinic acid and a co-crystal with L-malic acid.

Since here dicarboxylic acids are evaluated as additives for posaconazole and Affinisol 4M binary blends, initial trials were taken with all dicarboxylic acids with 40% posaconazole load in Affinisol 4M (Figure 6.21). Dicarboxylic acids were added in the stoichiometry of 1:1 ratio of molecular weight equivalent to posaconazole load. Oxalic acid and ascorbic acid trials as additives did not form single phase extrudates with 40% posaconazole and Affinisol 4M and hence were discarded for further trials. Maleic acid, succinic acid and L-malic acid trials gave single phase extrudates with 40% posaconazole and Affinisol 4M (Figure 6.22).

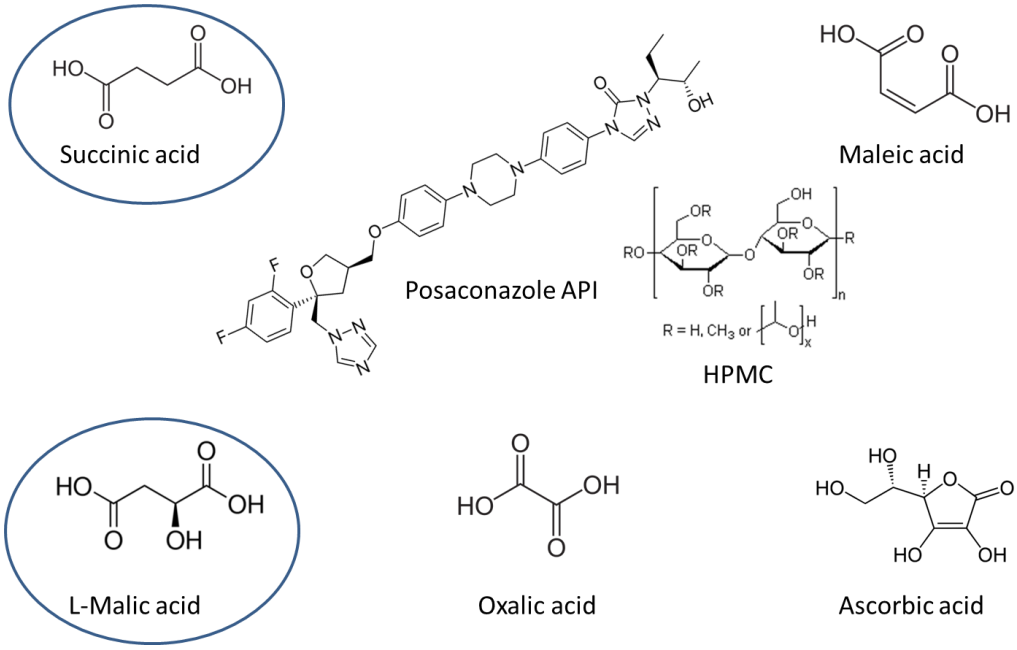

Figure 6.21 Primary screening for additive study for Posa and Affinisol 4M blends

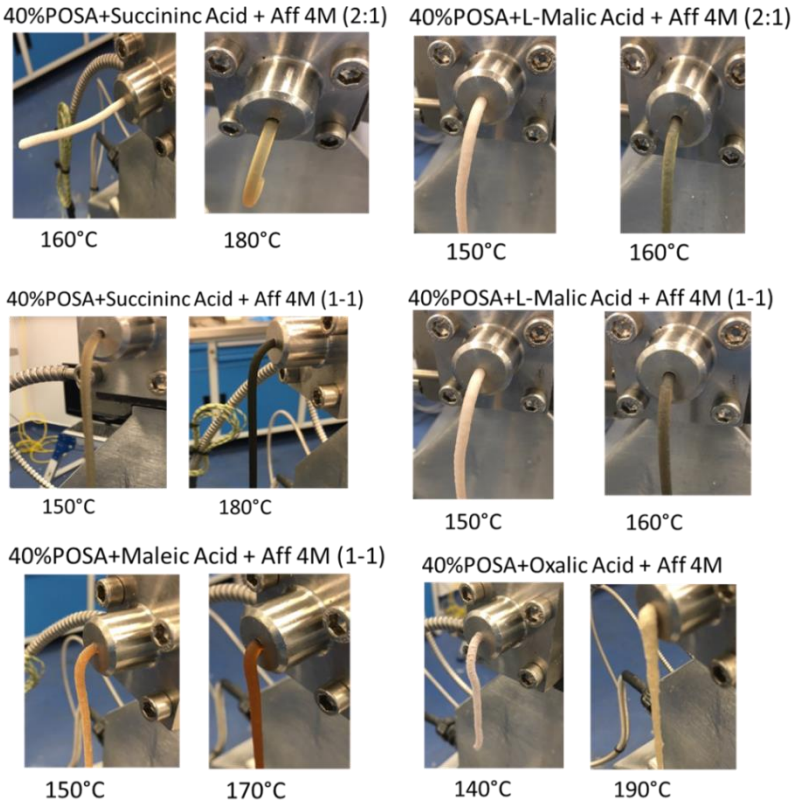

Figure 6.22 HME trials of dicarboxylic acids with Posa and Affinisol 4M blends

40%Posa+Maleic Acid+ Affinisol 4M (1-1) extrudates were dark brown in colour and were extruded at 170°C (Figure 6.22). However, dissolution studies showed an insignificant increase in drug release compared to 40%Posa+Aff 4M extrudates (Figure 6.23). Hence, maleic acid was not used for further trials.

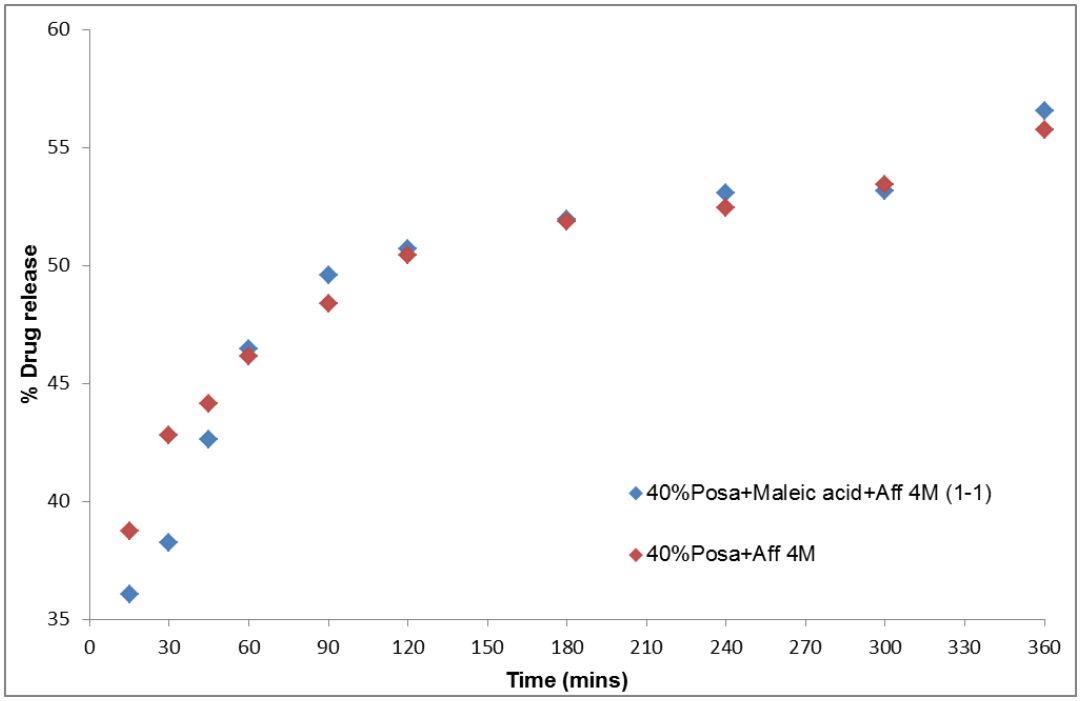

Figure 6.23 Dissolution study of Posa and Affinisol 4M milled samples with maleic acid as an additive

Thus, only succinic acid and L-malic acid were used for further trials. Trials of succinic acid and L-malic acid with 30%Posa and Affinisol 4M were also conducted in the stoichiometry of 1:1 molecular ratio. It was observed that posaconazole forms eutectic and co-crystal with succinic acid and L-malic acid in 2:1 ratio, hence for comparative purpose 40% posaconazole load was selected and equivalent 2:1 trials with Affinisol 4M were carried out (Figure 6.24). Increase in extrusion temperature was required for 40%Posa+Succinic acid+ Affinisol 4M (2-1) compared to 1-1 trials while the extrusion temperature remained constant for the L-malic acid trials. The extrudates were pelletised

and milled for further analysis. Additionally, the extrudates were stationed at three different stability conditions of 40°C/75%RH, 25°C/60%RH and room temperature for tracking of solid state stability.

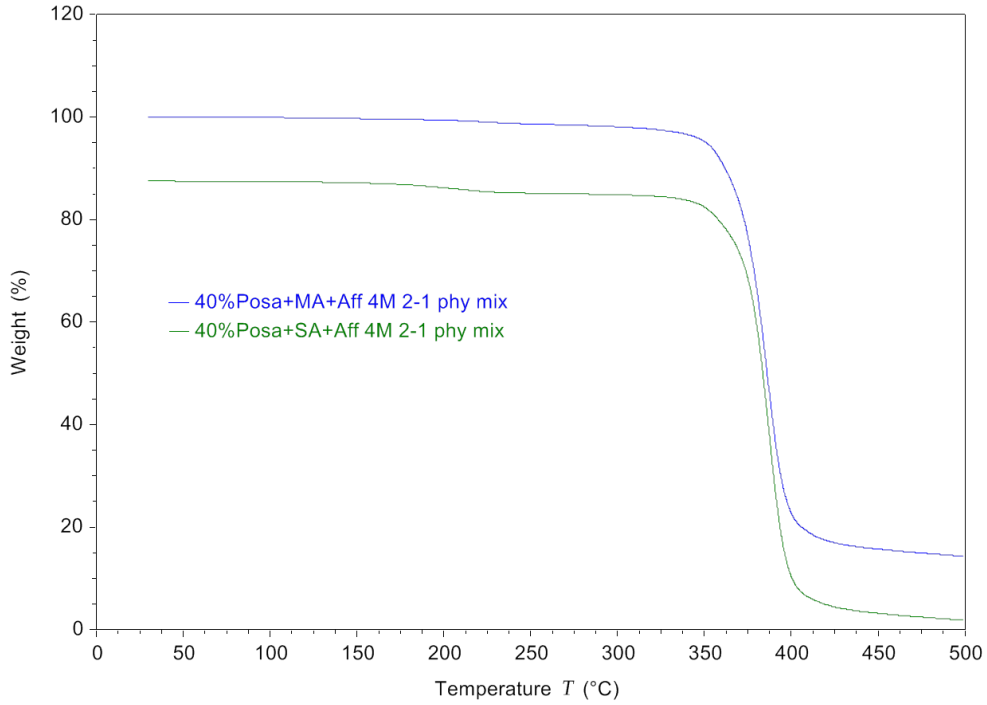

Figure 6.24 TGA thermograms of physical mix Posa and Affinisol with dicarboxylic acid

P-XRD results showed absence of crystalline domains and presence of halo region which confirmed amorphous nature of the extrudates on day 0 (Figure 6.25).

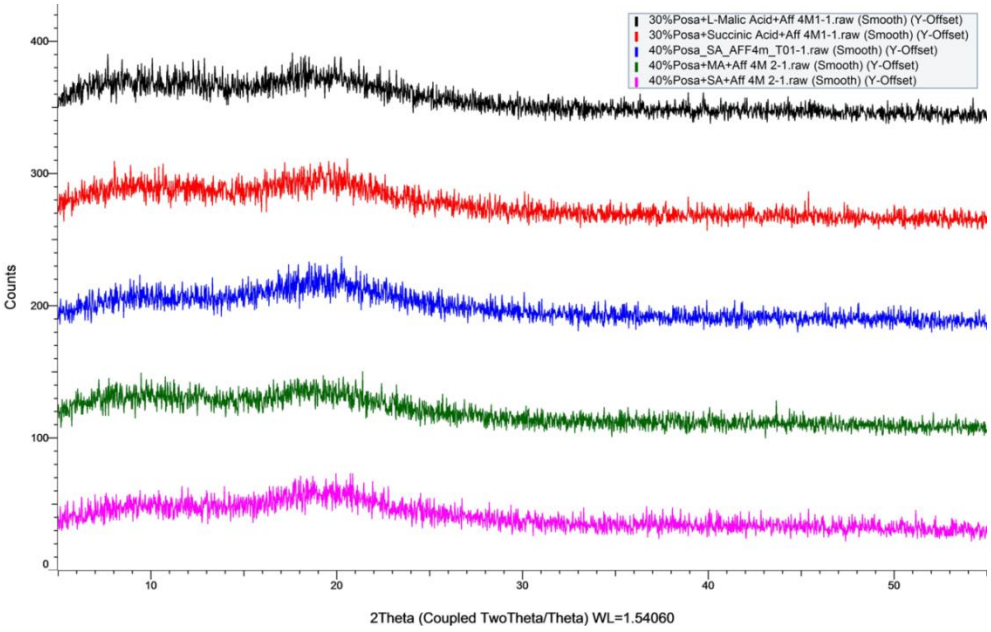

Figure 6.25 XRD diffractogram of milled extrudates of 40%Posa and Affinisol 4M with succinic and L-malic acid

DSC showed an absence of melting points of posaconazole and dicarboxylic acids respectively (not shown). ATR-FTIR showed presence of additional hump in the 1730-1740cm^{-1} region which could be due to interaction between posaconazole and dicarboxylic acid within Affinisol 4M. To confirm this, trials were taken with only dicarboxylic acid and Affinisol 4M. The additional hump was due to a shift observed in the dicarboxylic acid within Affinisol 4M and hence it can be inferred that no interaction was observed between posaconazole and dicarboxylic acids within Affinisol 4M and single phase extrudates were observed due to solid state miscibility and solubility (Figure 6.26).

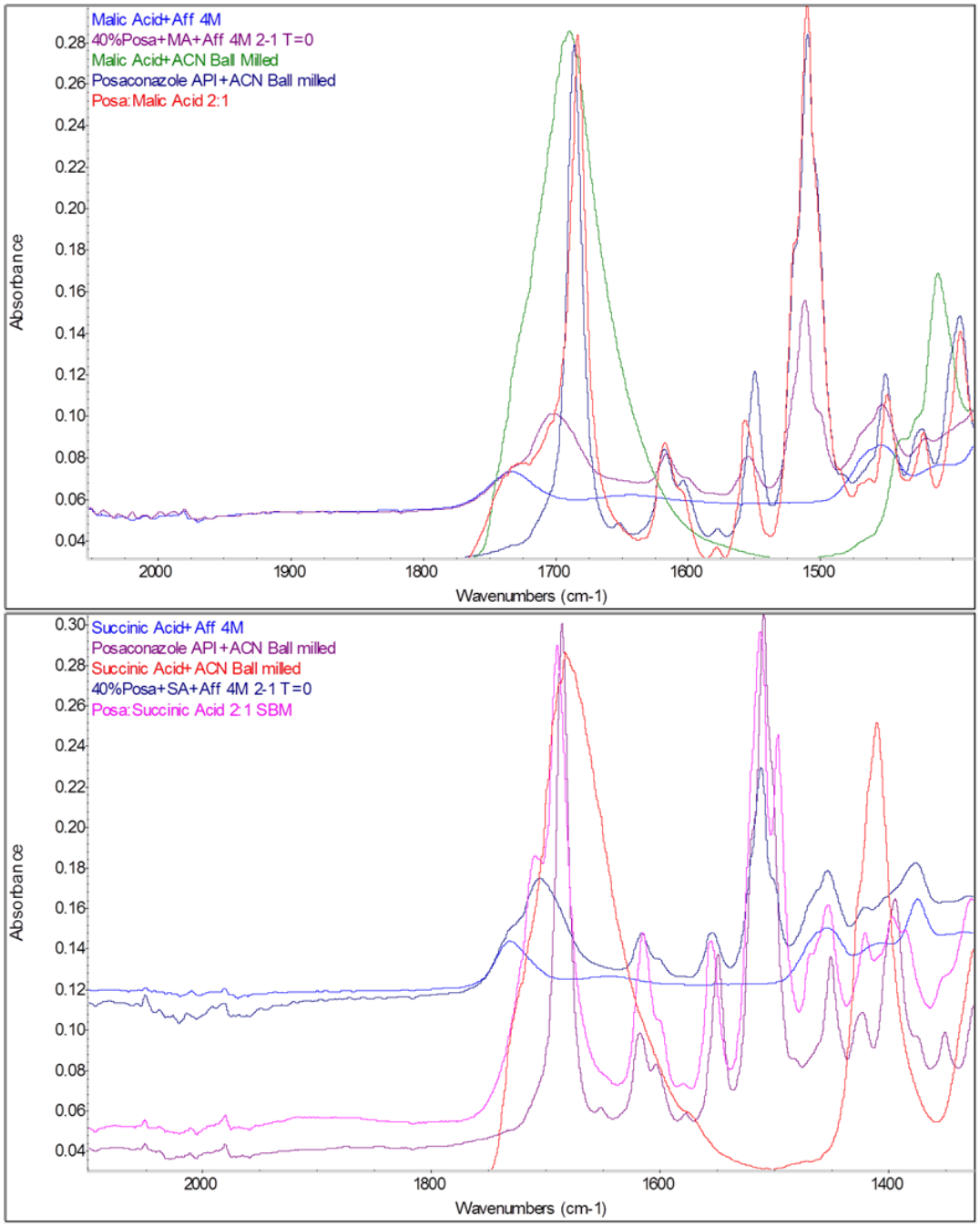

Figure 6.26 ATR-FTIR spectra of milled extrudates of 40%Posa and Affinisol 4M with succinic (top) and L-malic acid (bottom)

Day 0 dissolution studies of milled samples showed a slight increase drug release in 40%Posa+Malic acid+ Affinisol 4M (2-1) compared to 40%Posa+Affinisol 4M batch (Figure 6.27). However, highest release was observed in 40%Posa+Succinic acid+ Affinisol 4M batch.

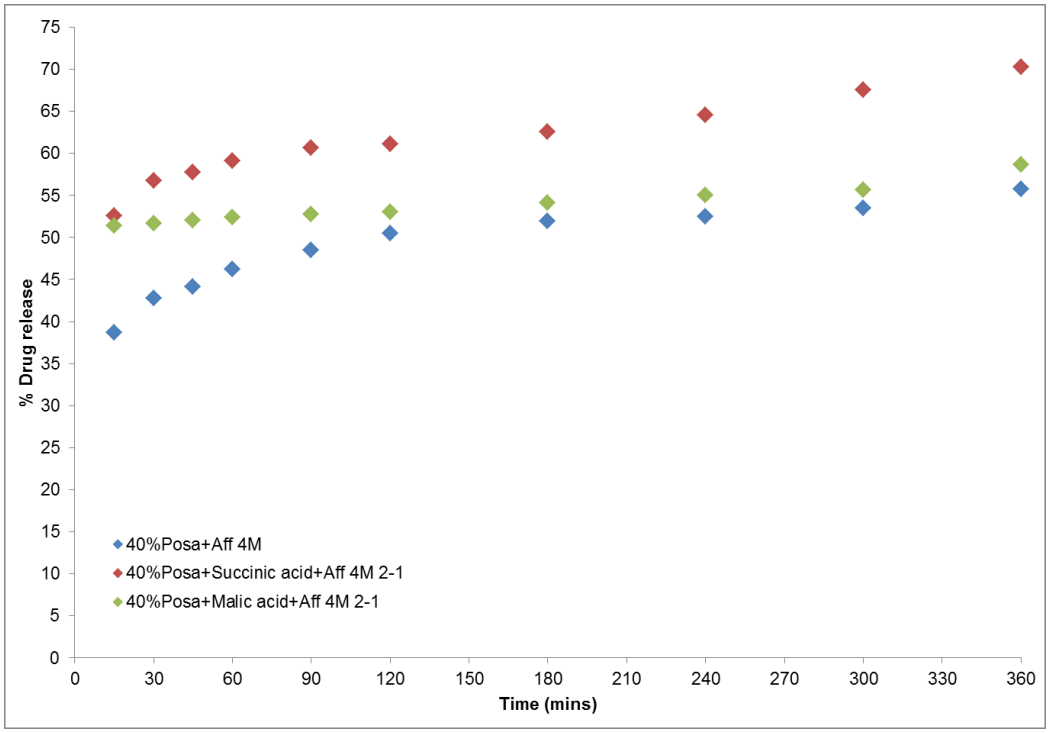

Figure 6.27 Dissolution studies of milled extrudates of 40%Posa and Affinisol 4M with succinic and L-malic acid at day 0

The current comparison is only based on the dose of 100mg of posaconazole; hence the release could increase with increase in drug content. Dissolution of pellets was also carried out but very low release was observed due to crystallisation of surface of the posaconazole pellets which formed a barrier for buffer (Figure 6.28).

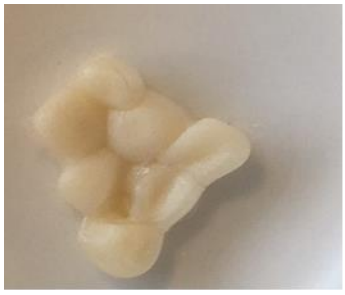

40%Posa+Aff 4M

40%Posa+SA+Aff 4M(2-1)

40%Posa+MA+Aff 4M(2-1)

Figure 6.28 Pellets of 40%Posa and Affinisol 4M with succinic and L-malic acid at day 0 post dissolution

Hence, dissolution studies for all Posa+ Affinisol 4M extrudates were carried out only on the milled samples.

Upon stability, it was observed that 40%Posa+Malic acid+ Affinisol 4M (2-1) batch recrystallised at 40°C/75%RH condition on the 30th day while 40%Posa+Succininc acid+ Affinisol 4M (2-1) batch recrystallised at same condition on the 60th day. 40%Posa+ Affinisol 4M batch was still stable at all conditions after 360 days.

However, when the extrudates were analysed for solid state stability, posaconazole was not found to be completely crystalline. ATR-FTIR spectra showed the shift of amorphous posaconazole band to crystalline posaconazole band for both succinic and L-malic acid (Figure 6.29).

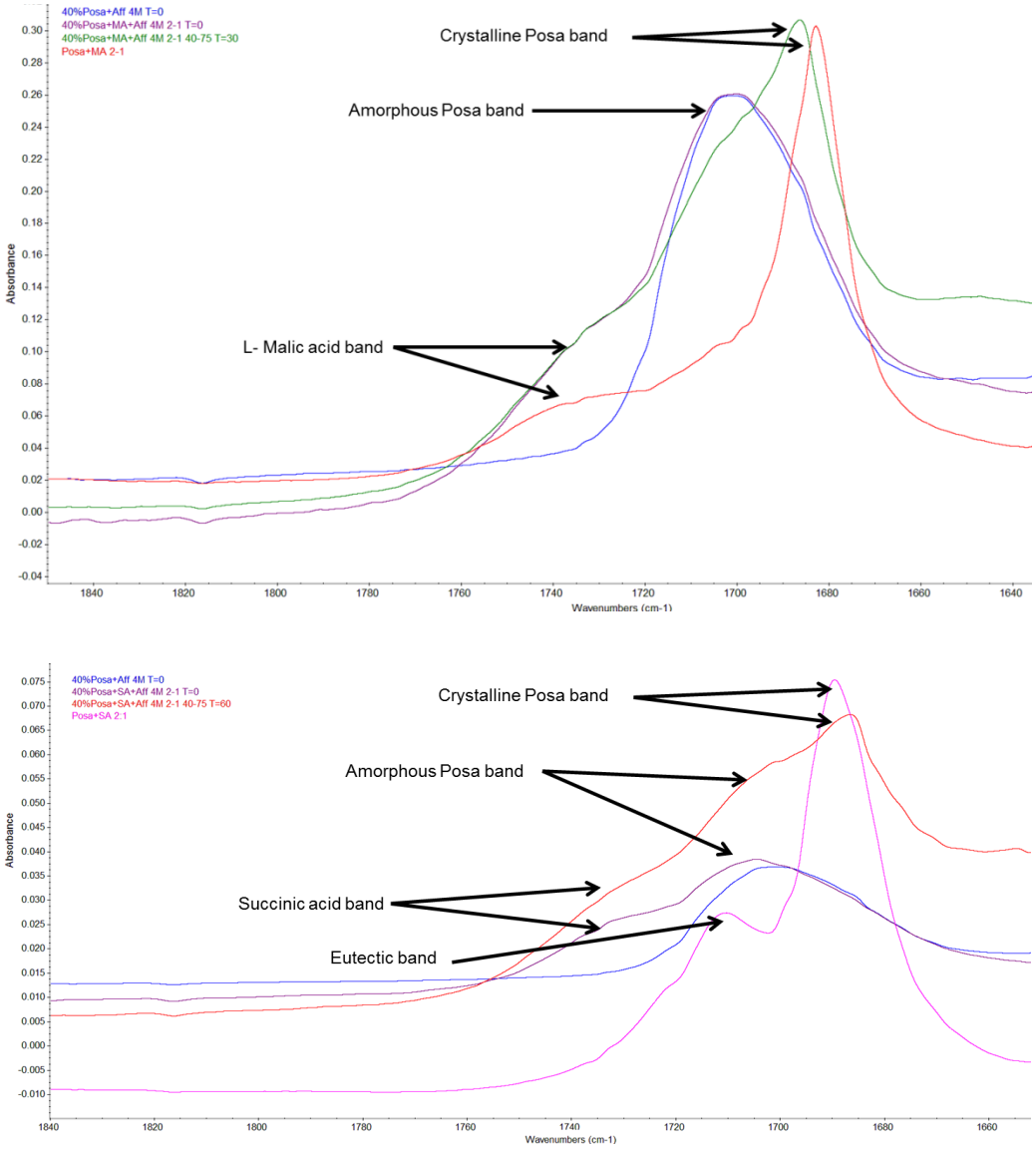

Figure 6.29 ATR-FTIR spectra of 40%Posa and Affinisol 4M with succinic and L-malic acid

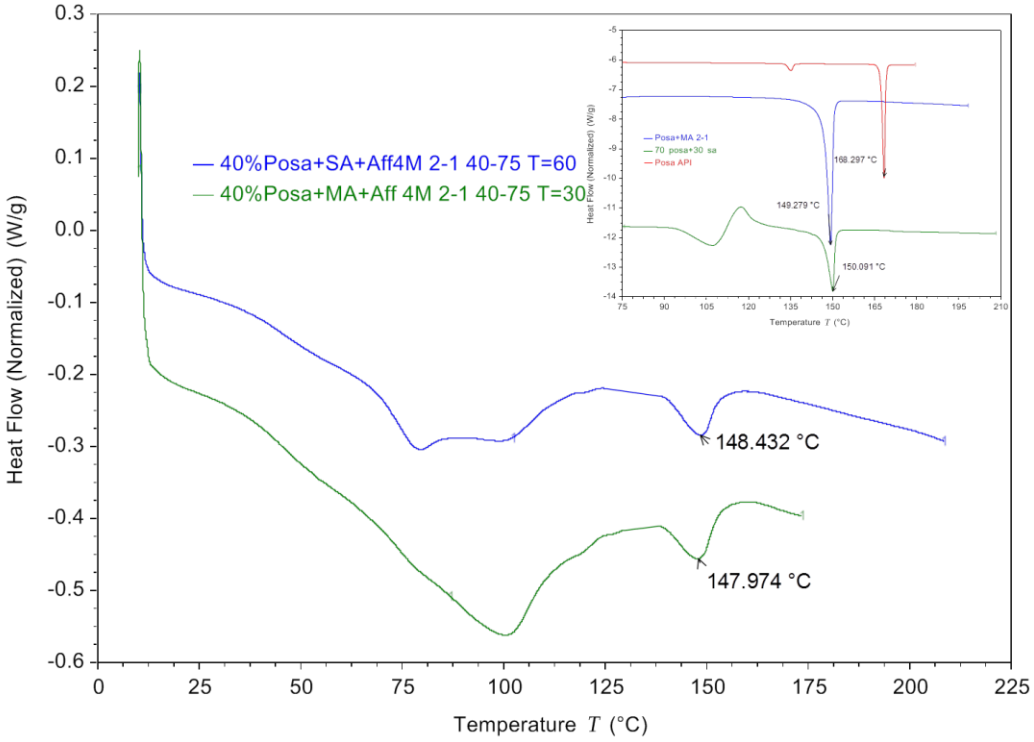

Figure 6.30 DSC thermogram of 40%Posa and Affinisol 4M with succinic and L-malic acid

DSC thermograms showed an absence of melting endothermic events for both the day 0 extrudates. Additionally, endothermic peak at the position of eutectic and co-crystal formed between Posa with succinic and L-malic acid was observed (Figure 6.30). Thus, it was interesting to note that crashing of the ternary system caused an interaction between crystalline posaconazole and succinic and L-malic acid to form eutectic and co-crystal within Affinisol 4M. Hence, posaconazole upon recrystallisation still was partly amorphous and partly eutectic/co-crystal with the additive dicarboxylic acids.

It would be worth studying the impact of the eutectic and co-crystal formed within Affinisol 4M on the drug release of posaconazole. Dissolution studies were again carried out on the milled samples to check for drug release.

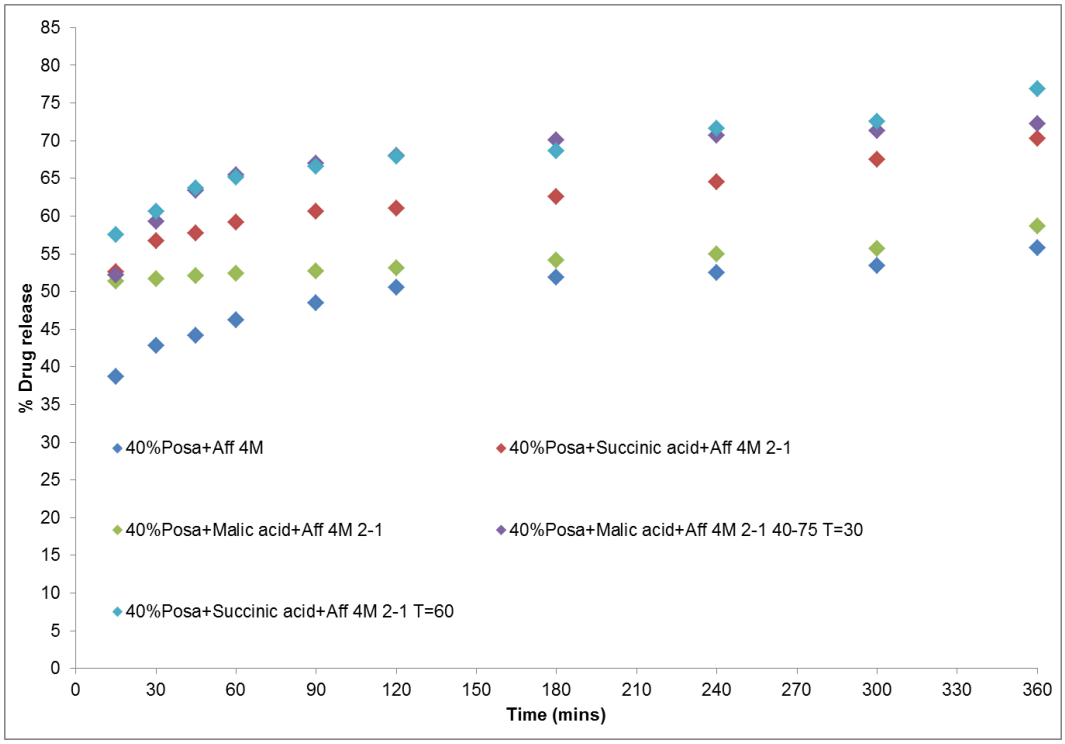

Figure 6.31 Dissolution studies of 40%Posa and Affinisol 4M with succinic and L-malic acid

The general convention would dictate a decrease in drug release due to formation of crystalline posaconazole. However, an increase in drug release was observed in both the batches. The release was also higher compared to the observed release on day 0 (Figure 6.31). But both the batches showed similar release patterns even though being analysed on 30th and 60th day respectively. This proves that the formation of either eutectic or co-crystal of posaconazole with succinic and L-malic acid within Affinisol 4M had a positive impact on the drug release. Thus, addition of dicarboxylic acids had a positive impact on the drug release of posaconazole in acidic pH.

T-Test paired two samples for means was applied to the % drug released at 360 mins for all samples. P-value for all the means was found to be significant and thus the difference in % drug release is significant (Table 6.4).

t-Test: Paired Two Sample for Means	40%Posa+Aff 4M	40%Posa+Succinic acid+Aff 4M 2-1
Mean	55.76408878	70.29953706
Variance	0.002579231	4.28633E-07
Observations	2	2
Pearson Correlation	1	
Hypothesized Mean Difference	0	
df	1	
t Stat	-410.0467277	
P(T<=t) one-tail	0.000776276	
t Critical one-tail	6.313751515	
P(T<=t) two-tail	0.001552551	
t Critical two-tail	12.70620474	

t-Test: Paired Two Sample for Means	40%Posa+Aff 4M	40%Posa+Malic acid+Aff 4M 2-1
Mean	55.76408878	58.62871715
Variance	0.002579231	0.000905919
Observations	2	2
Pearson Correlation	1	
Hypothesized Mean Difference	0	
df	1	
t Stat	-195.8269053	
P(T<=t) one-tail	0.001625451	
t Critical one-tail	6.313751515	
P(T<=t) two-tail	0.003250903	
t Critical two-tail	12.70620474	

t-Test: Paired Two Sample for Means	40%Posa+Succinic acid+Aff 4M 2-1	40%Posa+Succinic acid+Aff 4M 2-1 T=60
Mean	70.29953706	76.825
Variance	4.28633E-07	0.03125
Observations	2	2
Pearson Correlation	1	
Hypothesized Mean Difference	0	
df	1	
t Stat	-52.39776097	
P(T<=t) one-tail	0.006074138	
t Critical one-tail	6.313751515	
P(T<=t) two-tail	0.012148277	
t Critical two-tail	12.70620474	

t-Test: Paired Two Sample for Means	40%Posa+Succinic acid+Aff 4M 2-1	40%Posa+Malic acid+Aff 4M 2-1
Mean	70.29953706	58.62871715
Variance	4.28633E-07	0.000905919
Observations	2	2
Pearson Correlation	1	
Hypothesized Mean Difference	0	
df	1	
t Stat	560.5607212	
P(T<=t) one-tail	0.000567841	
t Critical one-tail	6.313751515	
P(T<=t) two-tail	0.001135683	
t Critical two-tail	12.70620474	

t-Test: Paired Two Sample for Means	40%Posa+Malic acid+Aff 4M 2-1 40-75 T=30	40%Posa+Succinic acid+Aff 4M 2-1 T=60
Mean	72.20151653	76.825
Variance	0.004701295	0.03125
Observations	2	2
Pearson Correlation	1	
Hypothesized Mean Difference	0	
df	1	
t Stat	-60.42463968	
P(T<=t) one-tail	0.005267401	
t Critical one-tail	6.313751515	
P(T<=t) two-tail	0.010534803	
t Critical two-tail	12.70620474	

t-Test: Paired Two Sample for Means	40%Posa+Malic acid+Aff 4M 2-1	40%Posa+Malic acid+Aff 4M 2-1 40-75 T=30
Mean	58.62871715	72.20151653
Variance	0.000905919	0.004701295
Observations	2	2
Pearson Correlation	1	
Hypothesized Mean Difference	0	
df	1	
t Stat	-498.9884471	
P(T<=t) one-tail	0.000637909	
t Critical one-tail	6.313751515	
P(T<=t) two-tail	0.001275819	
t Critical two-tail	12.70620474	

Table 6. 4 t-Test paired to sample for means of milled Posa extrudates.

6.3 Summary

For determining the maximum concentration for a stable Posa-Affinisol 4M extrudates, HME trials with varying in Posa concentration were carried out. 70%w/w of Posa concentration was found to be the maximum loading for HME processing. Due to the high melting point of posaconazole and degradation temperature of Affinisol 4M, the processing HME temperature window was narrow between 180°C-190°C. All the trials were carried out with same temperature profiles. All extrudates were stationed at different stability conditions to check for its solid state stability. 40%w/w Posa-Affinisol 4M

extrudates were found to stable for more than 8 months. Subsequently, concentrations below 40% were also found to be stable.

Marketed posaconazole suspensions had the drawback of negative effect of oral bioavailability due to the presence of food. Hence to overcome this drawback an enteric coated tablet is marketed which limits drug release in the stomach. However, a formulation strategy to overcome the effect of food by enhancing the drug release in an empty stomach has not previously been studied. In this chapter, an alternative strategy of incorporating dicarboxylic acid as additives was studied. The rationale was to use dicarboxylic acids to impart acidity to the product to enhance the drug release in empty stomach.

Posaconazole formed a eutectic and a co-crystal with succinic acid and L-malic acid respectively in the 2:1 stoichiometry. To confirm this, a binary phase diagram was plotted and solid state was confirmed using thermal, spectroscopic and diffraction methods. An improved intrinsic dissolution rate was observed in the eutectic and co-crystal states compared to posaconazole alone.

Of all the five selected additives, only maleic acid, succinic acid and L-malic acid trials gave single phase extrudates with 40% posaconazole and Affinisol 4M. Trials with maleic acid showed no comparable increase in dissolution compared to 40%Posa+Aff 4M extrudates. Increase in drug release was observed for the other two acids. Following stability studies, the 40%Posa+Malic acid+ Affinisol 4M (2-1) batch and 40%Posa+Succininc acid+ Affinisol 4M (2-1) batch recrystallised but showed increase in drug release as compared to 40%Posa+Aff4M batch. A positive effect in the drug release was

observed which could be due to formation of eutectic and co-crystal with the free succinic acid and L-malic acid.

Single crystal XRD or solid state NMR studies are needed to affirm the formation of eutectic or co-crystal of Posa with succinic acid and L-Malic acid. The formulation strategy to incorporate dicarboxylic acids as additives had a positive effect on drug release but had a negative effect on the solid state stability of the extrudates. Also, complete drug release was not observed. Trials with low molecular weight Affinisol^{TM}HPMC should be carried out to check its effect on dissolution.

Chapter 7: Global Conclusions and suggestions for future work

This chapter will summarise the conclusion made from studies carried out and provide suggestions for future work.

7.1 Global conclusions

The work carried out provides a detailed study of formulation development of pharmaceutical dosage forms using hot melt extrusion process. Focus was on the challenges and the findings of the work were divided into three main critical attributes important for process feasibility and optimisation. Further relevant studies focussing on the same were carried out to address the relevant issues arising during formulation development using HME. Robust HME process was developed using IBU and POSA as API and Affinisol^{TM}HPMC as amorphous polymer.

Understanding the material attributes affecting formulation development is one of the critical attribute during process development using HME. A detailed investigation in the physicochemical properties of IBU, Posa and Affinisol^{TM}HPMC was carried out. Theoretical methods like solubility parameters, fragility index and binary phase diagram were utilised to predict solid state solubility and miscibility between API-polymer combinations. Rationale, method development and validation of solid state characterisation methods like thermal, spectroscopic, diffraction, and water uptake were developed for both API-polymer combinations. All the above mentioned methods were used to identify the crystalline and amorphous domains of the APIs. HME trials for ibuprofen-Affinisol 100cP were carried out to form amorphous solid dispersion.

Material behaviour during melt processing is another critical quality attribute for process optimisation using HME. The behaviour is heavily dependent upon physicochemical properties. Effects of ibuprofen concentration on the rheological and mechanical properties of the extrudates with Affinisol 100cP were studied. A decrease in complex viscosity from rotational and capillary rheometer was observed with increase in ibuprofen concentration. The data generated was analysed using Carreau-Yasuda and Power law model. Shear thinning was observed for all the ibuprofen-Affinisol 100cP blends. Data obtained from rotational and capillary rheometer were fitted using Cox-Mertz rule. All the ibuprofen-Affinisol 100cP blends failed to follow the Cox-Mertz rule. Storage or elastic modulus (E') generated using DMA showed a decrease with increase in ibuprofen concentration. A similar trend was observed with tan delta (Δ) values. Thus, from melt rheology and visco-elastic properties of extrudates it was observed that an increase in ibuprofen concentration imparts plasticisation by decreasing the glass transition temperature of the extrudates. Tan delta (Δ) values were found to be in good correlation with predicted values by the Fox equation. Correlation between values obtained from the Fox equation and DMA confirmed the absence of inter-component interaction in the melt and glassy state of the ibuprofen-Affinisol 100cP mixture. An attempt was made to map the storage modulus E' & G' obtained from DMA and rotational rheometer over a range of temperature. A large difference was observed between the moduli of melt and a solid phase for all the ibuprofen-Affinisol 100cP blends. Thus, understanding shear thinning behaviour and visco-elastic nature of

extrudates provide a platform for optimisation of process for amorphous solid dispersion using HME.

Drug release from ibuprofen-Affinisol 100cP extrudates showed a dual mechanism of swelling and erosion. 10% and 20% loadings followed Peppas and zero order showing controlled release while higher drug loads of 30% and 40% followed Peppas and first order models showing sustained release.

Effect of process parameters on the product performance using HME was studied using the Taguchi method. Feed rate, screw speed and screw configuration were selected as process variables while mean residence time, torque, pressure, DSC and dissolution were used as response. Although the process study was carried out on 40% drug load only, but mean residence time was calculated for all drug loadings. Mean residence time increase with increase in ibuprofen concentration within extrudates.

Feed rate was found to be the only significant parameter to affect residence time measurement. Higher feed rate reduced residence time measurement by half. Torque was found to be affected by screw configuration and screw speed while pressure was affected only by screw speed. For dissolution, a screw configuration with two mixing zones had a positive effect on the drug release and was found to be the only significant factor. DSC and dissolution response confirm the assumption that higher mixing favoured an increase in solid state solubility and miscibility between 40%IBU-Affinisol 100cP extrudates.

For process optimisation of 40%IBU-Affinisol 100cP blends, feed rate should be kept the highest at 0.6kg/hr. Screw speed for the blend should be 500rpm. Screw configuration with no mixing element produces less torque, but it’s still

way below the process capability and hence screw configuration with two mixing zones should be preferred.

One of the critical formulation factors in the development of amorphous solid dispersions (ASD) is prediction of the maximum drug concentration which a stable ASD can support. Ibuprofen dimer in the solid dispersion was found to be an early indicator of solid-state stability. ATR-FTIR was used as a predictive tool to indicate long-term stability of ASDs by providing a mechanistic understanding of the drug-drug molecular association within the polymer matrix. This approach has significant advantages over conventional methods such as theoretical binary phase diagrams by Flory-Huggins polymer solution theory, or by subjecting samples to accelerated stability tests. 15% ibuprofen loaded extrudates were found to show an absence of dimer and were stable for more than 8 months. Lower IBU concentration extrudates at 20, 15 and 10% loadings were stable at all three stability conditions measured up to 8 months. The 20% IBU concentration extrudates were predicted to recrystallise due to decrease presence of ibuprofen dimer domains but this was not observed with 8 months of the study.

From formulation a perspective, it is desirable to incorporate maximum possible concentration of drug within polymer to for ASD. This will control size and weight and also minimise the cost and dose frequency of the final dosage form. Hence, finding out the API maximum concentration is one of the key critical attribute during product development. To overcome effect of food on the oral bioavailability of posaconazole, an alternative formulation strategy was studied. Rationale was to use additives containing dicarboxylic acid to

enhance dissolution of posaconazole in acidic pH. Since here dicarboxylic acids are evaluated as additives for posaconazole and affinisol 4M binary blends, initial trials were taken with all dicarboxylic acids with 40% posaconazole load in Affinisol 4M.HME trials and solid state stability of Posa and Affinisol 4M blends were carried out. 70% of Posa loading was found to be the maximum feasible concentration for HME. Due to high melting point of posaconazole, extrusion trials were extruded at same temperature. Processing temperature window was also found to be narrow, between 180°C and 190°C. All concentrations from 40%w/w and below of Posa loadings were found to be stable for more than 8 months. Of the five additives selected, posaconazole was found to form a eutectic and co-crystal with succinic acid and L-malic acid in the 2:1 stoichiometry. Stoichiometry was confirmed by plotting a binary phase diagram. Formation of eutectic and co-crystal were confirmed using thermal, spectroscopic and diffraction analytical methods. An improved intrinsic dissolution rate was observed in the eutectic and co-crystal compared to posaconazole alone. Only maleic acid, succinic acid and L-malic acid trials produced single phase extrudates with 40% posaconazole and Affinisol 4M. Trials with maleic acid showed no comparable increase in dissolution compared with 40%Posa+Aff 4M extrudates. Day 0 dissolution studies of milled samples showed a slight increase drug release in 40%Posa+Malic acid+ Affinisol 4M (2-1) compared to 40%Posa+Affinisol 4M batch (Figure 6.26). However, highest release was observed in 40%Posa+Succinic acid+ Affinisol 4M batch. Upon stability, it was observed that 40%Posa+Malic acid+ Affinisol 4M (2-1) batch recrystallised at 40°C/75%RH condition on the 30th day while 40%Posa+Succininc acid+

Affinisol 4M (2-1) batch recrystallised at same condition on the 60th day. 40%Posa+ Affinisol 4M batch was still stable at all conditions for over 360 days.

The general convention would dictate a decrease in drug release due to the formation of crystalline posaconazole. However, an increase in drug release was observed in both the batches. The release was also higher compared to the observed release on day 0. The formation of either eutectic or co-crystal of posaconazole with succinic and L-malic acid within Affinisol 4M had a positive impact on the drug release. Thus, addition of dicarboxylic acids had a positive impact on the drug release of posaconazole in acidic pH.

7.2 Suggestions for future studies

The aim of the project was to develop controlled/sustained release products using HME. Due to which, higher molecular weight grades of Affinisol^{TM}HPMC were used to achieve sustained release. However, feasibility studies need to be carried out to check the drug release using lower molecular weight grades of Affinisol^{TM}HPMC. The aim would be to check whether incorporation in lower molecular weight grades of Affinisol^{TM}HPMC show sustained release.

The study did not focus on one critical quality attribute of product impurity/relative substance. Relative substances for both the API-polymer blends need to be studied. Solution state degradation need to be studied in detail. Also, Studies to confirm drug purity within extrudates and pellets needs to be carried out by HPLC.

Drug release mechanism was concluded by visual observations of the pellet during and after dissolution. More studies should be carried out to confirm the mechanism of drug release during in-vitro dissolution. Analytical tools like particle video microscopy (PVM) and focussed beam reflectance microscopy (FBRM) should be used to confirm drug release. Surface dissolution can also be studied using in-situ monitoring by UV imaging. Pion's SDi2 is one such powerful analytical tool which can help in understanding the same.

Solid state degradation were indirectly studied using TGA and rotational rheometer but thermal/forced degradation of IBU and POSA during HME process needs to be studied in detail. Effect of high temperature and shear on Affinisol^{TM}HPMC degradation should be studied. This will help in building confidence on the process.

Down-streaming process like milling and tabletting should be investigated and studied to develop robust formulated products. With increase in IBU load an increase in plasticity was observed. Also, deviation to Fox equation was observed which could be due to saturated solubility between IBU and polymer. Taking values of Tan Δ as reference a study needs to be carried out to understand its implications on the milling process.

To fully understand the effect of process variables, a full factorial design of experiments should be carried out. The study will highlight the effect of interaction of variables. A more robust process model can be developed.

To confirm the sensitivity and selectivity of ibuprofen dimer as early indicator of solid state stability, trials need to be carried out with different polymers apart from cellulose based derivatives.

Single crystal XRD or solid state NMR studies are needed to affirm the formation of eutectic or co-crystal of Posa with succinic acid and L-Malic acid. The aim of this project was to achieve sustained release, however for Posa an immediate release profile is preferred due to its anti-fungal activity. Hence, trials with low molecular weight Affinisol^{TM}HPMC and Posa should be carried out to check its effect on dissolution.

Chapter 8: Bibliography

Adamska, K. and Voelkel, A. (2005) Inverse gas chromatographic determination of solubility parameters of excipients. *Int J Pharm* 304 (1-2) 11-7.

Aher, S., Dhumal, R., Mahadik, K., Paradkar, A. and York, P. (2010) Ultrasound assisted cocrystallization from solution (USSC) containing a non-congruently soluble cocrystal component pair: Caffeine/maleic acid. *European Journal of Pharmaceutical Sciences* 41 (5) 597-602.

Aho, J., Boetker, J. P., Baldursdottir, S. and Rantanen, J. (2015) Rheology as a tool for evaluation of melt processability of innovative dosage forms. *Int J Pharm* 494 (2) 623-42.

Aho, J., Edinger, M., Botker, J., Baldursdottir, S. and Rantanen, J. (2016) Oscillatory Shear Rheology in Examining the Drug-Polymer Interactions Relevant in Hot Melt Extrusion. *Journal of Pharmaceutical Sciences* 105 (1) 160-167.

Andrews, D. R., Leong, W. and Sudhakar, A. (2004) Crystalline antifungal polymorph. *US6713481B1* 1-19.

Andrews, D. R., Leong, W. and sudhakar, A. (2005) Crystalline anitfungal polymorph. *US6958337B2* 1-20.

Angell, C. A. (1988) Structural instability and relaxation in liquid and glassy phases near the fragile liquid limit. *Journal of Non-Crystalline Solids* 102 (1) 205-221.

Angell, C. A. (1991) Relaxation in liquids, polymers and plastic crystals — strong/fragile patterns and problems. *Journal of Non-Crystalline Solids* 131-133 (1) 13-31.

Angell, C. A. (1995) The old problems of glass and the glass transition, and the many new twists. *Proceedings of the National Academy of Sciences* 92 (15) 6675-6682.

Aubuchon, S. R. (2011) Detection and Quantification of Amorphous Content in Pharmaceutical Materials; Thermometric Application note TA 340. ---.

Babu, N. J. and Nangia, A. (2011) Solubility advantage of amorphous drugs and pharmaceutical cocrystals. *Crystal Growth and Design* 11 (7) 2662-2679.

Baghel, S., Cathcart, H. and O'Reilly, N. J. (2016) Polymeric Amorphous Solid Dispersions: A Review of Amorphization, Crystallization, Stabilization, Solid-State Characterization, and Aqueous Solubilization of Biopharmaceutical Classification System Class II Drugs. *J Pharm Sci* 105 (9) 2527-44.

Baird, J. A. and Taylor, L. S. (2012) Evaluation of amorphous solid dispersion properties using thermal analysis techniques. *Adv Drug Deliv Rev* 64 (5) 396-421.

Baishya, H., Gouda, R. and Qing, Z. (2017) Application of Mathematical Models in Drug Release Kinetics of Carbidopa and Levodopa ER Tablets. *Journal of Developing Drugs* 06 (02).

Baxevanis, F., Kuiper, J. and Fotaki, N. (2016) Fed-state gastric media and drug analysis techniques: Current status and points to consider. *Eur J Pharm Biopharm* 107 234-48.

Bennett, R. C., Brough, C., Miller, D. A., O'Donnell, K. P., Keen, J. M., Hughey, J. R., Williams, R. O. and McGinity, J. W. (2015) Preparation of amorphous solid dispersions by rotary evaporation and KinetiSol Dispersing: approaches to enhance solubility of a poorly water-soluble gum extract. *Drug Development and Industrial Pharmacy* 41 (3) 382-397.

Berry, D. J., Seaton, C. C., Clegg, W., Harrington, R. W., Coles, S. J., Horton, P. N., Hursthouse, M. B., Storey, R., Jones, W., Friščić, T. and Blagden, N. (2008) Applying Hot-Stage Microscopy to Co-Crystal Screening: A Study of Nicotinamide with Seven Active Pharmaceutical Ingredients. *Crystal Growth & Design* 8 (5) 1697-1712.

Bhardwaj, S. P., Arora, K. K., Kwong, E., Templeton, A., Clas, S. D. and Suryanarayanan, R. (2014) Mechanism of amorphous itraconazole stabilization in polymer solid dispersions: role of molecular mobility. *Mol Pharm* 11 (11) 4228-37.

Bhardwaj, S. P. and Suryanarayanan, R. (2012) Molecular Mobility as an Effective Predictor of the Physical Stability of Amorphous Trehalose. *Molecular Pharmaceutics* 9 (11) 3209-3217.

Borbas, E., Nagy, Z. K., Nagy, B., Balogh, A., Farkas, B., Tsinman, O., Tsinman, K. and Sinko, B. (2018) The effect of formulation additives on in vitro dissolution-absorption profile and in vivo bioavailability of telmisartan from brand and generic formulations. *Eur J Pharm Sci* 114 310-317.

Borde, B., Bizot, H., Vigier, G. and Buleon, A. Calorimetric analysis of the structural relaxation in partially hydrated amorphous polysaccharides. I. Glass transition and fragility. *Carbohydrate Polymers* 48 (1) 83-96.

Breitenbach J, S. W., Neumann J. (1999) Confocal Raman-Spectroscopy-Analytical Approach to Solid Dispersions and Mapping of Drugs. *Pharmaceutical Research* 16 (7) 1109-1113.

Broadhead, J., Edmond Rouan, S. K. and Rhodes, C. T. (1992) <u>The spray drying of pharmaceuticals</u> . *Drug Development and Industrial Pharmacy* 18 (11-12) 1169-1206.

Bunaciu, A. A., Udriştioiu, E. g. and Aboul-Enein, H. Y. (2015) X-Ray Diffraction: Instrumentation and Applications. *Critical Reviews in Analytical Chemistry* 45 (4) 289-299.

CDER/FDA (2015) Guidance for Industry, Waiver of in vivo bioavailability and bioequivalence studies for immediate release solid oral dosage forms based on a biopharmaceutics classification system. *Center for Drug Evaluation and Research* (May) 1-2.

Chadwick, K., Davey, R. and Cross, W. (2007) How does grinding produce co-crystals? Insights from the case of benzophenone and diphenylamine. *CrystEngComm* 9 (9) 732-734.

Chen, J., Mosquera-Giraldo, L. I., Ormes, J. D., Higgins, J. D. and Taylor, L. S. (2015) Bile Salts as Crystallization Inhibitors of Supersaturated Solutions of Poorly Water-Soluble Compounds. *Crystal Growth & Design* 15 (6) 2593-2597.

Chen, Y., Gao, Z. and Duan, J. Z. (2017a) Chapter 13 - Dissolution Testing of Solid Products. *Developing Solid Oral Dosage Forms (Second Edition).* Boston: Academic Press. 355-380 https://www.sciencedirect.com/science/article/pii/B9780128024478000133

Chen, Y., Wang, J. and Flanagan, D. R. (2017b) Chapter 9 - Fundamental of Diffusion and Dissolution. *Developing Solid Oral Dosage Forms (Second Edition).* Boston: Academic Press. 253-270 https://www.sciencedirect.com/science/article/pii/B9780128024478000091

Chen, Y., Wang, S., Wang, S., Liu, C., Su, C., Hageman, M., Hussain, M., Haskell, R., Stefanski, K. and Qian, F. (2016) Initial Drug Dissolution from Amorphous Solid Dispersions Controlled by Polymer Dissolution and Drug-Polymer Interaction. *Pharm Res* 33 (10) 2445-58.

Cherukuvada, S. and Guru Row, T. N. (2014) Comprehending the Formation of Eutectics and Cocrystals in Terms of Design and Their Structural Interrelationships. *Crystal Growth & Design* 14 (8) 4187-4198.

Cherukuvada, S. and Nangia, A. (2012) Fast dissolving eutectic compositions of two anti-tubercular drugs. *CrystEngComm* 14 (7) 2579.

Cherukuvada, S. and Nangia, A. (2014) Eutectics as improved pharmaceutical materials: design, properties and characterization. *Chem Commun (Camb)* 50 (8) 906-23.

Chiou, D., Langrish, T. A. G. and Braham, R. (2008) *The effect of temperature on the crystallinity of lactose powders produced by spray drying.* Vol. 86.

Cogswell, F. N. (1981) *Polymer Melt Rheology: A guide for industrial practice.* Great Britain: Woodhead Publishing Ltd. .

Costa, F. O., Sousa, J. J. S., Pais, A. A. C. C. and Formosinho, S. J. (2003) Comparison of dissolution profiles of Ibuprofen pellets. *Journal of Controlled Release* 89 (2) 199-212.

Cowie, J. M. G. (1968) Estimation of the cohesive energy density of a polymer from critical opalescence measurements.pdf. *Canadian Journal of Chemistry* 46 (24) 3919-3921.

Craig, D., Kett, V., Murphy, J. and Price, D. (2001) *The Measurement of Small Quantities of Amorphous Material—Should We Be Considering the Rigid Amorphous Fraction?* Vol. 18.

Craig, D. Q. M. (2002) The mechanisms of drug release from solid dispersions in water-soluble polymers. *International Journal of Pharmaceutics* 231 131-144.

Crowley, M. M., Zhang, F., Repka, M. A., Thumma, S., Upadhye, S. B., Kumar Battu, S., McGinity, J. W. and Martin, C. (2007) Pharmaceutical Applications of Hot-Melt Extrusion: Part I. *Drug Development and Industrial Pharmacy* 33 (9) 909-926.

Dahan, A., Miller, J. M. and Amidon, G. L. (2009) Prediction of Solubility and Permeability Class Membership: Provisional BCS Classification of the World's Top Oral Drugs. *The AAPS Journal* 11 (4) 740-746.

Daurio, D., Nagapudi, K., Li, L., Quan, P. and Nunez, F. A. (2014) Application of twin screw extrusion to the manufacture of cocrystals: scale-up of AMG 517-sorbic acid cocrystal production. *Faraday Discuss* 170 235-49.

David J. Greenhalgh, A. C. W., Peter Timmins, Peter York (1999) Solubility parameters as predictors of miscibility in solid dispersions. *Journal of Pharmaceutical Sciences* 88 (11) 1182-1190.

De Beer, T., Burggraeve, A., Fonteyne, M., Saerens, L., Remon, J. P. and Vervaet, C. (2011) Near infrared and Raman spectroscopy for the in-

process monitoring of pharmaceutical production processes. *International Journal of Pharmaceutics* 417 (1–2) 32-47.

Dekkers, B. G. J., Bakker, M., van der Elst, K. C. M., Sturkenboom, M. G. G., Veringa, A., Span, L. F. R. and Alffenaar, J. C. (2016) Therapeutic Drug Monitoring of Posaconazole: an Update. *Curr Fungal Infect Rep* 10 51-61.

Dengale, S. J., Grohganz, H., Rades, T. and Löbmann, K. (2016) Recent advances in co-amorphous drug formulations. *Advanced Drug Delivery Reviews* 100 116-125.

Descamps, M., Willart, J. F., Dudognon, E. and Caron, V. (2007) Transformation of pharmaceutical compounds upon milling and comilling: the role of T(g). *Journal of pharmaceutical sciences* 96 (5) 1398-1407.

Desiraju, G. (1995) Supramolecular Synthons in Crystal Engineering—A New Organic Synthesis. *Angewandte Chemie International Edition in English* 34 (21) 2311-2327.

Dey, B., Katakam, P., Assaleh, F. H., Chandu, B. R., Adiki, S. K. and Mitra, A. (2015) In vitro-in vivo studies of the quantitative effect of calcium, multivitamins and milk on single dose ciprofloxacin bioavailability. *J Pharm Anal* 5 (6) 389-395.

Dhumal, R. S., Kelly, A. L., York, P., Coates, P. D. and Paradkar, A. (2010) Cocrystalization and simultaneous agglomeration using hot melt extrusion. *Pharm Res* 27 (12) 2725-33.

Dong, Q., Zang, H., Liu, A., Yang, G., Sun, C., Sui, L., Wang, P. and Li, L. (2010) Determination of molecular weight of hyaluronic acid by near-infrared spectroscopy. *Journal of Pharmaceutical and Biomedical Analysis* 53 (3) 274-278.

Dong, Z., Chatterji, A., Sandhu, H., Choi, D. S., Chokshi, H. and Shah, N. (2008) Evaluation of solid state properties of solid dispersions prepared by hot-melt extrusion and solvent co-precipitation. *Int J Pharm* 355 (1-2) 141-9.

Dressman, J. B., Vertzoni, M., Goumas, K. and Reppas, C. (2007) Estimating drug solubility in the gastrointestinal tract. *Adv Drug Deliv Rev* 59 (7) 591-602.

Eby, G. N. (2004) Geochemistry, Principles of Environmental. *Brooks/Cole-Thomson learning* 212-214.

Elkhabaz, A., Sarkar, S., Dinh, J. K., Simpson, G. J. and Taylor, L. S. (2018) Variation in Supersaturation and Phase Behavior of Ezetimibe Amorphous Solid Dispersions upon Dissolution in Different Biorelevant Media. *Mol Pharm* 15 (1) 193-206.

Engers, D., Teng, J., Jimenez-Novoa, J., Gent, P., Hossack, S., Campbell, C., Thomson, J., Ivanisevic, I., Templeton, A., Byrn, S. and Newman, A. (2010) A Solid-State Approach to Enable Early Development Compounds: Selection and Animsal Bioavailability Studies of an Itraconazole Amorphous Solid Dispersion. *Journal of Pharmaceutical Sciences* 99 (9) 3901-3922.

Engisch, W. and Muzzio, F. (2016) Using Residence Time Distributions (RTDs) to Address the Traceability of Raw Materials in Continuous Pharmaceutical Manufacturing. *J Pharm Innov* 11 64-81.

Fang, L. Y., Wan, J. and Harris, D. (2011) ORAL PHARMACEUTICAL COMPOSITIONS IN A SOLID DISPERSION COMPRISING PREFERABLY POSACONAZOLE AND HPMCAS. *US20110034478* 1-15.

Fatouros, D. G., Deen, G. R., Arleth, L., Bergenstahl, B., Nielsen, F. S., Pedersen, J. S. and Mullertz, A. (2007) Structural development of self nano emulsifying drug delivery systems (SNEDDS) during in vitro lipid digestion monitored by Small-angle X-ray scattering. *Pharmaceutical Research* 24 (10) 1844-1853.

Figueiredo, C. B. M., Nadvorny, D., de Medeiros Vieira, A. C. Q., Soares Sobrinho, J. L., Rolim Neto, P. J., Lee, P. I. and de La Roca Soares, M. F. (2017) Enhancement of dissolution rate through eutectic mixture

and solid solution of posaconazole and benznidazole. *Int J Pharm* 525 (1) 32-42.

Forster, A., Hempenstall, J., Tucker, I. and Rades, T. (2001) Selection of excipients for melt extrusion with two poorly water-soluble drugs by solubility parameter calculation and thermal analysis. *International Journal of Pharmaceutics* 226 (1–2) 147-161.

G.Cole, B. B. *Secondary Pharmaceutical Production: An Engineering Guide.*

Garekani, H. A., Sadeghi, F., Badiee, A., Mostafa, S. A. and Rajabi-Siahboomi, A. R. (2001) Crystal habit modifications of ibuprofen and their physicomechanical characteristics. *Drug Dev Ind Pharm* 27 (8) 803-9.

Ghule, P. G., R. ; Jithan, A. ; Bairag, S. ; Aher, A. (2018) Amorphous solid dispersion: a promising technique for improving oral bioavailability of poorly water-soluble drugs. *S Afr Pharm J* 85 (1) 50-56.

Greenhalgh, D. J., Williams, A. C., Timmins, P. and York, P. (1999) Solubility parameters as predictors of miscibility in solid dispersions. *Journal of Pharmaceutical Sciences* 88 (11) 1182-1190.

Gupta, S., Kesarla, R. and Omri, A. (2013) Formulation strategies to improve the bioavailability of poorly absorbed drugs with special emphasis on self-emulsifying systems. *ISRN Pharm* 2013 848043.

Gupta, S. S., Solanki, N. and Serajuddin, A. T. (2016) Investigation of Thermal and Viscoelastic Properties of Polymers Relevant to Hot Melt Extrusion, IV: Affinisol HPMC HME Polymers. *AAPS PharmSciTech* 17 (1) 148-57.

Hancock, B. C. and Zografi, G. (1997) Characteristics and significance of the amorphous state in pharmaceutical systems. *Journal of pharmaceutical sciences* 86 (1) 1-12.

Hansen, C. (1999) Hansen-solubility-parameters.

Haque, M. K. and Roos, Y. H. (2005) Crystallization and X-ray diffraction of spray-dried and freeze-dried amorphous lactose. *Carbohydrate Research* 340 (2) 293-301.

Hedoux, A., Guinet, Y., Derollez, P., Dudognon, E. and Correia, N. T. (2011) Raman spectroscopy of racemic ibuprofen: evidence of molecular disorder in phase II. *Int J Pharm* 421 (1) 45-52.

Hens, B., Brouwers, J., Corsetti, M. and Augustijns, P. (2016) Supersaturation and Precipitation of Posaconazole Upon Entry in the Upper Small Intestine in Humans. *J Pharm Sci* 105 (9) 2677-2684.

Hens, B., Pathak, S. M., Mitra, A., Patel, N., Liu, B., Patel, S., Jamei, M., Brouwers, J., Augustijns, P. and Turner, D. B. (2017) In Silico Modeling Approach for the Evaluation of Gastrointestinal Dissolution, Supersaturation, and Precipitation of Posaconazole. *Mol Pharm* 14 (12) 4321-4333.

Herrmann, H. (1972) *Schneckenmaschinen in der Verfahrenstechnik.* 1 edition*.* Springer-Verlag Berlin Heidelberg.

Hirai, D., Iwao, Y., Kimura, S. I., Noguchi, S. and Itai, S. (2017) Mathematical model to analyze the dissolution behavior of metastable crystals or amorphous drug accompanied with a solid-liquid interface reaction. *Int J Pharm* 522 (1-2) 58-65.

Hitzer, P., Bauerle, T., Drieschner, T., Ostertag, E., Paulsen, K., van Lishaut, H., Lorenz, G. and Rebner, K. (2017) Process analytical techniques for hot-melt extrusion and their application to amorphous solid dispersions. *Anal Bioanal Chem* 409 (18) 4321-4333.

Huang, S., O'Donnell, K. P., Keen, J. M., Rickard, M. A., McGinity, J. W. and Williams, R. O., 3rd (2016) A New Extrudable Form of Hypromellose: AFFINISOL HPMC HME. *AAPS PharmSciTech* 17 (1) 106-19.

Huang, Y. and Dai, W.-G. (2014) Fundamental aspects of solid dispersion technology for poorly soluble drugs. *Acta pharmaceutica Sinica. B* 4 (1) 18-25.

Islam, M. T., Scoutaris, N., Maniruzzaman, M., Moradiya, H. G., Halsey, S. A., Bradley, M. S., Chowdhry, B. Z., Snowden, M. J. and Douroumis, D. (2015) Implementation of transmission NIR as a PAT tool for

monitoring drug transformation during HME processing. *Eur J Pharm Biopharm* 96 106-16.

Jampílek, J. (2012) - Investigation of Carbohydrates and Their Derivatives as Crystallization Modifiers N2 - It is my great honor and pleasure to introduce this comprehensive book to readers who are interested in carbohydrates. This book contains 23 excellent chapters written by experts from the fields of chemistry, glycobiology, microbiology, immunology, botany, zoology, as well as biotechnology. According to the topics, methods and targets, the 23 chapters are further divided into five independent sections. In addition to the basic research, this book also offers much in the way of experiences, tools, and technologies for readers who are interested in different fields of Glycobiology. I believe that readers can obtain more than anticipated from this meaningful and useful book. *Intech* - Ch. 5.

Janssen, L. P. B. M., Hollander, R. W., Spoor, M. W. and Smith, J. M. (1979) Residence time distributions in a plasticating twin screw extruder. *AIChE Journal* 25 (2) 345-351.

Jayachandra Babu, R., Brostow, W., Kalogeras, I. M. and Sathigari, S. (2009) Glass transitions in binary drug+polymer systems. *Materials Letters* 63 (30) 2666-2668.

Jayasankar, A., Good, D. J. and Rodríguez-Hornedo, N. (2007) Mechanisms by Which Moisture Generates Cocrystals. *Molecular Pharmaceutics* 4 (3) 360-372.

Jones, D. S., Margetson, D. N., McAllister, M. S. and Andrews, G. P. (2015) Characterisation and modelling of the thermorheological properties of pharmaceutical polymers and their blends using capillary rheometry: Implications for hot melt processing of dosage forms. *Int J Pharm* 493 (1-2) 251-9.

Jones, D. S., Tian, Y., Abu-Diak, O. and Andrews, G. P. (2012) Pharmaceutical applications of dynamic mechanical thermal analysis. *Adv Drug Deliv Rev* 64 (5) 440-8.

Jones, W., Motherwell, W. D. S. and Trask, A. V. (2011) Pharmaceutical Cocrystals: An Emerging Approach to Physical Property Enhancement. *MRS Bulletin* 31 (11) 875-879.

Jung, Y., Stevens, E., Ding, B., Kim, S., Woo, S.-K. and Lee, J.-K. (2013) *Microstructure and electrical conductivity in shape and size controlled molybdenum particle thick film.* Vol. 48.

K.Kolter, M. K., A.Gryczke (2012) Hot-Melt Extrusion with BASF Pharma Polymers. *Extrusion Compendium* 2.

Kalogeras, I. M. and Brostow, W. (2009) Glass transition temperatures in binary polymer blends. *Journal of Polymer Science Part B: Polymer Physics* 47 (1) 80-95.

Karandikar, H. (2015) *SUITABILITY OF CELLULOSE ESTER DERIVATIVES IN HOT MELT EXTRUSION*. PhD. Bradford, UK: University of Bradford.

Karandikar, H., Ambardekar, R., Kelly, A., Gough, T. and Paradkar, A. (2015) Systematic identification of thermal degradation products of HPMCP during hot melt extrusion process. *Int J Pharm* 486 (1-2) 252-258.

Karmwar, P., Graeser, K., Gordon, K. C., Strachan, C. J. and Rades, T. (2011) Investigation of properties and recrystallisation behaviour of amorphous indomethacin samples prepared by different methods. *International Journal of Pharmaceutics* 417 (1) 94-100.

Kelly, A. (1997) *On-Line Shear And Extensional Rheometry of Polymer Melts In The Extrusion Process.* Doctor Of Philosophy. University Of Bradford.

Kelly, A. L., Gough, T., Dhumal, R. S., Halsey, S. A. and Paradkar, A. (2012) Monitoring ibuprofen–nicotinamide cocrystal formation during solvent free continuous cocrystallization (SFCC) using near infrared spectroscopy as a PAT tool. *International Journal of Pharmaceutics* 426 (1–2) 15-20.

Kelly, A. L., Gough, T., Isreb, M., Dhumal, R., Jones, J. W., Nicholson, S., Dennis, A. B. and Paradkar, A. (2018) In-process rheometry as a PAT tool for hot melt extrusion. *Drug Dev Ind Pharm* 44 (4) 670-676.

Kimanius, D., Pettersson, I., Schluckebier, G., Lindahl, E. and Andersson, M. (2015) SAXS-Guided Metadynamics. *J Chem Theory Comput* 11 (7) 3491-8.

Kissi, E. O., Grohganz, H., Lobmann, K., Ruggiero, M. T., Zeitler, J. A. and Rades, T. (2018) Glass-Transition Temperature of the beta-Relaxation as the Major Predictive Parameter for Recrystallization of Neat Amorphous Drugs. *J Phys Chem B*.

Klein, S. (2010) The use of biorelevant dissolution media to forecast the in vivo performance of a drug. *AAPS J* 12 (3) 397-406.

Knopp, M. M., Tajber, L., Tian, Y., Olesen, N. E., Jones, D. S., Kozyra, A., Lobmann, K., Paluch, K., Brennan, C. M., Holm, R., Healy, A. M., Andrews, G. P. and Rades, T. (2015) Comparative Study of Different Methods for the Prediction of Drug-Polymer Solubility. *Mol Pharm* 12 (9) 3408-19.

Korang-Yeboah, M., Rahman, Z., Shah, D. A. and Khan, M. A. (2016) Spectroscopic-Based Chemometric Models for Quantifying Low Levels of Solid-State Transitions in Extended Release Theophylline Formulations. *Journal of Pharmaceutical Sciences* 105 (1) 97-105.

Köster, M. and Thommes, M. (2010) In-line dynamic torque measurement in twin-screw extrusion process. *Chemical Engineering Journal* 164 (2–3) 371-375.

Kostewicz, E. S., Abrahamsson, B., Brewster, M., Brouwers, J., Butler, J., Carlert, S., Dickinson, P. A., Dressman, J., Holm, R., Klein, S., Mann, J., McAllister, M., Minekus, M., Muenster, U., Mullertz, A., Verwei, M., Vertzoni, M., Weitschies, W. and Augustijns, P. (2014) In vitro models for the prediction of in vivo performance of oral dosage forms. *Eur J Pharm Sci* 57 342-66.

Kostewicz, E. S. B., U.; Becker, R.;Dressman, J.B. (2002) Forecasting the Oral Absorption Behavior of Poorly Soluble Weak Bases Using Solubility and Dissolution Studies in Biorelevant Media. *Pharm Res* 19 (3) 345-349.

Kothari, K., Ragoonanan, V. and Suryanarayanan, R. (2015) The role of drug-polymer hydrogen bonding interactions on the molecular mobility and physical stability of nifedipine solid dispersions. *Mol Pharm* 12 (1) 162-70.

Kourentas, A., Vertzoni, M., Symillides, M., Hens, B., Brouwers, J., Augustijns, P. and Reppas, C. (2016) In vitro evaluation of the impact of gastrointestinal transfer on luminal performance of commercially available products of posaconazole and itraconazole using BioGIT. *Int J Pharm* 515 (1-2) 352-358.

Kumar, P. and Singh, C. (2013) A Study on Solubility Enhancement Methods for Poorly Water Soluble Drugs. *American Journal of Pharmacological Sciences* 1 (4) 67-73.

Kumar, S. and Gupta, S. K. (2013) Pharmaceutical solid dispersion technology: a strategy to improve dissolution of poorly water-soluble drugs. *Recent patents on drug delivery & formulation* 7 (2) 111-121.

Lavasanifar, A., Samuel, J. and Kwon, G. S. (2002) Poly(ethylene oxide)-block-poly(L-amino acid) micelles for drug delivery. *Advanced Drug Delivery Reviews* 54 (2) 169-190.

Lerdkanchanaporn, S. and Dollimore, D. (1997) A thermal analysis study of Ibuprofen. *Journal of Thermal Analysis* 49 879-886.

Li, J., Gustavsson, C. and Piculell, L. (2016a) Time- and Space-Resolved SAXS Experiments Inform on Phase Transition Kinetics in Hydrated, Liquid-Crystalline Films of Polyion-Surfactant Ion "Complex Salts". *Langmuir* 32 (20) 5102-10.

Li, N., Mosquera-Giraldo, L. I., Borca, C. H., Ormes, J. D., Lowinger, M., Higgins, J. D., Slipchenko, L. V. and Taylor, L. S. (2016b) A

Comparison of the Crystallization Inhibition Properties of Bile Salts. *Crystal Growth & Design* 16 (12) 7286-7300.

Li, Y., Han, J., Zhang, G. G. Z., Grant, D. J. W. and Suryanarayanan, R. (2000) In Situ Dehydration of Carbamazepine Dihydrate: A Novel Technique to Prepare Amorphous Anhydrous Carbamazepine. *Pharmaceutical Development and Technology* 5 (2) 257-266.

Limbachiya, M. A., M; Sapariya, A; Soni, S (2012) SOLUBILITY ENHANCEMENT TECHNIQUES FOR POORLY SOLUBLE DRUGS A REVIEW. *International Journal of Pharmaceutical Research and Development* 4 (04) 071-086.

Lin, D. and Huang, Y. (2010) A thermal analysis method to predict the complete phase diagram of drug-polymer solid dispersions. *Int J Pharm* 399 (1-2) 109-15.

Liu, J. (2006) Physical Characterization of Pharmaceutical Formulations in Frozen and Freeze-Dried Solid States: Techniques and Applications in Freeze-Drying Development. *Pharmaceutical Development and Technology* 11 (1) 3-28.

Liu, J., Rigsbee, D. R., Stotz, C. and Pikal, M. J. (2002) Dynamics of pharmaceutical amorphous solids: The study of enthalpy relaxation by isothermal microcalorimetry. *Journal of Pharmaceutical Sciences* 91 (8) 1853-1862.

Liu, L. and Gao, H. (2012) Molecular structure and vibrational spectra of ibuprofen using density function theory calculations. *Spectrochim Acta A Mol Biomol Spectrosc* 89 201-9.

Loftsson, T. and Duchêne, D. (2007) Cyclodextrins and their pharmaceutical applications. *International Journal of Pharmaceutics* 329 (1-2) 1-11.

Lu, J., Ormes, J. D., Lowinger, M., Mann, A. K. P., Xu, W., Litster, J. D. and Taylor, L. S. (2017a) Maintaining Supersaturation of Active Pharmaceutical Ingredient Solutions with Biologically Relevant Bile Salts. *Crystal Growth & Design* 17 (5) 2782-2791.

Lu, J., Ormes, J. D., Lowinger, M., Mann, A. K. P., Xu, W., Patel, S., Litster, J. D. and Taylor, L. S. (2017b) Compositional effect of complex biorelevant media on the crystallization kinetics of an active pharmaceutical ingredient. *CrystEngComm* 19 (32) 4797-4806.

Lu, J., Ormes, J. D., Lowinger, M., Xu, W., Mitra, A., Mann, A. K. P., Litster, J. D. and Taylor, L. S. (2017c) Impact of Endogenous Bile Salts on the Thermodynamics of Supersaturated Active Pharmaceutical Ingredient Solutions. *Crystal Growth & Design* 17 (3) 1264-1275.

Maniruzzaman, M., Boateng, J. S., Bonnefille, M., Aranyos, A., Mitchell, J. C. and Douroumis, D. (2012) Taste masking of paracetamol by hot-melt extrusion: An in vitro and in vivo evaluation. *European Journal of Pharmaceutics and Biopharmaceutics* 80 (2) 433-442.

Maniruzzaman, M., Snowden, M. J., Bradely, M. S. and Douroumis, D. (2015) Studies of intermolecular interactions in solid dispersions using advanced surface chemical analysis. *RSC Adv.* 5 (91) 74212-74219.

Martínez, L., Peinado, A. and Liesum, L. (2013) In-line quantification of two active ingredients in a batch blending process by near-infrared spectroscopy: Influence of physical presentation of the sample. *International Journal of Pharmaceutics* 451 (1–2) 67-75.

Mathias, N., Xu, Y., Vig, B., Kestur, U., Saari, A., Crison, J., Desai, D., Vanarase, A. and Hussain, M. (2015) Food Effect in Humans: Predicting the Risk Through In Vitro Dissolution and In Vivo Pharmacokinetic Models. *AAPS J* 17 (4) 988-98.

Mehta, B. (2013) *Spray drying as a green technique for the development of co-crystals of incongruently soluble pair*. M.Phil. Bradford, UK: University of Bradford.

Mehta, M. and Suryanarayanan, R. (2016) Accelerated Physical Stability Testing of Amorphous Dispersions. *Mol Pharm* 13 (8) 2661-6.

Menard, K. P. (2008) *Dynamic Mechanical Analysis: A practical introduction.* Taylor & Francis Group.

Mezger, T. G. (2011) *The Rheology Handbook.* Vicentz Network GmbH & Co.KG, Hannover.

Michael A. Repka, S. K. B., Sampada B. Upadhye, Sridhar Thumma, Michael M. Crowley, Feng Zhang, Charles Martin & James W. McGinity (2007) Pharmaceutical Applications of Hot-Melt Extrusion: Part II. *Drug Development and Industrial Pharmacy* 33 (10) 1043-1057.

Michael M. Crowley, F. Z., Michael A. Repka, Sridhar Thumma, Sampada B. Upadhye, Sunil Kumar Battu, James W. McGinity & Charles Martin (2007) Pharmaceutical Applications of Hot-Melt Extrusion: Part I. *Drug Development and Industrial Pharmacy* 33 (9) 909-926.

Mistry, P. and Suryanarayanan, R. (2016) Strength of Drug–Polymer Interactions: Implications for Crystallization in Dispersions. *Crystal Growth & Design* 16 (9) 5141-5149.

Moneghini, M., Kikic, I., Voinovich, D., Perissutti, B. and Filipović-Grcić, J. (2001) Processing of carbamazepine-PEG 4000 solid dispersions with supercritical carbon dioxide: preparation, characterisation, and in vitro dissolution. *International journal of pharmaceutics* 222 (1) 129-138.

Montgomery, D. C. (2000) Design and Analysis of Experiments *Johhn Wiley & Sons, INC.* (5th Edition).

MSD (2014) *WC500168187*.

Mu, B. and Thompson, M. R. (2012) Examining the mechanics of granulation with a hot melt binder in a twin-screw extruder. *Chemical Engineering Science* 81 46-56.

Mueller, E. A., Kovarik, J. M., van Bree, J. B., Tetzloff, W., Grevel, J. and Kutz, K. (1994) Improved Dose Linearity of Cyclosporine Pharmacokinetics from a Microemulsion Formulation. *Pharmaceutical Research* 11 (2) 301-304.

Nehm, S. J., Rodríguez-Spong, B. and Rodríguez-Hornedo, N. (2006) Phase Solubility Diagrams of Cocrystals Are Explained by Solubility Product and Solution Complexation. *Crystal Growth & Design* 6 (2) 592-600.

Netchacovitch, L., Thiry, J., De Bleye, C., Chavez, P. F., Krier, F., Sacre, P. Y., Evrard, B., Hubert, P. and Ziemons, E. (2015) Vibrational spectroscopy and microspectroscopy analyzing qualitatively and quantitatively pharmaceutical hot melt extrudates. *J Pharm Biomed Anal* 113 21-33.

Netchacovitch, L., Thiry, J., De Bleye, C., Dumont, E., Cailletaud, J., Sacre, P. Y., Evrard, B., Hubert, P. and Ziemons, E. (2017) Global approach for the validation of an in-line Raman spectroscopic method to determine the API content in real-time during a hot-melt extrusion process. *Talanta* 171 45-52.

Newman, A., Engers, D., Bates, S., Ivanisevic, I., Kelly, R. C. and Zografi, G. (2008) Characterization of amorphous API:Polymer mixtures using X-ray powder diffraction. *Journal of pharmaceutical sciences* 97 (11) 4840-4856.

Nidhi, K., Indrajeet, S., Khushboo, M., Gauri, K. and Sen, D. J. (2011) Hydrotropy: A promising tool for solubility enhancement: A review. *International Journal of Drug Development and Research* 3 (2) 26-33.

Nie, H., Su, Y., Zhang, M., Song, Y., Leone, A., Taylor, L. S., Marsac, P. J., Li, T. and Byrn, S. R. (2016) Solid-State Spectroscopic Investigation of Molecular Interactions between Clofazimine and Hypromellose Phthalate in Amorphous Solid Dispersions. *Mol Pharm* 13 (11) 3964-3975.

Nollenberger, K., Gryczke, A., Meier, C., Dressman, J., Schmidt, M. U. and Bruhne, S. (2009) Pair distribution function X-ray analysis explains dissolution characteristics of felodipine melt extrusion products. *Journal of pharmaceutical sciences* 98 (4) 1476-1486.

Nonappa, Lahtinen, M., Kolehmainen, E., Haarala, J. and Shevchenko, A. (2012) Evidence of Weak Halogen Bonding: New Insights on Itraconazole and its Succinic Acid Cocrystal. *Crystal Growth & Design* 13 (1) 346-351.

Nurzynska, K., Booth, J., Roberts, C. J., McCabe, J., Dryden, I. and Fischer, P. M. (2015) Long-Term Amorphous Drug Stability Predictions Using Easily Calculated, Predicted, and Measured Parameters. *Mol Pharm* 12 (9) 3389-98.

O'Donnell, K. P. and Woodward, W. H. (2015) Dielectric spectroscopy for the determination of the glass transition temperature of pharmaceutical solid dispersions. *Drug Dev Ind Pharm* 41 (6) 959-68.

Ober, C. A. and Gupta, R. B. (2012) Formation of itraconazole-succinic acid cocrystals by gas antisolvent cocrystallization. *AAPS PharmSciTech* 13 (4) 1396-406.

Ober, C. A., Montgomery, S. E. and Gupta, R. B. (2013) Formation of itraconazole/L-malic acid cocrystals by gas antisolvent cocrystallization. *Powder Technology* 236 122-131.

Olabisi, O., Robeson, L. M. and Shaw, M. T. (1979) *Polymer-Polymer Miscibility.* Vol. 1. USA: Academic Press Inc. .

Otsuka, M., Nishizawa, J.-i., Fukura, N. and Sasaki, T. (2012) Characterization of Poly-Amorphous Indomethacin by Terahertz Spectroscopy. *Journal of Infrared, Millimeter, and Terahertz Waves* 33 (9) 953-962.

P. Sakellariou , R. C. R., E.F.T. White (1986) The solubility parameters of some cellulose derivatives and polyethylene glycols used in tablet film coating. *International Journal of Pharmaceutics* 31 (2) 175-177.

Paradkar, A., Kelly, A., Coates, P. and York, P. (2009) Shear and extensional rheology of hydroxypropyl cellulose melt using capillary rheometry. *J Pharm Biomed Anal* 49 (2) 304-10.

Parikh, D. M. (2005) *Pharmaceutical Granulation Technology.* Taylor and Francis, London:

Park, J. B., Lee, B. J., Kang, C. Y. and Repka, M. A. (2017) Process Analytical Quality Control of Tailored Drug Release Formulation Prepared via Hot-Melt Extrusion Technology. *J Drug Deliv Sci Technol* 38 51-58.

Patil, H., Tiwari, R. V. and Repka, M. A. (2016) Hot-Melt Extrusion: from Theory to Application in Pharmaceutical Formulation. *AAPS PharmSciTech* 17 (1) 20-42.

Patterson, J. E., James, M. B., Forster, A. H., Lancaster, R. W., Butler, J. M. and Rades, T. (2005) The Influence of Thermal and Mechanical Preparative Techniques on the Amorphous State of Four Poorly Soluble Compounds. *Journal of Pharmaceutical Sciences* 94 (9) 1998-2012.

Pauw, B. R. (2014) Corrigendum: Everything SAXS: small-angle scattering pattern collection and correction (2013 J. Phys.: Condens. Matter 25 383201). *Journal of Physics: Condensed Matter* 26 (23) 239501.

Perdikoulias, J. and Dobbie, T. (2003) *Pharmaceutical extrusion technology. Drug and the pharmaceutical sciences.* Volume 133 edition. New York: Marcel Dekkr, Inc.:

Potta, S. G., Minemi, S., Nukala, R. K., Peinado, C., Lamprou, D. A., Urquhart, A. and Douroumis, D. Development of Solid Lipid Nanoparticles for Enhanced Solubility of Poorly Soluble Drugs. *Journal of Biomedical Nanotechnology* 6 (6) 634-640.

Prudic, A., Lesniak, A. K., Ji, Y. and Sadowski, G. (2015) Thermodynamic phase behaviour of indomethacin/PLGA formulations. *Eur J Pharm Biopharm* 93 88-94.

Puaux, J. P. B., G. Ainser, A. (2000) Residence time distribution in a corotating twin-screw extruder. *Chem. Eng. Sci.* 55 1641–1651.

Qi, S., Gryczke, A., Belton, P. and Craig, D. Q. (2008) Characterisation of solid dispersions of paracetamol and EUDRAGIT E prepared by hot-melt extrusion using thermal, microthermal and spectroscopic analysis. *Int J Pharm* 354 (1-2) 158-67.

Qian, F., Huang, J. and Hussain, M. A. (2010) Drug-polymer solubility and miscibility: Stability consideration and practical challenges in amorphous solid dispersion development. *J Pharm Sci* 99 (7) 2941-7.

R.Liu (2008) *Water-Insoluble Drug Formulation.* Taylor and Francis, London:

Rabinow, B. E. (2004) Nanosuspensions in drug delivery. *Nature Reviews Drug Discovery* 3 (9) 785-796.

Randall, C. S., Dinenno, B. K., Schultz, R. K., Dayter, L., Konieczny, M. and Wunder, S. L. (1995) Solid-state transformation of a leukotriene antagonist. *International Journal of Pharmaceutics* 120 (2) 235-245.

Rask, M. B., Knopp, M. M., Olesen, N. E., Holm, R. and Rades, T. (2018) Comparison of two DSC-based methods to predict drug-polymer solubility. *Int J Pharm*.

Rautio, J., Kumpulainen, H., Heimbach, T., Oliyai, R., Oh, D., Järvinen, T. and Savolainen, J. (2008) Prodrugs: design and clinical applications. *Nature Reviews Drug Discovery* 7 (3) 255-270.

Rehder, S., Wu, J. X., Laackmann, J., Moritz, H. U., Rantanen, J., Rades, T. and Leopold, C. S. (2013) A case study of real-time monitoring of solid-state phase transformations in acoustically levitated particles using near infrared and Raman spectroscopy. *Eur J Pharm Sci* 48 (1-2) 97-103.

Reitz, E., Podhaisky, H., Ely, D. and Thommes, M. (2013) Residence time modeling of hot melt extrusion processes. *Eur J Pharm Biopharm* 85 (3 Pt B) 1200-5.

Repka, M. A., Bandari, S., Kallakunta, V. R., Vo, A. Q., McFall, H., Pimparade, M. B. and Bhagurkar, A. M. (2018) Melt extrusion with poorly soluble drugs - An integrated review. *Int J Pharm* 535 (1-2) 68-85.

Rippie, E. G. and Johnson, J. R. (1969) Regulation of dissolution rate by pellet geometry. *Journal of Pharmaceutical Sciences* 58 (4) 428-431.

Ryabenkova, Y., Jadav, N., Conte, M., Hippler, M. F., Reeves-McLaren, N., Coates, P. D., Twigg, P. and Paradkar, A. (2017) Mechanism of Hydrogen-Bonded Complex Formation between Ibuprofen and Nanocrystalline Hydroxyapatite. *Langmuir* 33 (12) 2965-2976.

Saerens, L., Dierickx, L., Lenain, B., Vervaet, C., Remon, J. P. and De Beer, T. (2011) Raman spectroscopy for the in-line polymer-drug

quantification and solid state characterization during a pharmaceutical hot-melt extrusion process. *Eur J Pharm Biopharm* 77 (1) 158-63.

Saerens, L., Dierickx, L., Quinten, T., Adriaensens, P., Carleer, R., Vervaet, C., Remon, J. P. and De Beer, T. (2012) In-line NIR spectroscopy for the understanding of polymer-drug interaction during pharmaceutical hot-melt extrusion. *Eur J Pharm Biopharm* 81 (1) 230-7.

Saerens, L., Ghanam, D., Raemdonck, C., Francois, K., Manz, J., Kruger, R., Kruger, S., Vervaet, C., Remon, J. P. and De Beer, T. (2014) In-line solid state prediction during pharmaceutical hot-melt extrusion in a 12 mm twin screw extruder using Raman spectroscopy. *Eur J Pharm Biopharm* 87 (3) 606-15.

Saleki-Gerhardt, A., Stoweell, J. G., Byrn, S. R. and Zografi, G. (1995) Hydration and Dehydration of Crystalline and Amorphous Forms of Raffinose. *Journal of Pharmaceutical Sciences* 84 (3) 318-323.

Sarode, A. L., Sandhu, H., Shah, N., Malick, W. and Zia, H. (2013) Hot melt extrusion (HME) for amorphous solid dispersions: predictive tools for processing and impact of drug-polymer interactions on supersaturation. *Eur J Pharm Sci* 48 (3) 371-84.

Schram, C. J., Smyth, R. J., Taylor, L. S. and Beaudoin, S. P. (2016) Understanding Crystal Growth Kinetics in the Absence and Presence of a Polymer Using a Rotating Disk Apparatus. *Crystal Growth & Design* 16 (5) 2640-2645.

Sekhon, B. (2009) *Pharmaceutical co-crystals-a review.* Vol. 50.

Serajuddin, A. T. (1999) Solid dispersion of poorly water-soluble drugs_ Early promises, subsequent problems, and recent breakthroughs. *Journal of Pharmaceutical Sciences* 88 (10) 1058-1066.

Shah, S., Maddineni, S., Lu, J. and Repka, M. A. (2013) Melt extrusion with poorly soluble drugs. *Int J Pharm* 453 (1) 233-52.

Shete, A., Murthy, S., Korpale, S., Yadav, A., Sajane, S., Sakhare, S. and Doijad, R. (2015) Cocrystals of itraconazole with amino acids: Screening, synthesis, solid state characterization, in vitro drug release

and antifungal activity. *Journal of Drug Delivery Science and Technology* 28 46-55.

Shevchenko, A., Bimbo, L. M., Miroshnyk, I., Haarala, J., Jelinkova, K., Syrjanen, K., van Veen, B., Kiesvaara, J., Santos, H. A. and Yliruusi, J. (2012) A new cocrystal and salts of itraconazole: comparison of solid-state properties, stability and dissolution behavior. *Int J Pharm* 436 (1-2) 403-9.

Shevchenko, A., Miroshnyk, I., Pietilä, L.-O., Haarala, J., Salmia, J., Sinervo, K., Mirza, S., van Veen, B., Kolehmainen, E., Nonappa and Yliruusi, J. (2013) Diversity in Itraconazole Cocrystals with Aliphatic Dicarboxylic Acids of Varying Chain Length. *Crystal Growth & Design* 13 (11) 4877-4884.

Sibik, J. and Zeitler, J. A. (2016) Direct measurement of molecular mobility and crystallisation of amorphous pharmaceuticals using terahertz spectroscopy. *Adv Drug Deliv Rev*.

Siepmann, J. and Siepmann, F. (2013) Mathematical modeling of drug dissolution. *Int J Pharm* 453 (1) 12-24.

Song, Y., Yang, X., Chen, X., Nie, H., Byrn, S. and Lubach, J. W. (2015) Investigation of drug-excipient interactions in lapatinib amorphous solid dispersions using solid-state NMR spectroscopy. *Mol Pharm* 12 (3) 857-66.

Subramaniam, B., Rajewski, R. A. and Snavely, K. (1997) Pharmaceutical Processing with Supercritical Carbon Dioxide. *Journal of Pharmaceutical Sciences* 86 (8) 885-890.

Takeuchi, H., Handa, T. and Kawashima, Y. (1987) Spherical Solid Dispersion Containing Amorphous Tolbutamide Embedded in Enteric Coating Polymers or Colloidal Silica Prepared by Spray-Drying Technique. *CHEMICAL & PHARMACEUTICAL BULLETIN* 35 (9) 3800-3806.

Takeuchi, H., Nagira, S., Yamamoto, H. and Kawashima, Y. (2004) Solid dispersion particles of tolbutamide prepared with fine silica particles by the spray-drying method. *Powder Technology* 141 (3) 187-195.

Thakkar, H. P., B.;, Thakkar, S. (2010) A REVIEW ON TECHNIQUES FOR ORAL BIOAVAILABILITY ENHANCEMENT OF DRUGS. *International Journal of Pharmaceutical Sciences Review and Research* 4 (3) 203-223.

Thakral, S., Terban, M. W., Thakral, N. K. and Suryanarayanan, R. (2015) Recent advances in the characterization of amorphous pharmaceuticals by X-ray diffractometry. *Adv Drug Deliv Rev*.

Thakral, S. and Thakral, N. K. (2013) Prediction of drug-polymer miscibility through the use of solubility parameter based Flory-Huggins interaction parameter and the experimental validation: PEG as model polymer. *J Pharm Sci* 102 (7) 2254-63.

Thakuria, R., Delori, A., Jones, W., Lipert, M. P., Roy, L. and Rodríguez-Hornedo, N. (2013) Pharmaceutical cocrystals and poorly soluble drugs. *International Journal of Pharmaceutics* 453 (1) 101-125.

Tian, B., Wang, X., Zhang, Y., Zhang, K., Zhang, Y. and Tang, X. (2015) Theoretical prediction of a phase diagram for solid dispersions. *Pharm Res* 32 (3) 840-51.

Tian, Y., Booth, J., Meehan, E., Jones, D. S., Li, S. and Andrews, G. P. (2013) Construction of drug-polymer thermodynamic phase diagrams using Flory-Huggins interaction theory: identifying the relevance of temperature and drug weight fraction to phase separation within solid dispersions. *Mol Pharm* 10 (1) 236-48.

Tian, Y., Caron, V., Jones, D. S., Healy, A. M. and Andrews, G. P. (2014) Using Flory-Huggins phase diagrams as a pre-formulation tool for the production of amorphous solid dispersions: a comparison between hot-melt extrusion and spray drying. *J Pharm Pharmacol* 66 (2) 256-74.

Torres, H. A., Hachem, R. Y., Chemaly, R. F., Kontoyiannis, D. P. and Raad, I. I. (2005) Posaconazole: a broad-spectrum triazole antifungal. *The Lancet Infectious Diseases* 5 (12) 775-785.

Trask, A. V., Motherwell, W. D. S. and Jones, W. (2006) Physical stability enhancement of theophylline via cocrystallization. *International Journal of Pharmaceutics* 320 (1) 114-123.

Treffer, D., Troiss, A. and Khinast, J. (2015) A novel tool to standardize rheology testing of molten polymers for pharmaceutical applications. *International Journal of Pharmaceutics* 495 (1) 474-481.

Troup, G. M. and Georgakis, C. (2013) Process systems engineering tools in the pharmaceutical industry. *Computers & Chemical Engineering* 51 (0) 157-171.

Tumuluri, V. S., Kemper, M. S., Lewis, I. R., Prodduturi, S., Majumdar, S., Avery, B. A. and Repka, M. A. (2008) Off-line and on-line measurements of drug-loaded hot-melt extruded films using Raman spectroscopy. *Int J Pharm* 357 (1-2) 77-84.

Van Duong, T., Ludeker, D., Van Bockstal, P. J., De Beer, T., Van Humbeeck, J. and Van den Mooter, G. (2018) Polymorphism of Indomethacin in Semicrystalline Dispersions: Formation, Transformation, and Segregation. *Mol Pharm* 15 (3) 1037-1051.

Van Krevelen, D. W. a. T. N., K. (1990) Chapter 7 - Cohesive Properties and Solubility. *Properties of Polymers (Fourth Edition)* 189-227.

Van Renterghem, J., Kumar, A., Vervaet, C., Remon, J. P., Nopens, I., Vander Heyden, Y. and De Beer, T. (2017a) Elucidation and visualization of solid-state transformation and mixing in a pharmaceutical mini hot melt extrusion process using in-line Raman spectroscopy. *Int J Pharm* 517 (1-2) 119-127.

Van Renterghem, J., Vervaet, C. and De Beer, T. (2017b) Rheological Characterization of Molten Polymer-Drug Dispersions as a Predictive Tool for Pharmaceutical Hot-Melt Extrusion Processability. *Pharm Res* 34 (11) 2312-2321.

Vankeirsbilck, T., Vercauteren, A., Baeyens, W., Van der Weken, G., Verpoort, F., Vergote, G. and Remon, J. P. (2002) Applications of Raman spectroscopy in pharmaceutical analysis. *TrAC - Trends in Analytical Chemistry* 21 (12) 869-877.

Varghese, S. and Ghoroi, C. (2017) Improving the wetting and dissolution of ibuprofen using solventless co-milling. *Int J Pharm* 533 (1) 145-155.

Vasconcelos, T., Sarmento, B. and Costa, P. (2007) Solid dispersions as strategy to improve oral bioavailability of poor water soluble drugs. *Drug Discovery Today* 12 (23-24) 1068-1075.

Verhoeven, E., De Beer, T. R., Van den Mooter, G., Remon, J. P. and Vervaet, C. (2008) Influence of formulation and process parameters on the release characteristics of ethylcellulose sustained-release mini-matrices produced by hot-melt extrusion. *Eur J Pharm Biopharm* 69 (1) 312-9.

Vertzoni, M., Dressman, J., Butler, J., Hempenstall, J. and Reppas, C. (2005) Simulation of fasting gastric conditions and its importance for the in vivo dissolution of lipophilic compounds. *Eur J Pharm Biopharm* 60 (3) 413-7.

Vigh, T., Drávavölgyi, G., Sóti, P. L., Pataki, H., Igricz, T., Wagner, I., Vajna, B., Madarász, J., Marosi, G. and Nagy, Z. K. (2014) Predicting final product properties of melt extruded solid dispersions from process parameters using Raman spectrometry. *Journal of Pharmaceutical and Biomedical Analysis* 98 (0) 166-177.

Vo, C. L.-N., Park, C. and Lee, B.-J. (2013) Current trends and future perspectives of solid dispersions containing poorly water-soluble drugs. *European Journal of Pharmaceutics and Biopharmaceutics* 85 (3) 799-813.

Wahl, P. R., Hörl, G., Kaiser, D., Sacher, S., Rupp, C., Shlieout, G., Breitenbach, J., Koscher, G. and Khinast, J. G. (2018) In-line measurement of residence time distribution in melt extrusion via video analysis. *Polymer Engineering & Science* 58 (2) 170-179.

Wahl, P. R., Treffer, D., Mohr, S., Roblegg, E., Koscher, G. and Khinast, J. G. (2013) Inline monitoring and a PAT strategy for pharmaceutical hot melt extrusion. *Int J Pharm* 455 (1-2) 159-68.

Wang, B., Wang, D., Zhao, S., Huang, X., Zhang, J., Lv, Y., Liu, X., Lv, G. and Ma, X. (2017) Evaluate the ability of PVP to inhibit crystallization of amorphous solid dispersions by density functional theory and experimental verify. *Eur J Pharm Sci* 96 45-52.

Wesholowski, J., Berghaus, A. and Thommes, M. (2018) Inline Determination of Residence Time Distribution in Hot-Melt-Extrusion. *Pharmaceutics* 10 (2).

Weuts, I., Van Dycke, F., Voorspoels, J., De Cort, S., Stokbroekx, S., Leemans, R., Brewster, M. E., Xu, D., Segmuller, B., Turner, Y. T., Roberts, C. J., Davies, M. C., Qi, S., Craig, D. Q. and Reading, M. (2011) Physicochemical properties of the amorphous drug, cast films, and spray dried powders to predict formulation probability of success for solid dispersions: etravirine. *J Pharm Sci* 100 (1) 260-74.

Wieser, J., Pichler, A., Hotter, A., Griesser, U. and Langes, C. (2008) A Crystalline form of posaconazole. *EP2141159A1*.

Willart, J. F., Caron, V., Lefort, R., Danède, F., Prévost, D. and Descamps, M. (2004) Athermal character of the solid state amorphization of lactose induced by ball milling. *Solid State Communications* 132 (10) 693-696.

Willart, J. F., Descamps, N., Caron, V., Capet, F., Danède, F. and Descamps, M. (2006) Formation of lactose-mannitol molecular alloys by solid state vitrification. *Solid State Communications* 138 (4) 194-199.

Wu, H., White, M. and Khan, M. A. (2011) Quality-by-Design (QbD): An integrated process analytical technology (PAT) approach for a dynamic pharmaceutical co-precipitation process characterization and process design space development. *Int J Pharm* 405 (1-2) 63-78.

Wu, J. X., Xia, D., van den Berg, F., Amigo, J. M., Rades, T., Yang, M. and Rantanen, J. (2012) A novel image analysis methodology for online monitoring of nucleation and crystal growth during solid state phase transformations. *Int J Pharm* 433 (1-2) 60-70.

Xu, L., Li, S. M., Wang, Y., Wei, M., Yao, H. M. and Sunada, H. (2009) Improvement of dissolution rate of ibuprofen by solid dispersion systems with Kollicoat IR using a pulse combustion dryer system. *Journal of Drug Delivery Science and Technology* 19 (2) 113-118.

Yang, F., Su, Y., Zhang, J., DiNunzio, J., Leone, A., Huang, C. and Brown, C. D. (2016) Rheology Guided Rational Selection of Processing Temperature To Prepare Copovidone-Nifedipine Amorphous Solid Dispersions via Hot Melt Extrusion (HME). *Mol Pharm* 13 (10) 3494-3505.

Yang, M., Wang, P. and Gogos, C. (2013) Prediction of acetaminophen's solubility in poly(ethylene oxide) at room temperature using the Flory-Huggins theory. *Drug Dev Ind Pharm* 39 (1) 102-8.

Yoshioka, T., Sternberg, B. and Florence, A. T. (1994) Preparation and properties of vesicles (niosomes) of sobitan monoesters (Span. *International journal of pharmaceutics* 105 1-6.

Yu, L. (2001) Amorphous pharmaceutical solids: Preparation, characterization and stabilization. *Advanced Drug Delivery Reviews* 48 (1) 27-42.

Zaheer, K. and Langguth, P. (2018) Formulation strategy towards minimizing viscosity mediated negative food effect on disintegration and dissolution of immediate release tablets. *Drug Development and Industrial Pharmacy* 44 (3) 444-451.

Zhao, Y., Inbar, P., Chokshi, H. P., Malick, A. W. and Choi, D. S. (2011) Prediction of the thermal phase diagram of amorphous solid dispersions by Flory-Huggins theory. *J Pharm Sci* 100 (8) 3196-207.

Ziegler, G. R. and Aguilar, C. A. (2003) Residence time distribution in a co-rotating, twin-screw continuous mixer by the step change method. *Journal of Food Engineering* 59 (2-3) 161-167.

Appendix 1

Ibuprofen dimer in the solid dispersion as an early indicator of solid-state stability (Publication draft)

A.D. Sabnis[1], T. Gough[2], A. Kelly[2], S. Forster[3], A. Paradkar[1]*

[1]Centre for Pharmaceutical Engineering Sciences, School of Pharmacy and Medical Sciences, University of Bradford, UK

[2]Centre for Pharmaceutical Engineering Sciences, IRC Polymer Engineering, Faculty of Engineering and Informatics, University of Bradford, UK

[3]Merck Research Laboratories, West Point, PA, USA

** Corresponding Author*

Prof. Anant Paradkar

Centre for Pharmaceutical Engineering Sciences, University of Bradford, BD7 1DP UK.

Contact no: +44(0)1274 233900

Email: A.Paradkar1@bradford.ac.uk

Graphical Abstract:

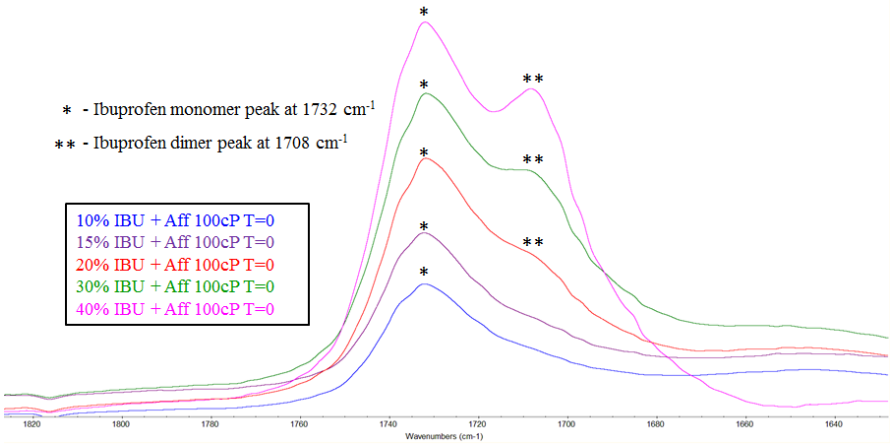

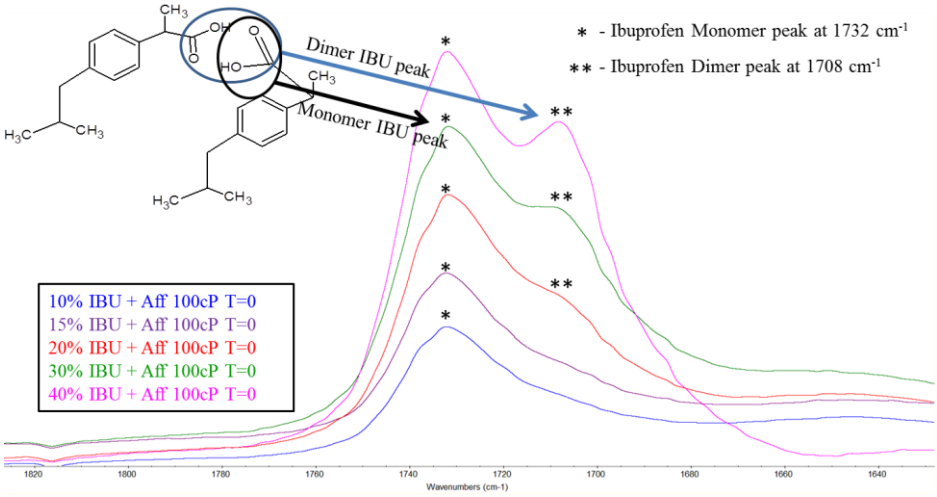

Abstract:

Achieving high drug load while maintaining stability of amorphous solid dispersions (ASD) is one of the critical formulation challenge during developmental phase. We propose here that early detection of ibuprofen dimer in the ASD is an indicator of potential physical destabilization of the ASD. Conventional approaches to determine this parameter involve exposure of prepared ASDs to different stress conditions in order to observe drug recrystallization. The approaches are time-consuming and often considered as limiting factor for the use of ASD. Attenuated Total Reflection Fourier Transform Infrared spectroscopy (ATR-FTIR) has been used as a tool to detect ibuprofen dimer in the ibuprofen and hydroxypropyl methylcellulose (HPMC) ASD prepared using hot melt extrusion (HME). X-ray diffractometry (XRD), Differential Scanning Calorimetry (DSC) and Raman spectrometry were used to support our hypothesis. Ibuprofen dimerization in the ASD was found to correlate well with the solid-state stability of ASDs. Results confirmed that 15%w/w drug loading of ibuprofen within HPMC ASD was the maximum drug concentration to produce a stable ASD.

Ibuprofen dimerization is used as an indirect approach to presage solid state stability of the amorphous solid dispersions (ASD). Prediction of the maximum drug concentration for stable ASD is one of the critical formulation factors during developmental phase. Conventional approaches to determine this parameter involve exposure of prepared ASDs to different stress conditions in order to observe drug recrystallization. The approaches are time-consuming and often considered as limiting factor for the use of ASD. Here Attenuated Total Reflection Fourier Transform Infrared spectroscopy (ATR-FTIR) has

been used as a tool to identify ibuprofen dimer formation as an early predictor of solid state stability of an ASD of ibuprofen and hydroxypropyl methylcellulose (HPMC). Predictive approach was further confirmed by exposing the extrudates of different ibuprofen concentration to various stress conditions. XRD, DSC and Raman spectrometry were used to confirm solid state stability of the ASD by providing an ortho-analytical approach. Drug aggregation approach observed after preparation of ASD was found to be in good correlation in forecasting the solid state stability of ASDs. Results confirmed that 15%w/w drug loading of ibuprofen within HPMC ASD was the maximum drug concentration to produce a stable ASD.

Keywords: Affinisol™ HPMC HME; hot melt extrusion; hydroxypropyl methylcellulose; solid dispersion; thermal analysis; FTIR Spectroscopy; Ibuprofen; Raman spectroscopy; solid-state stability; binary phase diagram

Introduction:

Poor water solubility of Active Pharmaceutical Ingredients (APIs) is a major challenge for the pharmaceutical industry.[1]One approach to address low solubility is to produce an amorphous solid dispersion (ASD), which is formed when the drug is molecularly dispersed and stabilized in a polymer matrix. The polymer matrix retards the molecular mobility of the API and stabilizes the API in an amorphous state.[2] Solid dispersions are obtained either by solvent evaporation or melt fusion methods.[3] Melt based processing involves melting a physical mixture of API and polymer to obtain a homogeneous molten phase, for example by application of shear and heat in a twin screw extruder.[4, 5] This is followed by cooling to ambient temperature to lock the API in its amorphous form. The concentration of the API in the solid dispersion is a critical factor affecting stability which depends on the miscibility of the API in the polymer.[6] The glass transition temperature (T_g) of the solid dispersion related to temperature and humidity during storage will affect the stability of the solid dispersion. It is generally desirable to incorporate the highest possible concentration of the API in ASD to control size and weight and to minimize the cost of the final dosage form. High drug loading is the preferred choice but has the drawback of solid-state stability.[6] Drug entrapped within the polymer, if not molecularly mixed, may recrystallize thus affecting the stability of the drug.

The objective of this work was to study the relationship between molecular association of the drug within an ASD and its long-term stability. Molecular associations like dimerization can provide insight about drug aggregation within ASD which can be further used as an indirect measure to study solid state stability. Current understanding of the stability of ASDs is predominantly

based on the theoretical predictions of drug-polymer miscibility[7-10], analytical measurements of molecular mobility and dynamics[11-13], onset of crystallization, crystal growth kinetics[14-16] and intermolecular interactions between the drug and polymer.[17-19]

One common approach for the prediction of the solid-state stability is to use the Flory-Huggins polymer solution theory as a function of temperature.[10, 20-23] However, the method fails to provide a link between molecular distributions of the drug within the polymer matrix and stability of the ASD. Hence, a basic practical screening tool is needed for early detection of the solid state stability of amorphous solid dispersions.

Currently, the stability of an ASD is determined empirically then estimated by exposing it to different temperature and humidity conditions while monitoring it for the appearance of crystalline API using suitable analytical tools such as powder XRD and DSC.[24, 25] Various studies using in-line and off-line spectroscopic techniques reported the monitoring of the crystalline phase.[26-29] Suryanarayanan et al. used dielectric spectroscopy (DES) to predict stability based on molecular mobility and studied the effect of hygroscopicity.[30-32] Findings from these works are selective and moreover, the approaches involved studying either the glass forming ability or crystal growth mechanism and not the molecular association of drug within the polymer matrix. Additionally, analytical techniques available for solid state detection are limited and require that samples be exposed to different time-consuming stability conditions. The difficulties in proving long term stability during storage can restrict use of amorphous solid dispersions for solubility enhancement of poorly soluble drugs.[1, 33]

Ibuprofen (IBU) or 2-(4-isobutylphenyl) propionic acid is a nonsteroidal anti-inflammatory drug (NSAID) used for reducing inflammation and pain in the body. It has a molecular weight of 206.29g/mol and melting point of 75-77°C.[34] It belongs to class II of Biopharmaceutical Classification System (BCS) due to its poor aqueous solubility. IBU exists as a cyclic bonded dimer in its crystalline state (Figure 1b).[34] Previous studies have shown the existence of this dimer in the melt state.[34, 35]

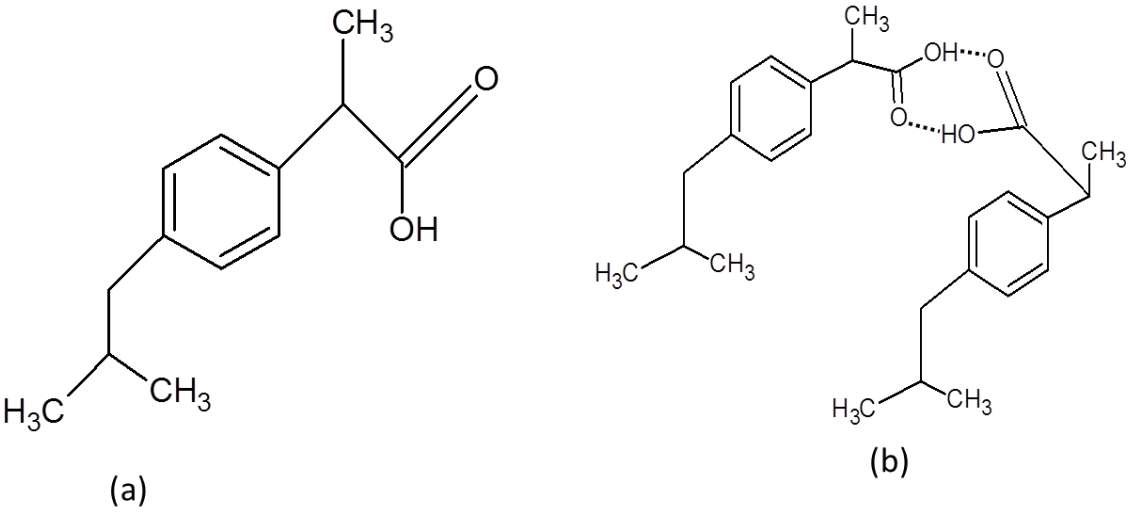

Figure 1. Structure of (a) ibuprofen monomer and (b) ibuprofen dimer with hydrogen bonding

Several studies have also reported the use of a solid dispersion of IBU with polymers to increase its oral bioavailability (Figure 1a).[35, 36] Main focus of those studies was on enhancing the product performance and investigation was about interfaces between ibuprofen and polymers. However, none have studied systematically the identification of the molecular association of ibuprofen within the polymer matrix and attempted its correlation with the solid state stability of the ASD.

The relatively recent emergence of melt-based techniques for preparation of ASD may be partially attributed to the lack of approved polymers for formulation. Conventionally used pharmaceutical polymers have major drawbacks of high T_g, and/or high melt viscosity, and thermal degradation.[1] To overcome this, various new polymers were developed either by co-polymerization or substitution and rearrangement within the monomers of the polymers.[37] This lead to the introduction of new polymers like Soluplus® (copolymer of PVC-PVA-PEG), HPMCAS, HPMCP, and Affinisol^{TM}HPMC. Affinisol^{TM}HPMC marketed by DowDupont is specifically developed for HME. It is amorphous in nature, water soluble and has a wide temperature window for hot melt processing.[37, 38] Three grades of Affinisol^{TM}HPMC 15cP, 100cP and 4M are commercially available of which 100cP was used for the current research.

In the current study, solid dispersions of ibuprofen and Affinisol^{TM}HPMC 100cP (Affinisol 100cP) of varying drug concentrations (10, 15, 20, 30 and 40%w/w) were prepared using HME. The extrudates were characterized using attenuated total reflection fourier transform infrared spectroscopy (ATR-FTIR) to identify the IBU aggregation and Raman spectroscopy, X-ray diffraction (XRD) and differential scanning calorimetry (DSC) to provide an ortho-analytical approach to monitor recrystallization of the extrudates. Prepared extrudates were subjected to conditions of 40°C/75% RH, 25°C/60% RH and room temperature (RT) to investigate stability. Attempts were also made to understand the solid state solubility and miscibility using the Flory-Huggins polymer solution theory.

Materials and Methods:

Materials:

Affinisol™ HPMC 100 cP (Affinisol 100cP) was provided as a gift sample by DowDupont., MI, USA. According to the manufacturer, the material was from batches prepared for distribution to researchers as experimental samples. Ibuprofen was procured from Medex UK.

Methods:

Theoretical considerations:

Melting point depression approach

The Flory-Huggins polymer solution theory proposes the drug-polymer temperature-composition phase diagram by understanding the interaction parameter χ between the drug-polymer and its change with temperature. This can be achieved by using melting point depression data to predict χ by using Equation 1:[9, 38]

$$\frac{1}{T_m} - \frac{1}{T_{mo}} = -\frac{R}{\Delta H}[log\ \phi_{drug} + \phi_{poly}\left(1 - \frac{1}{m}\right) + \chi\phi^{2}_{poly}]$$

Equation 1

Where $m = [(\text{Mol wt\_poly}/\text{Density\_poly})/(\text{Mol wt\_drug}/\text{Density\_drug})]$

T_m and T_{mo} are the melting points of the drug-polymer blend and pure drug respectively, ϕ is the volume fraction of the components. ΔH and R denote enthalpy of fusion and the gas constant respectively.

χ is a function of temperature which can be empirically described by Equation 2:

$\chi = A + B/T$ Equation 2

Where A is the entropic contribution and B is enthalpy contribution of the system.[9, 38]

Prediction of spinodal curve

According to the Flory–Huggins theory, the free energy of mixing for a drug-polymer solid dispersion can be described by Equation 3:

$$\Delta G_{mix} = RT[\phi_{\mathrm{drug}} \log \phi_{drug} + \frac{\phi_{\mathrm{poly}}}{\mathrm{m}} \log \phi_{poly} + \chi\, \phi_{\mathrm{drug}} \phi_{\mathrm{poly}}]$$

Equation 3

The second derivative of ΔG_{mix} at different temperatures will give the spinodal curve.

Theoretical glass transition temperature calculation by Fox equation

Researchers often co-relate the extent of plasticization based on T_g values of polymeric blends. Generally, values of T_g reduce with increase in plasticizer concentration and a plot of T_g against the concentration of plasticizer yields a relationship which determines the plasticization efficiency. Such a relationship can also be obtained theoretically using the Fox equation.[9]

$$1/T_g mixture = \left(w_1/T_{g1}\right) + \left(w_2/T_{g2}\right)$$ Equation 4

where w_1 & w_2 are weight fractions while T_{g1} & T_{g2} are the glass transition temperatures of drug and polymer respectively.

Preparation of ASDs using HME:

Pre-mixed dry blends of ibuprofen and Affinisol 100cP with varying drug concentration were prepared by HME using a 16mm twin screw Pharmalab extruder from ThermoScientific UK with screw length to diameter ratio of 40:1. A twin screw configuration consisting of one high mixing and kneading zone was used for all experiments; screw rotation speed of 100 rpm and feed rate of 0.4 kg/hr was kept constant for all experiments (Table S1). Temperature profiles were varied according to the blend concentrations used due to the plasticity induced by the ibuprofen and the associated decrease in T_g of the ibuprofen-Affinisol 100cP blends. Extrudates were air-cooled and pelletized for further analysis.

Analytical evaluations of the ASDs:

Raman spectroscopy

Raman spectra for all prepared samples were taken using a Thermo Scientific DXR spectrometer with a 780nm laser at 50mW power. A slit aperture of 50µm was used to give an estimated area spot size of 3.1µm. Samples were either placed in glass vials (for powder samples) or were placed on the sample plate as is (for extrudates). 64 scans of 30 secs duration were collected within the spectral range 50-3360 cm^{-1}. Total time of collection per sample was 33 mins.

X-ray Scattering

X-ray scattering of the samples was acquired using a SAXSspace from Anton Paar Austria. The samples were placed on the stainless steel sample holder and sealed with transparent film. The distance between sample and detector was 112mm and the intensity I (q) was monitored at a wavelength of 0.15418nm. An XYZ stage was used for auto-recognition of the sample stages.

A fast read-out detector (Pilatus 100K-S) was used with the total acquisition of 20 frames with an exposure time of 60 secs and data was analyzed using SAXSdrive™ software. The scattering vector q range was used to calculate 2Θ values ($q = 4\pi/\lambda \sin\theta$, where $\lambda = 0.15418$nm).[39-41]

ATR-FTIR spectroscopy

Fourier transform infrared (FTIR) spectra were acquired from extrudates using a Thermo-Scientific Nicolet iS50 FTIR spectrophotometer equipped with a diamond attenuated total reflection (ATR) module. A thin section of extrudate was sliced and placed on the ATR and clamped to avoid spaces between holder and sample. Spectra were recorded in absorbance mode from 4000 cm^{-1} to 400 cm^{-1} at 4 cm^{-1} resolution, and averaged over 64 scans. Total scan time was 1 min 35 secs.

Differential Scanning Calorimetry (DSC)

DSC runs were performed using TA Q2000 and TA Discovery calorimeters with standard aluminum pans. Samples of weight around 2mg were used and crimped with a pinhole in the aluminum lid. A heating rate of 10°C/min was applied up to the reported degradation temperature of the samples. Thermograms generated were analyzed using TA Universal Analysis and Trios software.

For melting point depression experiments, physical mixtures of various concentrations of ibuprofen and Affinisol 100cP were accurately weighed in standard aluminum pans and crimped with pin holed aluminum lids. Samples were run in duplicate at a heating rate of 2°C/min up to 85°C. Thermograms generated were analyzed using TA Instruments Trios software.

Accelerated Stability Studies:

To investigate solid-state stability, the ASDs were exposed to stability conditions at 40°C/75% RH, 25°C/60% RH, and room temperature. Samples were removed at regular intervals and analyzed using ATR-FTIR, Raman microscopy, XRD, and DSC.

Results and Discussion:

Construction of binary phase diagram:

The application of the Flory-Huggins solid-state solution theory assumes the drug solubilizes within the polymer with a similar principle as for a solid solute dissolving in a solvent to form a solution.[21] Table 1 provides the parameters used to calculate the interaction parameter and free energy of mixing.

Table 1. Calculated parameters for Ibuprofen and Affinisol

Parameter	Ibuprofen	Affinisol 100cP
M_w (g/mole)	206.29	231708
Density (g/cm^3)	1.03	1.326
Glass transition temperature (°C)	-44°C	128°C

The parameters for ibuprofen were obtained by ChemDraw software while experimental values obtained were used for Affinisol 100cP. Glass transition temperature values for ibuprofen and Affinisol 100cP were obtained from DSC and DMA respectively. The interaction parameter χ at the melting point was calculated by a melting point depression method using DSC and was found to be -0.6353 (Figure 2.).[9, 21, 22, 38]

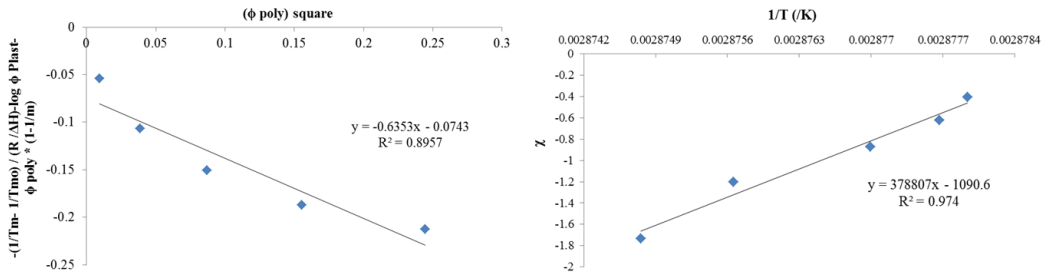

Figure 2. Calculation of interaction parameter χ at melting point (left) and over different temperatures (right) by Flory-Huggins equation

For the spinodal curve, the interaction parameter was plotted as a function of inverse temperature to get components A and B (Figure 2).

According to theory, at the melting temperature, the interaction parameter tends to infinity hence subtle changes in temperatures near the melting point will have a significant impact on the interaction parameter. Using values A and B obtained by plotting (figure 2), the free energy of mixing $\Delta Gmix$ at different temperature was theoretically calculated (Figure 3).

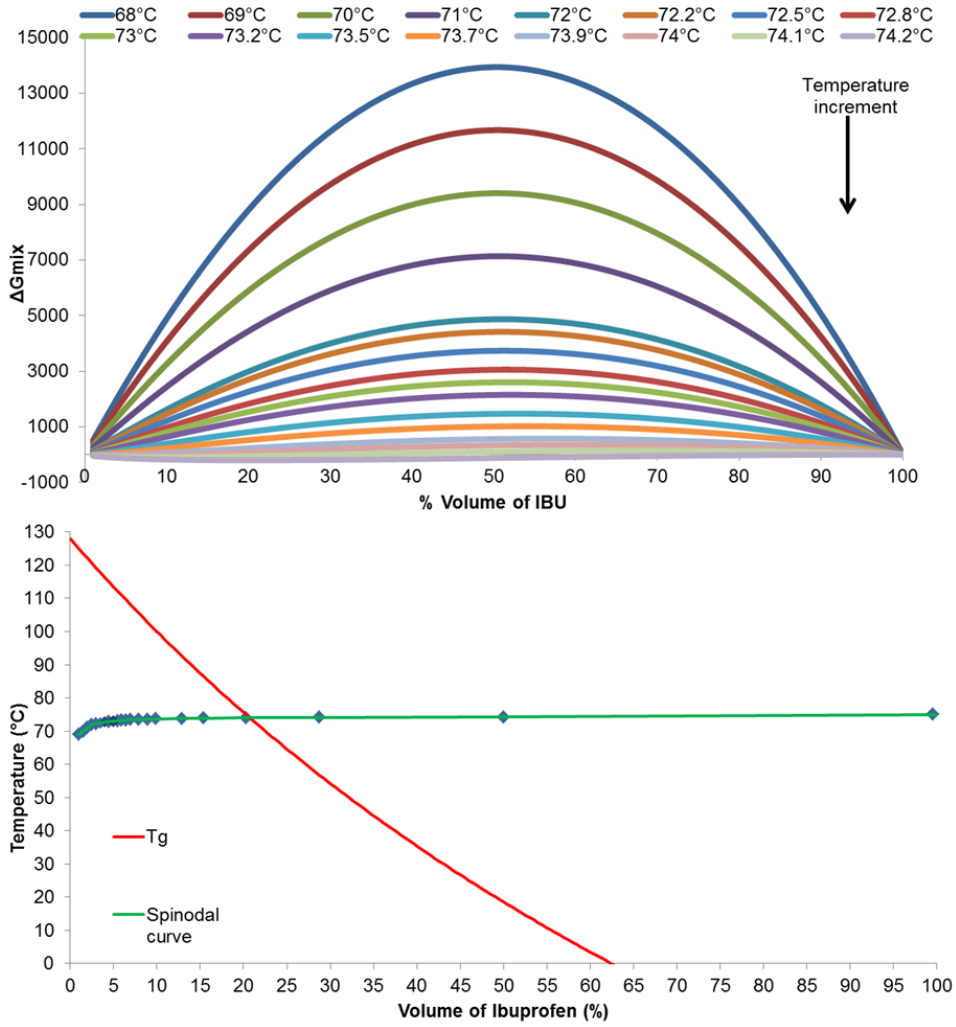

Figure 3. The plot of free energy of mixing (top) and phase diagram (bottom)

$\Delta Gmix$ values were found to be positive for temperatures below 74°C which indicates de-mixing. The spinodal curve was obtained by calculating the second derivate of $\Delta Gmix$ at various temperatures close to the melting temperature. The theoretical glass transition temperature profile for ibuprofen-affinisol 100cP was calculated using the Fox equation (Figure 3).

The molecular weight of Affinisol 100cP is more than 1000 times of that of ibuprofen. Due to which spinodal curve predicts complete solid-state miscibility between all the drug-polymer compositions and thus binary phase diagram fails to predict solid-state miscibility between ibuprofen and affinisol 100cP.[38]

Hence, it can be inferred that theoretical binary phase diagram by Flory-Huggins theory fails to predict the stability of the ASD formed using ibuprofen and Affinisol 100cP.

Confirmation of amorphous solid dispersion prepared by hot melt extrusion:

The formation of an ASD was confirmed through analysis by DSC, XRD, and Raman spectroscopy. The absence of any crystalline IBU melting endothermic peak in DSC confirmed the amorphous solid state of solid dispersions (figure S1).[34] No distinct crystalline ibuprofen peaks were observed in XRD diffractograms and a halo region confirmed the amorphous nature of the extrudates at all concentrations of ibuprofen (figure 4).[25, 35, 42] Raman spectra exhibited a peak shift from 1607cm^{-1} to 1612-1617cm^{-1}, attributed to aryl chain deformation and C-H stretching and bending which occurs due to disorder within the structure and is characteristic of the amorphous state of ibuprofen.[43] Thus, the peak shift affirmed the amorphous solid dispersions for all the ibuprofen-Affinisol 100cP extrudates at varying drug concentrations (Figure 4).

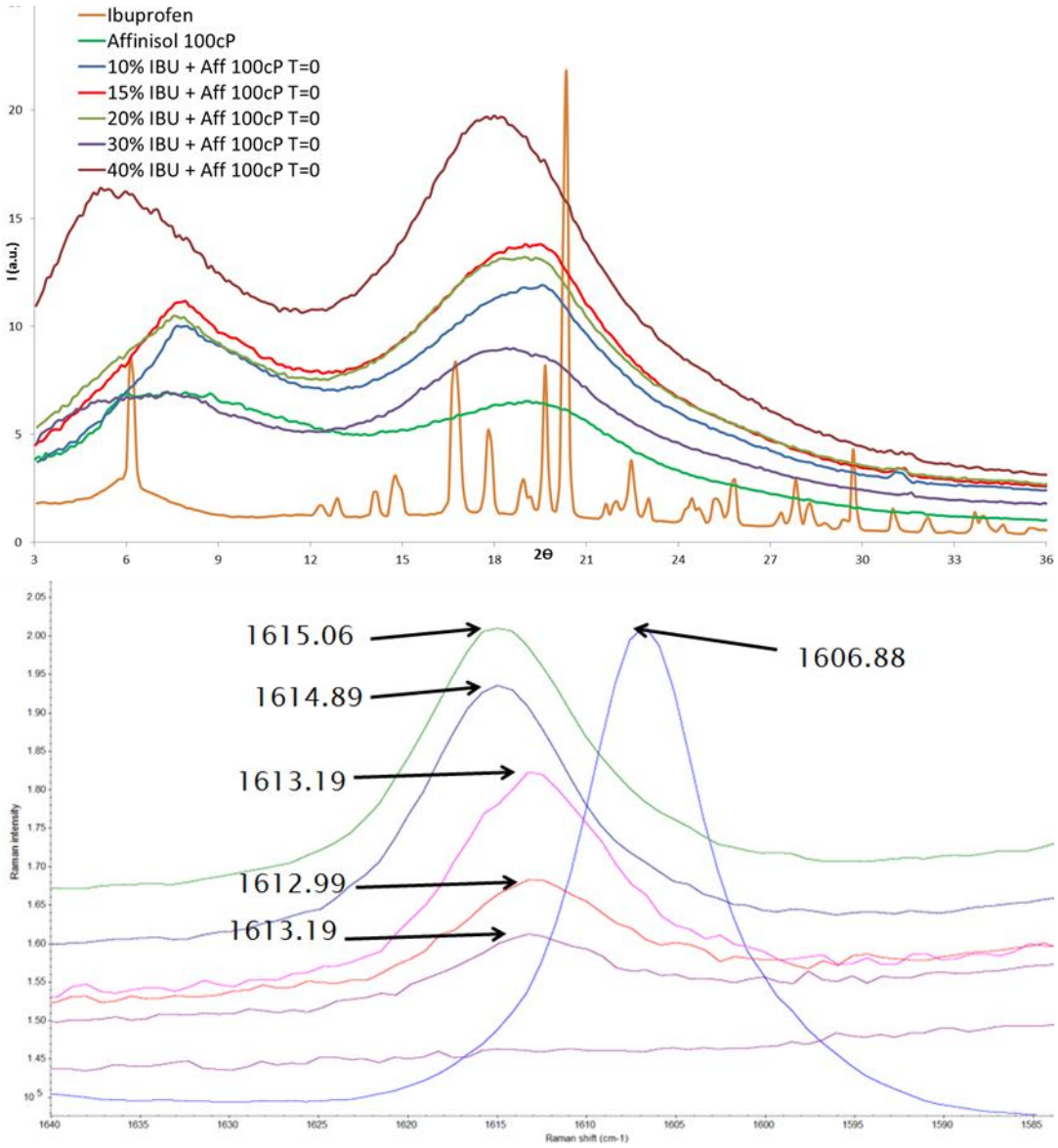

Figure 4. XRD patterns (top) and Raman spectra (zoomed view) for ibuprofen powder (blue), affinisol 100cP (purple), 10 (purple), 15 (red), 20 (pink), 30 (dark blue) and 40%w/w (green) ibuprofen-affinisol 100cP extrudates

Ibuprofen dimer as an early indicator of solid-state stability by ATR-FTIR:

Ibuprofen exists as a dimer in both its crystalline and melt states.[35] However, when IBU solubilizes within Affinisol 100cP, the dimer of IBU is broken down into its monomeric form either due to shear or by the effect of temperature during the process and is entrapped within the polymer resulting in an

amorphous solid dispersion. A single phase ASD affirmed uniform mixing between IBU and Affinisol 100cP. No chemical interaction was observed between the spectral bands of the drug and polymer which confirms the formation of a solid dispersion due to its solid state solubility and miscibility.

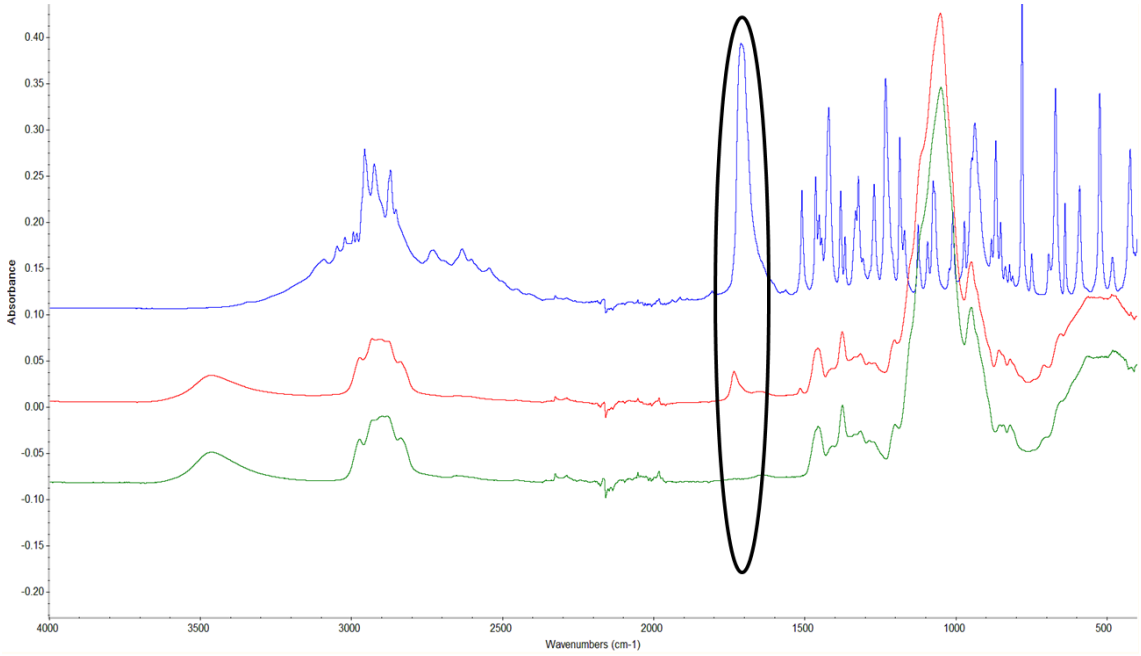

Figure 5. ATR-FTIR of IBU powder (blue), 10% IBU-affinisol 100cP extrudate (red) and affinisol 100cP powder (green)

It is evident from ATR-FTIR spectra, that active bands between 1800-1700 cm^{-1} can be considered as a non-interfering region for the detection of IBU within ASD (circled in figure 5). A distinct shift in the 1707 cm^{-1} band of IBU powder which is attributed to the carbonyl band to 1732 cm^{-1} in the solid dispersion was observed. Several studies have reported similar shifts which have been attributed to the breaking of hydrogen bonding of the IBU with other polymers within ASD.[34, 35] Thus, the shift in the carbonyl bond of the ibuprofen to 1732 cm^{-1} was due to the formation of monomeric form within the ASD.

Using this as a reference indirect measurement to understand the IBU solid state within the ASD, ASDs with different percent drug loading of IBU were prepared. It was observed that all ASDs above 15% drug loading showed the presence of the dimer along with some monomeric form (figure 6). This suggests that presence of ibuprofen dimer can be used as a measure in predicting the solid state stability of the ASDs.

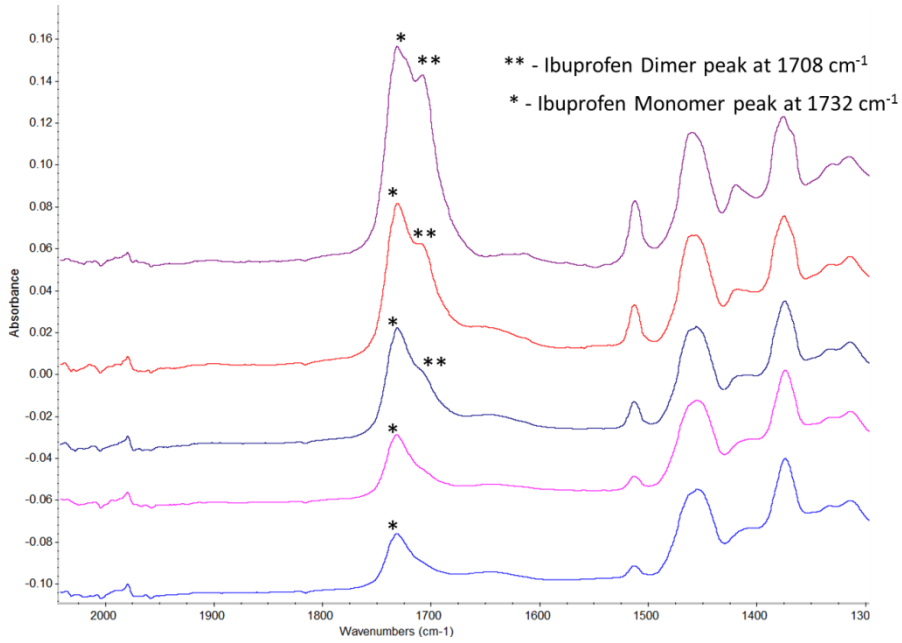

Figure 6. ATR-FTIR spectra (zoomed view) of 10 (blue), 15 (pink), 20 (dark blue), 30 (red) and 40%w/w (purple) ibuprofen-affinisol 100cP extrudates

Although all the extrudates above 15% IBU load showed some presence of the dimer form of IBU, traditional analytical techniques such as XRD, DSC, and Raman which are predominantly used in the detection of the crystalline phase of API within ASD showed the absence of crystalline domains (figures 4).

The theoretical binary phase diagram provided an overview of solid solubility and miscibility between the drug and polymer as a function of temperature.

However this is not a fair reflection of the process as it considers only the effect of temperature on the solubility. Furthermore, it fails to link the solid state solubility and miscibility to the actual stability of the ASD. Thus, the need for a simple, pre-formulation tool for the early detection of solid state stability of ASD led to the investigation of monomer and dimer formation of ibuprofen within ASD using ATR-FTIR.

To confirm the approach of ibuprofen dimer detection by ATR-FTIR studies, ASDs of different IBU concentration were stationed for accelerated stability studies. All the samples were stationed at three different stability conditions of 40°C/75% RH, 25°C/60% RH and room temperature. Extrudates were analyzed off-line at regular intervals using ATR-FTIR, Raman, XRD, and DSC to check for recrystallization of ibuprofen. Table 2 provides a summary of these stability studies. It was observed that 40% IBU loaded extrudates recrystallized within a week at 40°C/75% RH whereas 30% IBU loaded extrudates took 30 days to recrystallize (figure 7). Lower IBU concentration extrudates at 20, 15 and 10% loadings were stable at all three stability conditions measured up to 8 months (figure S2). The 20% IBU concentration extrudates were predicted to recrystallize due to presence of ibuprofen dimer domains but this was not observed with 8 months of the study.

Table 2. Summary of stability studies. (-) & (+) denotes amorphous and crystalline extrudates respectively.

IBU-Affinisol 100cP extrudates	Day 15	Day 30	Day 120	Day 180	Day 240	Ibuprofen dimer at Day 0
40% IBU	+	+	+	+	+	Yes
30% IBU	-	+	+	+	+	Yes
20%IBU	-	-	-	-	-	Yes
15%IBU	-	-	-	-	-	No
10%IBU	-	-	-	-	-	No

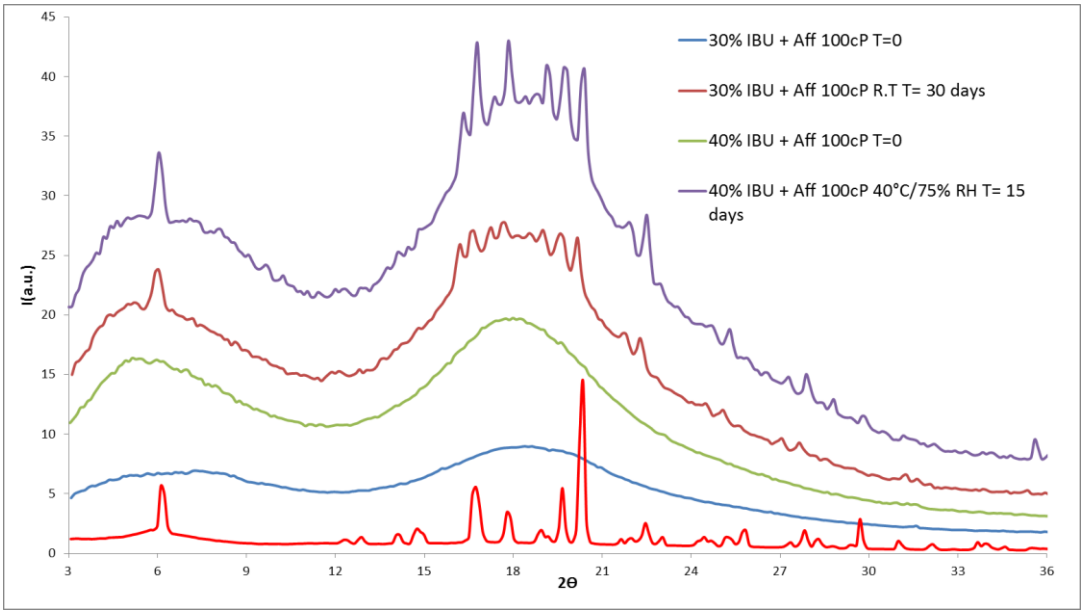

Figure 7: XRD diffractogram of ibuprofen powder (red), 30% T=0 day (blue), 30% R.T T=30 days (maroon), 40% T=0 day (green), and 40% 40°C/74% RH T=15 days (purple) of ibuprofen-Affinisol 100cP extrudates

ATR-FTIR was able to provide an early indication of the presence of the dimer form of ibuprofen within the ibuprofen—Affinisol 100cP ASDs. Detection of this dimer form within ASDs represents free IBU domains either in crystalline or melt form within the extrudates which appeared to correlate with IBU recrystallization. Thus, ATR-FTIR provided a quick and simple pre-formulation tool for detection of drug-drug interaction within the extrudates which could be used to predict the solid-state stability of the ASDs.

Conclusion:

The above results suggest that ATR-FTIR can be used as a predictive tool to indicate long-term stability of ASDs by providing a mechanistic understanding of the drug-drug molecular association within the polymer matrix. This approach has significant advantages over conventional methods such as theoretical binary phase diagrams by Flory-Huggins polymer solution theory, or by subjecting samples to accelerated stability tests. The use of advanced analytical tools can help identify molecular level interaction within ASDs at the initial stage and provide a simple, rapid and robust prediction technique to identify solid-state stability of the ASDs. Identification of molecular level interaction led to significant reduction of time required to confirm solid state solubility of ASD using conventional approach of monitoring crystallization by charging to accelerated stability conditions.

Acknowledgments:

The authors would like to acknowledge Merck & Co., Inc. for funding of the project. A.S would also like to thank Hrushikesh Karandikar for valuable discussion and contribution. Additional data related to the study is available at the University of Bradford in the Centre of Pharmaceutical Engineering Science department.

Appendix 2

PROFESSIONAL DEVELOPMENT:

- Poster titled ‘Effect of concentration of Ibuprofen on the rheological & mechanical properties of Ibuprofen-Affinisol^{TM}HPMC extrudates’ accepted for AAPS San Diego 2017.
- Delivered a presentation titled ‘Stability prediction for solid dispersion of Ibuprofen- Affinisol^{TM}HPMC extrudates using ATR-FTIR spectroscopy’ at PPE-AMRI Bradford UK 2017.
- Presented Poster titled ‘Suitability of Affinisol^{TM}HPMC HME polymers with Ibuprofen using thermal, spectroscopic and rheological properties’ at AAPS, Colorado 2016.
- Presented poster titled ‘Role of DMA in understanding the in-line effect of humidity on the Ibuprofen- Affinisol^{TM}HPMC extrudates’ at PharmSci 2016.
- Presented two posters titled ‘Mechanistic understanding of sphere formation during melt granulation of Lactose monohydrate and PEG-6000’ and ‘Effect of plasticisers on the degradation kinetics of cellulose ester derivative polymers’ at APGI 2016
- Presented poster titled 'Calculation of fragility index and prediction of binary phase diagram of Ibuprofen-HPMCP using DSC' at Thermal Activity Conference April 2015
- Student Representative of PhD (full-time) students of Pharmacy degree at University of Bradford.

CONFERENCES ATTENDED:

- AAPS Annual Meeting and Exposition 2017 – San Diego US
- PPE-AMRI annual meeting, Bradford 2017
- ShinEtsu conference on Solubility Enhancement, Bradford UK 2017
- AAPS Annual Meeting and Exposition 2016 – Colorado US
- PharmSci 2016 - Glasgow UK
- APGI 2016 - Glasgow UK
- Workshop on Synthesis, Characterization and Application of Nanoparticle Assemblies - Pune India
- CompFlu 2016 - Pune India
- APS Freeze Drying and Alternative Drying Technologies for Parenteral 2015
- DMU QbD Annual Symposium – Leicester 2015
- TAC conference 2015 - Univ of Cambridge
- International Health Symposium - Internationalising Your Health Business - Leeds UK 2014

HONOURS AND AWARDS:

- Student Leaders Award (Platinum Award) May 2017
- Student Representative of the Year 2015-2016
- Student Leaders Award (Gold Award) May 2016

- Fred Ellison Award to attend APGI 2016
- Student Bursary Award to attend TAC 2015
- People's choice award for 3MT Competition 2015 where scientific thesis was to be explained to non-scientific audience in 3 minutes with only one slide.

PUBLICATIONS:

- A.D. Sabnis*, N.B.Jadav, A.Naheed, X.Yin, J.Zhang, A.R. Paradkar; Mechanism for formation and internal structure of Lactose-PEG 6000 granules obtained by Hot Melt Granulation (Manuscript under preparation).
- A.D. Sabnis*, Arian Kelly, Tim Gough, Seth Forster, A.R. Paradkar; Effect of concentration of Ibuprofen on the mechanical properties of Ibuprofen-Affinisol^{TM}HPMC extrudates prepared using hot melt extrusion (Manuscript under preparation).
- A.D. Sabnis*, Arian Kelly, Tim Gough, Seth Forster, A.R. Paradkar; Ibuprofen dimer in the solid dispersion an early indicator of potential solid-state stability issues (Manuscript under preparation).
- A.D. Sabnis*, Arian Kelly, A.R. Paradkar; Physical characterization techniques to assess amorphous nature (Book chapter under preparation).